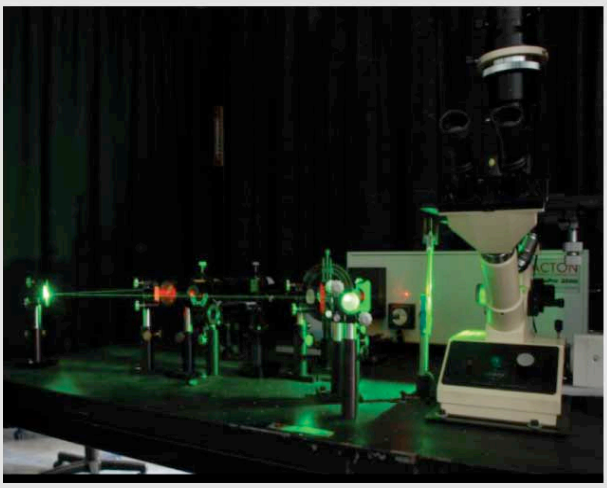

Advanced Laser Technologies

ALT' 09

17th International Conference on Advanced Laser Technologies

26 September – 01 October 2009, Antalya / TURKEY

BOOK OF ABSTRACTS

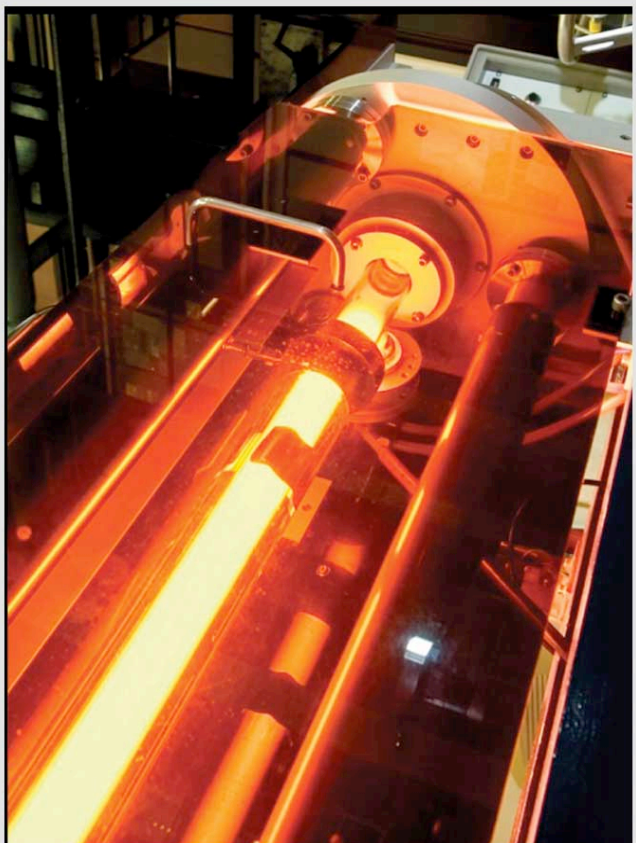

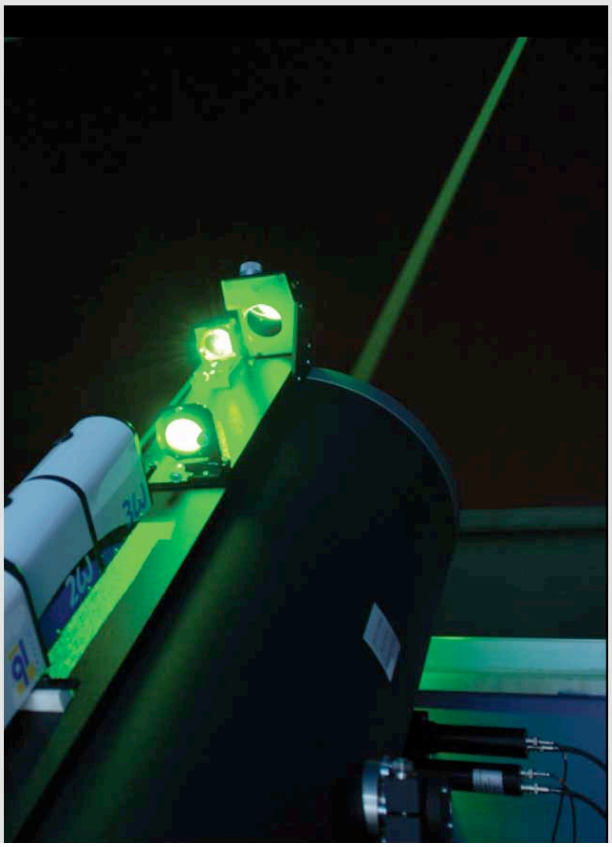

CONTENT

ALT'09 Organization

Conference Chairman

Ivan SHCHERBAKOV

Program Committee Co-Chairs

Vitaly KONOV

Kerim ALLAKHVERDIEV

Boris DENKER

Organizing Committee Co-Chairs

Vladimir PUSTOVOY

Sunullah OZBEK

Arif DEMIR

Local Organizing Committee

Elif KACAR

Timur CANEL

Zehra ALLAHVERDI

Fatih HUSEYINOGLU

Alper SECGIN

Nurullah AGCA

Erhan AKMAN

Belgin GENC

Secretariat

Kenan KELES

Levent CANDAN

Few notes about ALT'09

17th International Conference on Advanced Laser Technologies

The annual International Conference on Advanced Laser Technologies is established in 1993 by Nobel Prize Laureate Alexander Prokhorov, director of the General Physics Institute (GPI) of Russian Academy of Sciences.

ALT Conferences are focused on the recent developments and advances in laser technologies and their applications.

The 17th ALT conference is organized by GPI together with Türkish Scientific and Technological Research Council (TUBITAK) - Marmara Research Center (MRC), Kocaeli University - Laser Technologies Research and Application Center (LATARUM) (Turkey) and Moscow State University (Russia) and will follow this tradition.

The organizers of the ALT' 09 will make their best to provide perfect conditions for discussion and establishing contacts. Leading scientists are invited to give lectures, reviewing the latest achievements in their field of research.

Key Topics

In addition to the traditional issues, as photonics, laser-matter interaction and nonlinear processes, applications of nano-, pico- and femtosecond lasers in materials science, nanotechnology, spectroscopy, etc. separate sessions and presentations will be considered and focusing on:

- photonics
- applications of lasers in material science
- spectroscopy
- laser-matter interaction and nonlinear processes
- ultrashort laser technologies
- medical and biomedical applications of lasers including THz lasers
- solid state lasers and X-ray lasers and fiber lasers
- laser induced breakdown spectroscopy (LIBS)
- lasers in cultural heritage
- laser atmosphere monitoring
- photoacoustics

Letter From the Organizing Committee

Dear Ladies and Gentlemen, Dear Colleagues:

It is great pleasure and honor for me to welcome you to 17th International Conference of Advanced Laser Technologies here in Antalya/Turkey. ALT is a well known Annual Conference established by Nobel Prize Laureate Alexander PROKHOROV. We have assembled here to discuss the newest development and advances in Laser Technologies. We have participants from 33 countries.

The 17th ALT'09 Conference in Antalya, Turkey is organized by the General Physics Institute (GPI), Russian Academy of Sciences (RAS) together with the Turkish Scientific and Technological Research Council (TÜBİTAK) - Marmara Research Center (MRC), Kocaeli University - Laser Technologies Research and Application Center (LATARUM), Turkey and Moscow State University (Russia).
In addition to the traditional issues considered at latest ALT'08 Conference in Balaton, Hungary, such as: photonics, laser-matter interaction and nonlinear processes, applications of nano-, pico- and femtosecond lasers in materials science, nanotechnology, spectroscopy, etc. separate sessions focusing on: biomedical laser application; laser in atmosphere monitoring; laser systems; photoacoustics; light-matter interaction and diagnostics- will be functioning at ALT'09 in Antalya. Some new subjects (not considered at previous ALT Conferences) will be considered also in Antalya. Among the others are: ultrashort laser technologies; THz, solid state, fiber and X-ray lasers; lasers in cultural heritage; layered nonlinear crystals and photovoltaics.

I also hope that you will have a chance to make new friends and start talks about collaborations, as well as to get new ideas about the use of lasers in your research.
We will do our best that you will remember the hospitality you will experience during this meeting.

Prof. Dr. Kerim R. Allahverdiev

ALT'09 Program Committee Co-chair

ALT'09 PROGRAM

	26.09
	Saturday
9:00-19:30	**REGISTRATION**
20:00	**Welcome Buffet**

	September 27	
	Sunday	
9:00-09:30	**Registration**	
9:30-10:00	Welcome Speakers: Prof. Ivan SCHERBAKOV, Chairman of ALT09, Russia Prof. Nuket YETIS, President of TÜBİTAK, Turkey Prof. Vladislav PANCHENKO, Chairman of the Russian Foundation for Basic Research, Russia Prof. Sezer KOMSUOGLU, Rector of Kocaeli University , Turkey Prof. Mustafa AKAYDIN, Lord Mayor of Antalya, Turkey Prof. Kerim ALLAKHVERDIEV, Co-Chairman of Program Committee, Turkey.	
10:00-10:20	**Coffee Break**	
10:20-10:40	**BIOMEDICAL LASER APPLICATIONS**	**NON-LINEAR PHENOMENA**
	Raman Spectroscopy - A Powerful Tool in Biophotonics Jürgen Popp (Germany)	**Spectral Response of Molecular Media under Nanoporous Confinement** V.G. Arakcheev, V.B.Morozov, A.N. Olenin, A.A.Valeev (Russia)
10:40-11:00	**Biophotonic Methods for the Assessment of Burn Injury in Human Skin** Martin Leahy (Ireland)	**THz Source Based on Two-Color Diode-Pumped c-cut Vanadat Lasers and GaSe Nonlinear Crystal** A.A. Sirotkin, S.V. Garnov, A.I. Zagumennyi, Yu.D. Zavartsev, S.A. Kutovoi, V.I. Vlasov, I.A. Shcherbakov (Russia)
11:00-11:20	**Multi-Dimensional Laser Microscopy in Biomedical Sciences** Herbert Schneckenburger, Petra Weber, Thomas Bruns and Michael Wagner (Germany)	**Nonlinear Optics at the Single Optical Cycle Limit** Eleftherios Goulielmakis (Greece)
11:20-11:40	**Laser Cancer Phototherapy Enhanced by Gold Nanoparticles** Valery V. Tuchin, Irina L. Maksimova, Georgy S. erentyuk, Garif G. Akchurin, Boris N. Khlebtsov, Nikolai G. Khlebtsov (Russia)	**Pair Collisions of Optical Pulses in Non-Linear Dispersive Media: Frequency Tuning and Velocity Variation** A.P. Sukhorukov, V.E. Lobanov
11:40-12:00	**Imaging of Live Mammalian Embryos with Confocal Microscopy and Optical Coherence Tomography** Kirill V. Larin, Irina V. Larina, Saba Syed, Steven Ivers, Mary E. Dickinson (USA)	**Review for the Technique Development of Front end of SG Laser facility** Zhou Yi, Jianqiang Zhu, Xuechun Li, Wei Fan, Shaohe Chen, Zunqi Lin (China)
12:00-15:00	**Lunch**	

	BIOMEDICAL LASER APPLICATIONS	NON-LINEAR PHENOMENA
15:00-15:20	**Nonlinear Optical Properties of Biomineral Nanocomposite Structures** Yuriy Kulchin, A.V. Bezverbny, O.A. Bukin, S.S. Voznesenski, S.S. Golik, A.Yu. Mayor, Yu.A. Shipunov (Russia)	**Laser Resonator Mode Connection and Change of this Connection under Influence of an External Optical Signal** V.P.Bykov (Russia)
15:20-15:40	**Fluorescent Detection and Photodynamic Inactivation of Pathogenic Microorganisms** Ekaterina Borisova, V. Mantareva, I. Angelov, V. Kussovski, D. Woehrle, and L. Avramov (Bulgaria)	**Powerful Few Cycle Optical Pulse Production and New Spectral Component Formation under Filamentation in Gases** M. Kurilova, A. Mazhorova, D. Uryupina, n. Panov, G. golovin, S. gorgutsa, R. Volkov O. Kosareva, and A. Savel'ev (Russia)
15:40-16:00	**Laser Scattering and Diffraction Assessment of the Effect of Diamond Nanoparticles on Blood Microrheology** Alexander Priezzhev (Russia)	**Phase Retrieval Method for Reconstructing Wavefront Aberration of Ultrashort High-Power Laser Pulse** Moon Tae Jeong, Chu Min Kim, and Jongmin Lee (Korea)
16:00-16:20	**Laser-Based Nanoengineering for Biomedical Applications** Boris Chichkov (Germany)	**Phase-Lock and Frequency Stabilization of Nd:YAG Lasers** Cihangir Erdogan (Turkey)
16:20-16:40	**Sorption of the Ions with Different Ionic Radii on Protein Surface in the Process of Nanocluster Formation** Khlapov V.P, G.P. Petrova, Yu.M. Petrusevich (Russia)	
16:40-17:00	**Medical Applications of Laser Spectroscopic Gas Analyses** Markus Sigrist, R. Bartlome, and M. Gianella (Chehia)	
17:00-17:20	**Coffee Break**	
	BIOMEDICAL LASER APPLICATION	**LASER IN ATMOSPHERE MONITORING**
17:20-17:40	**"Clean" and "Cold" Laser Transfer of Biomaterials** Taras Kononenko, I.A.Nagovitsyn, G.K.Chudinova, V.I. Konov, I.N.Mihailescu, P.Alloncle, M.Sentis (Russia)	**LIDAR Technologies of Remote Monitoring** Anatoly Boreysho (Russia)
17:40-18:00	**The Optical Nose, Laser Based Trace Gas Detection for the Early Monitoring of Human Health** Frans Harren (Netherland)	**Reference and Phase Shift Technique in Multipass Laser Schemes for Trace Gas Particles Detection** I.V.Nikolaev, V.N.Ochkin, S.N.Tskhai (Russia)
18:00-18:20	**Spectral Domain Optical Coherence Tomography Imaging of the Human Posterior Eye** Tapio Fabritius, and Risto Myllyla (Finland)	**Retrieval of Dust Particle Parameters from Multiwavelength Lidar Measurements** Igor Veselovskii, Alexey Kolgotin, Oleg Dubovik, Sergey Vartapetov (Russia)
18:20-18:40	**Functionalized Plasmon-Resonant Nanoparticles: Fabrication, Optical Properties, and Biomedical Applications** Nikolai Khlebtsov (Russia)	**Quantum Cascade Laser Spectrometers for Atmospheric Gas Detection** Virginie Zeninari (France)
18:40-19:00	**Surface-Assisted Laser Desorption**	**A Multi-Angle Laser Light Scattering Aerosol**

	Mechanism and Applications. S.Alimpiev (Russia)	A. Nagy, A. Czitrovszky, A. Kerekes, W. Szymanski (Hungary)
17:00-19:30	**POSTERS**	

	September 28	
	Monday	
	PHOTOACOUSTICS	**LASER SYSTEMS**
9:00-9:20	**Optoacoustic Measurement of Optical Propertist in Biological Tissues** Pelivanov I.M., Barskaya M.I., Podymova N.B., Khokhlova T.D., Karabutov A.A (Russia)	**Numerical Analysis of Multilayer Optical Waveguides** A.G. Rzhanov, S.E. Grigas (Russia)
9:20-9:40	**Optoacoustic Array for Monitoring of Hemoglobin Concentration: Modeling and Experiment** Valeriy Andreev, Tatiana Khokhlova, Alexander Bykov (Russia)	**The Red and Infrared Emission Centers in Bismuth-Activated Silicate Glass.** B. Denker, E. Dianov, B. Galagan, S. Sverchkov, I. Shulman (Russia)
9:40-10:00	**Point Spread Function of Array Transducers in 2D Optoacoustic Tomography** Tatiana Khokhlova, Ivan M. Pelivanov, Varvara A. Simonova and Alexander A. Karabutov (Russia)	**Fluorescent and Optical Absorption Centers in Chromium-Doped $LiGaSiO_4$ Nano-Glass-Ceramics and Vitreous Precursors** Kirill A. Subbotin, Valery A. Smirnov, Evgeny V. Zharikov, Ivan A. Shcherbakov (Russia)
10:00-10:20	**Optoacoustic Cancer Diagnosis and Therapy** M. Jaeger, S. Preisser, L. Siegenthaler, M. Kitz, Martin. Frenz , D. Schol, M. Fléron, J.F. Greisch, M.C. De Pauw-Gillet, E. De Pauw J. Niederhauser, D. Schweizer (Switzerland)	**Photoluminensecence of CdTe Quantum Dots and Porous Silicon Oxide Nanocomposite** N.A. Piskunov , E.D. Maslennikov , L.A. Golovan , V.Yu Timoshenko , P.K. Kashkarov (Russia)
10:20-10:40	**Coffee Break**	
	PHOTOACOUSTICS	**LASER SYSTEMS**
10:40-11:00	**Imaging of Ultrasound Transmission Parameters in Photoacoustic Tomography** Srirang Manohar, Rene G.H. Willemink, Jithin Jose, Steffen Resnik, Cornelis H. Slump, Ferdi van der Heijdeb and Ton G. van Leeuwen (Netherlands)	**Thin Disk Laser: A Versatile Tool for Micro Machining** Friedrich Dausinger (Germany)
11:00-11:20	**Laser Induced Photoacoustic and Vaporization Pressure Signals in Water: New Experimental Results** A.A.Samokhin, V.I.Vovchenko, and N.N.Il'ichev (Russia)	**A cw Tm,Ho:YLF Laser Pumped by Raman Erbium Fiber laser at 1675 nm** Yu. L. Kalachev, V. A. Mihailov, V. V. Podreshetnikov, I. A. Shcherbakov (Russia)
11:20-11:40	**Evaluation of Microstructure of Severely Plastically Deformed Metals by Laser Ultrasound** V. V. Kazhushko, G. Paltauf, and H. Krenn (Austria)	**Pedestal Suppression in a Short-Pulse Fiber-Laser Output by Soliton Self-Frequency Shift in a Photonic-Crystal Fiber** D.A. Sidorov-Biryukov, E.E. Serebryannikov, A. Voronin, A. Fernandez, L. Zhu, A. Pugzlys, F.Ö. Ilday, J.C. Knight, A. Baltuška, and A.M.

11:40-12:00	**Characterization of Giant Photoacoustical Signals in Layered Crystals by a Novel Transient Free-Carrier Absorption Technique** Vytautas Grivickas, V. Gavryushin, K. Gulbinas, V. Bikbajevas, K. R. Allakhverdiev, and D. A. Huseinova (Latvia)	**Broadly Tunable Tm,Ho:KYW Laser Around 2 μm and its Mode-Locked Operation** A.A. Lagatsky, S. Calvez, N.V. Kuleshov, W. Sibbett (United Kingdom)
12:00-15:00	**Lunch**	
	PHOTOACOUSTICS	**LASER SYSTEMS**
15:00-15:20	**High Power Quantum Cascade Lasers and Applications to High Sensitivity, High Selectivity Detection of Chemical Warfare Agents and Explosives** C. Kumar N.Patel (USA)	**Diode-Pumped Disk and Slab Solid-State Lasers** Vladimir Tsvetkov, Vladimir Seregin, Andrew Lyashedko, Galina Bufetova, Dmitriy Nikolaev, Ivan Shcherbakov (Russia)
15:20-15:40	**Photoacoustic Spectroscopy: Low VS. High Laser Power** Dan Constantin Dumitras, D. C. A. Dutu, A. M. Bratu, M. Patachia, C. Achim, M. Petrus, C. Matei, S. Banita (Romania)	**CW and Pulsed Lasers Based on Er-doped GTWave Fiber** A.S.Kurkov, A.I.Ivanenko, S.M.Kobtsev, S.V.Kukarin (Russia)
15:40-16:00	**Three-Dimensional Acousto-Optic Mapping in Tissue Mimicking Phantoms Using Heterodyne Light-Scattering Spectroscopy.** Aliaksandr Bratchenia, R. Molenaar, R.P.H. Kooyman (Netherlands)	**Chemical Vapor Deposited (CVD) Diamond for Laser Applications** V.G. Ralchenko, V.I. Konov, A.P. Bolshakov, A.F. Popovich, V.V. Kononenko, M.N. Sinyavskiy, E.E. Ashkinazi, A.A. Kaminskii, A.Yu. Lukyanov, A.V. Khomich (Russia)
16:00-16:20	**Acousto-Optical Methods of Image Processing** Oleg Makarov, Wladimir Molchanov, Jewgenij Maximov (Germany)	**High Accuracy TN Optical Commutator of Laser Radiation for Application in Space Navigation** V. Pokrovsky, S. Studentsov, L. Soms, M. Tomilin (Russia)
16:20-16:40	**Self-Mixing Interferometry** Silvano Donati (Italy)	**Investigating Ultra-Intense Plasma-Based Soft x-ray Lasers** Philippe Zeitoun, Marta Fajardo, Pedro Velarde-Mayol, Frederic Burgy, Kevin Cassou, Julien Gautier, Jean-Philippe Goddet, Guillaume Lambert, David Ros, Anna Barszczak Sardinha, Stephane Sebban, Amar Tafzi (France)
16:40-17:00		**High Power Femtosecond Thin Disk Lasers** Thomas Südmeyer, Cyrill R. E. Baer, Christian Kränkel, Oliver H. Heckl, C.J. Saraceno, Matthias Golling, Rigo Peters, Klaus Petermann, Günter Huber, and Ursula Keller (Germany)
17:00-17:20	**Coffee Break**	
	LIGHT-MATTER INTERACTION	**LASER SYSTEMS**
17:20-17:40	**Three-Waves Interactions of Surface Defect-Deformational Waves and Their Role in Selforganization of Nano and Microstructures Under Laser Action on**	**High Power CW and Pulsed Fiber Lasers with China-Made Yb-Doped LMA Fiber at SIOM** Qihong Lou, Jun Zhou, Bin He and Songtao Du (China)

	V.I.□mel'yanov, D.□.Seval'nev (Russia)	
17:40-18:00	**Neutral and Charged Species Produced Through Lasers in Solid and Gas Phase: Spectroscopy and Mass Spectrometry.** A.Giardini, S. Orlando, A. Paladini, S. Piccirillo, F.Rondino, A. Santagata, P. Villani (Italy)	**Lasing Properties of a New Ytterbium-Doped Glass for Miniature Diode-Pumped Ultrashort Pulse Lasers** B.I.Denker, B.I.Galagan, I.N.Glushenko, V.E.Kisel, S.V.Kulchik,N.V.Kuleshov, S.E.Sverchkov (Russia)
18:00-18:20	**Direct-Write of 3-Dimensional Materials Structures from Gaseous Precursors and Applications** Michael Stuke (Germany)	**Diamond p-n-Junction for UV Streamer Laser** Sergei Buga, V. Blank, V. Bormashov, V. Denisov, S. Terentiev, A. Kirichenko, N. Kornilov, M. Kuznetsov, V. Mordkovich, E. Pel, S. Tarelkin (Russia)
18:20-18:40	**Ultrafast Light Blade: Anisotropic Sensitivity of Isotropic Medium to Femtosecond Laser Radiation** Peter G. Kazansky, Yasuhiko Shimotsuma, Jiarong Qiu, Weijia Yang, Masaaki Sakakura, Martynas Beresna, Yuri Svirko, Selcuk Akturkand Kazuyuoki Hirao (United Kingdom)	**High-Power Coherent Beam Combination from Two and Four Fiber Lasers** Jun Zhou, Bin He, Wei Wang, Qihong Lou (China)
18:40-19:00	**Turkish Accelerator Complex, FEL Resonator System** H. Duran Yildiz (Turkey)	**Laser Raman Microscopy, Pigments and the Arts/Science Interfaces** R.J.H. Clark (United Kingdom)
19:00-19:20		
17:00-19:30	**POSTERS**	
21:00	**Committee Meeting**	

	September 29
	Tuesday
9:00-19:30	**Social program**
20:00	**Gala dinner**

	September 30	
	Wednesday	
	LIGHT-MATTER INTERACTION	**DIAGNOSTICS**
9:00-9:20	**Laser Crystallisation Induced Multicrystalline Silicon Thin Film Solar Cells on Glass: European High-EF project** F. Antoni, E. Fogarassy, A. Slaoui, F. Falk, E. Ose, S. Christiansen, G. Sarau, J. Schneider, (France)	**Roughness Measurement with Laser Speckle Pattern of Milled Metals Using Speckle Statistics Analysis** Ersin Kayahan, Fikret Hacizade, Ozcan Gundogdu, Humbat Nasibov (Turkey)
9:20-9:40	**Femtosecond Laser Applied to Photovoltaic Cell processing** M. Sentis, Th. Sarnet and J. Hermann (France)	**Development of Laser-Based Metrology Methods for Extreme Light Infrastructure Project** Aladar Czitrovszky (Hungary)

9:40-10:00	**a-Si:H/c-Si Heterojunction for Photovoltaic Application** Osman Kodolbaş (Turkey)	**Lasers in Spectroscopy to Study Materials Under Extreme Conditions** Hans Dieter Hochheimer, (USA)
10:00-10:20	**Nanowires, Nanoloops and Nanorods by CVD** Michael Veith, Cenk Aktas (Germany)	**Structural Diagnostics of Polymer Materials by Raman Spectroscopy** Kirill Prokhorov, E.A. Sagitova, G.Yu. Nikolaeva, P.P. Pashinin, P. Donfack, and A. Materny (Russia)
10:20-10:40	**Coffee Break**	
	LIGHT-MATTER INTERACTION	**DIAGNOSTICS**
10:40-11:00	**A Review of Laser Ablation Propulsion** Claude Phipps, W. Bohn, T. Lippert, M. Michaelis, A. Sasoh, W. Schall and J. Sinko (USA)	**"An Ultrafast Single-Photon Image Diagnostics Sensor with APD Arrays for Industrial and Bio-Applications"** E.Charbon and S.Donati (Italy)
11:00-11:20	**High-Intensity Terahertz Pulses: Methods of Generation and Applications** Sergey V. Garnov (Russia)	**Investigation of Radio-Optic Resonances on Far Field and Free Space Condition** Mustafa Cetintas, R. Hamid, S. Çakir, O. Sen (Turkey)
11:20-11:40	**Laser Cleaning of Metals: Fundamentals, Practical Applications and Future Prospects** Vadim Veiko, V.N. Smirnov, T.Yu. Moutin, E.A. Shakhno (Russia)	**Optical Characterization and Thin Film Electronics Applications of Carbon Nanobuds and -Tubes** Esko I. Kauppinen (Finland)
11:40-12:00	**LIBS-study of Components Migration in Steel Weld Joints** Elena L. Surmenko, Tatiana N. Sokolova, and Ivan A. Popov (Russia)	**Nano-Aquarium Integrated with Functional Microcomponents in Photostructurable Glass by Femtosecond Laser Microprocessing for Microorganism Analysis** Y. Hanada, K. Sugioka, H. Kawano, I. Ishikawa A. Miyawaki, M. Iida, H. Takai K. Modrikawa (Japan)
12:00-15:00	**Lunch**	
	LIGHT-MATTER INTERACTION	**LASER SYSTEMS**
15:00-15:20	**Laser-Assisted Fabrication of Silicon Nanocrystals in Liquids** S.V. Zabotnov, P.A. Perminov, A.A. Ezhov, I.O. Dzhun, L.A. Golovan, P.K. Kashkarov (Russia)	**A New Approach for Developing Highly effective Solid-State HV Pulse Generators for Laser Pumping** Sergey Moshkhunov (Russia)
15:20-15:40	**Theoretical and Experimental Characterization of Nanosecond-Laser-Induced Plasmas for Ignition** Ernst Wintner (Austria)	**A Novel Pattern Recognition Approach for Noisy Frequency-Resolved-Optical-Gating Traces** Chao-Kuei Lee, Wei-Hong Su, Sung-Hui Lin, T. R. Tsai (Taiwan)
15:40-16:00	**Laser-Induced Surface Modification of Organic polymers** Lokman Torun (Turkey)	**Plasma-Based Extreme Ultra-Violet Lasers** G.J. Tallents, I. Al'Miev, N. Booth, L.M.R. Gartside, H. Huang, A. K. Rossall, E. Wagenaars, D. S. Whittaker, Z. Zhai (United Kingdom)
16:00-16:20	**Synthesis by Pulsed Laser Ablation in Ar and SERS Activity of Silver Thin Films with Controlled Nanostrucure**	**Temporal Optimization of 0.1- Hz.0.5- PW Laser Pulses** Jae Hee Sung, Tae Jun Yu, Seong Ku Lee, Tae

	Sebastiano Trusso (Italy)	(Korea)
16:20-16:40	**Zinc Oxide Nanostructured Layers for Gas Sensing Applications** A.P. Caricato, A. Cretí, A. Luches, M. Lomascolo, M. Martino, R. Rella, D. Valerini (Italy)	**Recent Advances of High Power 1 µm Lasers** Manfred Berger (Germany)
16:40-17:00	**Terahertz Reflection Response Measurement Using a Photon Polariton Wave** Kenji Katayama (Japan)	**Z-Scan Investigation of Concentration Dependency of Nonlinear Optical Responses in Triphenylmethane Dye Solutions** Humbat Nasibov, Izmir Mamedbeili (Turkey)
17:00-17:20	**Coffee Break**	
	LIGHT-MATTER INTERACTION	**LASER SYSTEMS**
17:20-17:40	**Terahertz Applications of Nanostructured Alumina Oxyhydroxide Based Artificial Materials** A.V. Andreev, M.N.Esaulkov, A.□. Khodan, M.M. Nazarov, A.A. Konovko, D.A. Sapozhnikov, I.N.Smirnova, A.P. Shkurinov (Russia)	**Nano-Imaging and Nano-Patterning with Compact EUV Lasers: New Opportunities in Nanotechnology with a Table Top System** Mario Marconi (USA)
17:40-18:00	**Functional Surface Structures Using Femtosecond Ablation** Paivasaari Kimmo, Jääskeläinen Timo (Finland)	**Laser Designator and Range Finder Design** Birol Erenturk (Turkey)
18:00-18:20	**Application of the Pulse Laser Deposition Method for Preparation Film Nanostructure of Metals and Semiconductors** O.A. Novodvorsky, E.V. Khaydukov, A.A. Lotin, L.S. Parshina, V,V. Rocheva, V.Ya. Panchenko (Russia)	**New Frontiers in Tunable Laser Technology: Optical Parametric Oscillators Spanning the Ultraviolet to Mid-Infrared** Majid Ebrahim-Zadeh (Spain)
18:20-18:40	**Laser Modification of 1D Al/Al_2O_3 Nanostructures** C. Aktas, C. Akkan, M. Veith (Germany)	**Pishaper-Beam Shaping Optics for Advanced Laser Technologies** Aleksandr Laskin (Germany)
18:40-19:00	**Optimization of Ultrashort Pulsed Laser Radiation for Precise and Productive Micromashining** P. Pivovarov, S. Klimentov, V. Konov, D. Walter, M. Kraus, F. Dausinger (Russia)	**High Power Fiber Lasers** Bulend Ortac (Germany)
17:00-19:30	**POSTERS**	

	October 01	
	Thursday	
	LIGHT-MATTER INTERACTION	**LASER SYSTEMS**
9:00-9:20	**Obtaining of Extremely Homogeneous Volume Self -Sustained Discharge for Powerful CO_2-Lasers Pumping** Vladimir Yamshchikov (Russia)	**$GaS_{0.4}Se_{0.6}$: Relevant Properties and Potential for 1064 nm Pumped Mid-IR OPOs and OPGs Operating above 5 µm** Valentin Petrov, Vladimir Panyutin, Alexey Tyazhev, Georgi Marchev, Alexander I. Zagumennyi, Fabian Rotermund and Frank Noak (Germany)

9:20-9:40	**Stable Laser-Plasma Picosecond kHz X-ray Source Using Melted Metal Target** Konstantin Ivanov, D.S. Uryupina, R.V. Volkov, A.B. Savel'ev, I.A. Ozheredov, A.P. Shkurinov (Russia)	**Ultrafast Low-Noise High-Power Fiber Lasers: Applications from Material Processing to Next-Generation Accelerators** Omer Ilday (Turkey)
9:40-10:00	**Waveguides in Laser Crystals Inscribed by a Femtosecond Laser Beam** Andrey Okhrimchuk, A.V. Shestakov, V. Mezentsev, and I. Bennion (United Kingom)	**Alternative Materials for High Power Lasers** Zelmon D. (USA)
10:00-10:20	**Effect of CO2 Laser Focusing on Groove Cutting into Steel Surfaces** Suleyman Biyikli , J. Yilmazkaya Sungu (Turkey)	**Polycrystalline Yttrium Aluminum Garnet for Fiber Lasers** Randall S. Hay, Geoff Fair, Hee Dong Lee, Triplicane Parthasarathy, Kristin Keller, Pavel Mogilevsky (Canada)
10:20-10:40	**CLOSING CEREMONY**	

POSTERS SESSIONS

BIOMEDICAL LASER APPLICATIONS — September 27

1. **Broadband Optical Illumination in a TD-OCT System for Live Imaging in Developmental Biology at 1300 nm Wavelength**
   R.Cernat, .Dobre, A.Bradu and A.Gh.Podoleanu (Romania)
2. **Noninvasive Detection of Breath Ammonia Levels in Renal Diseases Using Laser Photoacoustic Spectroscopy**
   R. Cernat, D.C.A. Dutu, M. Patachia, C. Achim and D.C. Dumitras (Romania)
3. **Formation of Biocompatible Silicon Nanocrystals with Desired Structure and Optical Properties**
   T. Yu. Bazylenko, L. A. Osminkina, R. A. Abidulina, A. I. Efimova, M. B. Gongalsky, A. V. Motuzyuk, V. Yu. Timoshenko, A. H. Gaydarova, G. T. Sukhih, and A. D. Durnev (Russia)
4. **Laser Stereolithography in Cosmetic Surgery**
   S.A. Cherebylo, A.V. Evseev, P.N. Mitroshenkov (Russia)
5. **Effect of the Ions with Different Ionic Radius on Lysozyme in Water Solutions.**
   Ksenya V. Fedorova, Irina A. Sergeeva, Galina P. Petrova, Y.M. Petrusevich (Russia)
6. **Photodynamic Therapy on B16 Cells With Tetrasulphonated Porphyrin and Different Light Sources**
   Simona Florentina Pop, R.M. Ion, M. Neagu and C. Constantin (Romania)
7. **A New Method of Herpes Keratitis Treatment by means of 1.4um Laser Diode.**
   P.A. Gonchar, M.A. Frolov, N.V. Rodionova, Yu. L. Kalachev, V. A. Mihailov, I. A. Shcherbakov (Russia)
8. **Experimental Study of the Multiple Scattering Effect on the Flow Velocity Profiles Measured in Intralipid Phantoms by DOCT**
   Janne Lauri, Alexander V. Bykov, Alexander V. Priezzhev and Risto Myllylä (Finland)
9. **Histological Studies of Pathological ENT Tissues Irradiated by Laser Diode and CO_2 Laser Surgical System**
   M. Petrus, D.C. Dumitras, D.C. Dutu (Romania)
10. **Dynamic Light Scattering Studies of Collagen Solutions Containing Metal Ions with Different Ionic Radii**
    I.A. Sergeeva, M.S. Ivanova, K.V. Fedorova, G.P. Petrova, Yu.M. Petrusevich. (Russia)
11. **Luminescent Porous Silicon for Biosensing Applications**
    Viktoriia Shevchenko (Ukrain)
12. **HCN Detection in Human Breath Using a CW Optical Parametric Oscillator**
    M. Spunei, D. Arslanov, S. Persijn, S. Cristescu, P. Merkus, F. J.M. Harren (Netherlands)
13. **Simulation of Optical Radiation Propagation in Plant Tissue**
    V. P. Zakharov, I. A. Bratchenko, E.V.Timchenko (Russia)
14. **The Possibilities of the Oxygen Saturation Spectral Imaging Method**
    Tatiana A. Savelieva, Maxim V. Loschenov , Sergey Yu. Petrov and Sergey Yu. Vasilchenko (Russia)
15. **Controlled Laser Hyperthermia of Subdermal Neoplasms**
    Nina A. Kalyagina, Irina A. Shikunova, Tatiana A. Savelieva, Viktor B. Loschenov (Russia)
16. **Sunscreen-Grade Nanoparticles: Aspects of Interaction with Skin**
    A.P. Popov, A. Zvyagin, M.S. Roberts, J. Lademann, A.V. Priezzhev, and R. Myllyä (Russia)
17. **Terahertz Time-Domain Spectroscopy of Biological Molecules**

NON-LINEAR PHENOMENA — September 27

18. **Nonlinear Photolimunescence of Gallium Selenide and Related Compounds: Caused by Resonance Enhanced Two-Photon Absorption Rather than Second-Harmonic Generation**
Kerim Allakhverdiev, D. Huseinova, T. Baykara, E. Salaev, C. Angermann, P. Karich, and L. Kador (Turkey)
19. **Influence of the Resonator Losses on the Possible Squeezing at the Resonator Parametrical Excitation**
Vladimir Bykov (Russia)
20. **Polarization-Resolved Study of Passively Q-switched Diode-Pumped Nd:YVO4 Lasers with Cr^{4+}:YAG and V^{3+}:YAG Saturable Absorbers**
A.A. Sirotkin, D.V. Sizmin, S.V. Garnov (Russia)
21. **1,3 μm Passively Q-switched Diode Pumped Lasers with Co^{2+} Doped Crystals as the Saturable Absorbers**
A.A.Sirotkin, S.P. Sadovskiy, S.V. Garnov (Russia)
22. **Laser-Induced Diffraction and Reflection in the Nonlinear Defocusing Media**
Valery E. Lobanov, Aleksey A. Kalinovich, Anatoly P. Sukhorukov (Russia)
23. **Blue Laser Light Generation by Frequency Doubling of a Cesium Vapor Laser**
B. V. Zhdanov, Yalin Lu, M. K. Shaffer, W. Miller, D. Wright, W. Holmes, and R. J. Knize (USA)
24. **Second-Harmonic Generation and Optical Bistability in Thin $Ge_xSb_{40-x}S_{60}$ Chalcogenide Films**
Sashka Alexandrova, Vitalii I. Krasovskii, Igor A. Maslyanitsyn, Vladimir B. Tsvetkov, and Vladimir D. Shigorin (Russia)
25. **Modulation for Compression Dynamics of Quadratically Phase-Modulated Few-Cycle Pulses in Dispersive Medium**
Olga I. Paseka, Valery E. Lobanov and Anatoly P. (Russia)
26. **Evaluation of Laser Speckles Generated by Microspheres - Z-Scan Investigation of Concentration Dependency of Nonlinear Optical Responses in Triphenylmethane Dye Solutions**
Humbat Nasibov (Turkey)
27. **Intermittency and Chaos in a Semiconductor Laser Subjected to Strong Coherent and Incoherent Feedback**
Enrico Randone and Silvano Donati (Italy)
28. **Structure Elucidation 4,4'''-Bis-(2-butyloctyloxy)-p-quaterphenyl in Cyclohexane by the Joint Application of FTIR, Raman, UV and Visible Spectroscopy**
Ipek Karaaslan (Turkey)
29. **Thermally Induced Depolarization Ratio in 23 and m3 Symmetry Classes of Cubic Crystals**
Anton Vyatkin, Efim Khazanov (Russia)
30. **Nonlinear Interaction of Optical Beams in Gradient Waveguides**
A.K. Sukhorukova, A.P. Sukhorukov, A.S. Grankin (Russia)

LASERS IN ATMOSPHERE MONITORING — September 27

31. **Vertical Concentration Distribution Measurement of Atmospheric Aerosols by Laser Light Scattering**
Daniel Oszetzky, Attila Nagy, Attila Kerekes, Aladár Czitrovszky (Hungary)
32. **New Multiwavelength MIE-Raman Lidar in Turkey for Aerosol Studies**

K. Allakhverdiev, T. Baykara, M. Bekbolet, Fatih Huseyinoglu, S. Ozbek, Z. Salaeva, A. Secgin, S. Vartapetov, I. Veselovskii (Turkey)

33. **The Possibility of Wideband CO Laser and Sr Vapor Laser Using for Atmosphere Monitoring**
Kharchenko O.V., Romanovskii O.A. (Russia)

34. **Atmospheric Environment: Impacts of the Transport of Aerosols from Saharan Dust and Lidar Techniques**
Nihal Yucekutlu, Yavuz Yucekutlu (Turkey)

35. **Lidars in Forestry**
Surhay Allahverdi (Turkey)

36. **Hot-Air Atmospheric Turbulence Generator for the Improvement of Laser Based Free-Space Communication Systems with Adaptive Optics Systems**
Onur Keskin, H. Nasibov, F. Hacızade (Turkey)

PHOTOACOUSTICS **September 28**

37. **Evaluation of Ammonia Absorpsion Coefficients by Photoacoustic Spectroscopy for Detection of Ammonia Levels in Human Breath**
C. Achim, D. C. Dumitras, D. C. A. Dutu, R. Cernat (Romania)

38. **Optoacoustic Phenomenon in a Submicron Metal Coating Covered by a Transparent Liquid: Theory and Application for Evaluation of Coating Properties**
Kopylova D.S., Pelivanov I.M., Podymova N.B., Karabutov A.A (Russia)

39. **Development of Back-Mode Photoacoustic Transducer for Measuring Consistency of Paper Pulp Suspensions**
Zumoin Zhao, M. Törmänen, R. Myllylä (Finland)

LASER SYSTEMS **September 28**

40. **Nonlinear GaSe and GaSexS1-x Layered Compounds for Near IR Laser Light Visualization**
Kerim Allakhverdiev, Tarik K. Baykara, Sunullah Ozbek, Eldar Yu. Salaev (Turkey)

41. **Supercontinuum Generation in Transparent Biomimetical Nanocomposites**
Alexander Bezverbny, Yu.N. Kulchin, Yu.A. Shchipunov, S.S. Voznesensky, S.S. Golik, A.Yu. Mayor, I.V. Postnova (Russia)

42. **Investigation on the Mode Hope Free Tunability of a 852 nm Laser Diode without Anti Reflection Coating**
Cengiz Birlikseven, E. Şahin, M. Çelik, R. Hamid (Turkey)

43. **Photonic Crystal Si-based Structures for Optics and Sensorics**
A.I. Efimova, V.B. Zaitsev, L.A. Golovan, S.M. Afonina, A.D.Sladkov (Russia)

44. **Numerical Investigation of Laser Resonator for Generating Radially or Azimuthally Polarized Beams**
V.D. Dubrov, R.V. Grishaev, M.D. Homenko, Yu.N. Zavalov (Russia)

45. **Growth and Structural Peculiarities of the Epitaxial Films of GaSe and InSe in Correaltion with the Electrophysical Properties**
E. Yu. Salaev, Hidayat Nuriyev (Azerbaijan)

46. **Tunable Infrared Liquid Crystalline Filters**
Tahir Ibragimov, N.J.Ismailov, G.M.Bayramov, A.R.Imamaliyev (Azerbaijan)

47. **Actively Q-switched Diode Pumped Tm:YLF Laser**
J. K. Jabczynski, L. Gorajek, W. Zendzian, J. Kwiatkowski, K. Kopczynski, H. Jelinkova, M. Němec, J Šulc (Poland)

48. **Photoalignment in a Dye-doped Liquid Crystal by Linearly Polarized Laser Light**

Ridvan Karapinar, D. Fedorenko, E. Ouskova and Y. Reznikov (Turkey)

49. **GaSe and InSe Crystals in Quantum Electronics**
V.M.Salmanov, A.A.Salmanova, E.M.Kerimova, D.A.Huseinova (Azerbaijan)
50. **Femtosecond Pulse Self-Compression Under Filamentation of Collimated Beam**
M. Kurilova, A. Mazhorova, N. Panov, S.Gorgutsa, D. Uryupina, R. Volkov, O. Kosareva, A. Savel`ev (Russia)
51. **Ho:YAG Tunable Hybrid Laser Pumped by a Tm-Doped Fiber Laser**
Jacek Kwiatkowski, J.K. Jabczynski, W. Zendzian, L. Gorajek, H. Jelinkova, J. Sulc, M. Nemec, P. Koranda (Poland)
52. **Spectral-Luminescent Properties of Ions in Semiconductive Glasses of La2S3, Ga2O3**
G. I. Abutalybov, Arzu Mamedov (Azerbaijan)
53. **The Spectral-Luminescent Properties of TlInS2 and TlGaS2 Crystals Activated by Rare-Earth Ions**
Tofig Mammadov, G.I.Abutalybov, A.A. Mamedov (Azerbaijan)
54. **Photovoltaic Spectra of TlMSe2 Single Crystals**
Solmaz Mustafaeva
55. **High Power Fiber Lasers**
Bulend Ortac (Germany)
56. **Near- and Mid-Infrared Optical Parametric Oscillator Pumped by an Yb Fiber Laser - Continuous-Wave, Single-Frequency Optical Parametric Oscillator Pumped by a Frequency-Doubled Fiber Laser**
Majid İbrahim Zadeh (Spain)
57. **TEM_{00}, 30mJ, 2.94-μm Q-switched Er:YAG Laser Working at the Repetition Rate up to 25Hz**
M. Skorczakowski, J. Swiderski, A. Zajac, W. Pichola, S. Gross, A. Heinrich, T. Bragagna (Poland)
58. **Detailed Theoretical Analysis of Thermal Effects in Er-Yb Phosphate Glass Microchip Lasers**
Feng Song, Teng Li ,Fang Wang, Shujing Liu, Hong Cai, and Jianguo Tian (China)
59. **Investigation on Carriers Confinement in Photonic-Corral-Mode Quantum Ring Lasers**
G. A. Stanciu, R. Hristu, S.G. Stanciu, O'Dae Kwon (Romania)
60. **Broad-Area Semiconductor Laser Diode with Sectioned Electric Contact into External Bragg Resonator.**
V.V. Svetikov, V.A. Sychugov (Russia)
61. **The Q-switched Hybrid Er:YAG Laser**
Waldemar Zendzian, . K. Jabczynski, L. Gorajek, J. Kwiatkowski, K. Kopczyński, H. Jelinkova, M. Němec, J Šulc (Poland)
62. **Tunable YAG:Cr^{4+} Bidirectional Ring Laser**
Yu.Yu. Broslavets, M.A. Georgieva, A.A. Fomitchev (Russia)
63. **High Voltage Solid-State Pumping Source for Excimer Laser**
M. V. Malashin, S. I. Moshkhunov, E. A. Shershunova, V. U. Khomich (Russia)
64. **The Project of High Power Cryogenic Laser Based on Yb:YAG Disks**
E. A. Perevezentsev, I. B. Mukhin, O. V. Palashov, E. A. Khazanov (Russia)

LIGHT-MATTER INTERACTION **September 30**

65. **Optimization of Ultrashort Pulsed Laser Radiation for Precise and Productive Micromashining.**
P. Pivovarov, S. Klimentov, V. Konov, D. Walter, M. Kraus, F. Dausinger (Russia)

P.K. Kashkarov, D.A. Mamichev, S.V. Zabotnov, A.V. Zoteyev, L.A. Golovan, V.Yu. Timoshenko (Russia)

67. **Photovoltaics in X-irradiated InSe–GaSe–InSe Heterojunctions**
MirSalim Asadov (Rusya)
68. **Selective Laser Sintering, Magnesium, Microstructural Features, Porous Structure**
Chi Chung Ng (China)
69. **Roughness Measurement with Laser Speckle Pattern of Milled Metals Using Speckle Statistics Analysis**
Kayahan Ersin (Turkey)
70. **Creation of Ohmic Contacts on n - and p - Type ZnO Films by PLD Method.**
Ye.A. Cherebilo, L.S. Parshina, O.A. Novodvorsky, V.Ya. Panchenko, E.V.Khaydukov, O.D. Khramova, C. Wenzel, N. Trumpaicka, J.W. Bartha (Russia)
71. **Selective Laser Sintering of Magnetium Powder for Fabrication of Porous Structures**
Chi Chung Ng (China)
72. **Silicon Nanoparticles with Previously Defined Parameters Creation from Silicon Tetra Fluoride by CO_2-Laser Permanent Irradiation for Biology and Medicine**
Ershov I.A., Orlov A.N., Pustovoy V.I., Surkov A.A. (Russia)
73. **The Erosive Laser Plume Researches at the Silicon Ablation in Vacuum**
Khaydukov E.V., Rocheva V.V., Lotin A.A. Novodvorsky O.A., Parshina L.S. (Russia)
74. **The Influence of Annealing on Characteristics ZnO:N Films.**
O.D. Khramova, O.A. Novodvorsky, V.Ya. Panchenko, V.I. Sokolov, L.S. Parshina, Ye.A. Cherebilo, A.A. Lotin, E.V. Khaydukov, V,V. Rocheva, C. Wenzel, J.W. Bartha , V. T. Bublik, K. D. Chtcherbatchev (Russia)
75. **Optical and Structural Properties of Quantum Wells $Mg_{0,27}Zn_{0,73}O$/ZnO Produced by Pulsed Laser Deposition**
A.A. Lotin, O.A. Novodvorsky, E.V. Khaydukov, O.D. Khramova (Russia)
76. **Development of Photo-Curable Composition and Technique for Thin-Layer (till 10 μm) Objects Manufacturing.**
Evseev A., Kamayev S., Kotzuba E., Markov M., Michrin V., Novikov M., Surovtsev M. (Russia)
77. **Polymeric Surfaces During MEMS Fabrications**
E. Mocanu , P. Sterian (Romania)
78. **Electric Properties of Heterogeneous Transitions Between n - and p - type ZnO Films and n - and p - Type Silicon Substrates**
L.S. Parshina, O.A. Novodvorsky, V.Ya. Panchenko, O.D. Khramova, Ye.A. Cherebilo, A.A. Lotin, C.Wenzel, N. Trumpaicka, J.W. Bartha (Russia)
79. **Specific Character of the Sn Thin Films Growth on Amorphous Si by CBPLD Method**
Rocheva V.V., Khaydukov E.V., Novodvorsky O.A., Khramova O.D. (Russia)
80. **Manifestation of Electrophysical Phenomena Under Femtosecond Laser Action on Semiconductor**
R.V. Dukin, G.A. Martsinovsky, G.D. Shandybina, E.B. Yakovlev (Russia)
81. **Nanostructured Thin Film Formation in Ultra-Short PLD of Vanadium Oxide**
A. De Bonis, A. Galasso, A. Santagata, P. Villani, R. Teghil (Italy),
82. **Synthesis of Luminescent Si Nanoparicles Using Laser-Induced Pyrolysis**
A. Vladimirov, S. Korovin, A. Surkov, V, Pustovoy (Russia)
83. **Direct Laser Materials Nanostructuring in Absence of Melting**
S.V. Nebogatkin, V.Yu. Khomich, V.A. Shmakov, V.N. Tokarev, V.A. Yamshchikov (Russia)
84. **Investigation of Formation Nanostrucurized Thin Films in Processes of Femtosecond Laser Deposition**
Gerke M.N, Kutrovskay S.V., Kucherik A.O., Prokoshev V.G., Arakelian S.M. (Russia)

V.Yu. Khomich, V.A. Shmakov, V.N. Tokarev, V.A. Yamshchikov (Russia)

86. **Production of THz Radiation by Short Laser Pulses via Tunnel Ionization of a Gas under the Effect of External Magnetic Field**
Anil K. Malik and Hitendra K. Malik (India)

87. **Wakefield Excited by Laser Pulses of Different Field Profiles: Contribution of Electron Thermal Energy**
Hitendra K. Malik (India)

88. **Formation Dynamics of Gold Nanoparticles Detected by Single-Shot Near-Field Heterodyne Transient Grating Method**
K. Katayama, Y. Nakazato, K. Taniguchi, T Eitoku (Japan)

89. **Lifetime and Diffusion Coefficient of Active Oxygen Species Generated in TiO2 sol Solutions**
K. Katayama, M. Okuda, and T. Tsuruta (Japan)

90. **Pulsed Nd:YAG Laser Drilling Process of Alumina Ceramic for Printed Circuit Board**
P. Demir, E. Akman, M. Mutlu, S. Babur, E. Suvaci, E. Kacar, A. Demir (Turkey)

91. **Laser Pulse Shape Effects on the Hardness of Steel**
E. Akman, L.Candan, M. Zeren, E. Kacar, A. Demir (Turkey)

92. **Spectroscopic Measurements and Modelling of the Spectrum Emitted from Laser-Induced Argon Plasma**
B. Genc, S. Sipahioglu, E. Akman, P. Demir, E. Kacar, A. Demir (Turkey)

93. **Laser Surface Treatment of Ceramic Material**
M. Mutlu, E. Kacar, E. Suvaci, A. Demir, E. Akman (Turkey)

94. **Size-Dependent Features of Diamond Bulk Microstructuring with Ultrashort Laser Pulses**
T.V. Kononenko, S.M. Pimenov, V.I. Konov, M. Neff, V. Romano (Russia)

95. **Thermally Induced Light Scattering in Laser Ceramics with Arbitrary Grain Size**
Anton Vyatkin, Efim Khazanov (Russia)

96. **KDP Crystal Coped by Anatase Nanoparticles in Terahertz Applications**
V.A.Enikeeva, I.A.Ozheredov, A.P.Shkurinov, V.Ya.Gayvoronsky, I.M.Prytula (Russia)

97. **Light Emission from Silicon Nanoclusters in Silicon Suboxide Matrix**
V. Yu. Timoshenko, D. M. Zhigunov, N. E. Maslova, S. A. D'yakov, P. K. Kashkarov, V. N. Seminogov, V. I. Sokolov, V. N. Glebov, and V. Ya. Panchenko (Russia)

DIAGNOSTICS **September 30**

98. **Laser-Stimulated Luminescence of Ag Nanoparticles in Glass**
I.V. Andreeva, S.B. Korovin (Russia)

99. **Filamentation of Femtosecond Laser Pulses: First Experimental Observation and Real-Time Measurement of Flying Filament Front**
V.V. Bukin, S.V. Garnov, T.V. Shirokih, , V.A. Tserevitinov (Russia)

100. **Application of Digital In-Line Holographic Microscopy (DIHM) for 4D Tracking of the Colloid Particles**
Dmitry Ekimov (Russia)

101. **Improving Spatial Resolution of Infrared Image Converter Based on the Semiconductor-Liquid Crystal Structure for Real Time Optical Application**
Namig Ismailov, T. Ibraimov (Azerbaijan)

102. **Determining Resolution of a Digital In-Line Holography Microscope**
Ville Kaikkonen, Anssi J. Mäkynen (Finland)

103. **Straightforward Measurement of the Doppler Shift of Light Scattered by Moving Particles in Colloids**
A. Karpo, S. Korovin, V. Pustovoy (Russia)

104. **Infrared Spectroscopy to Characterize Shock Interaction**

Korovin S., Pustovoy V., Beklemishev V., Makhonin I. (Russia)

105. **Accurate Spectral Measurement of Absorption and Scattering Coefficients with Double Integrating Spheres**
Markku A. Lehto, Ville T.J. Keränen, and Anssi J. Mäkynen (Finland)
106. **Fiber-Optic Sensing System for Nanometer Displacement Measurements**
I. Likhachev, V. Pustovoy (Russian)
107. **Experimental Investigation of Optical Time-of-Flight and Amplitude on Pulp at Different Refining Stages**
Jan Niemi (Sweden)
108. **Tree Mapping Using a Time-of-Flight 3D Camera**
Arttu Ollikkala, Anssi J. Mäkynen (Finland)
109. **Spectroscopy of Multisites Chromium in Garnet Crystals**
H. Örucu, J. Collins, B. DI Bartolo (Turkey)
110. **Place of Laser Induced Dielectric Breakdown and Speed Sound in Milky Water Measured with a Laser Doppler Vibrometer**
Juha Saarela, Torbjörn Löfqvist, Kerstin Ramser, Per Gren, Erik Olson, Jan Niemi, and Mikael Sjödahl (Finland)
111. **Diffraction of Plasmon-Polariton Beams on Metal/Metamaterial-Dielectric Interfaces**
Daria O. Saparina and Anatoly P. Sukhorukov (Russia)
112. **Compact Raman Spectrometer for Active Test of Liquid and Solid Samples**
Kerim Allakhverdiev, Tarik Baykara, Alper Secgin, Sunullah Ozbek, Aydin Ulubey, Zehra Salaeva, Fatih Huseyinoglu, S. L. Druzhinin, K. A. Konovalov, O. N. Smirnov, V. Y. Shchagin, S. Yu. Strakhov (Turkey)
113. **Lasers in Confocal Raman Research of Prehistoric Stones and Painted Hellenistic Potteries in Anatolian Archaeology**
Aydın Ulubey, B. Erdogu, A.Seçgin, S.Özbek (Turkey)
114. **High Temperature Effects at Laser Heating of Ceramics in Different Ambient Atmospheres.**
Olga G. Tsarkova, Sergey V. Garnov (Russia)
115. **Measurement of Refractive Index Variation of Water as Function of Temperature and Wavelength with a Fiber Optic Sensor**
Serafettin Yaltkaya, E. Kendir and S. Bayır (Turkey)
116. **Optical Methods and Systems for Distance and Contact Dangerous Matters Detection**
S.Yu.Strakhov (Russia)
117. **Elliptically Polarized Laser Light For Characterization of Micro-Size Object(s) from Angular Scattering Profiles**
Mustafa M. Aslan and Kerim Allakhverdiev (Turkey)
118. **Gas Pumping Through Membranes by Resonance Radiation**
V.V. Levdansky, J. Smolik, P. Moravec (Russia)

ABSTRACTS

Optical and structural properties of quantum wells $Mg_{0,27}Zn_{0,73}O/ZnO$ produced by pulsed laser deposition

□.□. Lotin, □.□. Novodvorsky, □.V. Khaydukov, O.D. Khramova
RAS, Institute on Laser and Information Technologies, Shatura, Russia

The series of multiple quantum wells (MQW) $Mg_{0,27}Zn_{0,73}O/ZnO$ with various well width (L_w=1,8-15 nm) have been grown on the single crystal sapphire substrates (0001) by pulsed laser deposition method. The studies by a x-ray spectroscopy method of quantum wells indicated the high quality of interfaces between layers (fig.1). It was research low temperature photoluminescence (PL) spectra of MQW $Mg_{0,27}Zn_{0,73}O/ZnO$. The blue shift of exciton peak in PL spectra of the quantum wells due to quantum confinement effect observed even at room temperature (fig.2). It was established that the exciton energy decreased smaller and it binding energy greater on comparison with thin films ZnO.

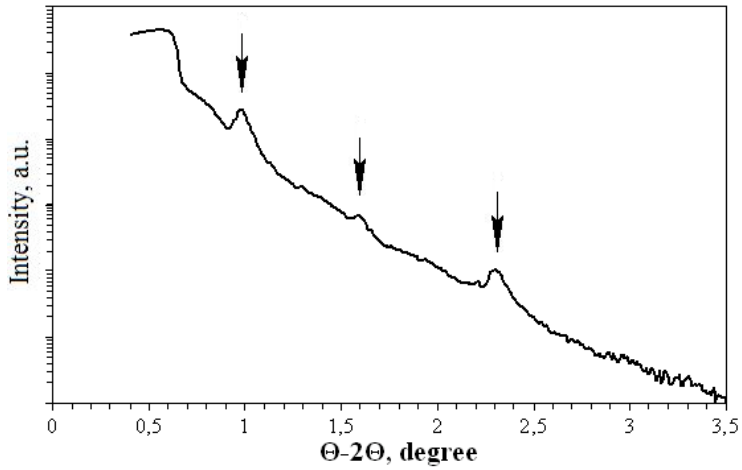

Fig.1. Specular reflection curve of 15 periods quantum well $Mg_{0,27}Zn_{0,73}O/ZnO$ with L_w=5,9 nm.

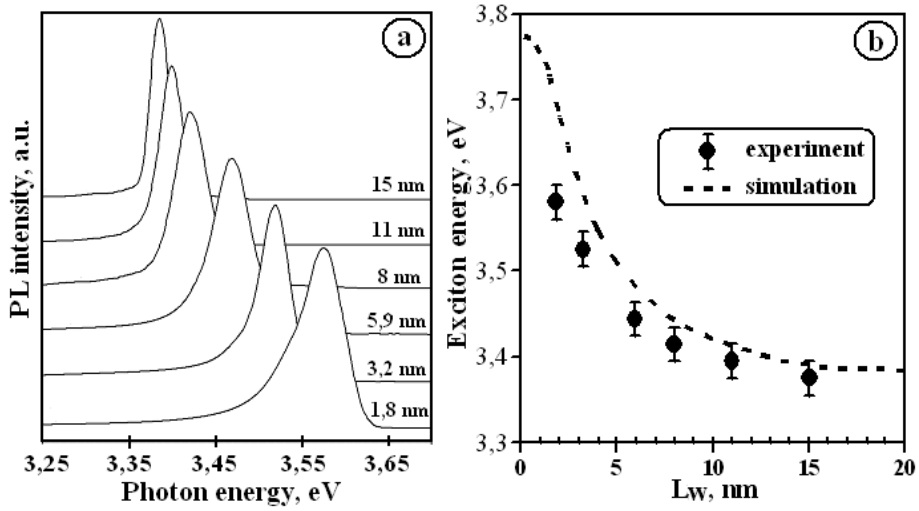

Fig.2. The low temperature normalized PL spectra (a) and exciton energy dependence of MQW $Mg_{0,27}Zn_{0,73}O/ZnO$.

Lased Induced Photoacoustic and Vaporization Pressure Signals in Water: New Experimental Results

A.A.Samokhin, V.I.Vovchenko, and N.N.Il'ichev
A.M.Prokhorov General Physics Institute of RAS
Vavilov St. 38, Moscow, 119991, Russia
asam40@mail.ru

Pressure pulses generated during laser action in absorbing condensed matter due to photoacoustic, surface and bulk vaporization effects are discussed. New experimental results for water exposed to erbium laser pulses with 150-200 ns duration and wavelength 2.94 μm are presented.

At low laser intensity the well established pressure behavior is observed when bipolar form of the pressure pulse transforms to monopolar form as laser intensity increases. This transformation is due to increasing value of surface vaporization pressure as compared with photoacoustic pressure signal determined by heat expansion of condensed matter without phase transition.

At higher laser fluence E>0.6 J/cm^2 short (subnanosecond) pressure peaks above smooth pressure signal are observed which can be interpreted as a manifestation of bulk vaporization (explosive boiling) process which develops in the thin submicron layer of superheated metastable liquid when the superheating limit (or spinodal line) is attained.

At lower fluence photoacoustic and surface evaporation pressure signals are investigated in the case when laser intensity was modulated with period 5 ns. It was found that amplitude of high frequency part of the pressure signals shows one or two minima during laser pulse. Such behavior is possibly due to destructive interference (mutual compensation) of photoacoustic and surface evaporation pressure signals.

Thermally induced depolarization ratio in 23 and m3 symmetry classes of cubic crystals

A. G. Vyatkin, E. A. Khazanov
Institute of Applied Physics of the Russian Academy of Sciences, Nizhniy Novgorod, Russia
vyatkin@appl.sci-nnov.ru

Nowadays several *m3* symmetry group oxides (Y_2O_3, Sc_2O_3, Lu_2O_3) are becoming available for optical applications. The photoelastic tensor of these crystals as well as of *23* symmetry group crystals has a different structure than most known cubic crystals including garnets have: $\pi_{12} \neq \pi_{21}$ [1]. We investigated thermally induced depolarization ratio in a *m3* crystal.

We assumed long rod geometry and top-hat heating and scanning beam profiles. Strain field in an isotropic approximation is available in [2]. The local depolarization rate in both cases of small and strong birefringence has been derived. The global depolarization rate, the optimal and the worst crystal orientations have been calculated numerically.

The local depolarization rate depends on two parameters: $\xi = 2\pi_{xyxy}/(\pi_{xxxx} - \frac{1}{2}(\pi_{xxyy}+\pi_{yyxx}))$ is the common photoelastic anisotropy parameter [3], $\xi_d = (\pi_{xxyy} - \pi_{yyxx})/(\pi_{xxxx} - \frac{1}{2}(\pi_{xxyy}+\pi_{yyxx}))$ is a novel parameter.

The optimal orientations are mainly determined by the $\xi_d/(\xi - 1)$ ratio and are not the same as found in [3] for a "common" cubic crystal. In case of small birefringence the minimal depolarization rate is always larger for a "novel" crystal than for the "common" one with the same ξ. In case of strong birefringence it can be either smaller or larger depending on both heating and scanning beam diameters.

References

1. J. F. Nye, *Physical properties of crystals*, University Press, London, 1964.
2. A. V. Mezenov, L. N. Soms and A. I. Stepanov: *Thermooptics of solid-state lasers*, Mashinostroenie, Leningrad, 1986.
3. I. B. Mukhin, O. V. Palashov, E. A. Khazanov and A. I. Ivanov, "Influence of the orientation of a crystal on thermal polarization effects in high-power solid-state lasers", *JETP Letters*, **81**, 120-124 (2005).

Thermally induced light scattering in laser ceramics with arbitrary grain size

A. G. Vyatkin, E. A. Khazanov
Institute of Applied Physics of the Russian Academy of Sciences, Nizhniy Novgorod, Russia
vyatkin@appl.sci-nnov.ru

Laser ceramics combines large aperture like glasses and high thermal conductivity like crystals but is affected by thermally induced light scattering. The special case of the grain size d to wavelength λ ratio $R >> 1$ was studied in [1] in geometrical optics approximation. We considered a medium with an arbitrary R value and isotropic variations of dielectric permeability ε in case of small fluctuations magnitude and small mean scattered power to incident power ratio K.

The scattered electric field was calculated by small perturbations method [2]. Only once scattered light term was considered. We figured out that mean scattered light intensity depends on ε fluctuations intensity spatial spectrum (correlation function (CF) Fourier-transform).

The magnitude of ε CF can be estimated as $<\varepsilon_{xx}^2>$. The CF shape was evaluated in spherical grain shape approximation in both cases of single scale grains and grain size varying in the range of ($d-\Delta$, $d+\Delta$). The actual difference between these cases is sufficient for $\Delta/d > 0.33$.

The K ratio obtained was compared with mean fundamental mode power loss ratio $1-<\chi>$ [1]. The curves fit qualitatively in the range $R > 1$ where $1-<\chi>$ calculation is valid. However the amount of scattered power is overestimated by ~ 8 in the current study.

References

1. I. B. Mukhin, O. V. Palashov, I. L. Snetkov and E. A. Khazanov, "Thermally induced wavefront distortions in laser ceramics", *Proc. SPIE*, **6610**, 66100N-1-66100N-12 (2007).
2. S. M. Rytov, Yu. A. Kravtsov and V. I. Tatarskiy, *Introduction to statistical radiophysics*, Vol. 2, Nauka, Moskva, 1978.

Neutral and charged species produced through lasers in solid and gas phase: spectroscopy and mass spectrometry.

A.Giardini[a], S. Orlando[a], A. Paladini[a], S. Piccirillo[c], F.Rondino[b], A. Santagata[a], P. Villani[a]
[a] *CNR – IMIP, Sede di Potenza, zona industriale, 85050 Tito Scalo (PZ), Italy*
[b] *Dip. di Scienze e Tecnologie Chimiche, Università di Roma 2 "Tor Vergata", Rome, Italy*
[c] *Dip. di Chimica e Tecnologie del Farmaco, Università di Roma "La Sapienza", Rome, Italy*

This paper aims to review the characteristics of the process of laser desorption on non-volatile and thermally labile organic systems. The apparatus consists of a multiport stainless steel vacuum chamber provided with a laser window entrance, a gas inlet system and other windows for diagnostic purposes. In the chamber a rotating target and a substrate holder are positioned at a variable distance. The incidence angle of the laser beam on the target can be varied from 45° up to 90°. In some cases, ablation is performed at atmospheric pressure. A Quanta System frequency doubled Nd: YAG laser (Handy Model, 532 nm emission wavelength, 6 ns pulse duration, 10 Hz repetition rate) and a Light Conversion doubled Nd:glass laser (529 nm emission wavelength, 250 fs pulse duration, 10 Hz repetition rate) are used for the ablation experiments. The highest laser fluences employed are 2.5 and 2.0 Jcm^{-2} in the fs regime and 18 Jcm^{-2} in the ns one.

The composition and temporal evolution of the transient products formed by short and ultrashort laser pulses are characterized to obtain structural and dynamical information. The optical emission spectra are detected by means of a ICCD Princeton device. The width of the entrance spectrograph slit and the grating employed are 80 mm and 2400 grooves/mm, respectively. Thus, the spectral width obtained is of about 7 nm with a resolution of 0.03 nm. The gated system has a time resolution of 10 ns and each acquisition is integrated on 50 laser shots in order to increase the signal to noise ratio. Varying the position of the optical elements by a micrometric translation stage, it is possible to obtain space-resolved emission spectra at different distances from the ablated target surface. Both ICCD fast imaging and time resolved spectra are accomplished by delaying the data acquisition of the plasma emission in the range of 10-1000 ns with respect to the laser pulse. The acquisition is performed both by single shot and by accumulating up to 20 shots. In all cases, every acquisition is carried out on a not previously irradiated surface.

Different organic systems, as neurotransmitters, Schiff bases, and fluorinated drugs have been examined. To shed more light on the structure of these systems, complementary experiments of resonant enhanced multiphoton laser ionisation (REMPI) and mass spectrometric analysis, have been performed using a nanosecond dye laser pumped by a doubled Nd:Yag laser (0.1 Jcm^{-2}). For example, in the REMPI mass spectrum of (1S,2S)-N-methyl pseudoephedrine (MPE) neurotransmitter, a fragmentation is observed, with breaking of the C_a-C_b bond [1]. At large fluences, an almost complete atomisation is observed in both femto and nanosecond regimes [2].

References

[1] A. Giardini Guidoni, A. Paladini, S. Piccirillo, F. Rondino, M. Satta, M. Speranza, Org. Biomol. Chem. **4** (2006) 2012–2018
[2] P. Villani, S. Orlando, A**.** Santagata, A. De Bonis, S. Veronesi, A. Giardini, Applied Surface Science **253**(19) (2007) 7783-7786.

Nonlinear Interaction of Optical Beams in Gradient Waveguides

A.K. Sukhorukova, A.P. Sukhorukov, A.S. Grankin

Lomonosov Moscow State University

We investigate the interplay of two optical beams at different frequencies in an inhomogeneous medium with defocusing nonlinearity. Earlier it has been shown, that dark solitons can be formed with negative nonlinearity [1]. Later the total reflection of optical beams from the induced defocusing inhomogeneity has been predicted [2]. Now we take into account the potential hole in a Bose-Einstein condensate or a fiber with parabolic focusing profile. Total internal reflection of the tilted signal wave from negative channel induced by the basic beam is considered.

The beam propagation is described by the set of NSE for envelopes. The basic beam distortions were insignificant. Using geometrical optics approach we received and analyzed the equation for a trajectory of the signal beam. The simple formula for critical angle was obtained. It is proportional to square root from the refractive index change at the basic beam axes due to both cross modulation and inhomogeneity. The critical angle equals to half of degree when the index change is about equals to ten to minus four.

At small nonlinearity the reflection does not occur, the signal beam passes through basic beam and oscillates in the potential hole. With increase in nonlinearity the signal reaches the basic beam and is reflected from it. In this case the signal beam oscillates between external border of potential and the basic beam which plays a role of a wall of a wave guide.

Diffraction is considered also at collinear propagation of beams. In induced defocusing channel the signal beam can split into two parts which then get together in one beam owing to action of parabolic potential.

The results of the analytical theory are in good agreement with numerical simulation.

References

1. KIVSHAR, Y. S., LUTHER-DAVIES, B. // Physics Reports, 1998. V. 298. P. 81-197.
2. Lobanov, V.E., Sukhorukov, A.P. // Bull. RAS. Physics, 2005. V. 69. P. 1986.

Straightforward measurement of the Doppler shift of light scattered by moving particles in colloids

A. Karpo, S. Korovin, V. Pustovoy
General Physics Institute RAS, Moscow, Russia

In this work is presented the investigation of instantaneous velocities of silicon nanoparticles in colloid. The investigation was made by measuring the Doppler shift of the optical signal. We used the heterodyne detection scheme in which the scattered light was mixed with the reference signal (in our case laser). The phase difference of these two signals, which is caused by motion of particles, is usually small. Therefore, to accumulate this difference we used a long optic fiber to enlarge the optical path length. We developed the theoretical model which considers instantaneous velocities of the particles utilizing the approximation of Rayleigh particle. It allows to evaluate the value of the particle radius. Experiments were made in water and acetone and, also, in water with added silver nitrate.

Selective Laser Sintering of Magnesium Powder for Fabrication of Compact Structures

Ng Chi Chung[1]

[1] *The Advanced Manufacturing Technology Research Centre, Department of Industrial and Systems Engineering, The Hong Kong Polytechnic University, Hung Hom, Hong Kong, China*

Main author email address: eddyncc1@yahoo.com.hk

In past decades, considerable research effort has been reported in the area of selective laser sintering (SLS). However, rarely work has previously been found on the laser sintering of magnesium and its alloy powder. Magnesium possesses of low density, high specific strength and good mechanical properties, making it become a potential candidate for the fabrication of compact structures in automotive and aerospace industries. The novelty of the present research lies in the fabrication of compact structures by laser sintering of magnesium powder using a Nd:YAG laser. The laser sintering of single tracks and single layers of magnesium powder were carried out for demonstrating the process feasibility and for examining the influences of several processing parameters (laser power, pulse duration and scan speed) on microstructural characteristics and mechanical properties of the final compact structures. The experimental results demonstrated that compact structures of magnesium have been successfully fabricated by selective laser sintering technique. The results also give valuable information about geometrical features and microstructural evolution of magnesium powder under a Nd:YAG laser irradiation, which would facilitate the fabrication and controllability of compact structures by deliberating the associated effect of different processing parameters, whilst achieving superior quality for the laser sintered parts using this rapid one step laser sintering technique.

Acousto-optic Methods of Image Processing

OlegMakaromtberlinao@aol.com

The detection and recognition of objects is one of the mostly discussed problems in the modern applied optics. Spectral imaging systems allow to get images of objects at the different wavelengths. The spectral content can be effectively used for identification because objects and backgrounds besides their different shapes have different spectral brightness, varying over the spectral range. The principles of spectral image processing by acousto-optical methods are discussed in the present work. Specific requirements imposed on the filters intended for the spectral analysis of images are studied. The factors influencing on image quality are discussed also. The laboratory tests of imaging spectrometer, as well as outdoor experiments are presented.

Manifestation of Electrophysical Phenomena Under Femtosecond Laser Action on Semiconductor

R.V. Dukin, G.A. Martsinovsky, G.D. Shandybina, E.B. Yakovlev

St.Petersburg State University of Information Technologies, Mechanics and Optics
49 Kronverksky pr., 197101, St.Petersburg, Russia

Main author email address: shandyb@lastech.ifmo.ru

The technology of excitation of plasmon-polaritons on nanoscopic structures paves the way for creation of superfast computers and supersensitive molecular sensors. It also serves as a fine tool for diagnostics of change of surface state under ultra-short laser action.

In this paper we would like to discuss the role of electrophysical phenomena under femtosecond laser action. We deliver the results of numerical modeling of space–time distribution of nonequilibrium carriers concentration under ultra-short laser pulses action on semiconductor with provision for electron photoemission. Analytical calculation of stationary distribution of concentration of nonequilibrium electrons at the same physical system parameters agreed with the results of the numerical count. The calculation demonstrated that stationary state of substance in the electron system is achieved in the first part of the impulse and confirmed the relevance of a stationary case analysis. Numerical modelling allowed detecting complicated dynamics in distribution of concentration of nonequilibrium carriers in depth of the material during pulse action, and determining the effect of photoemission current on space–time distribution of nonequilibrium electrons. Obtained results are compared with experimental conditions of excitation and propagation of surface plasmon-polaritons in silicon under femtosecond pulse action.

The work was supported by RFBR Grant 09-02-00932.

Atmospheric Environment: Impacts of the Transport of Aerosols from Saharan Dust and Lidar Techniques

N. Yücekutlu[1], Y. Yücekutlu[2]
[1] *Faculty of Science, Department of Chemistry, Hacettepe University, Beytepe, Ankara/Turkey*
[2] *The Ministry of Environment and Forestry, Air Management Department, Beştepe, Ankara/Turkey*

In recent years, Saharan dust storms were investigated for atmospheric transport and deposition processes and for their strong impact on the concentration levels and composition of atmospheric aerosol. Researches have been performed integrating tropospheric aerosol optical properties measured by an Elastic/Raman Lidar system and daily concentrations of particulate matter (PM_{10}) measured at ground level by means of a low-volume gravimetric sampler. Lidar vertical resolved measurements allowed characterizing the dust cloud. Moreover, measurements performed during complete diurnal cycles, allowed to follow the temporal evolution of the aerosol vertical distribution. The observations point out the influence of vertical exchanges from higher to lower atmospheric levels on daily PM_{10} concentrations. This complete set of measurements must include basic number densities, size distributions, mass distributions, chemical composition, optical properties, and basic microphysical properties. Our measurement strategy is aimed at obtaining a significant amount of information on the nature of the Saharan dust aerosols during extreme events in which the dust is transported and deposited in the plot region of Lidar data. European Union integration process and the reduction of air quality limit values for dust which comes from the atmosphere is important to know the amount of contributions.

Lidar Observations of Impact of Emissions from Atmospheric Deposition on Cultural Heritage

N. Yücekutlu[1], Y. Yücekutlu[2]
[1] *Faculty of Science, Department of Chemistry, Hacettepe University, Beytepe, Ankara/Turkey*
[2] *The Ministry of Environment and Forestry, Air Management Department, Beştepe, Ankara/Turkey*

Cultural heritage is very important for our world and even for history. The modern approach to the study of cultural heritage is strongly interdisciplinary. Protecting of monuments is very big duty for conveying of them for next generation. Today, written sources, photographs, maps, archives, plans are some documentation methods. Laser scanners are used more and more as instruments for various tasks in cultural heritage conservation.

We know that West Africa is a major source region for natural and anthropogenic aerosols. Depending on the season aerosols particles are a mixing, in variable proportion, of soil dust coming from the Saharan source. Indoor and outdoor air pollution can cause chemical damage onto surfaces of paintings, frescoes, sculptures etc., by deposition of particulate material or absorption of present gases. The conservation of our cultural heritage and its protection against possible damage due to indoor air pollution has only recently received growing scientific interest. The clearly demonstrated damaging nature of many aerosol components (acidic species, elemental carbon and of specific carboxylic acids (including oxalate), PaH, POPs, PCBs, VOCs, metals, among others), led many countries to impose limit values enforced by legislation. In any given country, such standards tend to become stricter as awareness of the problem increases. Emphasis is placed on identifying biologically-relevant, temporal and spatial scales of atmospheric motion and other atmospheric variables which help control the abundance and dispersal of airborne biota, specifically insects, spores, pollen, fungi, and plant pathogens. Recent advances in meteorological technologies and techniques are providing new insight into microscale, mesoscale, and macroscale aerobiological processes. For example, Lidar systems have identified microscale characteristics of atmospheric turbulence over cultural heritage fields. In this context, lidar observations combined with punctual measurements have been used to evaluate the impact of long range transport phenomena related to Saharan dust outbreaks on the particulate matter (PM_{10}) measured at ground level.

Fluorescent Detection and Photodynamic Inactivation of Pathogenic Microorganisms

E. Borisova[1], V. Mantareva[2], I. Angelov[2], V. Kussovski[3], D. Woehrle[4], and L. Avramov[1]

1) Institute of Electronics, Bulgarian Academy of Sciences, 72, Tsarigradsko chaussee Blvd., 1784 Sofia, Bulgaria
2) Institute of Organic Chemistry, Bulgarian Academy of Sciences, Acad. G. Bonchev str., Bl. 9, 1113 Sofia, Bulgaria
3) The Stefan Angeloff Institute of Microbiology, Bulgarian Academy of Sciences, Acad. G. Bonchev str., Bl. 26, 1113 Sofia, Bulgaria
4) Institute of Organic and Macromolecular Chemistry, University of Bremen, 330 440, 28334 Bremen, Germany

Photodiagnosis (PD) and photodynamic therapy (PDT) are innovative light-drug initiated treatment, based on the photoactive compound irradiated with proper light – in the first case to fluoresce and be detected, and in second case - to produce oxygen spices that are toxic to the biological objects – bacteria, viruses, tumor cells. Photodynamic treatment that appears as an alternative modality for therapy of infections and especially for caused from antibiotic resistant microorganisms is developed in the last several years, and it is known as a process of photodynamic inactivation (PDI).

We will present some of our recent results, received with application of phthalocyanine derivatives as photosensitizing compounds, for treatment of aerobic and anaerobic, Gram-positive and Gram-negative bacterial strains and fungi, using variety of treatment conditions – drug concentration, cell density, irradiation regimes and light doses, needed for optimization of the process of PDI for different microbial species.
Diode lasers in the red spectral region (635 nm and/or 665 nm) are applied for fluorescence excitation and for photodynamic irradiation of the bacterial strains investigated. Process of bacterial samples' inactivation is monitored by the fluorescence at the region of 670-800 nm of the phthalocyanines compounds applied using microspectrometer and the signal detected is used for evaluation of PDI effect, observation of dynamics and drug uptake in the bacterial cells treated. Based on the fluorescence data analysis, we could compare relative effectiveness of different phthalocyanine compounds synthesized and optimize irradiation regime of PDI treatment for different pathogenic microorganisms, which could be used for in vivo applications.
The challenge in local antimicrobial PDI is to find an optimal therapeutic regime – drug concentration, light density and irradiation time conditions, where bacteria are killed without harming the surrounding human tissue. Initial experimental results are very promising about a development of a PDI treatment protocol, but only a controlled, randomized clinical trial can demonstrate the efficacy of PDT for the inactivation of bacteria in vivo. Therefore, further experiments are in progress to demonstrate the efficacy of the new phthalocyanine complexes to be use as an antimicrobial treatment modality for antibiotic resistant microorganisms causing infections in humans.

Synthesis by pulsed laser ablation in Ar and SERS activity of silver thin films with controlled nanostructure

C. D'Andrea[1], F. Neri[1], P.M. Ossi[2], N. Santo[3], S. Trusso[4]

[1] *Dipartimento di Fisica della Materia e Tecnologie Fisiche Avanzate, Università di Messina, Salita Sperone 31, 98166 Messina, Italy*

[2] *Dipartimento di Energia & Centre for NanoEngineered MAterials and Surfaces - NEMAS Politecnico di Milano, Via Ponzio, 34-3, 20133 Milano, Italy*

[3] *Centro Interdipartimentale di Microscopia Avanzata, Università degli Studi di Milano,Via Celoria 26, 20133 Milano Italy.*

[4] *Istituto per i Processi Chimico-Fisici del CNR, S.ta Sperone, C.da Papardo, Faro Superiore, 98158 , Messina, Italy.*

Thin silver films were deposited by pulsed laser ablation in a controlled Ar atmosphere and their SERS activity was investigated. The samples were grown at Ar pressures between 10 and 70 Pa and at different laser pulse number. Other deposition parameters such as laser fluence, target to substrate distance and substrate temperature were kept fixed at 2.0 J/cm2, 35 mm and 297 K. Film morphologies were investigated by scanning and transmission electron microscopies (SEM, TEM). Surface features range from isolated nearly spherical nanoparticles to larger islands with smoothed edges. The predictions of a phenomenological model for the size of nanoparticles grown in the propagating plasma plume are tested against experimental results. Cluster growth is favoured by plume confinement induced by background gas. After landing on the substrate clusters start to coalesce giving rise to larger structures as long as the deposition goes on. Such a path of film growth allows controlling the surface morphology as a function of laser pulse number and Ar pressure. These two easy-to-manage process parameters control the number density and the average size of the as-deposited nanoparticles. Surface enhanced Raman scattering measurements were performed by soaking the samples in rhodamine 6G aqueous solutions over the concentration range between 1.0×10^{-4} M and 5.0×10^{-8} M. The dependence of the film SERS activity on their surface morphology is discussed.

Ultrafast light blade: Anisotropic sensitivity of isotropic medium to femtosecond laser radiation

Peter G. Kazansky[1], Yasuhiko Shimotsuma[2], Jiarong Qiu[3], Weijia Yang[1], Masaaki Sakakura[2], Martynas Beresna[1], Yuri Svirko[4], Selcuk Akturk[5]and Kazuyuoki Hirao[2]

[1]*Optoelectronics Research Centre, University of Southampton, SO17 1BJ, U.K.*
pgk@orc.soton.ac.uk
[2]*Department of Material Chemistry, Graduate School of Engineering, Kyoto University, Kyoto, Japan 615-8510*
[3]*Department of Materials Science, Zhejiang University, Hangzhou 310027, China, and State Key Laboratory of High Field Laser Physics, Shanghai Institute of Optics and Fine Mechanics, Chinese Academy of Sciences, Shanghai 201800, China*
[4]*Department of Physics and Mathematics, University of Joensuu, FI-80101, Finland*
[5]*Department of Physics, Istanbul Technical University, Maslak 34469 Istanbul, Turkey*

Material processing with ultrafast lasers has recently attracted considerable interest mainly due to a wide range of applications including laser surgery and 3D micro- and nano-structuring. However, we have recently demonstrated that in-depth investigation of the processes occurring in condensed medium in presence of intense ultrashort laser pulses opens new insight on the light-matter interaction at high intensities. In particular, we discovered that photosensitivity of non-centrosymmetric crystal is not necessary reciprocal [1], i.e. the light-induced modification depends on light propagation direction. We observed also strong dependence of the isotropic glass modification on the orientation of writing direction relative to the direction of pulse front tilt (quill writing effect) [2]. These effects indicate that at high intensities, a homogeneous illumination can produce essentially inhomogeneous modification in the medium, i.e. the presence of the hidden anisotropy in the light-matter interaction at high intensity. However until now this anisotropy manifested itself only when laser beam moves with respect to the sample. The question of fundamental importance is can this anisotropy manifest itself in the conventional material processing, i.e. when femtosecond light beam interacts with non-moving sample. One may recall that until now only two types of optical anisotropy have been identified. The first one is attributed to anisotropy of material structure being inherent, e. g. in crystals or externally produced e. g. by stress. Another type assigned to anisotropy of geometric structure, e. g. anisotropy of Fresnel reflections or form birefringence, is produced by macro or sub-wavelength scale interfaces and gradients of material. Here we demonstrate experimentally that uniform illumination an isotropic homogeneous medium can give rise to its inhomogeneous modification, i.e. the new mechanism of the optical anisotropy that manifests itself at ultrahigh intensities. Specifically, we observe dependence of the refractive index and absorption coefficient induced by intense ultrashort light pulse in an isotropic glass on the orientation of the polarization plane azimuth. This new phenomenon originates from the absorption anisotropy of electron plasma produced by the femtosecond light pulse with tilted intensity front [3]. Our results present the evidence of new type of collisionless heating mechanism [4] arising at the oblique interface produced by the pulse front tilt. We would like to point out that the observed anisotropic photosensitivity is intrinsic property of the light-matter interaction at high intensities. We anticipate that the observed phenomenon, which offers the orientation of a light polarization plane relative to the direction of pulse front tilt as a new tool to control interaction of matter with ultrashort light pulses, will open new opportunities in laser material processing, optical manipulation and data storage. We refer the observed phenomenon as ultrafast light blade, drawing an analogy between material modification produced by ulrashort light pulse with tilted front and cutting with a blade.

References

[1] W. Yang, P. G. Kazansky and Yu. P. Svirko, "Non-reciprocal ultrafast laser writing," Nature Photonics, **2**, 99-105 (2008).
[2] P. G. Kazansky, W. Yang, E. Bricchi, J. Bovatsek, A. Arai, Y. Shimotsuma, K. Miura and K. Hirao,"Quill" writing with ultrashort light pulses in transparent materials," Appl. Phys. Lett. **90**, 151120 (2007).
[3] S. Akturk, M. Kimmel, P. O'Shea, and R. Trebino, "Measuring pulse front tilt in ultrashort pulse using GRENOILLE," Opt. Express **11**, 491-501 (2003).
[4] U. Teubner, J. Bergmann, B. Wonterghem, F.P. Schafer and R. Sauebrey, "Angle-dependent x-ray emission and resonance absorption in laser-produced plasma generated by high intensity ultrashort pulse," Phys. Rev. Lett.**70**, 795-797 (1993).

Place of laser induced dielectric breakdown and speed sound in milky water measured with a laser doppler vibrometer

Juha Saarela[1], Torbjörn Löfqvist[2], Kerstin Ramser[2], Per Gren[3], Erik Olson[3], Jan Niemi[2], and Mikael Sjödahl[3]

[1]*Department of Electrical and Information Engineering and Infotech Oulu, University of Oulu, P.O. Box 4500, 90014 University of Oulu, Finland, fax +358-8-553 2774, juha.saarela@oulu.fi*

[2] *Department of Computer Science and Electrical engineering, Luleå University of Technology, SE-97187 Luleå, Sweden*

[3]*Department of Applied Physics and Mechanical Engineering, Luleå University of Technology, SE-97187 Luleå, Sweden*

The optoacoustic effect is generated when the absorption of a short electromagnetic pulse in matter causes a heat release that is strong enough to create an acoustic wave. Many imaging systems are created based on this effect. In this experiment a laser pulse with λ = 1064 nm and 9 ns pulse length was aimed at a volume of liquid. Liquids were deionized water with 0% to 8,3% milk. Milks had fat 0.1 % or 3.0 %. When a collimated laser beam was focused using a lens of 16 mm focal length a single dielectric breakdown spot occurred. These breakdowns were imaged using a double shutter camera. The acoustic wave generated by the dielectric breakdowns was detected at a free surface using a surface scanning laser doppler vibrometer. The vibrometer is as point-measuring heterodyne interferometer based on the Doppler effect of the light backscattered from a moving object. The laser doppler vibrometer signal was used to calculate speed of sound and the location of the dielectric breakdown. Speed of sound was determined with accuracy of 10 m/s and the location of the breakdown with an accuracy of 1 mm. The location of the breakdown was calculated from vibrometer data and the calculated position matched the breakdown location recorded by the camera. It is found that scattering and absorption caused by milk stop deelectic breakdowns before the amount of milk has a measurable effect on speed of sound.

The Spectral-Luminescent Properties of $TlInS_2$ and $TlGaS_2$ Crystals Activated by Rare-Earth Ions.

G.I.Abutalybov, A.A. Mamedov, T.G.Mammadov

Institute of Physics of the National Academy of Sciences of Azerbaijan
AZ-1143, H. Javid ave., 33, Baku
Fax: (+99412)4470456 e-mail: mamedov_tofik@mail.ru

Last time the interest on semiconductor materials as laser active mediums has quickened. The above mentioned fact is caused by the possibility of recombination of excitation center by the way of zone-zone intensive absorption band. The spectral-luminescent properties of these crystals have been studied for clearing-up of perspective view of triple layered compounds of $TlB^3C_2^6$ (B-Ga, In; C-S, Se) as laser active mediums.

At T=77K the intensive wideband radiation (775÷1060nm) with maximum at λ~960nm caused by structural defects is observed at excitation by argon laser with λ =488,8nm in $TlInS_2$ crystals in the comparison of $TlGaS_2$. These radiation characteristics confirm the perspective view of this material as the active medium of frequency-tuned laser.

Note that the doping of $TlInS_2$ by Yb^{3+} ions leads to disappearance of observable wideband radiation.

$TlInS_2$-Nd^{3+} and $TlGaS_2$-Nd^{3+} crystals have been investigated with the aim of studying of excitation energy transfer from matrix to ion activating agents. It is observed that excitation energy transfer in $TlGaS_2$-Nd^{3+} is more effective one than in $TlInS_2$-Nd^{3+} at light excitation with λ =488,8nm. The luminescent centers of Nd^{3+} ions are identified and stark level design for these centers in $TlGaS_2$ and $TlInS_2$ is constructed by selective laser excitation method.

The lifetimes of metastable level of Nd^{3+} $^4F_{3/2}$ ions in both crystals for all centers are obtained. The carried out complex investigations of Nd^{3+} ion spectral-luminescent properties in these matrices confirm the perspective view of $TlGaS_2$-Nd^{3+} crystals as the active medium of miniature lasers at zone-zone excitation.

Spectral-luminescent properties of $TlInS_2 - Nd^{3+}$ and $TlGaS_2 - Nd^{3+}$

G.I.Abutalybov , A.A. Mamedov, T.G. Mammadov
Institute of Physics of the National Academy of Sciences of Azerbaijan, Baku, Azerbaijan

Recently, new solid-state laser materials applicable for designing of tunable, near-IR lasers became of great interest. We have investigated spectral-luminescent properties of $TlInS_2$, as of possible active element of tunable laser.

When exciting $TlInS_2$ crystal with the use of argon laser line λ =488,8 nm at 77K strong wide-range emission was observed within the region 775 ÷ 1060nm with maximum at λ ~ 960 nm. This emission proved to be highly suppressed as it could not be observed at room temperature. Analysis of this band has shown that it is polarized. At $E_L \perp c$, $E_R \perp c$ (E_L and E_R - direction of electric vector of exciting light and of registration respectively; c - direction of crystalline axis) shape of wide line has changed and its maximum became equal 928 nm. At $E_L \perp c$, $E_R \parallel c$ line maximum became at λ ~963.2 nm. This fact confirms that observed wide line is stipulated by existence of two different sets of centers.

Study of kinetics of luminescence decay has shown that it is non-exponential. At the initial stage lifetime of excitation was found to be equal 4.4 μ ks, at the later stages of decay-12.6 μ ks.

As result of doping of $TlInS_2$ crystal with the use of Yb^{3+} ions wide emission line disappears. Taking into account that TR^{3+} ions add to crystal perfection we might conclude that wide-rage emission is induced by structural defects of the crystal.

Use of intensive absorption lines «zone-zone» at excitation of TR^{3+} ions allows to obtain more efficient semiconductor lasers activated by TR^{3+}. With this point in mind we investigated spectral-luminescent properties of $TlGaS_2$ activated by Nd^{3+}.

Investigations have shown, that when exciting with light falling into its own absorption band(λ =514,5 nm illumination intensity at $^4F_{3/2} \rightarrow {}^4I_J$ transitions, wherein J =9/2, 11/2, 13/2, 15/2 was considerable lower than in case of excitation through zones(λ =488,8 nm). Kinetics of luminescence decay of $^4F_{3/2}$ level of Nd^{3+} in $TlGaS_2$ at room temperature is non-exponential, at the late atages of decay lifetime was found to be equal 45 μ ks and at nitrogen temperature 80 μ ks.

After excitation of Nd^{3+} ions luminescence using tunable rhodamine 6G laser, shape and position of the line changed. This fact shows that Nd^{3+} ions form different types of centers in $TlGaS_2$. Using method of selective laser excitation we investigated radioactive centers of Nd^{3+}.

Laser Modification of 1D Al/Al_2O_3 Nanostructures

C. Aktas, C. Akkan, M. Veith
Leibniz-Institut für Neue Materialien gGmbH
Campus D2 2, D-66123 Saarbrücken

CVD methods have been used successfully in fabrication of fibers, filaments, nanotubes and nanowires of various materials for more than 20 years. CVD has a number of advantages as a method for depositing thin films. One of the primary advantages is that CVD films are generally quite conformal, which is critical for coating the complex-shaped objects. Another advantage of CVD is that the wide variety of materials can be deposited with a precise thickness control. Recently we have presented fabrication of various 1D Al/Al_2O_3 nanostructures using a single source concept. Such combination of metal and metal oxide opens up further possibilities for modification of the material structure. For instance in case of laser assisted heat treatment of Al/Al_2O_3 composite, Al acts as an additive which is oxidized further to Al_2O_3 and this forms a compromise approach to synthesize dense and pure alumina. Different laser power densities can be applied to control the morphology of the alumina layers. Ultra-hard □-Al_2O_3 layers were synthesized successfully by heat treatment of 1D Al/Al_2O_3 nanostructures using a low energy Ar^+ laser. On the other hand, use of a high energy (nano-second pulsed) Nd:YAG laser leads to porous alumina surface which forms a model system to study cell-surface interactions.

Experimental study of the multiple scattering effect on the flow velocity profiles measured in Intralipid phantoms by DOCT

Janne Lauri[1], Alexander V. Bykov[1,2], Alexander V. Priezzhev[2] and Risto Myllylä[1]

[1]*University of Oulu, Optoelectronics and Measurement Techniques Laboratory, P.O. Box 4500, 90014 University of Oulu, Oulu, Finland*
Tel.: +358 8 553 2760; Fax: +358 8 553 2774; E-mail: janne.lauri@ee.oulu.fi
[2]*M.V. Lomonosov Moscow State University, Physics Department, Moscow, Russia*

Doppler optical coherence tomography (DOCT) is a relatively new noninvasive technique based on the low coherence interferometry and allowing for measuring the flow velocities inside highly scattering media, in particular, blood flow velocities in the superficial layers of human skin, retina or other tissues. However, multiply scattered photons that contribute to the DOCT signal acquire random Doppler frequency shifts. This leads to a distortion of the reconstructed velocity profile in comparison with the real one.

In this work, we analyze the distortions of the measured velocity profiles of the flow embedded into the scattering medium at different embedding depths in order to develop the method for the correction of these distortions. For this purpose a tissue phantom consisting of the glass capillary embedded into a slab of Intralipid solution mimicking human skin has been designed. Intralipid is a polydisperse suspension of almost spherical particles of about 0.3 □m mean radius suspended in glycerine and water solution. The particles are soybean oil droplets covered with a 2.5-5.0 nm thick lipid membrane. In the field of biomedical optics, this liquid is frequently used for the fabrication of tissue phantoms.

The designed phantom has the form of parallelepiped containing plain glass capillary (inner diameter 0.3 mm, wall thickness 0.23 mm) located along to the side wall made of glass with the thickness of 200 μm. The distance between this wall and the outer surface of the capillary (embedding depth) varies from 0 up to 3 mm which corresponds to the tilting angle between glass wall and capillary of ~ 4 deg. A certain embedding depth can be chosen by the positioning the probing beam to the corresponding point along the capillary. The phantom was filled with the 1 % Intralipid solution. The Intralipid solution of the same concentration was pumped through the capillary at a constant flow rate of 100 ml/h. The designed phantom was placed into the measurement arm of DOCT setup. Superluminescent diode with a central wavelength of 840 nm and spectrum band of 50 nm is used as a light source. Determined by these parameters, the depth resolution of the system is about 6 μm in air and 4.5 μm in the phantom medium. The angle between the glass wall of the phantom and the probing beam was set to 90 deg.

A series of experiments to study the effect of the multiple scattering both in the static surrounding of the capillary and in the flowing medium on the flow velocity profiles reconstructed from the DOCT signals has been performed for the capillary embedding depth of 100 - 600 μm. It was assumed that the flow velocity profile has a parabolic shape. In this respect, the parabolic approximation of the measured profiles was performed. It is well know that parabola is defined by three parameters such as the position of its center, the value in the central point and the width at a certain level. We have determined the behavior of these parameters of the parabolic approximation of the measured flow velocity profiles with increasing embedding depth. The results show that an increase in the embedding depth of the studied flow shifts the velocity maximum position towards the region of greater depths, the maximal velocity value decreases and the width of the profile increases. This is due to the fact that with an increase of the embedding depth the number of photons caring reliable information about the flow velocity decreases. The photons, which come from greater depths, have more complicated and longer trajectories as well as the random Doppler shifts and thereby exert destructive influence on the reconstructed velocity profile. Additionally, we have also performed the measurements for higher Intralipid concentrations (2% - 4%) of capillary surrounding. The results show that with the increase of Intralipid concentration the similar changes of the approximation parameters occur at lower embedding depths. The experimental results are in good correspondence with the results of Monte Carlo simulations that we performed earlier and published in [A.V. Bykov, et al. *Quantum Electronics,* 35 (11), 2005].

This work was supported by RFBR-Academy of Finland grant □ 08-02-91760.

Fiber-optic sensing system for nanometer displacement measurements

I. Likhachev, V. Pustovoy

Center of Laser Technology and Material Sciences, Moscow, Russia
e-mail: iglikhachev@gmail.com

Interferometric fiber-optic sensing system for mechanical displacement measurement demonstrating subnanometric resolution is proposed. The measuring system includes a set of small size probes connected to the processing unit by the standard fiber optical cable and the computer for data processing. High sensitivity of the system is provided by the Fabry-Perot interferometer used as a probe.

The operation of the system is based on the straightforward detection and processing of the spectrum of the light reflected from sensing element. The spectral distribution unambiguously characterises the value of measurand which is recovered by proper processing technique.

The probe represents the Fabry-Perot interferometer formed by two fiber ends polished at the right angle to the fiber axis and serving as semi-reflective mirrors. If Fabry-Perot interferometer is illuminated by a broadband light source, the output optical spectrum acquires a periodic modulation determined by the interferometer optical path difference (OPD). The key idea of the signal processing technique is in treatment of the spectral distribution as a hole to receive the frequency dependence of the phase difference of the interfering beams. The goal is achieved by the Fourier transformations and an appropriate filtering of signals. Then the absolute value of the sensor OPD can be found as a slope of the phase difference dependence on the frequency. Providing the absolute value measurements the system does not need recalibration after switch on and during the operation. This feature is very important in applications where long term monitoring is required.

The employment of spectral encoding demonstrated high noise resistance of the system and insensitivity to the optical power variations. The system demonstrates 200 micrometer full range and 0.05 nm displacement resolution at 100 ms detection time.

Fluorescent and optical absorption centers in chromium-doped $LiGaSiO_4$ nano-glass-ceramics and vitreous precursors

Kirill A. Subbotin[1], Valery A. Smirnov[1], Evgeny V. Zharikov[2], Ivan A. Shcherbakov[1]
1.- *A.M.Prokhorov General Physics Institute Russian Academy of Sciences, Vavilova str. 38, Moscow, 119991, Russia*
2.- D.I.Mendeleyev University of Chemical Technology of Russia Miusskaya sq. 9, Moscow, 125047, Russia

Chromium doped $LiGaSiO_4$ nano-glass-ceramics was synthesized for the first time by partial controlled crystallization of vitreous precursors of various compositions in Cr-Li-Ga-Si-O system. Obtained samples contained the crystallites of α- and γ-$LiGaSiO_4$:Cr polymorphous modifications, distributed in residual parent glass. The content of each polymorph and sizes of crystallites depend on both precursor composition and ceramming regimes. The spectroscopic studies of the sintered vitreous and cerammed samples (absorption and fluorescence spectra, fluorescence decay kinetics at 300 and 77K) were performed. The strong absorption bands of octahedrally coordinated Cr^{3+} ion (with peak positions $\lambda_1 \sim 450$ nm, transition $^4A_2 \rightarrow {}^4T_1$, and $\lambda_2 \sim 640$ nm, transition $^4A_2 \rightarrow {}^4T_2$), and tetrahedral Cr^{6+} ion ($\lambda = 360$ nm, ligand-to-metal charge transition), as well as weak absorption bands of tetrahedral Cr^{4+} ion ($\lambda_1 \sim 700$ nm, transition $^3A_2 \rightarrow {}^3T_1$, $\lambda_2 \sim 950$-1000 nm, transition $^3A_2 \rightarrow {}^3T_2$) have been observed in vitreous samples. No fluorescence of Cr^{4+} was observed in precursors at 77K or 300K.

After ceramming the intensity of Cr^{4+} absorption bands drastically increased with slight shift of peak positions, while the intensity of Cr^{6+} absorption band drastically decreased. The typical for Cr^{4+} fluorescence appears at λ_{max} ~1280 nm, with FWHM ~ 270 nm. The fluorescence decay of the major part of cerammed samples is non-single exponential. Two components of the fluorescence decay can be easily distinguished: the slower component has the lifetime ~ 65-70 μsec at 77K and ~ 12 μsec at 300K. These values are close to that for earlier investigated α-$LiGaSiO_4$:Cr single crystals. Thus, the structure of the slower Cr^{4+} emitting center is, apparently, similar to that in α-$LiGaSiO_4$:Cr single crystals.

Another, faster Cr^{4+} emitting center observed in nano-glass-ceramics has the lifetime ~ 7-8 μsec at 77K and ~ 1-1.5 μsec at 300K. This center was not observed in Cr:$LiGaSiO_4$ single crystals, and its structure is not completely clear to the moment. Probably, this center is Cr^{4+} ion located in the crystallites of metastable γ-$LiGaSiO_4$. The data about phase compositions of sintered samples, chromium concentrations and fluorescent properties are systematized.

Dynamic light scattering studies of collagen solutions containing metal ions with different ionic radii

I.A. Sergeeva, M.S. Ivanova, K.V. Fedorova, G.P. Petrova, Yu.M. Petrusevich.
Faculty of Physics, M.V. Lomonosov Moscow State Universitry, Leninskie Gory, Moscow

The study of the water solution properties of collagen relating to the type of fibrillar proteins is quite important. Collagen plays a major structural role in an organism. Approximately 40% of an organism's collagen is found in the skin, 10–20% - in the bones and teeth, and 7–8% - in blood vessels. The extraordinary structure of the collagen molecule (a triple helix) causes its peculiar optical properties and molecular mobility.

Proteins in water solutions tend to aggregation depending on their physicochemical condition. This process often happens irreversible and can be a sign of some serious illness in a human body. Aggregation and other processes occurring to protein macromolecules in solutions, depend by the nature of proteins, their concentration, type of solvent, salts, metal ions, acids, the bases, an □□, temperature and other factors.

Thus, studies involving both collagen's structural modifications in water solutions and processes leading to molecule connection into collagen chains (fibrils) determining unique bone, skin and other tissue properties are very important.

Optical methods can be successfully used to investigate intermolecular interactions and molecular dynamics in solutions. In the present study the photon-correlation spectroscopy method of scattered light was used to study the dynamics of collagen molecules.

Dynamic light scattering depends on fluctuations in the concentration of scattering particles. In macromolecule solutions the correlation function of the signal $g(t)$ for scattered light can be found as a function of the translational diffusion coefficient D_t:

$$g^{(1)}(t) = a\left\langle E^{*}(0)E(t)\right\rangle = c_0 \exp(-D_t k^2 t),$$

a and c_0 are constants.

The appropriate method for $g(t)$ definition of correlation functions is the method of photon correlation. The values of the particles translational diffusion coefficients D_t and their hydrodynamic radii can be obtained using this method.

The molecular parameters of collagen in water solutions containing $CaSO_4$, NaCl, KCl, and $Pb(CH_3COO)_2$ salts were studied using the light scattering method. It was observed that the size of the metal's ion radius significantly influences the electrostatic interactions between protein macromolecules. Interactions between K^+ ions, as well as ions of one of the heavy metals, Pb^{2+}, that were characterized by relatively large ionic radii (K^+ = 1.33 Å and Pb^{2+} = 1.2 Å) results in the formation of macromolecule complexes (nanoclusters) in collagen solutions, viz., protein doublet nanostructures. While collagen solutions contain calcium or sodium ions characterized by smaller ionic radii (Ca^{2+} =0.99 Å, Na^+ = 0.8 Å), the formation of nanostructures has not been demonstrated.

We have received angular dependences of intensity of scattered light in collagen water solutions at three angles: 45°, 90° and 135°. Experimental results have been processed by means of two methods: the method of asymmetry and the method of double extrapolation.

It has been received, that in pure water solutions of collagen and in solutions with salt NaCl protein molecules have the form of rods with the sizes ~ 2500 Å. And in solutions with salts KCl and $Pb(CH_3COO)_2$ scattered particles become larger (nanoclusters) and get the form of balls with a size about ~ 4500 Å. As we assume, it is the forms and the sizes of nanoparticles formed in a solution.

Changes of collagen molecules properties can lead to heavy pathologies in living organisms (collagen illnesses). The behaviour of collagen macromolecules in solutions studied in the work and their interaction with ions of various salts, including with ions of heavy metals, allows to establish possible pathological processes in a human body, occurring under the influence of adverse factors of environment.

Plasma-Based Extreme Ultra-Violet Lasers

G J Tallents, I Al'Miev, N Booth, L M R Gartside, H Huang, A K Rossall,
E Wagenaars, D S Whittaker, Z Zhai

Department of Physics, University of York, York YO10 5DD, United Kingdom

Work on the development and understanding of plasma-based extreme ultra-violet (EUV) lasers will be reviewed. The production of short pulse (< 1 ps) EUV lasers by injecting short pulse harmonic radiation into a plasma amplifier is discussed using Maxwell-Bloch modelling. Comparisons are made with the output obtained with amplified spontaneous emission (ASE). The use of the developed EUV lasers in probing the opacity of plasma is discussed. The opacity of iron plasmas found in the outer convection zone of the Sun has been measured using EUV laser probing.

Optoacoustic cancer diagnosis and therapy

M. Jaeger, S. Preisser, L. Siegenthaler, M. Kitz, M. Frenz
Institute of Applied Physics, University of Bern, Sidlerstrasse 5, CH-3012 Bern, Switzerland
Fax: +41 31 6313765
martin.frenz@iap.unibe.ch
D. Schol, M. Fléron, J.F. Greisch, M.C. De Pauw-Gillet, E. De Pauw
University of Liège, Liège, Belgium
J. Niederhauser, D. Schweizer
Fukuda Denshi Switzerland AG, Basel, Switzerland

Optoacoustic imaging is a hybrid technique which combines the advantages of echo-ultrasound and optics. Optoacoustics images absorbed photons by detecting thermoelastically generated ultrasound. It therefore provides high optical contrast without the handicap of poor resolution characterized by optical tomography. The absorption is given either by endogenous chromophores such as oxy- or deoxy-hemoglobin or exogenous chromophores e.g. dyes, nanoparticles or quantum dots. By varying the excitation wavelength different chromophores can be quantitatively identified. The laser-induced ultrasound transients propagate to the tissue surface and are detected by an acoustic transducer. The time delay between laser pulse and detected pressure transient, its amplitude and temporal profile provide information about location, strength and spatial dimension of the acoustic source. Detection of early stage tumors in the millimeter range is shown by labeling the tumor cells with antibody-gold nanoparticle conjugates. The use of gold nanoparticles together with antibodies makes optoacoustic imaging highly sensitive and selective. In addition, the selectively bound particles can be used for thermal therapy of the tumor.

To fully exploit all the advantages of classical echo-ultrasound and optoacoustics, we combined both techniques to simultaneously provide complementary information obtained from both imaging modalities. To fully take advantage of the maximum image depth given by the optical penetration of the exciting laser radiation we developed a novel image reconstruction method based on acquiring in parallel a series of optoacoustic and echo-ultrasound images while the tissue sample is gradually deformed by an externally applied force.

Three-dimensional cell spheroids were used for evaluation of the optoacoustic system Spheroids of 2 mm to 5 mm diameter were grown from LNCaP cells and incubated with PSMA-targeted nanorods, and with unspecifically targeted nanorods for control. Echo images of the spheroids were acquired alternately with OA signals, such that reconstructed OA sources could be localized inside the spheroids. The distribution of the gold nanoparticles inside the spheroid was imaged by two-photon luminecence microscopy. To study the mechanisms underlying cell damage we additionally studies the interaction processes taken place when single nanoparticles are irradiated. Threshold fluences for cavitation bubble formation could be determined.

The results show that functionalized gold particles work as contrast agent in the LNCaP spheroid model, and that our OA imaging system is well suited to detect them with high resolution. The results also demonstrate that the particles are not homogeneously distributed within the spheroids, but are concentrated in small areas. When a spheroid was repeatedly scanned several times, a decrease in the OA signal was observed. This is attributed to deformation or fragmentation of the gold particles upon laser irradiation.

Synthesis of luminescent Si nanopaticles using laser-induced pyrolysis.

A. Vladimirov, S. Korovin, A. Surkov, V, Pustovoy
General Physics Institute, RAS, Moscow, Russia

In this report we present silicon nanoparticles synthesis in the reaction of silane pyrolysis. The reaction of silane decomposition occurred in a flow reactor under the influence of continuous CO_2-laser. As-prepared Si nanoparticles explored by means of transmission electron microscope, fiber spectrometer, FTIR spectrometer and Raman scaterring. Obtained Si nanoparticles have spherical shape and average diameter about 15 nm. From Raman scattering spectrum nanoparticles have crystalline structure.

As-prepared nanoparticles practically have no luminescence, therefore nanoparticles was etched in acid vapor in order to increase luminescence yield. After acid etching average size of nanoparticles decreased to 5 nm and luminescent peak centered at 730 nm appeared on luminescent spectrum.

"Clean" and "cold" laser transfer of biomaterials

T.V. Kononenko[1], I.A. Nagovitsyn[1], G.K. Chudinova[1], V.I.Konov[1],
I.N. Mihailescu[2], P.Alloncle[3], M.Sentis[3]

[1] *Natural Sciences Center, A.M. Prokhorov General Physics Institute, Moscow, Russia*
[2] *National Institute for Lasers, Plasma, and Radiation Physics, Bucharest, Romania*
[3] *LP3 Université Aix-Marseille, Marseille, France*

Fabrication of micro-dimensioned patterns of biomaterials on a solid substrate is one of the cornerstones for the development of next-generation biomedical devices such as microfluidic biosensors and biochips, gene and protein recognition microarrays. The laser induced forward transfer (LIFT) technique is an interesting alternative to pin microspotting, ink-jet printing and photolithography, which are most extended techniques allowing production of high-density surface microarrays for the current moment. The given method consists in the local transfer of material from a thin film covering a special target to a close receiving substrate under the action of a laser pulse. It has been shown for different proteins, DNA, living cells and tissue that the main part of the transferred material retains specific functionality.

Here we present the newest variety of the LIFT techniques demonstrating several important advantages comparing with other known laser-based approaches. The material for the transfer is spread over a thin metal film, which is irradiated from the rear side by single laser pulses through a transparent support. The laser action under optimized conditions causes appearance of a transient blister at the metal-support interface, which provides ejection and transfer of the covering material. First, the blister-based laser induced forward transfer (BB-LIFT) is absolutely clean as the absorbing metal film is not sputtered by the laser radiation. Second, laser-induced heating of the transferred material can be reduced to negligible values due to optimization of the metal thickness and the pulse duration. Third, safe transfer of different organic materials can be performed avoiding usage of an additional liquid matrix or solvent.

Large-scale patterns of mesotetraphenylporphyrin and immunoglobulin consisting of numerous overlapping microspots were produced via BB-LIFT of mono- and multilayered Langmuir films applying nanosecond and subnanosecond IR laser pulses. The patterns were studied with fluorescent microscopy and UV-visible absorption spectroscopy to verify possible changes in chemical composition and specific functions. Clean transfer of the organic materials was found possible within the limited range of experimental conditions including laser fluence and target parameters. The requirement to minimize the heat-induced material degradation applies additional restriction on the processing parameters.

The examined biomaterials show close resemblance with behavior of inorganic nanopowders subjected to the BB-LIFT. It makes possible usage of the experimental data on laser transfer of diamond nanoparticles to consider other important aspects of the process including transverse scattering of the flying particles, effect of the pulse duration on the appropriate fluence range, contribution of different physical mechanisms in the material ejection, etc.

Size-dependent features of diamond bulk microstructuring with ultrashort laser pulses

T.V. Kononenko[1], S.M. Pimenov[1], V.I. Konov[1], M. Neff[2], V. Romano[2]

[1] *Natural Sciences Center, A.M. Prokhorov General Physics Institute, Moscow, Russia*
[2] *Institute of Applied Physics, University of Bern, Bern, Switzerland*

Femtosecond lasers are known to be a highly efficient tool for three-dimensional micro- and nanostructuring of various transparent materials required for applications in photonics, microoptics, microfluidic devices, etc. Recently, formation of local graphitized regions (graphitic "wires") inside the diamond bulk under the action of 100 fs pulses has been demonstrated avoiding visible mechanical damage of the surrounding diamond [1]. Diameter of the wires varies from tens micrometers down to submicrometer values due to control of the beam caustic, energy of the laser pulse and speed of the focal point movement.

Here we consider the effects, which accompany formation of relatively thick (>10 μm) graphitic "wires" and provoke essential reduction of the wire's quality. The first is increasing mechanical stresses resulted from change of the material density under the laser-induced phase transition. Occurrence of the cracks around the graphitic wires is found to depend on both the wire radius (R) and speed (v) of the wire growth. To avoid damage of the diamond matrix, the following phenomenological condition must be fulfilled: $v<V_{max}/(\pi R^2)$, where $V_{max}\approx 20\ \mu m^3$.

Rise of the laser power being necessary to produce thicker wires, results finally in the second unwanted effect, namely, self-focusing of the laser beam inside the diamond sample. The given phenomenon causes small-scale modulation of the laser intensity across the beam, which, in turn, leads to transformation of the thick compact graphitic channel into a bunch of thinner wires. Two possible solutions of the given problem are proposed including increase of the pulse duration and usage of more complicated scanning technique- 3D instead of 1D.

References

1. T.V. Kononenko, M. Meier, M.S. Komlenok, S.M. Pimenov, V. Romano, V.P. Pashinin, V.I. Konov, "Microstructuring of diamond bulk by IR femtosecond laser pulses", Applied Physics A, **90**, 645-651 (2008)

Classification of Main Reliefs in Laser Nanostructuring Technological Materials

VladislavKhomich[a], Vyacheslav Shmakov[b], Vladimir Tokarev[b], Vladimir Yamschikov[a]

a) Institute of Electrophysics and Energetics, Russian Academy of Sciences, 18 Dvortsovaya nab., 191186 Sankt-Peterburg, Russia
b) A.M. Prokhorov General Physics Institute, Russian Academy of Sciences, 38 Vavilov st., 119991 Moscow, Russia

We experimentally demonstrated a possibility of direct laser surface nanostructuring germanium, nickel, platinum silicide, silicon nitride, stainless steel and titanium by nanosecond ArF laser multipulse irradiation with the wavelength 193 nm. Similar results were obtained also for titanium and platinum when using nanosecond KrF laser irradiation with wavelength 248 nm. It was found that 5 main types of laser-induced profiles are possible. They correspond to five zones of laser spot when laser intensity decreases with an increase of the distance from the spot centre, i.e. to zones (1) of intense ablative material removal (in the crater in the central part of the spot irradiated with a high intensity), (2) of "deep" laser melt without significant ablative material removal, when melt layer thickness is of the order of 1 or few hundreds of nanometers, (3) of "shallow" melt, i.e., at laser intensity around or just above the melting threshold, when melt thickness is small compared to the case (2), (4) of spot periphery outside melting zone, and (5) of original non-irradiated surface. Besides of this, mentioned 5 main reliefs can also be exhibited in the form of corresponding superpositions in various transient regions between mentioned zones. It can give rise to a co-existence in some parts of the spot, for example, of micron and submicron reliefs, or of two different submicron reliefs. The proposed classification of reliefs for the first time unites in one scheme the results of previous papers, where many authors have observed the formation of micron structures under nanosecond laser irradiation, with recent results on studies of laser-induced submicron reliefs (or nanostructures). The physical mechanisms for formation of mentioned 5 main reliefs are proposed.

Blue Laser Light Generation by Frequency Doubling of a Cesium Vapor Laser

B. V. Zhdanov, Yalin Lu, M. K. Shaffer, W. Miller, D. Wright, W. Holmes, and R. J. Knize

US Air Force Academy, Department of Physics, Laser and Optics Research Center, 2354 Fairchild Dr., Ste. 2A31,USAF Academy, CO 80840, USA
FAX : +1-719-3337098
Email: boris.zhdanov.ctr@usafa.edu,

High power lasers operating in the blue spectral range are highly desirable for many important applications such as data recording, high definition laser projection, underwater communication, etc. One possible way to generate such blue laser radiation is a frequency doubling of the output of near infrared lasers. Recently developed diode pumped alkali vapor lasers are the perfect candidates for frequency doubling because of their ability to generate high power beams with excellent beam quality and very narrow emission linewidth – all important features that are required to realize an efficient frequency conversion.

In this paper, we report a 447.3 nm blue light generation through direct frequency doubling of a continuous-wave Cesium vapor laser operating at 894.6 nm. The diode-pumped Cs vapor laser had an output power about 10 W with an emission linewidth less than 10 GHz. The second harmonic generation was performed in a commercial periodically poled KTP crystal (PPKTP). In this experiment, the PPKTP crystal was selected because of its large optical nonlinearity and good transparency in short wavelengths, high material damage threshold, the maturity in electrical poling for realizing high quality domain structures, and its easy availability from commercial vendors. The second harmonic generation efficiency achieved in our experiments for moderate pump power (up to 1 W continuous wave) was about 4.4 %/W that is close to calculated value (4.6 %/W). At higher pump powers, the second harmonic power depletion from the quadratic low and corresponding conversion efficiency decrease were observed that can be explained by the absorption related thermal effects, most noticeable at high pump power, long pulse duration, or high repetition rate. The crystal's sensitivity over the light-introduced thermal effect was experimentally monitored by recording the temporal profile of both fundamental and harmonic pulses.

Using of intracavity second harmonic generation, where the PPKTP crystal was assembled inside a Cs laser cavity, allowed us to increase the blue laser power to several watts. Other nonlinear crystals with lower thermal effects were studied in this system as well.

Laser Crystallisation Induced Multicrystalline Silicon Thin Film Solar Cells on Glass: European High-EF Project

F. Antoni[1], E. Fogarassy[1], A. Slaoui[1], F. Falk[2], E. Ose[2], S. Christiansen[2], G. Sarau[2], J. Schneider[3], N. Lichtenstein[4], B. Valk[4], M. Leclercq[5], R. Lewandowska[5], J. Michler[6], X. Maeder[6], A.-S. Dehlinger[7], J. Lábár[8], G. Sáfrán[8],

[1]*InESS-CNRS/UdS, Strasbourg, France*

[2]*IPHT, Jena, Germany*

[3]*CSG Solar AG, Thalheim, Germany*

[4] *Oclaro, Switzerland AG*

[5] *Horiba Jobin Yvon, Lille, France*

[6] *Swiss Federal Laboratories for Materials Testing and Research, Thun, Switzerland*

[7] *ALMA Consulting Group, Lyon, France*

[8] *Research Institute for Technical Physics and Materials Science Hungarian Academy of Science, Budapest, Hungary*

The European project HIGH-EF is developing a unique process for silicon thin films based solar cells. To provide high solar cells efficiency (> 10 %), a combination of laser crystallisation of a seed layer (50 to 200 nm) and an additional Solid Phase Crystallisation process of a thick (2 µm) layer is realised. The absorbing Si-based seed layer is deposited onto a borosilicate glass (3.3 mm thick) coated with a thin SiNx layer, used as a thermal barrier during the laser crystallisation process and as an antireflective layer for the final active cell.

The crystallisation of the seed layer is obtained by scanning a focused laser beam obtained by the combination of multiple diodes aligned behind an optical lens system, shaping the beam to a sharp line (0.3 mm large) able to crystallise in a single pass a full 1.4 m² panel (at the speed of 3 to 6 cm/s). Epitaxial growth of a large grains active silicon layer is obtained by Solid Phase Epitaxy (furnace annealing). Process optimisation is supported by numerical simulations of both the laser melting and crystallization process of the seed layer as well as for the epitaxial SPC process. Correlation between absorbed energy in the seed layer, energy density of the 806 nm diode laser beam and initial substrate temperature are investigated in order to optimise the crystallisation process.

Nanowires, Nanoloops and Nanorods by CVD

M. Veith, C. Aktas
Leibniz-Institut für Neue Materialien gGmbH
Campus D2 2, D-66123 Saarbrücken

Recently, one-dimensional (1D) nanostructures have attracted considerable interest of nanoscience studies as well as nanotechnology applications. Especially 1D hetero-structural nanowires with a combination of two different materials, for instance metal/metal oxide composites, hold a great potential for various bio, photonic and electronic applications. Thus, $Al{\cdot}Al_2O_3$ core-shell nanowires, which were firstly reported by Veith et al., form an interesting class of such hetero-nanostructures. Present work describes the preparation of functional surfaces composed of such 1D $Al{\cdot}Al_2O_3$ nanostructures by CVD of a single source precursor, (^{t}BuOAlH$_2$). Firstly, main attention is given to understand the underlying mechanisms controlling the 1D growth of $Al{\cdot}Al_2O_3$ nanostructures. By applying systematically different deposition temperatures and flow rates, various nanostructures were synthesized. No catalysis is needed to produce the different morphologies, as the growth mechanism proceeds in a self catalytic way At high deposition temperatures chaotic $Al{\cdot}Al_2O_3$ nanowires form, whereas at low deposition temperatures worm- and loop-like nanostructures are achieved. Our approach represents an effective, single step and easy method to fabricate various nanostructures.

Tree Mapping Using a Time-of-Flight 3D Camera

Arttu V.H. Ollikkala, Anssi J. Mäkynen
Measurement and Sensor Laboratory, University of Oulu, Kajaani, Finland

The purpose of this work was to study the use of a time-of-flight (TOF) 3D camera for tree mapping. The need to map trees is to make an inventory of the biomass of the forest and also to plan the tree harvesting. TOF 3D cameras such as those manufactured by PMDTech, Canesta and Mesa Imaging, for example, are low-cost non-scanning (staring) range imagers based on CMOS imager chips that are capable of providing range images at full video speed. The range image is generated by illuminating the whole field-of-view with sine modulated light and measuring the phase delay of reflected light concurrently in each pixel. [1]

The 3D camera was set on a pan-tilt unit to make possible accurate movement of the camera. The 3D camera has a field-of-view of 22.5° and 64*48 pixels. In laboratory environment several round sticks 25 mm in diameter were measured to model forest. At the analyzing phase, cartesian coordinates are calculated by Matlab algorithm for each pixel. The measured data was segmented into clusters which represented the used sticks. Segmenting is done by using different thresholds such as maximum distance difference of the adjacent pixels etc. The segmenting algorithm needs at least two enough close pixels to decide if the found cluster is a stick or not. Experiments showed that the sticks can be found till some distance when the spatial resolution is limiting the segmenting. To increase the spatial resolution, two or more range images can be overlapped.

At the final point the idea is to measure panoramic range image of a forest area in several measuring points and map the trees. The possible affect of different weather conditions to distance values were also tested. Measurements showed that the rain was the most problematic.

References

1. T. Möller, H. Kraft, J. Frey, M. Albrecht, and R. Lange, "Robust 3D Measurement with PMD Sensors", in: Proceedings of the First Range Imaging Research Day at ETH Zurich, ISBN 3-906467-57-0, 2005.

Optoacoustic Array for Monitoring of Hemoglobin Concentration: Modeling and Experiment

Valeriy Andreev[1], Tatiana Khokhlova[2], Alexander Bykov[3], Rinat Esenaliev[4]
[1] *Acoustics Dept, Faculty of Physics, Moscow State University, Moscow, Russia*
[2] *Applied Physics Laboratory, University of Washington, Seattle, USA*
[3] *Optoelectronics and Measurement Techniques Lab, University of Oulu, Oulu, Finland*
[4] *University of Texas Medical Branch at Galveston, USA*

Optoacoustic technique can be used for noninvasive monitoring of total hemoglobin concentration (THb). Recently one-element optoacoustic probe was successfully tested in clinical studies at UTMB. It was shown that for accurate measurement of THb concentration one has to scan the probe on the skin surface over the blood vessel of interest to obtain the best optoacoustic signal for processing. Another approach is to use optoacoustic arrays which have multiple acoustic detectors. In this work, we designed and built a novel optoacoustic array for probing blood vessels without scanning. The array has 8 piezoelements and can detect simultaneously and in real time a set of 8 optoacoustic signals from blood vessels. We performed numerical modeling and *in vitro* tests of the array in this study.

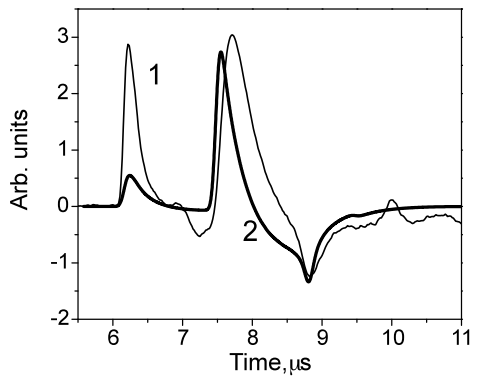

Fig. 1. Profiles of acoustic pulses generated in 2-mm tube at 2 mm depth. Thin line – experimental (THb=11.64 g/dL), thick line – calculated (THb=12 g/dL)

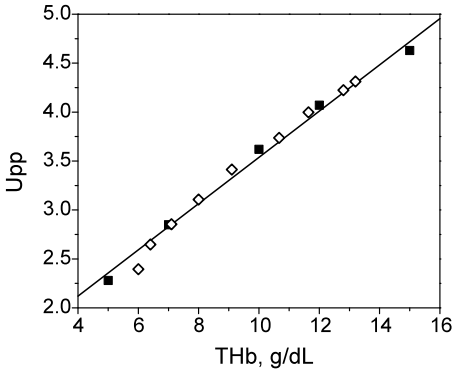

Fig. 2. The peak-to-peak signal amplitude from 2-mm tube vs. total hemoglobin concentration. Calculated and experimental results are shown by solid and empty symbols, correspondingly.

Experiments were performed with silicon tubes immersed into turbid liquid with optical properties similar to human tissue. The tubes were filled with heparinized arterial sheep blood which THb concentration was varied from 6 to 15 g/dL. In experimental profile (thin line in Fig.1) the first positive peak at 6.3 □s was generated at the boundary of the optoacoustic probe and the scattering liquid. The second peak belongs to the signal from the tube that has a bipolar shape typical for a cylindrical optoacoustic source. The time delay between the positive and the negative peak is determined by the tube diameter and speed of sound in the blood. Numerical calculations were performed for the same parameters as used in the experiment. Thermal sources resulting from the absorption of photons in the blood and surrounding medium were calculated using Monte Carlo simulations. To improve the calculation perfomance and increase the accuracy the Monte Carlo code was implemented on the multiprocessor computer with the parallel architecture. For calculation of the excited optoacoustic signal each voxel of the medium was considered as a source of an ultrasound N-shaped wave with the amplitude proportional to the energy absorbed in the voxel. The resulting waveform was calculated as a superposition of the N-waves by integrating over the entire illuminated volume. The output signals of the transducers were calculated with the use of Rayleigh integral (thick line in Fig.1). The size and position of the transducers matched those in the experimental probe. The experimental and calculated signals are in a good agreement. We demonstrated that peak-to-peak amplitudes of the experimental and calculated signals (Fig.2) are directly proportional to hemoglobin concentration. We proposed to use this parameter for THb monitoring *in vivo* studies. This work was supported in part by NIH and ISTC (grant#3691).

Physical properties, phase matching and frequency conversion in $GaSe_{1-x}S_x$, $Ga_{1-x}In_xSe$ and $GaSe_{1-x}Te_x$

Yurii M. Andreev[1], Gregory V. Lanskii [1], Sergey N. Orlov[2], and Yurii N. Polivanov[2]
[1] *Ecological Instrument-Making Department, Institute of Monitoring of Climatic and Ecological Systems SB RAS, Tomsk, Russia*
[2] *Optical Spectroscopy Department, Prokhorov General Physics Institute RAS, Moscow, Russia*

Physical properties of modified GaSe (S, In, Te doped and mixed $GaSe_{1-x}S_x$, $Ga_{1-x}In_xSe$, $GaSe_{1-x}Te_x$) crystals are studied. Crystal structures are determined by both x-ray and proposed non-linear method. Main attention is paid to study of optical (linear, non-linear, damage threshold) and mechanical properties. $GaSe_{1-x}S_x$ crystals are found to be best choice for practical application due to a shift of transparency range toward short-wavelength range versus mixing ratio x and a set of it physical properties that are responsible for frequency conversion efficiency. Best dispersion equations for mid-IR are identified through SHG and DFG experiments, and modeling. Temperature dispersion of Er^{3+}:YSGG and CO_2 laser SHG within 100-560 K is analyzed in detail. First results on design of THz range dispersion equations will be discussed, so as different ways for THz emission generation in modified crystals.

Terahertz time-domain spectroscopy of biological molecules

O.P.Cherkasova[1], M.M.Nazarov[2], A.P.Shkurinov[2]
1. Institute of Laser Physics SB RAS, Lavrentyeva 13/3, Novosibirsk 630090, Russia
2. Departament of Physics and International Laser Center, M.V.Lomonosov Moscow State University,
Leninskie Gory, GSP-1, Moscow 119991, Russia

Terahertz range is specific region of electromagnetic field which occupies an intermediate position between optical and radio ranges of electromagnetic waves. In this frequency range rotary and collective libratory transitions and also hydrogen bond modes of biological molecules are located. These transitions determine a change of molecule conformation. The frequencies of intermolecular interactions are also located in this region. We have performed terahertz time-domain spectroscopy (THz TDS) of several biological molecules in the frequency range 0.1-4.0 THz at room temperature.

Amino acid tryptophan, proteins trypsin and bovine serum albumin (BSA), DNA from calf thymus and corticosteroids have been measured. For THz TDS measurements cylindrical pellets of various thicknesses (d=0.2-0.5 mm, 2.5-5.0 mg, 5 mm diameter) were formed and the thin-films evaporated on substrates were prepared. Our common TDS apparatus has been reported previously [1, 2]. For the case of solutions we developed total internal reflection (TIR) scheme using silicon right angle Dowe prism. The practical advantage of TIR are the large signal amplitude (|R| is close to 1) for strong absorbing media. Water solutions of BSA and DNA were studied.

It was obtained that for pellets of both trypsin and BSA the absorbance increases with frequency. The absorbance is strong, nearly featureless and broadband. DNA absorbance increases more rapidly and absorption peak at 3.6 THz is observed. THz absorption spectrum of tryptophan has six major peaks at 1.45, 1.79, 2.22, 3.07, 3.67 and 3.94 THz.

In natural environment biological molecules are surrounded by liquid water, which absorbs terahertz radiation considerably. For the case of solutions we have constructed total internal reflection (TIR) scheme. We observe small changes in reflection spectra relative to reflection from pure water. Those changes are attributed mostly to water molecules bounded (by hydrogen bonds) to large biological molecules. With careful evaluation of concentrations and molar extinctions it may provide information about weak interaction between molecules in solution

The possibilities of the oxygen saturation spectral imaging method

Tatiana A. Savelieva[1], Maxim V. Loschenov [1], Sergey Yu. Petrov[2]
and Sergey Yu. Vasilchenko[1]
[1] *Laser Biospectroscopy Lab., Natural Science Research Center*
General Physics Institute RAS, Moscow, Russia
savelevat@mail.ru
+7(499)503 8759
[2] *Eye Diseases Institute RAS, Moscow, Russia*

A simple method to evaluate the spatial distribution of hemoglobin oxygen saturation in different biological tissues from diffuse reflectance spectra in the visible wavelength spectrum range is presented. It was assumed that while oxygenated and deoxygenated hemoglobin contributions to the attenuation are strongly variable functions of wavelength all other contributions to the attenuation including scattering are smooth wavelength function and may be approximated by Taylor series expansion. Basing on this assumption a robust algorithm suitable for real-time monitoring of the spatial distribution of hemoglobin oxygen saturation has been worked out. Spectra of the oxygenated and deoxygenated forms of hemoglobin are the most distinguished in the green area (520nm – 600nm) and have there several characteristic points. Thus four band-pass filters were used for multi-spectral imaging.

For qualitative oximetry of scleral vessels obtained images was processed to recognize the vessels tree and esteem the diffuse reflectance for each vessel profile. The diffuse reflectance spectra of melanin was took into account for qualitative skin oximetry.

Infrared Spectroscopy to Characterize Clay Intercalation

Korovin S., Pustovoy V., Beklemishev V*., Makhonin I.*
GPI of RAS, Moscow, Russia, E-mail: korovin@kapella.gpi.ru
** Institute of Applied Nanotechnology, Moscow, Russia*

We used of infrared spectroscopy as a technique for characterizing the state of intercalation nanocomposites prepared from montmorillonite. The nanocomposite samples were based on samples of clays, ion exchanged with Ag^{+} and solvated with water. It was shown that the shape of the clay band is in the 1350□750 cm^{-1} region, which includes four Si□O stretching modes, varies with the degree of processing and is sensitive to the quality of intercalation. Peak fitting was used to elucidate the nature of the changes and to develop quantitative indicators. The out-of-plane Si□O mode near 1070 cm^{-1} is particularly sensitive and undergoes significant changes. Infrared spectroscopy is a valuable complement to established techniques like X-ray diffraction and transmission electron microscopy and has the added advantage of being able to provide a relatively fast indication of the overall degree of intercalation, including clay particles with interlayer spacing. Furthermore, it offers the possibility of use as a quality control method, either in the laboratory or on-line.

Obtaining of extremely homogeneous volume self -sustained discharge for powerful CO_2-lasers pumping

V.A. Yamshchikov

Institute for Electrophysics and Electric Power, Russian Academy of Sciences, 18, Dvortsovaya nab., Sankt-Peterburg, 191186, Russia

Main author email address: yamschikov52@mail.ru

For pumping of the powerful CO_2-lasers the volume self-sustained discharge (VSSD) used. In the VSSD, usually, are formed local inhomogeneous in the form of plasma strings, channels or cathode spots. Presence and development of these inhomogeneous leads to restriction of duration of steady burning of the discharge, reduction of value both specific energy load and discharge volume, decreases frequency of impulses of radiation that worsens output characteristics of CO_2-lasers. It is important to solve the problem on an opportunity of obtaining extremely homogeneous VSSD in which local inhomogeneous are absent.

In the given work the mechanism and conditions of obtaining of extremely homogeneous VSSD in a mix of gases CO_2 : N_2 : He are investigated. The influence of value of initial electron concentration $n_0 = 10^7$-10^{12} sm^{-3} on uniformity of the VSSD and energy of radiation of CO_2-lasers both experimentally also theoretically are investigated. At $n_0 \sim 10^{12}$ sm^{-3}, owing to formation extremely homogeneous VSSD, in mixtures of gases CO_2 : N_2 : He =1 : 2 : 3 atmospheric pressure, the VSSD in volume of 60 litre with duration of steady burning 10 □s is obtained. Thus energy of radiation of the CO_2-laser has made 2 kJ.

Lidars in forestry

S. R. Allahverdi
Bartin University, Faculty of Forestry, 74100 Bartin/Turkey
E-mail address: surhay@mail.ru

LIDAR (Light Detection and Ranging) is an active remote sensing technique, analogous of RADAR (Radio Detection and Ranging; detection with extremely hihg-ferquency radio pulses), but using laser light. LIDAR measures the roundtrip time for a pulse of laser energy to travel between the detector and a target. The development of airborne LIDARs goes back to the 70th of last century. Good quality data may be obtained by using traditional techniques as: photography, photogrammetry and field research. All of these methods are relatively expensive and require considerable time.

LIDARs in forestry is breakthrough emerging technology to investigate different aspects of remote sensing.

At the same time multi-return LIDAR gives an opportunity to detect dense point data defining the first surface (canopy) and penetration into the vegetation cover with many points hitting the ground. Latter gives a possibility to obtain the map of the canopy and its characteristics (height, volume, basal area and aboveground biomass).

LIDAR systems for forestry applications is considered and classified according to their characteristics (recording the range to the first/last return or fully digitize the return signal; small or large footprint syatems; sampling rate/scanning pattern).

In this work a brief background on LIDAR remote sensing, and its current uses in forestry are considered. This work has been done in a frame of evaluation of multi-return LIDAR for Bartin forest service applications.

Broad-area semiconductor laser diode with sectioned electric contact into external Bragg resonator

V.V. Svetikov, V.A. Sychugov
A.M. Prokhorov General Physics Institute, Russian Academy of Sciences,, 119991, Russia, Moscow, Vavilov Str., 38

Main author email address: svetikov@nsc.gpi.ru

The experimental results of the investigations of the sectioned laser diode periodical structure selective properties are presented. An emitting of broad-area semiconductor laser diode with sectioned electric contact has been investigated from the point of view of coupled waveguides system forming the transmission Bragg hologram. The spectral selectivity of that structure has been estimated by using the Kogelnik theory for thick hologram gratings [1]. The sectioned semiconductor laser diode with an emitting area of 500mkm and an operating wavelength of 980nm has been investigated experimentally in various external cavity Bragg geometries, geometry with wavelength tuning has been included. The high order transverse mode selection has been experimentally obtained in Bragg resonator.

References

[1] H. Kogelnik: The Bell System Technical Journal, v.48, No.9, pp. 2909-2947 (1967)

Reference and Phase Shift Technique in Multipass Laser Schemes for Trace Gas Particles Detection

I.V.Nikolaev, V.N.Ochkin, S.N.Tskhai
P.N.Lebedev Physical Institute of Russian Academy of Sciences Russia, 119991 Moscow, Leninski prospect, 53
ochkin@sci.lebedev.ru

The high-sensitive spectroscopy with the aid of tunable lasers for atmosphere and other gas mixture content monitoring became of practical interest presently. For the atmosphere admixtures control the typical sensitivity really needed is about ~1ppb or ~10^{10}cm^{-3}. At the absorption cross-section in visible ~10^{-19}cm^2 it leads to the absorption sensitivity ~10^{-9}cm^{-1}. Taking into account the fundamental noise to signal ratio limitations and the requirement of reasonable measurements localization it follows in turn that such technique has to be completed with the multipass optical schemes. Different versions of such systems are described (CRDS, ICLS, ICOS…) which are the versions of high quality resonant cavities with different sets of eigen frequencies. So the common problem is the matching of the modes and frequencies with those of the laser as a light source. The mutual fluctuations and mismatching gives the rise of N/S value. Two versions related to this problem are investigated.

The first one is the improvement of ICOS scheme. The laser beam splits in three channels – analytic, basic line and reference. In the analytic channel the signal corresponds the transmittance of cavity including the media absorption, basic line channel takes into account the change of the laser intensity during the frequency tuning. The reference beam is the light reflected by the resonant cavity. Thus the analytic and the reference beam intensities as being supplement has the oppositely same fluctuations due to occasional mismatch of analytic cavity and laser modes. When combining that signals it is possible to improve the absorption sensitivity with the signal storage time ca 10 times less compare with traditional ICOS technique.

In the second version phase-shift measurements have been performed. It appears that in such approach the influence of modes mismatch effects are less pronounced then in the case of purely intensity measurements.

Both methods have been verified for the measurements of NO_2 molecules in atmosphere when using the cavity mirrors with reflection ~99.99% at the wavelength 415nm. In case of modified ICOS the sensitivity 0.05ppb with the storage time 6s was preliminary demonstrated. In case of phase measurements the corresponding values are 0.02ppb and 400s. It permits the monitoring of such molecules in typical atmosphere conditions with the accuracy ca 1%.

This work was supported by the Russian Foundation for Basic Research (projects 08-02-12164-ofi-a and 08-02-00145-a) and the Department of Physical Sciences of the Russian Academy of Sciences (Program Fundamental Optical Spectroscopy and Its Applications)

Terahertz applications of nanostructured alumina oxyhydroxide based artificial materials

A.V. Andreev, M.N.Esaulkov, A.□. Khodan, M.M. Nazarov, A.A. Konovko, D.A. Sapozhnikov, I.N.Smirnova, A.P. Shkurinov

M.V.Lomonosov Moscow State University, Leninskie Gory, 119992, Moscow, Russia
Institute of Physical Chemistry and Electrochemistry of RAS, Moscow, 119991, Russia

The properties of new porous materials made from nanostructured alumina oxyhydroxides (NAO) were studied in terahertz range. Analysis of the experimental results obtained with the raw , annealed, and chemically modified NOA samples show potential application of such materials for development light driving terahertz devices in the form of photonic band gap (PBG) and low loss holey waveguides. We report the results of THz-TDS detection of adsorbed molecular layers at the NAO surface.

Metamaterials can be used for obtaining the optical properties "on-demand". This study was focused on NOA based materials possessing very low density ~ 0.04 g/cm^3), high specific surface area (300 – 800 m^2/g) and fine fibrous structure. The particular interest of this work was terahertz properties of porous NOA samples after physical and chemical treatment. The chemical modification by using gaseous or liquid absorption at the NAO surface allows predictable changes in the optical properties. The preliminary results of the studies of the native, thermally treated and chemically modified NAO in the terahertz frequency range are presented. The first application of NAO based materials for photonic band gap (PBG) and a waveguide application was demonstrated. We also report an attempt to use NOA based composites with TiO_2 and ZrO_2 nanocrystals for making light driving terahertz devices.

The essential part of the work is concerned with the detection of OH^- and H_2O molecules absorbed on the NAO surface and bonded inside phase structure. At room temperature the NAO structure consists of amorphous nanofibrils of aluminum oxihydroxide with composition $Al_2O_3 \cdot 3.6H_2O$. In the work the possibility of the detection and separation of the different state of OH^- and H_2O molecules are discussed. We show for the first time the THz detection of molecular monolayers at the NAO surface and also the properties of NAO composites with TiO_2 and ZrO_2 nanocrystals and we observed the real-time condensation and desorption of the atmospheric water on and out of the NAO surface.

Tunable YAG:Cr^{4+} bidirectional ring laser

Yu.Yu. Broslavets, M.A. Georgieva, A.A. Fomitchev
Moscow Institute of Physics and Technology (State University), Dolgoprudny, Russia

Permanently growing requirements to measurement accuracy and operational performance of gyroscopes stimulate the search of fresh ideas to solve the problem of developing of sensitive devices for measurement and imaging of angular motion. To our mind gyros based on ring lasers with solid-state active media can be convenient for use and manufacturing. Construction of a laser gyro on a broadband active medium is of great interest by several reasons. First, Kerr-lens mode locking with femtosecond pulse generation enables to enhance the gyroscope accuracy due to the decrease of natural width of line. Meanwhile the competition between counterpropagating waves in the ring laser becomes less as the synchronizing pulses traverse the gain medium by turns and interaction between them decreases significantly. In addition one can take advantages of multifrequency generation: the angular values can be determined by use of several pairs of opposite waves. Lasers on these media have a good lifetime; heat generation in the active medium is less than in gas laser gyros because of greater generation effectiveness. They can be pumped by diode lasers.

We worked out the mathematical model for dynamics of bidirectional generation in a ring solid-state laser with a broadband active medium; it is based on the reduced equations for the slowly-varying amplitudes of the counterpropagating waves and the population inversion [1,2]. We determined the conditions under those the beat note regime, the unidirectional regime and various self-modulation regimes take place. We have also studied the influence of the active medium parameters, resonator construction and radiation wavelength on the size of lock-in zone. We performed also numerical simulation for operating regimes of the laser and showed that the lock-in zone decreases with increasing number of locked longitudinal modes.

In order to study the features of bidirectional generation and to explore the possibility of gyroscopic effect in the ring laser with the broadband active media we constructed an experimental setup including a wavelength-tunable YAG:Cr^{4+} laser pumped by the Yb-doped fiber laser. An YAG:Cr^{4+} crystal rod with faces cut at the Brewster angle was used as an active element. The laser resonator has a Z-configuration, includes two spherical and two flat mirrors and a quartz prism. Wavelength and spectrum width can be changed by turn of the prizm and mirrors and by variation of width and position of the aperture. At the laser output we set a wave mixer that can register the beat note of the counterpropagating waves.

The bidirectional generation with possibility of wavelength tuning was obtained in this laser. We observed both antiphase and in-phase self-modulation oscillations (fig.1), researched self-modulation and beat note regimes of laser operation. The measurements of different parameters of laser generation, spectral characteristics of laser radiation and luminescence were made at various temperatures of the active crystal. The features of beat note regime in case of multifrequency generation and in case when the laser generates several pairs of opposite waves with utterly different frequencies were investigated.

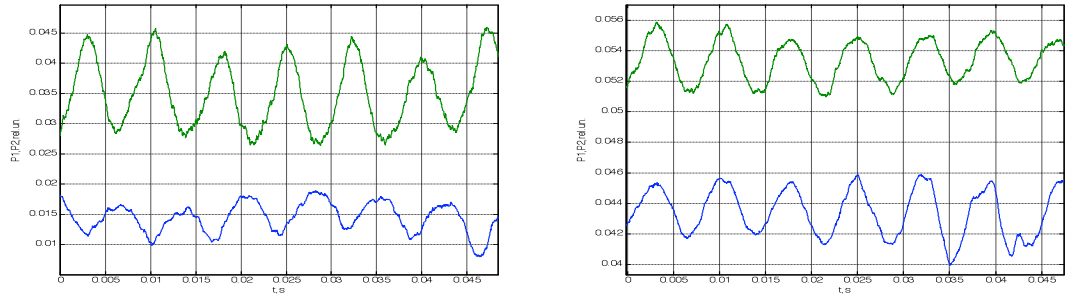

Fig. 1. CW and CCW intensities oscillate in antiphase (a) and in phase (b).

Thereby, as our investigation has shown, ring laser with broad spectrum of radiation can operate in various self-modulation and beat note regimes that can be used for rotation sensing.

References

1. Ya.I. Khanin. Osnovy *dinamiki lazerov (Foundations of Laser Dynamics)*. — Moscow: Nauka, 1999.
2. Yu.Yu. Broslavets, M.A. Georgieva, A.A. Fomitchev Possibility of construction of a solid-state laser gyroscope based on the ring wavelength-tunable YAG:Cr^{4+} laser. — *15th Saint Petersburg international conference on integrated navigation systems. Saint Petersburg, Russia*, (2008).

The Optical Nose, Laser Based Trace Gas Detection for the Early Monitoring of Human Health

Frans J.M. Harren

Life Science Trace Gas Facility
Institute for Molecules and Materials, Radboud University, Nijmegen, the Netherlands

E-mail: F.Harren@science.ru.nl, URL: www.ru.nl/tracegasfacility

A sample of normal human breath can contain more than 1200 different volatile organic compounds (VOC's), most of them in picomolar concentrations. Some of these VOC's are markers of diseases, i.e. their absolute concentrations/ concentration ratios can be used for early non-invasive diagnosis. Presently, detection requires invasive tests, such as biopsy, endoscopy and x-rays, that may be painful and potentially harmful. Breath testing, on the other hand, is the least invasive of all diagnostic tests, presenting minimal risk and negligible discomfort to patients. Breath tests as a diagnostic tool are an emerging science at the international level. Examples are the successful introduction of $^{13}CO_2$ breath test for the detection of stomach ulcers, caused by bacterial infection (Nobel prize 2005), and tests based on the biomarker NO (Nobel price 1998), for determining the severity of the inflammation in the airways. There is an imperious need for such devices in the medical community to replace, or to be used in combination with, existing instrumentation. Once developed and validated such tests could be used to monitor the health status of a patient in daily practice.

In our analytical research and development programme we develop advanced sensors based on mid-infrared laser sources, ranging from near infrared 'telecom' lasers, miniaturized photonic devices, optically pumped solid state lasers to OPO's in combination with ultra-sensitive spectroscopic methods. For a real-time profiling of the trace-gas contents, e.g. of a breath sample, the laser wavelength has to be tuned rapidly (second timescale) over a large portion of the so-called infrared fingerprint region of organic molecules. In addition, accurate detection of specific gases becomes into reach thanks to high laser powers and the exact tuning capabilities of lasers. When the lasers are combined with sensitive spectroscopic techniques, such as photoacoustic spectroscopy and cavity ring down spectroscopy, gases can be determined extremely sensitive. The laser based gas sensors typically reach detection limits around 1 part per billion volume for molecules and possess a time resolution of only a few seconds. This can make lasers applicable for a wide variety of applications.

Possibility of Increasing Excimer Laser Emission Duration

Malashin M.V., Khasaya R.R., Khomich V. U., Yamschikov V.A.
Institute for Electrophysics and Electric Power Russian Academy of Sciences
30/6, Vavilova St, 119991, Moscow, RUSSIA

Duration of excimer lasers radiation, is defined by duration of a pumping current of the active media. Depending on that, radiation time usually takes □ = 5-20 nanoseconds, measured on half amplitude of laser impulses. Laser emission with artificially increased duration of impulses uses in a number of the important applications, such as a photolithography, inscribing of fiber Bragg gratings, obtain diffractional optical microstructures and etc. Such emission have, the smaller divergence, improved spatial coherence, narrower width of spectral structure. Besides, as a result of increasing of duration of a laser impulse, the intensity of a laser beam decreases and the light loading operating on optical elements in powerful laser installations is weakened.

In the present work possibilities of increasing of duration of excimer lasers radiation by change of duration of the active media pumping are investigated: 1) using the scheme of the pumping generator with an artificially forming line and the system of magnetic compression of high-voltage impulses; 2) using pumping mode of the active media with aperiodic discharge current. Experimental dependences of energy and duration of lasers emission on pumping voltage, composition and pressure of gas mixtures in discharge gap of the laser are received. For the ArF-laser with the maximum radiated energy to 15 mJ the emission by the duration changed in limits □ = 7 - 18 nanoseconds is received. For the KrF laser with the maximum radiated energy to 40 mJ the emission with □ = 16 - 45 nanoseconds is received.

High Voltage Solid-State Pumping Source for Eximer Laser

M. V. Malashin, S. I. Moshkhunov, E. A. Shershunova, V. U. Khomich

Russian Academy of Sciences, Institute for Electrophysics and Electric Power, Russia

Main author email address: serg-moshkunov@yandex.ru

The pulse generators for pumping eximer lasers are conventionally based on gas discharge switches (thyratrons, dischargers) [1-3] , which limit the operational life time of generators. At present, an increasing number of IGBT transistors and modules are being developed that are competitive with tubes and thyratrons in power and response speed but have lifetimes that are many times longer. However, the power and the limiting operating voltages of a single device are not high enough, obliging one to use several devices jointly. The problem of generating high-voltage pulses using IGBT transistors is solved earlier by connecting several devices in parallel and using step-up pulse transformers. Typical disadvantages of such generators are large losses and time response of step-up pulse transformer, the problem of current shearing between IGBTs, large number of magnetic-compression sections. Another approach is to develop a high-voltage switch capable of ensuring the required operation voltage and duration and the pulse and mean power across the load. [4]

In the present work describes pulse generators for pumping eximer lasers with new high-voltage solid-state switch based on parallel-series connection of IGBT. The switch has allowed to construct all solid-state power generator of sub-microsecond range for pumping of high power eximer laser. The generator's maximal output power is 2kW. It operates at frequency up to 2kHz with output voltage level 20-27kV and with rise-time less than 70ns.

References

1 V.V. Atezhev, M.A. Kurzanov, A. Z. Obidin, S.K.Vartapetov, V. A. Yamschikov, A.V. Zhukov. Conditions of Effective Exciting of Electric Discharge F2-laser. //Quantum Electronics 33, □7 8, p. 677-683 (2003)

2 V. Yu. Khomich, K.E. Lapshin, A.Z. Obidin, S. K.,Vartapetov, V. A. Yamschikov, A. A. Zhigalkin. Research of Electric Discharge VUF Laser on Molecular Phluorine.//Quantum Electronics, 36, □5, 393 (2006)

3 M.A.M. El-Osealy, T. Jitsuno, K. Nakamura, Y.,Uchida, T. Goto Oscillation and gain characteristics of longitudinally excited VUV F2 laser at 40 Torr total pressure//Optics Communications 207 (2002) 255-259

4 E. V. Ivanov, V. Yu. Khomich, S. I. Moshkunov. High Voltage Nanosecond Generator on a Base of Bipolar Transistors with Isolated Gate//Preprint IEEP RAS.- M., 2004. – 50ps.

The influence of annealing on characteristics ZnO:N films

O.D. Khramova[1], O.A. Novodvorsky[1], V.Ya. Panchenko[1], V.I. Sokolov[1], L.S. Parshina[1], Ye.A. Cherebilo[1], A.A. Lotin[1], E.V. Khaydukov[1], V.V. Rocheva[1], C. Wenzel[2], J.W. Bartha[2], V.T. Bublik[3], K.D. Chtcherbatchev[3].

[1] *RAS, Institute on Laser and Information Technologies, Shatura, Russia*

[2] *TU Dresden, Institute of Semiconductor and Microsystems Technology, Dresden, Germany*

[3] *TU, Moscow State Institute of Steel and Alloys, Moscow, Russia*

N-doped ZnO thin films were received by PLD method. Nitrogen doping was made from gas phase (N_2O, N_2, NH_3) and the condensed phase (Zn_3N_2), and also by the codoping method ZnO:(Ga, N) at joint doping from condensed (GaN) and a gas phase (N_2O). For codoping of films by nitrogen and gallium from condensed phase we used nitride of gallium at preparation of tablets of targets. At doping by gaseous nitrogen, ammonia, nitrogen oxide a nitro- containing gases moved in chamber for deposition through precision system. Positions of maxima of emission strips in PL spectra depends on film reception conditions – substrate temperatures, ablation parameters, doped level, set by composition of a target and buffer gas pressure.

The influence of annealing in vacuum and in an atmosphere of oxygen on optical and structural characteristics ZnO:N films was investigated. Gradual change of the PL spectrum form with increase in concentration N-doping components is observed. This phenomenon was investigated in width temperature range (10K-400K). On spectra of a photoluminescence change of shallow acceptor levels concentration and occurrence deep donor levels as a result of annealing is established. PL signal has been appeared in UV areas, and the amplitude and position of peak of a photoluminescence depend on N-doping level of films. Passage through a maximum of PL intensity depending on time high-temperature annealing is observed. The behavior of PL signal of films in a mode of annealing with gradual rise in temperature (with step 50^o) has threshold character.

The work has been supported by ISTC Project 3294 and RFBR-09-07-00208-a.

Diode-pumped disk and slab solid-state lasers

Vladimir Tsvetkov, Vladimir Seregin, Andrew Lyashedko, Galina Bufetova, Dmitriy Nikolaev, Ivan Shcherbakov
General Physics Institute, 119991, GSP-1, Vavilov str., 38, Moscow, Russia
e-mail: tsvetkov@lsk.gpi.ru

The main goal of experiments was the study of conditions of a pumping and cooling of active disks and slabs for high power diode pumped 1-μm solid-state lasers which can operate both in CW and in pulse lasing modes with high efficiency and beam quality.

In experiment with slab lasers we used as monolithic active slabs with the sizes 6x2x62 mm (height x thickness x length), and composite one with the same sizes. The slab end faces have been cut off at 45^0. Composite slabs consisted of the central 40-mm section of 0.6 % doped Nd: YAG and 11-mm long undoped YAG ends diffusion-bonded to the central part. Cooling of the active medium was done by a water cooled heat sink.

In experiments there were investigated the heat generation and temperature of the active medium and also the uniformity of absorbed pump power distribution on slab length and on its cross-section. Temperature distribution along an active slab was measured with the Fabry-Perot interferometer. Simultaneously the changes of an optical phase difference along optical axes of the laser cavity were measured with the Twyman-Green interferometer.

It is shown that at change of pumping diodes temperature and in accordance with it the pumping wavelength from 804 nm to 810 nm the lasing efficiency practically was not changed. However the heat generation map and the maximum temperature in the active medium demonstrated considerable variation. In the paper there are experimentally shown advantages and lacks of monolithic and composite designs of an active slab and various ways of a pumping are discussed.

Study of an active disk bending which occurs due to its non-uniform heating and influence of the disk shape on laser cavity characteristics was the second goal of our work. Researches of a heat distribution in a disk volume have been carried out, and also measurements of radius of curvature of a disk surface at various values of pumping power have been done. Estimations were made in the assumption that the shape of an active disk becomes spherical.

We used the unconstrained active disk which was pressed to a heat sink while using a low thermal resistance interface. In our experiment the temperature of the active Nd:YAG disk was monitored by the change of interference figure. It gave the chance to estimate both temperature gradients, and the thermal optical phase distortions (OPD) brought in the laser resonator. The carried out researches have shown, that thermolens compensation occurs at the expense of a crystal bending because of non-uniform heating at one-sided cooling of an active mirror.

Studying of a question on heat diffusion in the active medium was other direction of researches. The obtained results show the necessity of the account of influence of thermolens in active disk on laser output characteristics.

A new method of herpes keratitis treatment by means of 1.4um laser diode

P.A. Gonchar[(1)], M.A. Frolov[(1)], N.V. Rodionova[(1)], Yu. L. Kalachev[(2)], V. A. Mihailov[(2)], I. A. Shcherbakov[(2)]

[(1)] *Peoples' Friendship University of Russia, 6 Miklukho-Maklay street, 117198 Moscow, Russia*

[(2)] *A.M. Prokhorov General Physics Institute, RAS, 38 Vavilov street, 119991 Moscow, Russia*

Herpes Simplex keratitis is a widely common and severe viral infection, which according to the severity takes one of the first places among the other cornea diseases.

We developed a new method of treatment of the herpes keratitis, using diode laser-coagulation, which helps to decrease risk of relapses, to short the period of recovering.

The features of the method

Diagnosed the herpes keratitis, under local anesthesia Sol. Dicaini1%, we performed laser coagulation of the herpetic vesicles.

First, while developing the technique we made laser - coagulator on the base of 1.4 um fiber coupled laser diode. Output power of light was ~300 mW in cw mode and exposition time in single pulse was varying from 0.1 to 3.0 sec. In the postoperative period we saw intensive coagulates of the cornea, which came to the middle of the stroma. Using higher power or more quantity of the impulses we had more rasping focuses of coagulation.

Necessary power dosage of the affecting by the laser and time of affecting according to the place and depth of the cornea's lesion were experimentally found out. The most common energy per pulse was in range 0.12 .. 0.3 J.

Clinical case

Patient G. 22 years old. Complaints of light-fear, tearing and redness of the eye. During examination we saw 2 lines of subepithelium vesiculars and decrease of the cornea's sensitivity. Herpes keratitis was diagnosed. Special antivirus therapy was recommended and we made laser-coagulation along herpes tree. Using biomicroscope, in impulse mode we destructed vesiculars. We made 3 impulses of 0.15 J in the periphery of the cornea and 2 impulses in the central part. In the place of laser action we had mild focuses of opalescence and epithelium desquamation 0.5-0.7 mm in diameter.

14 procedures were made. After recovery there were no traces of coagulation. The period of postoperative observation was 8 months, and we had no relapses.

1. Karu T. Photobiological fundamentals of low–power laser therapy// The 1–st international congress Limawssol ,1997–P.207–210

2. Bihari J. Mester A.// Laser therapy–1989–Vol 1(2) P.97

Enhanced Raman Scattering in Photonic Crystals Based on Grooved Silicon

Pavel K. Kashkarov[1,2], Dmitry A. Mamichev[2], Stanislav V. Zabotnov[2,1], Andrey V. Zoteyev[2], Leonid A. Golovan[2], and Viktor Yu. Timoshenko[2,1]

[1] *Russian Research Center "Kurchatov Institute", Moscow, Russia*

[2] *Physics Department, M.V. Lomonosov Moscow State University, Moscow, Russia*

Grooved silicon structures (GSS) consisting of the alternating layers of crystalline silicon walls and grooves [1, 2] attract the attention of researchers as new artificial media which can be easily integrated into devices for the microelectronics and optoelectronics. It was found that periodical GSS possess the properties of one-dimensional photonic crystals [3] or single axis negative crystals [4, 5] depending on the wavelength of a light beam propagating in the plane of the silicon substrate. In the both cases the local field effects in such inhomogeneous dielectric media play the dominant role. The largest manifestation of the local field effects can be expected for Raman scattering, and nonlinear optical processes. In our work the Raman scattering in the GSS has been investigated by using the different excitation wavelengths (514, 633 and 1064 nm) comparable with the characteristic thicknesses of the silicon walls in these structures. Also we have shown a possibility to use the GSS as sensors for the detection of harmful liquids in the environment.

The samples of the GSS were fabricated by the wet anisotropic etching (for details see Refs. [3-5]). The samples have the lattice periods varied from 4 to 7 μm and the silicon wall thicknesses from 1 to1.6 μm. The depth of the grooves and silicon walls was in the range from 15 μm to 60 μm.

The experiment showed that the Raman scattering spectra of the GSS measured at the excitation wavelengths of 633 and 514 nm were close to those detected for the crystalline silicon substrate. However a significant increase of the Raman scattering intensity (up to 8 times for the Stokes component) was revealed in the GSS under excitation at 1064 nm. The enhancement of the scattering intensity was nearly independent on the GSS period and the silicon wall thicknesses. Also the significant increase for the ratio of the Stokes to anti-Stokes intensities up to 70-80 times revealed for the GSS at the excitation wavelength of 1064 nm. At that, this ratio does not reach such high values for the smaller excitation wavelengths. Such behaviour can not be explained in the frameworks of the traditional theory for the spontaneous Raman scattering. We suppose the influence of the weak light localization within the grooved structures on the Raman scattering growth. The effective scatter volume increases in the medium, when the excitation wavelength approaches the silicon wall thickness. The observed effect can be used for the highly sensitive analysis of the Raman scattering of different compounds localized in the silicon grooves. We filled the grooves by the carbon tetrachloride and benzene. The growth of the Raman signal was observed up to 10 times for the both liquids.

Thus, the obtained results demonstrate the possibility of the significant enhancement of the Raman scattering in the GSS under the excitation with the wavelength close to the silicon wall thickness. Such structures may be used as high sensitive sensors of different compounds localized in the silicon grooves.

References

1 A.-Sh. Chu, S. H. Zaidi, S. R. J. Brueck, "Fabrication and Raman scattering studies of one-dimensional nanometer structures in (110) silicon", *Appl. Phys. Lett.*, **63**, 905-907 (1993).

2 S. H. Zaidi, A.-Sh. Chu, S. R. J. Brueck, "Optical properties of nanoscale, one-dimensional silicon grating structures", *J. Appl. Phys.*, **80**, 6997-7008 (1996).

3 V.A. Tolmachev, E.V.Astrova, Yu.A. Pilyugina, et al., "1D photonic crystal fabricated by wet etching of silicon", *Optical Materials*, **27**, 831-835 (2005).

4 E.V.Astrova, T.S. Perova, V.A. Tolmachev, et al., "IR birefringence in artificial crystal fabricated by anisotropie etching of silicon", *Semiconductors*, **37**, 399-403 (2003).

5 E. Yu. Krutkova, V. Yu. Timoshenko, L. A. Golovan, et al., "Infrared and submillimeter spectroscopy of grooved silicon structures", *Semiconductors*, **40**, 834-838 (2006).

Pulsed Nd:YAG Laser Drilling Process of Alumina Ceramic for Printed Circuit Board

P. Demir[1,2], E. Akman[1], M. Mutlu[1], S. Babur[1], E. Suvaci[3], E. Kacar[1,2], A. Demir[1,2]

[1] *Laser Technologies Research and Application Center, Kocaeli University, 41275 Kocaeli/Turkey*
[2] *Faculty of Arts and Science, Department of Physics, Kocaeli University, 41380 Kocaeli/Turkey*
[3] *Faculty of Engineering and Architecture, Department of Materials Science and Engineering, Anadolu University, 26480 Eskisehir/Turkey*

Main author email address: pinardemir@kocaeli.edu.tr

Ceramics are commonly used in microelectronics for the manufacture of printed circuit boards and electronic components, due to its electrical, mechanical and thermal properties. In micro-processing application of ceramics, lasers have become very important devices [1,2]. In this study, alumina ceramic material is drilled using nanosecond pulsed Nd:YAG laser to obtain holes for printed circuit board (PCB). Results of laser drilling process of alumina ceramic for varied laser pulse parameters are presented to observe effects on produced hole structure and to obtain optimum conditions for producing better quality processing of alumina PCB. Emission spectra of plasma produced by laser-material interaction during laser drilling of alumina ceramic are recorded by spectrometer.

References

1 E. Kacar, M. Mutlu, E. Akman, A. Demir, L. Candan, T. Canel, V. Gunay, T. Sınmazcelik: Journal of Materials Processing Technology, 209, (2009), 2008 – 2014
2 V. Oliveira, O. Conde, R. Vilar: Advanced Engineering Materials, 3, (2001), No. 1-2

Three-dimensional acousto-optic mapping in tissue mimicking phantoms using heterodyne light-scattering spectroscopy.

A. Bratchenia [1], R. Molenaar[1], R.P.H. Kooyman[1]
[1] *University of Twente, Faculty of Science & Technology, Institute of Biomedical Technology, PO Box 217, NL-7500 AE Enschede, the Netherlands*

Main author email address: a.bratchenia@tnw.utwente.nl

We have used acousto-optic modulation of scattered light to investigate the possibility of three-dimensional mapping of tissue mimicking phantoms with a resolution of a few millimeters. The phantom under investigation mimicked the blood vessel surrounded by tissue. For that purpose we used a silicon rubber tube embedded in an Intralipid based gel (μ_s=1.5 cm^{-1}). We have applied the acoustic pressure in a predefined volume of phantom by insonifying it with a microsecond length ultrasound bursts. The insonificaton in combination with irradiation of the phantom with a microsecond length light pulses resulted in the localized acousto-optic modulation of phase of scattered light in hat volume. The detection technique, based on the parallel speckle detection in the transmission mode, allowed us to quantify the ratio of the modulated light intensity over unmodulated intensity. The measured modulation depth depends on the absorption coefficient of tissue phantom in the focal volume of the ultrasound beam. By varying the delay time between ultrasound burst initiation and light pulse initiation we could perform a scan in the ultrasound-propagation direction. By moving the ultrasound transducer in a plane perpendicular to ultrasound-propagation, we could build up a volumetric map of modulation depth values. We have experimentally determined the acousto-optical modulation depth in phantom volume voxels, and we have compared these results with those obtained from diffusive optical imaging simulations. The simulations were based on the finite elements method solution of the diffusion approximation of the radiation transfer equation. We have reconstructed the image of the tube with absorber with a spatial resolution of a few millimeters. The use of calibration curves allowed us to extract quantitative information on dye concentration in the tube. Our findings demonstrate the outlook to apply this technique for non-invasive three-dimensional mapping of local absorbances in turbid media by means of acousto-optic modulated light scattering spectroscopy.

Numerical Investigation of Laser Resonator for Generating Radially or Azimuthally Polarized Beams

V.D. Dubrov, R.V. Grishaev, M.D. Homenko, Yu.N. Zavalov
Institute on Laser and Information Technologies, Shatura, Russia

The increased attention to high-power laser beams with radial or azimutal polarization in recent years has been caused by the advantage of such beams in material processing (cutting and drilling). Though there are only a few lasers for generation of high-power axially symmetric polarized beams. Recently radially polarised high power CO2 lasers were demonstrated [1, 2]. Investigations are also focused on the application of this technology to thin-disk lasers [3].

In this paper we present the numerical simulation of optical resonators with circular mirror with polarization selectivity. The simulation includes vectorial calculation of the paraxial wave propagation through the loaded or empty resonators. Geometry of the resonator and the reflectivity difference between p and s polarizations makes one of low-order mode with minimum losses to oscillate and suppresses other modes. The purpose of the present work was the study of resonator, mirror and active medium parameters on the output power and efficiency of the laser.

References

1 M. Endo, "Azimuthally polarized 1 kW CO2 laser with a triple-axicon retroreflector optical resonator", Optics Letter, 33, 1771-1773 (2008).
2 M. Ahmed *et al*, "Radially polarized 3 kW beam from a CO2 laser with an intracavity resonant grating mirror", Optics Letters 32 (13), 1824-1826 (2007)
3 M. Abdou Ahmed *et al*, "Radially polarized high-power lasers", Proc. SPIE, 7131, 71311I (2008)

Surface-Assisted Laser Desorption Ionization of Organic Compounds. Mechanism and Applications.

S.Alimpiev
A.M.Prokhorov General Physics Institute of Russian Academy of Sciences,
Vavilov str.38, 119991, Moscow, Russia.

The generation of ions from silicon substrates in Surface-Assisted Laser Desorption Ionization (SALDI) has been studied using silicon substrates prepared and etched by a variety of different methods. Mass spectra of a wide range of analytes with varying basicity and molecular weights were obtained using laser wavelengths from UV to IR. Ionization efficiencies were measured as a function of desorption conditions. It is demonstrated that both the chemical properties of the substrate surface and the presence of a highly disordered structure with a high concentration of "dangling bonds" or deep gap states are required for efficient ion generation. In particular, amorphous silicon is shown to be an excellent SALDI substrate with ionization efficiencies in excess of one percent. Based on the results, a novel model for SALDI ion generation is proposed. with the following reaction steps: 1) the adsorption of neutral analyte molecules on the SALDI surface with formation of a hydrogen bond to surface Si-OH groups; 2) the laser electronic excitation of the substrate to form free electron/hole pairs. Their relaxation dynamics leads to trapped positive charges in near-surface deep gap states, resulting in an increase in the acidity of the Si-OH groups and proton transfer to the analyte molecules; and 3) the thermally activated dissociation of the analyte ions from the surface over a "loose" transition state.

The application of SALDI technique for ultra high sensitive detection of organic compounds in liquid and gas samples is discussed.

Retrieval of Dust Particle Parameters from Multiwavelength Lidar Measurements

Igor Veselovskii[1], Alexei Kolgotin[1], Oleg Dubovik[2], Sergei Vartapetov[1]

[1] Physics Instrumentation Center of General Physics Institute, Troitsk, Moscow reg.,142190 Russia. E-mail:igorv@pic.troitsk.ru
[2] Laboratoire d'Optique Atmospherique, CNRS Universite de Lille 1, Bat P5 Cite scientifique, 59655 Villeneuve d'Ascq Cedex, France, E-mail: dubovik@loa.univ-lille1.fr

The desert dust aerosols play an important part in Earth's radiation budget, thus development the methods for remote study of particle microphysical properties is highly demanded. During the last decade the multi-wavelength (MW) Raman lidars have demonstrated their potential to provide this kind of information. Up to the present the physical models in retrieval algorithms for processing of MW lidar data were based on Mie theory. However, this model is applicable for modeling light scattering by spherical particles only and does not adequately reproduce the scattering by non-sherical particles. This fact imposes serious limitations on the interpretation of the lidar observations of the desert dust. Indeed, there is a large number of theoretical and experimental evidences of the high sensitivity of lidar measurements to the light scattering effects caused by the non-sphericity of dust aerosol particles. At the same time, there are several examples of successful attempts to account for particle non-sphericity in interpretation of desert dust scattering observations by laboratory and passive remote sensing methods. For example, the model of randomly oriented spheroids has been included into AERONET retrieval algorithm for accounting for effects of aerosol particle shape irregularities. Scattering properties of particles of irregular shape can be simulated by the set of randomly oriented spheroids. Such approach has resulted in significant improvements of retrieved desert dust properties from AERONET observations.

Here we present the algorithm using spheroid model for inversion of multi-wavelength lidar data. Following the positive experience of AERONET retrieval developments, we model the aerosol as a mixture of spherical and non-spherical aerosol components. The non-spherical component is an ensemble of randomly oriented spheroids with size independent shape distribution. It is fixed to the axis ratio distribution providing the best fit to the detailed polarimetic laboratory measurements for desert dust sample. We considered the Raman lidar based on a tripled Nd:YAG laser. Such lidar provides three backscattering (β), two extinction (α) coefficients and particle depolarization ratio δ at single or multiple wavelengths. Simulations were performed for bimodal particle size distribution with modal radii of fine and coarse modes of 0.1 μm and 2 μm respectively. Comparison the results obtained with $3\beta+2\alpha$ and $3\beta+2\alpha+3\delta$ input data sets demonstrates that the use of depolarization ratio as an input data is essential to stabilize retrieval. The accuracy for retrieval of particle surface, volume concentration and effective radius for 10% errors in input data is estimated to be about 30-40%. It is demonstrated that if the effect of particle non-sphericity is not accounted the error of parameters estimation is notably increased.

Silicon nanoparticles with previously defined parameters creation from silicon tetra fluoride by CO_2-laser permanent irradiation for biology and medicine

Ershov I.A., Orlov A.N., Pustovoy V.I., Surkov A.A/

*Centre natural science investigations at
*Prokhorov General Physics Institute, Russian Academy of Sciences,
*Vavilova str. 38, Moscow, 119991 Russia
*E- -mail: grr@nsc.gpi.ru , orlov1@kapella.gpi.ru , pustovoy@nsc.gpi.ru

Silicon nanoparticles creation from silicon tetra fluoride is possible to implement the most effectively by making use the permanent CO_2-laser with wave length about 9.7 mkm. The silicon tetra fluoride molecule is a stable enough. None the less the silicon tetra fluoride decomposition had been carried out successfully with the permanent CO_2-laser radiation of moderate intensity usage. The gaseous silicon tetra fluoride molecule decomposition in CO_2-laser resonant field was regarded. The surfaces of these silicon nanoparticles has been covered with fluorine atoms, that leads to surface protection and dangling bonds absent.

Experimental investigation of different refining stages influences on optical and ultrasonic signals in paper pulp suspensions

Jan Niemi

EISLAB, Department of Computer Science and Electrical Engineering,
Lulea University of Technology, SE-971 87 Lulea, Sweden

An important parameter to control in papermaking is the fibre mass fraction in a pulp suspension. Poor control of the mass fraction leads to an unstable process that compromises the production, quality and the energy efficiency in the pulp mill. Estimation of the mass fraction can be obtained using optical measurement techniques or ultrasound measurement techniques or a combination of both. If the fibres stems from a chemical process the fibres are beaten in a refiner. The refining influences the fibre by cutting, reshaping, removing parts of the outer fibre wall and delamination of the inner fibre wall. The motivation for this study is to examine if and how a light pulse and a sound pulse are affected by refining

Two different types of chemical pulp are considered; bleached hardwood and unbleached softwood pulp. The pulp samples stems from four refining steps. At each refining step four mass fractions are mixed. The mass fraction ranges from 0.25% to 1.3%. Altogether, a set of 16 pulp samples with four refining levels and four consistency levels for each pulp type was investigated.

The optical measurements were conducted using a custom designed LIDAR measurement system CMP3 from Noptel Oy, Finland. The wave length of the light was 905 nm. Both the received amplitude and time-of-flight of the light pulse was recorded for each pulp sample. The ultrasonic measurements were performed in a pulse-echo setup with a pulser/receiver that excite and amplify a transducer. The transducer center frequency was 25 MHz. A freeness tester was used for measuring the influence of refining intensity on the fibres.

The result shows that for unbleached softwood pulp the used measurement techniques are influenced by refining. For bleached hardwood pulp the influence of refining intensity on the tested measurement techniques was not observable or minor. The results indicate that refining can potentially influence accurate consistency estimation for unbleached softwood pulp but not for bleached hardwood pulp using the investigating measurement techniques.

The result forms a base for development of a photoacoustic sensor to monitor fibre mass fraction.

Review for the technique development of Front end of SG Laser facility

Jianqiang Zhu, Xuechun Li, Wei Fan, Shaohe Chen, Zunqi Lin
National Laboratory on High Power Lasers and Physics
Shanghai Institute of Optics and Fine Mechanics CAS, Shanghai 201800

In China, we had developed several high power laser facilities since 1964, and now the much large laser system will be established also. The Front end is the key part of the laser facility, it takes on the ability of pulse duration, stability, reshaping and spectrum width etc.. We reviewed the Front end technique used in different laser facilities, and some special technique we had developed.

Raman spectroscopy a powerful tool in Biophotonics

Jürgen Popp

[1]*Institute of Physical Chemistry, Friedrich-Schiller University, Jena, Germany*
[2]*Institute of Photonic Technology, Jena, Germany*
juergen.popp@uni-jena.de

Raman based microspectroscopy has been recognized as a powerful tool to study biological cells and tissues because the method provides molecular information without external markers such as stains or radioactive labels. Raman spectroscopy is a non destructive technique and does in general, require only minimal or no sample preparation. However while the specificity of Raman spectroscopy is very high its sensitivity i.e. the conversion efficiency of the Raman effect is rather poor. To overcome the disadvantage of low signal intensities from most biomolecules, special Raman signal enhancing techniques can be applied. The two most prominent approaches are the resonance Raman effect and the surface enhanced Raman scattering (SERS). Besides these two linear Raman signal enhancing techniques a nonlinear variant of Raman spectroscopy called coherent anti Stokes Raman spectroscopy (CARS) belongs to the most promising Raman techniques because it combines signal enhancement due to the coherent nature of the process with further advantages such as directional emission, narrow spectral bandwidth and no disturbing interference with autofluorescence.

We will start with a discussion of the application of Raman microspectroscopy allowing the identification of chemical structures by comparison of spectral data with databases of known substances or by analyzing the molecular structure using the spectral information. In particular Raman microspectroscopy is used to study microorganisms. Here, different Raman excitation wavelengths achieve information about different chemical groups. Resonance Raman excitation in the UV region yields selectively enhanced signals of macromolecules like DNA / RNA and proteins. Using excitation wavelengths in the visible region monitors the chemical composition of the whole cell.

The presented SERS examples convincingly demonstrate that SERS is an extremely potent tool in bioanalytical science because the technique comprises high sensitivity with molecular specificity. Here the first applications of tip-enhanced Raman spectroscopy (TERS) for bio-diagnostics are of particular relevance. TERS combines SERS spectroscopy and atomic force microscopy (AFM) or scanning tunnelling microscopy (STM) and thus the high spatial and topological resolution of AFM and the chemical sensitivity of Raman scattering. We succeeded in recording TERS spectra of the surface of a single microorganism or even on a single virus.

Furthermore we present for the first time a systematic experimental evaluation of the information content of the two complimentary techniques, Raman and CARS microscopy which may define future spectral imaging trends. The presented CARS microscopy results establish the foundation for further development of the CARS technology to assess tissue and offers great prospects for clinical diagnoses. CARS images were recorded from various tissue sections (colon, brain, liver etc.) and compared with Raman images. Based on these results we suggest a complementary application of Raman and CARS imaging. Raman imaging defines spectral regions and spectral markers that are essential for tissue classification. CARS imaging at different Stokes shifts probes these spectral descriptors at video-rate speed. Such a combination offers great prospects for clinical diagnoses.

Overall within this contribution it will be shown that Raman spectroscopy and its various techniques are powerful tools for bioanalytical and biomedical applications.

Second-Harmonic Generation and Optical Bistability in Thin $Ge_xSb_{40-x}S_{60}$ Chalcogenide Films

Sashka Alexandrova[1], Vitalii I. Krasovskii[2], Igor A. Maslyanitsyn[2], Vladimir B. Tsvetkov[2], and Vladimir D. Shigorin[2]

[1]*Institute of Solid State Physics, Bulgarian Academy of Sciences, Sofia, Bulgaria*

[2]*A.M. Prokhorov General Physics Institute, Russian Academy of Sciences, Moscow, Russia*

her
ent
cal

Z-
on
lly
ich
ice

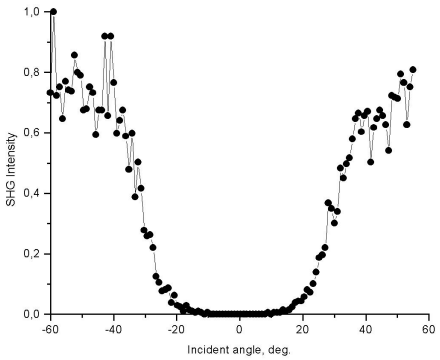

Fig 1. Dependence of SH intensity on the angle of incidence for $Ge_{35}Sb_5S_{60}$ film

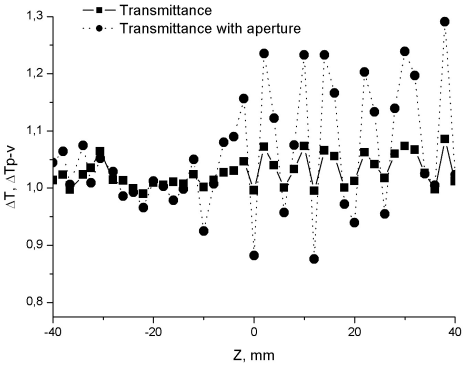

Fig 2. Optical bistability, measured by Z-scan technique in $Ge_{35}Sb_5S_{60}$ film

Effect of bistability was observed in the measurement of nonlinear absorption and absorption through the aperture in the geometry of Z-scan (Fig.2). Since the obtained dependence is not characteristic of the Z-scan technique [1], the interpretation of these measurements was carried out by the numerical solution of the Kirchhoff-Fresnel integral [2] for each point , *Dn(I)* and *Da(I)* which were obtained according followed by the application theory for bistability model for dispersion Kerr nonlinearity in Fabry-Perot interferometer [3, 4].

References

1. M. Sheik-Bahae, A. A. Said, T. Wei, D. J. Hagan, and E. W.Van Stryland, IEEE J. Quantum Electron., 26, 760 (1990).
2. J. A. Hermann, T. J. McKay, R. G. McDuff, Optics Communications, 154, 225-233 (1998).
3. T. Bichofberger, Y.R. Shen, Appl. Phys. Lett, 32, 156 (1978).
4. T. Bichofberger, Y.R. Shen, J.Opt.Soc.Am., 68, 642 (1978).

Laser Cancer Phototherapy Enhanced by Gold Nanoparticles

Valery V. Tuchin, Irina L. Maksimova, Georgy S. □erentyuk, Garif G. Akchurin,

Saratov State University, Department of Optics and Biophotonics, 83 Astrakhanskaya, Saratov, 410012 Russia
Tel. +7 8452 21 07 22, Fax +7 8452 27 85 29, tuchin@sgu.ru

Boris N. Khlebtsov, Nikolai G. Khlebtsov,

Institute of Biochemistry and Physiology of Plants and Microorganisms, Russian Academy of Science, 13 Prospekt Entuziastov, Saratov, 410049 Russia
Tel. +7 8452 97 04 44, Fax +7 8452 27 85 29, khlebtsov@ibppm.sgu.ru

The possibility of effective application of gold nanoparticles to laser therapy of cancer is discussed. To enhance cancer photothermal therapy we have applied plasmonic silica (core)/gold 140/20 nm-nanoshells. The gold nanoshells with maximum of extinction in the NIR spectral range were synthesized in Institute of Biochemistry and Physiology of Plants and Microorganisms RAS (Russia). Spectral characteristics of design nanoparticles were in a good agreement with theoretical ones calculated on the basis of Mie theory. The parameter verification (size and shape) was executed by TEM. Absorbing in NIR, nanoshells allowed us to produce a controllable laser hyperthermia in tissue depth using powerful diode lasers with the wavelength of 810 nm. Laser irradiation parameters were optimized on the basis of experimental studies with laboratory rats. Temperature distributions on the animal skin surface at hypodermic and intramuscular injection of gold nanoparticle suspensions were measured *in vivo* using a thermal imaging system. The comparison of thermal and histological studies of laser treated tissues that were photosensitized by nanoparticles was done.

By experimental investigations using a test-tube, the dependences of temperature rise of solutions upon concentration of nanoparticle were measured, as well as the depth and time interval of laser heating. It was found that at continuous wave (CW) laser heating the time needed to reach the steady-state temperature conditions was of 100-150 sec. The back reflectance spectral measurements using a fiber-optical probe allow for monitoring of subcutaneously injected nanoparticles in the rat skin. The results of study of laser heating kinetics allow one to optimize clinical protocols for cancer treatments via induction of pathology cell apoptosis or their photothermolysis by NIR laser irradiation. For instance, both CW and pulse laser heating have the similar short time kinetics (temperature rise up to 46-50°C over time no more than 40 sec) however due to compensatory response of the organism pulsed laser heating is more controllable than CW at large time scale. In that sense pulsed irradiation (on-off time ratio of 0.25, and pulse duration of 1 msec) is preferable because gives fast and prolonged self-limited temperature rise.

Temperature distributions and corresponding morphological alterations in tissues caused by laser heating at different depths of inserted nanoparticles were analyzed. Gold nanoshell mediated laser destruction of muscle tissue was achieved *in vivo* in the region of nanoparticle localization (in depth of 4 mm) without any damage of the surface tissues. These findings are important for the successful translation of plasmonic nanoparticle technology for early cancer detection and selective laser photothermal therapies to clinical settings.

Safety problems with measurements of gold nanoparticle distribution within the organs of experimental animals are also highlighted.

Direct laser materials nanostructuring in absence of melting

S.V. Nebogatkin[1], V.Yu. Khomich[1], V.A. Shmakov[2], V.N. Tokarev[2], V.A. Yamshchikov[1]

1- Institute for Electrophysics and Electric Power, Russian Academy of Sciences, 18, Dvortsovaya nab., Sankt-Peterburg, 191186, Russia
2- A.M. Prokhorov General Physics Institute, Russian Academy of Sciences, 38 Vavilov st., Moscow, 119991, Russia
snebogatkin@gmail.com

In the given paper a so-called "direct" laser nanostructuring is considered, when surface profile is modified by only one laser beam. As a result of performed theoretical studies [1] we found out that two types of nanostructures can be obtained in this case:

(1) A development of laser-induced surface instability in a form of wavy disturbances having characteristic periods $d < L_T$, where $L_T = 2(\chi\tau)^{1/2}$ is heat diffusion length for pulse duration τ. For action of nanosecond laser pulses ($\tau = 20$ ns) L_T becomes less than 1 μm and hence a formation of submicrometer reliefs is possible, if a material on a high-temperature stage of heating has a low thermal diffusivity: $\chi < 0.1$ cm^2/s. For example, for graphite, diamond films and ceramics, which have χ of the order of 10^{-2} cm^2/s, L_T is around 300 nm. For a number of polymers having χ of the order of 10^{-3} cm^2/s L_T is around 100 nm.

(2) Profile in the form of an array of cones having characteristic sizes along the material surface $d > L_T$. We have shown that for obtaining cones of minimal sizes both a short laser wavelength λ and a small heat diffusion length are important. Under nanosecond irradiation such situation is possible when ultraviolet lasers (λ = 157 and 193 nm) and materials having on high-temperature stage thermal diffusivity χ of the order of $(1\text{-}3)\times10^{-2}$ cm^2/s and less are used. Such materials are graphite and diamond films and also a number of ceramics and polymers. Obtained theoretical conclusions agree well with our experimental data on F_2 laser (λ = 157 nm) irradiation of diamond films, where cones with unusually small sizes d = 200-600 nm have been observed [2].

[1]. V.N. Tokarev, V.Yu. Khomich, V.A. Shmakov, V.A. Yamshchikov, Possibility of direct laser surface nanostructuring in absence of material melting, Physics and Chemistry of Materials Processing, No. 4, pp. 18-25 (2008) – in Russian.

[2]. K.E. Lapshin, A.Z. Obidin, V.N. Tokarev, V.Yu. Khomich, V.A. Shmakov, V.A. Yamshchikov, Direct laser surface nanostructuring of diamond film and silicon nitride by nanosecond pulses of F_2 laser radiation, Russian Nanotechnologies, vol. 2, No. 11, 12, pp. 50-57 (2007) – in Russian.

Zinc Oxide Nanostructured Layers for Gas Sensing Applications

A.P. Caricato[1], A. Luches[1], R. Rella[2], D. Valerini[1]
[1] *Università del Salento, Dipartimento di Fisica, 73100 Lecce, Italy*
[2] *Istituto per la Microelettronica ed i Microsistemi, IMM-CNR, Lecce, Italy*

Zinc oxide presents many interesting properties, like a wide band gap, a large exciton binding energy, chemical stability, biocompatibility and piezoelectricity, among others. ZnO nanostructures, due to their high surface-to-volume ratio, high luminescence efficiency and possible quantum confinement effects, are particularly appealing for many applications, like optoelectronic and sensor devices. Pulsed laser deposition (PLD) is a convenient technique to fabricate good quality nanometric ZnO films. In fact, depending on the deposition parameters, like laser wavelength, substrate temperature, oxygen background pressure, nanostructured films with many different morphologies can be fabricated. In particular, we have demonstrated the growth of various ZnO nanostructures, such as columns, pencils, hexagonal pyramids, hexagonal hierarchical structures, as well as smooth and rough films, by means of excimer PLD, without the use of any catalyst. ZnO films were deposited at substrate temperatures from 500 to 700 °C and oxygen background pressures of 1, 5, 50 and 100 Pa. In particular, very different morphologies were observed when different laser wavelengths (248 nm or 193 nm) were used to ablate the bulk ZnO target: smooth, rough thin films as well as nanostructures were obtained. The sensing properties of the different nanostructures were tested against low concentrations of NO_2. The variation in the photoluminescence emission of the films when exposed to NO_2 was used as transduction mechanism to reveal the presence of the gas. The nanostructured films with higher surface-to-volume ratio and higher total surface available for gas adsorption presented higher responses, detecting NO_2 concentrations down to 3 ppm at room temperature.

The possibility of wideband CO laser and Sr vapor laser using for atmosphere monitoring

Olga V. Kharchenko, Oleg A. Romanovskii
Institute of Atmospheric Optics SB RAS, Tomsk, Russia

The development of laser remote IR-spectroscopy calls for the elaboration and promotion of new mid-IR laser radiation sources capable of lasing in the spectral range as wide as possible with small-step frequency tuning.

In the present paper the possibility of application of the wideband CO and Sr lasers for atmosphere monitoring is analyzed. A compact slit high-frequency-excited CO laser has generation range 4.7–8.2 □m for fundamental vibrational transitions and 2.5–4.2 □m for overtone transitions. Generation range for strontium vapor laser (SrI- SrII) is - 1-6.2 □m. These spectral ranges are most informative from the viewpoint of laser sensing of minor gaseous components (MGC) in the atmosphere.

The differential absorption lidar (DIAL) method based on the effect of resonant laser radiation absorption by gases is most widespread among the methods of laser sensing of gaseous atmospheric components. The effect of resonant laser radiation absorption has a maximum interaction cross section in comparison with other phenomena (Raman scattering and resonant fluorescence) used to determine gaseous composition of the atmosphere. To find CO-laser wavelengths suitable for sensing of the atmospheric MGC by the DIAL method, we used the justified criteria for line selection. The informative wavelengths of the substances N_2O, NO_2, H_2CO, CH_4, C_2H_2, HCl, HF, HBr, and HCN for lidar technique have been found. Numerical modeling of lidar measurements of atmosphere MGC using wideband CO laser was carried out.

To retrieve wavelengths informative for MGC sensing by strontium laser we used the same technique. Results of these calculations demonstrates that it is rather difficult to use some of the strontium laser lines in base methods of gas analysis of the atmosphere because of the strong interfering component caused by the radiation absorption by water vapor. However, alongside with lines whose radiation is completely absorbed on the path 1 km long, there are lines in the Sr laser spectrum that fall within the atmospheric transparency micro-windows and can be used for remote sensing by DIAL. Strong water vapor absorption lines centered at 2.69 and 2.92 μm are promising for measurements of humidity profiles in the atmosphere on paths of 10-100 m. As demonstrated the calculated results, the strontium laser line around 3 μm can be used to detect HCN emissions on a level of 0.1 ppm using paths 1 km long.

As a whole, our calculations have confirmed that the wideband CO and Sr vapor lasers are promising for remote laser sensing of the atmospheric minor gaseous components by the differential absorption lidar method.

This work was supported in part by the Russian Foundation for Basic Research (grants Nos. 07-05-00765-a and 09-05-99035-r_ofi).

Femtosecond pulse self-compression under filamentation of collimated beam

Maria Kurilova, Anna Mazhorova, Nikolai Panov, Stepan Gorgutsa, Daria Uryupina, Roman Volkov, Olga Kosareva, and Andrei Savel'ev
International Laser Centre & Faculty of Physics, Lomonosov Moscow State University, Leninskie gory, Moscow, 119991, Russia
e-mail: kuma_hotel@mail.ru

Few cycle high peak power optical pulses are extensively exploited now in various area of research including attosecond science, high harmonic generation, non-adiabatic laser-matter interaction, etc. Recently it was shown that self-compression down to 8–10 fs without external dispersion compensation could be achieved by loosely focusing of 30–50 fs 30–50 GW 800 nm pulses in noble gases ([1,2,3]). In [4] the new approach was introduced and numerically backed in which self-compression takes place from the initially collimated beam instead of the focused one. Now we exploited this scheme and achieved more than threefold compression of 55 fs 80 GW laser pulses with high energy efficiency and shot-to-shot stability. We traced pulse shape and spectrum changes along the filament in dependence on laser pulse parameters, diameter of the diaphragm inserted into the filament, as well as gas type and pressure and obtained optimal set of characteristics. Numerical simulations well reproduced experimental data and predicted how even higher compression could be achieved.

Single filament was created by 80 GW, 55 fs, 805 nm laser pulse at repetition rate of 10 Hz. To launch filamentation at the proper distance laser beam (M_2=1.8) was telescoped down to the diameter of 1.3 mm. The tube 2–4 m long filled with pure gas of variable pressure (argon, nitrogen, etc.) was placed at 0.5 m away from the telescope exit. We measured energy, temporal and spectral intensity distributions as well as spectral phase (using SPIDER technique) of the radiation passing through the aperture with diameter of 100-1000 □m placed at different positions along the tube.

At the optimal conditions (4.5 mJ input energy, no initial chirp, 0.85 atm Ar pressure, 300 m diaphragm located 2 m apart from the 0.6 mm thick input silica window of the tube) we obtained 0.3 mJ, 15 fs pulse having good shot-to-shot stability and nearly flat spectral phase (phase deviation not more than 0.2 rad). The compressed pulse has the flat spectral phase with substantial suppression of pre- and post-pulses. Even higher compressed pulse energy of 3-3.5 mJ was obtained when 700 m aperture was used. Simultaneously the pulse lengthens to 23 fs. At the above mentioned optimum conditions pulse temporal envelope shows remarkable stability. At the pressure ~0.8—0.9 atm we managed to reach both the shortest duration of the self-compressed pulse and the best stability of its duration. The same figure contains numerical data demonstrating that even sub 5 fs pulse can be produced with 100 m aperture, but it implies much higher beam pointing stability for stable pulse compression.

References

1 G. Stibenz, N. Zhavoronkov, G. Steinmeyer, □Self-compression of millijoule pulses to 7.8 fs duration in a white-light filament□, *Opt. Lett.,* **31**, 274 (2006).
2 C.P. Hauri., A. Trisorio, M. Merano, G. Rey, R.B. Lopez – Martens, G. Mourou □Generation of high-fidelity, down chirped sub-10fs mJ pulses throught filamentation for driving relativistic laser-matter interactions at 1 kHz□, *Appl. Phys. Lett.*, **89**, 151125 (2006).
3 A. Zaïr1, A. Guandalini, F. Schapper, M. Holler, J. Biegerti, L. Gallmann, U. Keller, A. Couairon, M. Franco, A. Mysyrowicz, □Spatio-temporal characterization of few-cycle pulses obtained by filamentation□, *Opt. Exp.,* **15,** 9, 5394 (2007).
4 O.G. Kosareva., N.A. Panov., D.S. Uryupina, M.V. Kurilova, A.V. Mazhorova, A.B. Savel'ev, R.V. Volkov, V.P. Kandidov, S.L. Chin, □Optimization of a femtosecond pulse self-compression region along a filament in air□, *Appl. Phys. B.,* **91**, 35 (2008).

Growth of Laser Crystals of $NaBi(WO_4)_2$-Nd^{3+}

A.Kholov, Kh.Muminov

Physical-Technical Institute, Academy of Sciences of the Republic of Tajikistan, 299/1 Aini Ave, Dushanbe 734063, Tajikistan

Main author email address: khikmat@inbox.ru

One of the primary goals of creation of new laser systems is development of enough cheap and simple technologies of the laser crystals growth, capable to provide their wide production. Monocrystals of molybdates (and wolframates) of alkaline elements with bismuth are the material which can be received by crystallization in platinum crucible on air by use of Tchochralsky method. In the present work on the basis of the developed technology an opportunity of reproduced growth of large (diameter up to 55 mm and length 150 mm) of optically homogeneous crystals of $NaBi(WO_4)_2$ -Nd^{3+} has been shown. Growth of the crystals of $NaBi(WO_4)_2$-Nd^{3+} has been conducted bu Tchochralsky method on the installation with high-frequency heating with platinum crucibles of the diameters of 50, 70, 80 mm. Initial furnace was prepared from industrial reactants Na_2CO_3, i_20_3, $W0_3$ and Nd_20_3 of CDA mark, their synthesis has been conducted at a temperature of 750° during 5 hours at air. In order to acieve a high optical quality of the crystals of $NaBi(WO_4)_2$-Nd^{3+} the prepared by this method furnace has been twice recrystallized. Alloying impurity was entered as a compounf Nd_2O_3. Crystals with concentration from 0.5 up to 3.0 mol.% that corresponded to the concentration Nd^{3+} from $0.6x510^{20}$ cm"^{3} up to $3.9\square10^{20}$ cm"^{3}. To grow an optical homogeneous crystals mass speed of crystallization should not exceed 40 g/hour. Growth of laser crystals of $NaBi(WO_4)_2$ was conducted along a direction [001]. At convex at a melt direction of the front of crystallization ions are non-uniformly distributed on the section of a crystal. For elimination of this defect conditions of growth of $NaBi(WO_4)_2$-Nd^{3+} with flat front of crystallization were chosen. It was achieved, first, due to reduction of a heat-conducting path on a crystal for what the active platinum screen above a crucible with melt was used, and, second, due to increase of heat transfer from a melt to front of crystallization for what speed of rotation of a crystal was increased up to 100 rev/min. In the work distribution of alloying impurity Nd^{3+} and the basic components along the grown crystals $NaBi_{l\_x}Nd_x(WO_4)_2$ was investigated. The mechanism of entry of ions of Nd^{3+} in to the lattice of $CaWO_4$ is established on the basis of the data of the micro-X-ray analysis. It is shown, that concentration of the basic components varies a little bit (in the limits of 1 %). Concentration of Nd^{3+} decreases on length of a crystal that corresponds to reduced the factor of distribution Nd≈1.3. Thus, by the melt method tetragonal disordered crystals $NaBi(WO_4)_2$-Nd^{3+} were grown and some technological features of this process were studied.

Laser Heating Method for Monocrystal Growth from Melt

A.Kholov, Kh.Muminov

Physical-Technical Institute, Academy of Sciences of the Republic of Tajikistan,
299/1 Aini Ave, Dushanbe 734063, Tajikistan

Main author email address: khikmat@inbox.ru

.Among beam sources of heating the special prospect has the laser heating described by high temporal and spatial radiation coherency. Namely the high coherence distinguishes laser heating from other kinds of heating. Spatial coherence provides very high orientation of radiation, creating such high density of energy in unit of volume which cannot be received by use of thermal radiation. As it is known, lasers represent a unique opportunity to penetrate to a mix consisting of many compounds and selectively conduct only one reaction, not mentioning other elements. In the previous works [1-2] development of methods of monocrystal growth at high temperatures from melt by laser heating and its advantage is in part reflected. In this paper we study the use of laser heating for additional changes of a local gradient of temperature directly near to the border of crystal-melt and study of morphology of a surface of front of crystallization. It is known, that the important parameters influencing on to the defective structure of a lattice and the form of crystals at the growth by Tchochralsky method are the melt temperature, growth rate and a gradient of temperature on the border of division a crystal - melt. The form of front of crystallization is determined by a ratio of temperature gradients in the melt, above melt and in a crystal; a heat-conducting path; thermal properties of a melt and a crystal; a ratio of speed of pull up and rotations of a crystal. At influence of a laser beam change convection streams in a melt and change of the form of front of crystallization is visible. As a result of experiments monocrystals of yttrium-aluminium garnet with use of laser influence for additional local heating and without it were received.The grown crystals were investigated by microscope on a gleam and it is confirmed, that at use of local laser heating the form of front of crystallization changes.

References

1 Kh. S. Bagdasarov, V.V. Dyachenko, A.M. Kevorkov, A. Kholov. In the collected papers "Crystal growth", Moscow, Nauka, 1980, p. 314 (in Russian)
2 Kh. S. Bagdasarov, V.V. Dyachenko, A. Kholov. Crystallography, 1979, v. 24, no. 6, p. 1303 (Russian journal)
3 Kh. S. Bagdasarov, A. Kholov. Proceedings of the Academy od Sciences of the Rep. Tajikistan., 1981, n. 1, p. 24

Growth and structural pecularities of the epitaxial films of GaSe and InSe in correlationN with the electrophysical properties

E. Yu. Salaev, H. R. Nuriyev
Institute of Physics Azerbaijan National Academy of Sciences, *370143 Baku*, *Azerbaijan*

Layered chalcogenide materials of GaSe- type (Gallium Selenide) are well known as one the outstanding materials for nonlinear optical applications. GaSe is a highly anisotropic material, which consists of thin layers of covalently bond gallium and selenium atoms with a thickness of four atoms. Between the layers, weak forces of van der Waals type are present, whereas in the stacking direction (along the crystallogrphic z- axis which is in the direction of the optical c- axis), the layers can be arranged in different ways, whic leads to the existence fo different polytypes. For modifications have been described in the literature [1]. Most investigated is the noncentrosymmetric ε- modificatrion, which consists of 2 layers per unit cell. It belongs to space group D_{3h}^{1}.

Bulk properties of GaSe crystals are well invetsigated [1], whereas less have been done concerning epitaxially grown thin films.

The peculiarities of formation and the structure of the epitaxially grown thin films of GaSe and InSe (Indium Selenide) has been investigated in the present work. The method used included the standard vacuume evaporation system by using the method of the molecular beams and previously synthesized polycrystalline materials (GaSe and InSe). Growth were performed at different conditions by using different substrate. Optimal conditions for formation of oriented amorphous, polycrystalline and epitaxial films were determined. Structural, electrical and optical properties of grown f'ilms were measured.

The domain structure of grown films is discussed as studied by confocal Raman microscopy experiments. The results are compared with the confocal Raman spectra of bulk crystals. Photolumiscence spectra due to defect and also from surfaces of the films are observed and discussions are rpesented in this report. Raman scattering spectra are analyzed and compared with that fro bulk crystals.

Strong second harmonic signals (excitation by 1.06 μm line of YAG:Nd laser) say ina favour of perspective to use thin films of Gase in nonlinear optical devices.

Refernces

1. K. Maschke, F. Levy, in: S. Flugge (Ed.), New Series, Group III: Crystal and Solid State Physics, 17, Springer-Verlag, Berlin, 1983.
2. K. R. Allakhverdiev, M. Ö. Yetis, S. Özbek, T. K. Baykara, E. Yu. Salaev, ″Effective Nonlinear GaSe Crystal. Properties and Applications″, *Laser Physics*, **19**, 1092 (2006).

Light Emission from Silicon Nanoclusters in Silicon Suboxide Matrix

V. Yu. Timoshenko[1,2], D. M. Zhigunov[1], N. E. Maslova[1], S. A. D'yakov[1], P. K. Kashkarov[1,2], V. N. Seminogov[3], V. I. Sokolov[3], V. N. Glebov[3], and V. Ya. Panchenko[2,3]

[1] *M.V.Lomonosov Moscow State University, Physics Department, 119991 Moscow, Russia*

[2] *Russian Research Center "Kurchatov Institute", 123182 Moscow, Russia*

[3] *Institute on Laser and Information Technologies RAS, 142190 Troitsk, Russia*

Silicon nanocrystal (nc-Si) structures are known to be light-emitting under optical or electrical excitation. One of the methods of nc-Si structure preparation is SiO_x ($1<x<2$) thin layer deposition and subsequent high temperature annealing [1,2]. The nc-Si formation occurs at the annealing temperatures higher than some critical one, while at lower temperatures presumably amorphous nanoclusters grow [3]. In our work the structure and optical properties of thermally annealed SiO_x ($x\sim1$) films were investigated using transmission electron microscopy (TEM) and spectroscopic methods of infrared absorption, Raman scattering and photoluminescence (PL).

The reactive evaporation of SiO powder was used to grow 500 nm SiO_x films on quartz and sapphire substrates. The deposited films were then annealed in N_2 atmosphere at temperatures (T_a) ranged from 350 °C to 1200 °C. The samples annealed at $T_a<950$ °C exhibit the Raman scattering band at about 480 cm^{-1}, which is typical for amorphous Si. The Raman line at 519 cm^{-1} is detected for the samples annealed at $T_a=950$ °C that indicates the formation of nc-Si. The intensity of the peak at 519 cm^{-1} grows with increasing T_a, which can be explained by an expansion of the nc-Si fraction in SiO_x matrix. It should be noted that the maximum of the Raman spectra of nc-Si is shifted down as compared with 520.5 cm^{-1} peak position for the bulk crystalline Si. This shift is usually attributed to the phonon confinement in nc-Si with sizes of 3- 4 nm. The Raman scattering analysis agrees with the TEM data.

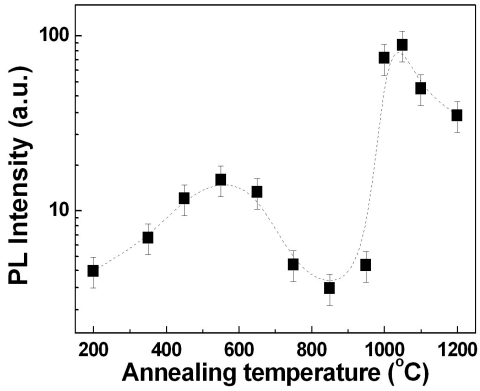

Fig. 1. Dependence of the PL yield of Si nanoclusters on annealing temperature.

It was found that PL intensity of SiO_x films depends non-monotonically on T_a, namely two PL intensity maxima were observed at 600 °C and 1100 °C. The first one can be attributed to the formation of amorphous nanocluster network [4], while $T_a = 1100$ °C is sufficient to grow a large amount of nc-Si. The samples annealed at $T_a \geq 950$ □□ show the PL spectra at 1.3-1.4 eV, which are typical for nc-Si with mean sizes of about 4 nm. The PL of nc-Si is usually attributed to the radiative recombination of excitons confined in nc-Si. The annealing at $T_a > 1100$ °C was found to give a decrease of the PL intensity of nc-Si. This fact can be explained by the exciton migration through the nc-Si network. In general, the observed modifications of the Raman and PL spectra of SiO_x films are explained by a model of the structure transformations of silicon-rich suboxide, which result in growth of amorphous or crystalline nanoclusters in SiO_2 matrix. The samples with nanocluster network can be recommended for applications in Si-based light emitting devices excited by electrical current.

This work is supported by the Russian Foundation for Basic Research (grants # 08-02-01041-□) and by the Ministry of Education and Science of the Russian Federation.

Quantum cascade laser spectrometers for atmospheric gas detection

Virginie Zeninari

Groupe de Spectrométrie Moléculaire et Atmosphérique (GSMA), UMR CNRS 6089,
Université de Reims Champagne-Ardenne (URCA), Faculté des Sciences,
BP 1039, F-51687 Reims Cedex 2 – France
Tel. +33.3.2691.8788, Fax. +33.3.2691.3147
virginie.zeninari@univ-reims.fr

Since the first realization of a quantum cascade laser, many applications have been studied: communications, detection and quantification of trace gases, and high-resolution spectroscopy. Continuous-wave distributed feedBack quantum cascade lasers have demonstrated to be high-performance tools for the study of the atmosphere: their powerful emission in the mid-infrared permit to develop spectrometers' capabilities thanks to the presence of fundamental absorption bands of most of the molecules. I will report the development of several spectrometers and the results obtained with various quantum cascade lasers emitting from 5 to 10 µm.

The powerful emission of quantum cascade lasers in the mid-infrared is of great interest for photoacoustic spectrometry where the photoacoustic signal is proportional either to the laser power and to the absorption coefficient of the gas. Various quantum cascade lasers may be used in conjunction with a photoacoustic spectrometer without changing any part of the spectrometer except the laser. Results on CH_4 and N_2O detection in the 8 µm region [1,2] and on NO detection in the 5.4 µm region [3] will be presented. The quantum cascade lasers have also been demonstrated to be excellent local oscillators when using a heterodyne radiometer. Results on measurements around 10 µm of atmospheric ozone concentrations from the ground have been realized and will be presented [4]. Finally, quantum cascade laser direct-absorption spectrometers can be used in order to measure atmospheric concentrations of the main atmospheric constituents involved in the greenhouse gases effect. Results on H_2O around 6.7 µm [5] and CH_4 and N_2O around 8 µm [6] will be presented.

References

1 A. Grossel et al, Spectrochimica Acta Part A, **63**, 1021-1028 (2006).
2 A. Grossel et al, Applied Physics B: Lasers and Optics, **88**, 483–492 (2007).
3 A. Grossel et al, Infrared Physics and Technology, **51**, 95-101 (2007).
4 B. Parvitte et al, Spectrochimica Acta Part A, **60**, 3285-3290 (2004).
5 L. Joly et al, Optics Letters, **31**, 143-145 (2006).
6 L. Joly et al, Applied Optics, **47**, 1206-1214 (2008).

Sunscreen-grade Nanoparticles: Aspects of Interaction with Skin

A.P. Popov[1,2], A. Zvyagin[3], M.S. Roberts[4], J. Lademann[5], A.V. Priezzhev[1], and R. Myllyä[2]
[1]*International Laser Center, M.V. Lomonosov Moscow State University, Moscow, 119992, Russia*
[2]*University of Oulu, Department of Electrical Engineering, Optoelectronics and Measurement Techniques Laboratory, P.O. Box 4500, FI-90014, Oulu, Finland*
[3]*Macquarie University, Department of Physics, Centre of MQ Photonics, Sydney NSW 2109, Australia*
[4]*University of Queensland, School of Medicine, Therapeutics Research Unit, Princess Alexandra Hospital, Australia*
[5]*Center of Experimental and Applied Cutaneous Physiology, Department of Dermatology, Universitätsmedizin-Charité Berlin , D-10117 Berlin, Germany*
Main author email address: dwelle@rambler.ru

Zinc oxide (ZnO) and titanium dioxide (TiO_2) nanoparticles are widely used in skin care products such as sunscreens. Although such products have been in use for many years, effects of sunscreen nanoparticles on human health are highly debated nowadays. There are, e.g. fears about particle penetration into viable layers of skin through stratum corneum after multiple applications of sunscreens onto body surface. Due to small particle sizes (at a range of tens of nanometers) these concerns are to be addressed. Size also matters if UV protection is considered: not all the sizes are equally attenuating. And the third issue we report here is comparison between amounts of free radical generated by nanoparticles and skin under UV irradiation.

In order to reveal in-depth distribution of nanoparticles in skin, X-ray fluorescence in combination with consecutive tape stripping (for TiO_2) and multiphoton microscopy (MPM) imaging (for ZnO) were used. We show that ZnO nanoparticles rubbed for 5 min into human skin, stayed in the stratum corneum and accumulated into skin folds and/or hair follicle roots of human skin not reaching epidermis within 24 h. TiO_2 nanoparticles after multiple applications within four days were also detected within stratum corneum and in hair follicles (1%) so that most of them were located superficially within the depth of 2-3 μm.

In order to simulate the propagation of UV light within the stratum corneum with embedded TiO_2 (or Si) particles the Monte Carlo method implemented in a developed computer 3D code was applied. The computational model of the stratum corneum consists of an infinitely wide plain layer, the upper part of which (1-μm-thick) contains TiO_2 (or Si) particles. The total thickness of both parts is 20 μm, which corresponds to the real dimension of this skin layer on the back and arms; only the palms and soles have thicker stratum corneum (up to 150 μm) because of more intensive use of hands and feet.

For radical-revealing experiments ears of freshly slaughtered domestic pigs were used. The samples were UV-irradiated immediately after preparation. Even with statistical errors taken into account, the effect of UV irradiation is clearly seen in all cases (the points corresponding to such samples are located below the non-irradiated); the magnitude of the effect is almost the same for all samples. This means that the amounts of short-lived free radicals appearing under UV irradiation are comparable and do not depend on the presence of the particles on the skin surface. In other words, the contribution of skin to free-radical generation under UV irradiation exceeds that of the particles.

Our research focused on effects on nanoparticels-skin interactions shows that TiO_2 mineral compound of sunscreens is not an issue of concerns so far. Even after multiple applications of sunscreens, the particles are localized superficially and their radical production ability does not surpass that of porcine skin *in vitro*. However, the latter effect could be more distinct under *in vivo* conditions; applicability of the result to human skin is still to be elucidated.

Authors thank Russian Fund for Basic Research (project No. 07-02-01000).

Powerful few cycle optical pulse production and new spectral component formation under filamentation in gases

Maria Kurilova, Anna Mazhorova, Daria Uryupina, Nikolai Panov, Grigory Golovin, Stepan Gorgutsa, Roman Volkov, Olga Kosareva, and Andrei Savel'ev
International Laser Centre & Faculty of Physics, Lomonosov Moscow State University, Leninskie gory, Moscow, 119991, Russia
e-mail: ab_savelev@phys.msu.ru

Few cycle high peak power optical pulses are extensively exploited now in various area of research including attosecond science, high harmonic generation, non-adiabatic laser-matter interaction, etc. Recently it was shown that self-compression down to 8–10 fs without external dispersion compensation could be achieved by loosely focusing of 30–50 fs 30–50 GW 800 nm pulses in noble gases. Filaments created during propagation of an ultrashort laser pulses in gases and solids combine high non-linearity with huge intensity and long interaction path. Different non-linear processes were observed such as four-wave mixing, coherent Raman scattering, third harmonic production, etc.

In [1] the new approach was introduced and numerically backed in which self-compression takes place from the initially collimated beam instead of the focused one. Now we exploited this scheme and achieved more than threefold compression of 55 fs 80 GW laser pulses with high energy efficiency and shot-to-shot stability. We traced pulse shape and spectrum changes along the filament in dependence on laser pulse parameters, diameter of the diaphragm inserted into the filament, as well as gas type and pressure and obtained optimal set of characteristics. Numerical simulations well reproduced experimental data and predicted how even higher compression could be achieved.

The radiation spectrum inside the filament undergone impressive changes along the propagation path. In particular we observed new spectral component on the red side of the initial spectrum. Spectral shift of this component increases along the filament up to 100 nm from the initial wavelength of 800 nm at the distance of 4 m. In the filament core (approximately 300 m in diameter) this new component amplitude was much higher as compared to the spectral amplitude at the fundamental frequency. Energy of this component was as high as 2 mJ (700 m aperture) while its duration was estimated as 50–70 fs from the SPIDER measurements. The newly generated spectral components at the red side of the fundamental spectrum take part in the four-wave mixing processes in the filament. As a result new components arise also at the red side of the spectrum.

Hence spectral transformation of collimated radiation undergone filamentation in molecular gases differs drastically from that in noble gases. In particular we did not observed prominent spectral broadening toward blue side in the filament core that is specific for filamentation in noble gases. It is this broadening that provides for efficient self-compression of femtosecond laser pulses down to few optical cycles.

References

1 O.G. Kosareva., N.A. Panov., D.S. Uryupina, M.V. Kurilova, A.V. Mazhorova, A.B. Savel'ev, R.V. Volkov, V.P. Kandidov, S.L. Chin, "Optimization of a femtosecond pulse self-compression region along a filament in air", *Appl. Phys. B.,* **91**, 35 (2008).

CW and pulsed lasers based on Er-doped GTWave fiber

A.S.Kurkov[1], A.I.Ivanenko[2], S.M.Kobtsev[2], S.V.Kukarin[2].
[1]*General Physics Institute of the Russian Academy of Sciences, 119991, Vavilov St. 38, Moscow, Russia, Fax: +7 499 135-027*
[2]*Novosibirsk State University, 630090, Novosibirsk, Pirogov St. 2.*
E'mail: kurkov@kapella.gpi.ru

GTWave active fiber is a modification of the cladding pumped fibers allowing one to use high power pump sources. GTWave fiber constitutes a collection of the fiber with an active core and passive multimode fiber in the general polymer coating with a refractive index lower than that for silica glass. In this design a pump power is delivered through the passive fiber that makes this medium comfortable for the applications in lasers and amplifiers. Typically, the active fiber contains Yb-ions. To get a high power emission in the range of 1.55 μm, fibers co-doped by Er- and Yb-ions are used. In this paper we suggest to use Yb-free Er-GTWave fiber lasers. The fiber had an active core diameter of 20 micron with absorption of the pump emission at 975 nm of approximately 1 dB/m. This fiber was used as an active medium of CW and pulsed lasers.

To build CW laser we have used 10 m of GTWave fiber. A multimode Bragg grating was used as the input laser reflector and the cleaved fiber end – as the output reflector. The Bragg grating was arranged between the source pigtail and the taper. Resonance wavelength was chosen near 1.6 micron to prevent the signal reabsorption. A laser oscillation was observed starting from a threshold pump power of 2.3 W. A maximum output power of 1.2 W was achieved for the pump power of 5.5 W. Slope efficiency was measured as 35%.

To get the pulsed oscillation we have used a ring laser cavity composed of Er-doped GTWave fiber, standard fiber to compensate the chromatic dispersion, isolator, polarization controller and polarization beam splitter. An effect of the non-linear polarization rotation was exploited to get mode-locking regime. Under pumping at 975 nm the stable pulse train with an average output power up to 250 mW was observed. The measured pulse duration was not more than 270 fs with a repetition rate of 14 MHz. Maximum pulse energy has achieved 20 nJ and pulse energy – 65 kW.

The same Er-doped fiber was used to amplify the realized pulsed train. We have applied the fiber piece with a length of 14 m and a pump power up to 12 W. As result the output power was increased up to 2 W with a rise of the pulse duration up to 360 fs. Maximum pulse energy was increased up to 150 nJ and pulse energy – 450 kW without any spectrum broadening under amplification.

Then for the first time we have applied Er-doped GTWave fiber to build two laser types and amplifier. Our results have shown that such fibers are promising for the application as an active medium for CW and pulsed fiber laser.

A cw Tm,Ho:YLF laser pumped by Raman erbium fiber laser at 1675 nm

Yu. L. Kalachev, V. A. Mihailov, V. V. Podreshetnikov, I. A. Shcherbakov

A.M. Prokhorov General Physics Institute, RAS, 38 Vavilov street, 119991 Moscow, Russia

One of the promising method of Tm,Ho:YLF pumping is using of absorption band near 1682 nm corresponding to the $^3F_4$ manifold of Tm^{3+} ions. In the previous work [1] the self-made liquid nitrogen cooled tunable Co:MgF_2 laser was used for such kind of pumping. In this paper we present results of experimental investigations of Tm,Ho:YLF laser pumped at fixed wavelength 1675 nm by a 3 W Raman erbium fiber laser. The main advantages of this commercially available laser are single mode of operation, polarized emission and high stability of output power. Besides a fiber coupled diode laser array lasing at 795 nm was used for comparison.

The uncoated a-cut Tm,Ho: YLF active element (AE) with 5% Tm^{3+} and 0,5% Ho concentrations had dimensions 5 x 5 mm in cross section and 2 mm in length. The AE was hold in the copper heat sink keeping at room temperature. Pump spot sizes inside AE for Raman fiber laser and diode laser were about 100 mm. Laser cavity of length from 5 to 20 mm was formed by flat 100% mirror and output coupler with radius of curvature ~ 50 mm and reflectivity ~ 97%. AE was placed perpendicular to the cavity optical axis.

Lasing took place at 2…4 wavelengths near 2.052 mm with linewidth <0.5 nm each. Output power up to 450 mW was obtained with total and slope efficiencies ~ 45 % and 50% respectively. Slightly lower results were obtained under diode pumping. For comparison, slope lasing efficiency under pumping by Co:MgF_2 laser [1] was 59% at 200mW output power.

Benefit of Raman erbium fiber laser as a pumping device become apparent in such fields of applications where there is necessity to use AE with small (< 2%) Tm-ions concentration. In this case traditional pumping in absorption band $^3H_4$ near 795 nm is not effective due to lack of cross relaxation effect in Tm^{3+}.

References

[1]. Cornacchia F., Di Lieto A. , Maroni P., Minguzzi P., Toncelli A., Tonelli M., Sorokin E., Sorokina I., "A cw room-temperature Ho, Tm:YLF laser pumped at 1.682 □m" Appl. Phys. B **73**, N3, pp. 191-194 (2001)

Three-Dimensional Acousto-Optic Mapping in Tissue Mimicking Phantoms Using Heterodyne Light-Scattering Spectroscopy.

A. Bratchenia [1], R. Molenaar[1], R.P.H. Kooyman[1]
[1] *University of Twente, Faculty of Science & Technology, Institute of Biomedical Technology, PO Box 217, NL-7500 AE Enschede, the Netherlands*

Main author email address: a.bratchenia@tnw.utwente.nl

We have used acousto-optic modulation of scattered light to investigate the possibility of three-dimensional mapping of tissue mimicking phantoms with a resolution of a few millimeters. The phantom under investigation mimicked the blood vessel surrounded by tissue. For that purpose we used a silicon rubber tube embedded in an Intralipid based gel (μ_s=1.5 cm^{-1}). We have applied the acoustic pressure in a predefined volume of phantom by insonifying it with a microsecond length ultrasound bursts. The insonificaton in combination with irradiation of the phantom with a microsecond length light pulses resulted in the localized acousto-optic modulation of phase of scattered light in hat volume. The detection technique, based on the parallel speckle detection in the transmission mode, allowed us to quantify the ratio of the modulated light intensity over unmodulated intensity. The measured modulation depth depends on the absorption coefficient of tissue phantom in the focal volume of the ultrasound beam. By varying the delay time between ultrasound burst initiation and light pulse initiation we could perform a scan in the ultrasound-propagation direction. By moving the ultrasound transducer in a plane perpendicular to ultrasound-propagation, we could build up a volumetric map of modulation depth values. We have experimentally determined the acousto-optical modulation depth in phantom volume voxels, and we have compared these results with those obtained from diffusive optical imaging simulations. The simulations were based on the finite elements method solution of the diffusion approximation of the radiation transfer equation. We have reconstructed the image of the tube with absorber with a spatial resolution of a few millimeters. The use of calibration curves allowed us to extract quantitative information on dye concentration in the tube. Our findings demonstrate the outlook to apply this technique for non-invasive three-dimensional mapping of local absorbances in turbid media by means of acousto-optic modulated light scattering spectroscopy.

Compact Raman Spectrometer for the Active Test of Liquid and Solid Samples

K. Allakhverdiev [1,3], T. Baykara [1], A. Secgin [1], S. Ozbek [1], A. Ulubey [4], Z. Salaeva [1], F. Huseyinoglu [1], S. L. Druzhinin [2] K. A. Konovalov [2], O. N. Smirnov [2], V. Y. Shchagin[2], S. Yu. Strakhov [2**]

[1] *TÜBITAK, Marmara Research Center, Materials Institute, P.K. 21, 41470 Gebze/Kocaeli, Turkey*

[2] *Laser Systems Ltd., Krasnoarmeyskaya str., 1, 190005, Saint-Petersburg, Russia*

[3] *Institute of Physics ANAS, 370143, Baku, Azerbaijan*

[4] *University of Thrace, Faculty Art and Science, Department of Physics, 22030 Edirne, Turkey*

E-mail: *Alper.Secgin@mam.gov.tr ** Strakhov@lsystems.ru

Fax: (+90 262 641 23 09)

The advantages of optical techniques for contactless probing of objects with respect to their quality and purity are manifold; for example they possess a reasonable resolution, they are non-perturbing and easily movable.

Raman spectroscopy takes advantage of the inelastic scattering of laser light by molecules. Laser energy is exchanged in such a way that the scattered photons have higher or lower energy when comparing with the incident energy. Since different molecules show different energy changes, the Raman effect have found a wide application as a qualitative or quantitative analysis method.

In the present report the compact Raman spectrometer for remote detection of liquid and solid samples has been developed. The spectrometer is intended for active analysis of liquid and solid samples in different environmental conditions, including food samples checking and narcotics and explosives spreading.

The spectrometer consists of the block for spectral analysis, two lasers, two fiber-optical sensors and sampling probe and can work with two types of laser sources without reconfiguration the optics and lasers. It includes also narrow-line-width/frequency stabilized 785 nm laser.

Scattered radiation via fiber enters the spectral block. Raman spectrum is separated in 4096 receiver components (pixels) by help of the TEC- regulated CCD array. Developed spectrometer can operate by accumulator battery and is considered as portable. The spectrometer is capable to detect the spectral coverage in the range between 150 and 4000 cm^{-1} and may be used for liquids (including water solution, alcohol, different types of gasoline) and solids (including pills, powders, explosives and drugs) analysis.

Our fully integrated Raman system provides a portable instrument with the best performance and quality and may be used for: chemical analysis for various substances identification and authentication; academic research and industrial laboratories.

Range of applications of the developed Raman system includes: forensics; pharmaceuticals; real time reaction monitoring and process control; gemotology; recycling; semiconductors; microwave assisted synthesis.

Polarization-resolved study of passively Q-switched diode-pumped Nd:YVO_4 lasers with Cr^{4+}:YAG and V^{3+}:YAG saturable absorbers

A.A. Sirotkin, D.V. Sizmin, S.V. Garnov
Prokhorov General Physics Institute of the Russian Academy of Sciences,119991, Vavilov 38, Moscow, Russia
E-mail: saa@kapella.gpi.ru

We have experimentally investigated the operation of diode-pumped passively *Q*-switched Nd:YVO_4 lasers with either *a*-cut (π- and □-polarization) and *c*-cut Nd:YVO_4 crystals and compared their relative advantages and drawbacks.

By using the natural birefringence of an *a*-cut Nd:YVO_4 crystal, we experimentally investigate laser operation under different light polarizations (π- and □-polarized emissions) and compare their performance. The laser performance is further compared with a diode-pumped *c*-cut Nd:YVO_4 laser of the same parameters. It is known, that too large emission cross-section of vanadate crystals is a shortcoming for Q-switched lasers, because it limits their energy-storage capacity, leading to smaller pulse energies [1]. Usial methods to avoid this drawback are to use *c*-cut crystals [2-3] or mixed vanadates Nd:$Gd_xY_{1-x}VO_4$. Laser operation under different light polarizations investigated for Nd:$GdVO_4$ [5]. However C-cut vanadate crystals have nonpolarised radiation and wavelengths distinct from a-cut crystals [6].

Two Cr^{4+}:YAG and V^{3+}:YAG saturable absorbers, one with initial transmission *85* % and the other with *9*0%, oriented with their normal along the (111)-crystal axis, were used as the passive *Q* switch.

We have shown experimentally that the *c*-cut Nd:YVO_4 laser could have good passively *Q*-switched performance in a low-pump-power region but the best passively *Q*-switched performance obtained in our experiments is from the *a*-cut □-polarized laser, which gives the narrowest pulse of 9 ns with the highest peak power of 2 kW. In addition *a*-cut □-polarized vanadate crystals have the polarized radiation, and wavelengths of radiation coincide with a-cut π-polarized emission. It allows creating effective master oscillator-amplifier systems.

References

1. X. Y. Zhang, S. Z. Zhao, Q. P. Wang, Q. D. Zhang, L. K. Sun, and S. J. Zhang, "Optimization of Cr4_-doped saturable absorber Q-switched lasers," IEEE J. Quantum Electron. **33**, 2286–2294 (1997).
2. Y. F. Chen and Y. P. Lan, "Comparison between c-cut and a-cut Nd:YVO4 lasers passively Q-switched with a Cr4_:YAG saturable absorber," Appl. Phys. B **74**, 415–418 (2002).
3. J. Liu, J. M. Yang, and J. L. He, "Diode-pumped passively Q-switched c-cut Nd:GdVO4 laser," Opt. Commun. 219, 317– 321 (2003).
4. J. Liu, Zh. Wang, X. Meng, Z. Shao, B. Ozygus, A. Ding, H. Weber, "Improvement of passive *Q*-switching performance reached with a new Nd-doped mixed vanadate crystal Nd:$Gd_{0.64}Y_{0.36}VO_4$", Opt. Lett. **28**, 2330-2332 (2003)
5. S. P. Ng, D. Y. Tang, L. J. Qin, X. L. Meng, and Z. J. Xiong, «Polarization-resolved study of diode-pumped passively Q-switched Nd:GdVO4 lasers». Appl. Opt. . **45**, 6792– 6797 (2006).
6. A.A. Sirotkin, L. Di Labio, A.I. Zagumennyi, Yu.D. Zavartsev, S.A. Kutovoi, V.I. Vlasov, W. Lüthy, T. Feurer, A.A. Onushchenko, I.A. Shcherbakov, "Mode-locked diode-pumped vanadate lasers operated with PbS quantum dots", Appl. Phys. B., **94**, 375-379 (2009).

THz source based on two-color diode-pumped C-cut vanadat lasers and GaSe nonlinear crystal

A.A. Sirotkin, S.V. Garnov, A.I. Zagumennyi, Yu.D. Zavartsev, S.A. Kutovoi, V.I. Vlasov, I.A. Shcherbakov
Prokhorov General Physics Institute of the Russian Academy of Sciences,119991, Vavilov 38, Moscow, Russia
E-mail: saa@kapella.gpi.ru

We have demonstrated a novel THz source based on Q-switch two-color diode-pumped solid state c-cut Nd:GdVO4 laser with Filter Lio as selective element and the GaSe nonlinear optical crystals as convertor. Terahertz radiation with wavelength 436 μm (0.56 THZ) was detected.

Terahertz-wave radiation has been wide used in THz spectroscopy, biomedical applications, DNA analysis and security applications. THz sources based on femtosecond Ti:Sapphire-laser and photoconductive antennas or nonlinear optical crystals which generate the THz radiation is extremely expensive and complex. One of alternative cost-effective and robust THz sources to use optical two-color light sources with THz converters. Difference frequency generation with photoconductive antennas or nonlinear optical crystals can be directly used to generate corresponding THz radiation. Such a two-color laser systems with THz convertors is probably the cheapest and the most compact sources for terahertz radiation.

Here, we present a THz source based on a novel two-color diode-pumped solid state c-cut $Nd:GdVO_4$ laser and the GaSe nonlinear optical crystals as convertor.

C-cut neodymium-doped vanadate crystals ($Nd:YVO_4$, $Nd:GdVO_4$, or mixed $YGdVO_4$) are efficient laser media and have a considerable potential to produce spectrally tunable radiation, two-frequency lasing and short pulse generation [1].

Two-color lasing has been obtained in the C-cut $Nd:GdV0_4$ and $Nd:YVO_4$ crystal at the spectral lines separated by 2.3 nm and 3.8 nm.

QW, mode-locking and Q-switching regimes with acoustic-optical modulators were realised .

Q-switching yielded 15-20 ns pulses with an average output power of 1.2 W at a repetition rate of 6-12 kHz. At 3 to 5 W of pump power the Q-sw - mode-locking laser produced a stable train of pulses with a pulse duration of about 30-40 ps FWHM and an output power of 340 mW at pulse repetition rate 140 MHz .

The use of GaSe crystal for the generation of pulsed THz radiation was demonstrated recently [2-3]. This crystal is excellent nonlinear optical element for difference-frequency generation (DFG). GaSe crystal has the lowest absorption coefficient in the THz spectral range and, furthermore, a large second-order nonlinear coefficient.

The two-color C-cut $Nd:GdV0_4$ and $Nd:YVO_4$ lasers served as an optical pump source. Laser emitted dual wavelength at 1063.2 nm and 1065.5 nm. After passing through lens the pump beam was focused in a GaSe crystal. The GaSe crystal is mounted on a rotational stage. The generated THz waves are combaned and separated from pump beams by two teflon lens and focused onto a piroelectric detector or an opto-acoustic detector. The THz signal from the detector is in turn low-noise voltage preamplifier SR560 and lock-in amplifiers SR830. A Si and black polyethylene plates are used to block the two pump beams.

Terahertz radiation with wavelength 436 mkm (0.56 THZ) was detected.

This work partially supported by RFBR grant 07-02-12109.

References

1. V.I. Vlasov, S.V. Garnov, Yu.D. Zavartsev, A.I. Zagumennyi, S.A. Kutovoi, A.A. Sirotkin, I.A. Shcherbakov "New possibilities of neodymium-doped vanadate crystals as active media for diode-pumped lasers", Quantum Electronics, **37** (10), 938-940 (2007)
2. W. Shi, Y. J. Ding, N. Fernelius, and K. Vodopyanov, "Efficient, tunable, and coherent 0.18 5.27-THz source based on GaSe crystal", Opt. Lett. **27**, 1454-1456 (2002).
3. W. Shi, M. Leigh, J. Zong, and S. Jiang, "Single-frequency terahertz source pumped by Q-switched fiber lasers based on difference-frequency generation in GaSe crystal", Opt. Lett. **32**, 949-951(2007).

1,3 μm passively Q-switched diode pumped lasers with Co^{2+} doped crystals as the saturable absorbers

A.A. Sirotkin, S.P. Sadovskiy, S.V. Garnov
Prokhorov General Physics Institute of the Russian Academy of Sciences,119991, Vavilov 38, Moscow, Russia
E-mail: saa@kapella.gpi.ru

Lasers with wavelength near 1.3 μm represent considerable practical interest in fiber-optical communication systems, in an optical location and others. One of simple and reliable ways to obtain the short pulses is the passive Q-switching, however in this spectral range the set of saturable absorbers is limited (YAG:V^{3+} [1], singlewall carbon nanotube [2], glasses with quantum dots [3]). Therefore research of saturable absorbers based on crystals doped by ions Co^{2+} is actual now.

As far as we know experimental investigations of diode pumped Nd:YAG (=1.31 μm), Nd:YVO_4 (=1.34 μm) and Nd:$GdVO_4$ (=1.34 μm) lasers on transition of Nd $^4F_{3/2}$-$^4I_{13/2}$, working in passively Q-switching with saturable absorbers crystals Co^{2+}:$MgAl_2O_4$ and Co^{2+}:GGG for the first time are presented.

We have obtain absorption spectrum this saturable absorbers.

Energy and temporal dependences for two type of a saturable absorbers, three active elements, and different resonator configurations are presented.

Pulse duration of 20 nanoseconds with average power 200 mW, pulse energy 18 mJ on frequency repetition rate - 2-20 kHz are reached.

This work partially supported by RFBR grant 07-02-12109.

References

1 M.J.Weber, L.A.Risenberg. Optical Spectra of Vanadium Ions in Yttrium Aluminum Garnet. // The Journal of Chemical Physics, V.55, N5, pp.2032-2038, (1971).

2 N N Il'ichev, E D Obraztsova, S V Garnov, S E Mosaleva, "Nonlinear transmission of single-wall carbon nanotubesin heavy water at a wavelength of 1.54 m and self-mode locking in a Er^{3+}: glass laser obtained using a passive nanotube switch», Quantum Electronics, **34** , p.572–574 (2004).

3 A.A. Lagatsky, C.G. Leburn, C.T.A. Brown, W. Sibbett, A.M. Malyarevich, V.G. Savitski, K.V. Yumashev, E.L. Raaben, A.A. Zhilin. Passive mode-locking of a Cr 4+ :YAG laser by PbS quantum-dot-doped glass saturable absorber**.** Optics Communications , v.**241** , pp. 449-454 (2004).

Pair Collisions of Optical Pulses in Non-Linear Dispersive Media: Frequency Tuning and Velocity Variation

A.P. Sukhorukov, V.E. Lobanov

Faculty of Physics, Lomonosov Moscow State University, Leninskie Gory, 119991, Moscow, Russia
apsmsu@gmail.com

We first present the crucially new effects of optical pulse frequency tuning and time delay (advancing) caused by two-pulse nonlinear collision. This phenomenon is a temporal analogue of the total beam reflection in a defocusing medium. The total reflection from moving pump pulse in defocusing media can occur only in the case of anomalous group velocity dispersion (GVD) at the signal frequency; and vice versa if nonlinearity is focusing, GVD must be normal. As a result of collision the signal frequency and group velocity change. It means that signal pulse obtains a push, after which it moves away from the pump pulse with another velocity.

As a result of reflection the group velocity mismatch changes a sign. The signal frequency change is proportional to the group velocity mismatch and inversely proportional to the GVD coefficient. These effects are described by NSE for envelopes of colliding pulses. In the report analytical results and results of numerical simulation are presented.

We have developed an asymptotic method similar to a method of geometrical optics and have deduced the equation for a of a signal pulse trajectory in a field of a powerful pump pulse at other frequency. The condition for the total reflection from any pump pulses was obtained. The problem about the total pulse reflection is completely solved for pump pulse in the form of a hyperbolic secant. We also derived that the frequency shift is proportional to the group velocity mismatch and inversely proportional to the GVD coefficient. These effects are discussed in the media with cubic, photorefractive and cascade-quadratic nonlinearities.

We also first investigate the effect of discrete dispersion on the laser-induced moving lattice which is the temporal analogue of the discrete diffraction phenomenon. The discrete dispersion gives the ample opportunities of multiplexing input signal for different applications in ultrafast photonics. We also demonstrate that single pulse could be locked between two neighbor pump pulses. The parameters of cascade-induced lattices could be easily controlled by the varying of the intensity and the frequency shift of the initial pump pulses. The simplicity of lattice parameters variations and the small power of all pulses are the advantages of such temporal lattices in fibers and photonic crystals.

Laser-induced Diffraction and Reflection in the Nonlinear Defocusing Media

Valery E. Lobanov, Aleksey A. Kalinovich, Anatoly P. Sukhorukov
Faculty of Physics, Lomonosov Moscow State University, Leninskie Gory, 119991, Moscow, Russia

The report presents the new laser technology to simulate the diffraction of optical waves on opaque objects in nonlinear defocusing media. We first investigate diffraction and reflection of narrow and wide laser beams from laser-induced cylindrical inhomogeneity in the media with both local photorefractive and nonlocal thermal nonlinearities. Just mention that the induced object becomes opaque when the cross-angle less than the critical value for total reflection. The observed effects are given hydrodynamic interpretation by comparison with the fluid flow around obstacles.

The profile of narrow signal beam remains almost undistorted after reflection. If the beams are comparable to the width, the reflected beam takes the characteristic sickle shape. Wide signal wave flows around a thin cylinder, forming the shadow area, small ripples, and the cone of diffraction.

The main problem for experimental observation of the effect in 3D geometry is pump beam defocusing. To suppress this effect is to use anisotropic a material with strong electro-optic anisotropy; pump wave must be polarized in non-electro-optic direction (ordinary polarization) and signal wave must have extraordinary polarization. For example, in the highly anisotropic SBN:75 crystal the nonlinear coefficient for ordinarily polarized wave is more than 20 times smaller that the nonlinear coefficient for extraordinarily polarized wave. In this arrangement pump wave dynamics is practically linear while signal wave experiences both pump wave action and screening nonlinearity. The efficiency of such approach was proved by the results of numerical simulation. Induced diffraction can be used to all-optical switching the optical characteristics of laser beams, for example, for deviation in the given angle.

In the medium with thermal nonlinearity the influence of defocusing can be decreased by means of preset pump beam focusing. The influence of linear absorption and thermal defocusing are investigated too, and optimal parameters for observation of nonlinear diffraction of wide beams and total reflection of narrow beams are found under such approximation. We realize numerical modeling of the process of nonlinear reflection of laser beam from the beam of another laser in color ethanol. Numerical results are in a good agreement with experimental data.

Production of THz Radiation by Short Laser Pulses via Tunnel Ionization of a Gas under the Effect of External Magnetic Field

Anil K. Malik and Hitendra K. Malik
Plasma Waves and Particle Acceleration Laboratory, Department of Physics, Indian Institute of Technology Delhi, New Delhi – 110 016, India

The potential applications of THz radiation in the fields like time domain spectroscopy, remote sensing, biological spectroscopy, communication etc. has made the subject of THz generation an interesting field of research [1 – 3]. The use of collective properties of laser-produced plasma underlies a number of methods of THz generation that include mechanisms based on the phenomenon of nonlinear ponderomotive force induced excitation of plasma wake oscillations. However, conversion efficiency of these schemes is poor [4, 5].

We present a theoretical and simulation study for THz generation, where two short laser pulses are focused on to a gas in the presence of external static magnetic field. Here, one laser is taken as circularly polarized and another one as linearly polarized with same frequency but with different amplitude and phase. The mechanism is based on tunnel ionization of gas, where subsequent transverse transient current is realized due to the presence of residual momentum after passing the laser pulse. Due to this oscillatory current, THz radiation is emitted in the forward direction of propagation of the laser pulses. The directionality of emitted THz radiation is observed to be controlled with the help of the phase difference of incident laser pulses. Moreover, this mechanism provides tunablity in the frequency range of THz radiation with the application of external magnetic field. Under the situation of external static magnetic field and the superposition of two laser pulses, the THz radiation of high power is obtained.

References

1. G. Segschneider, F. Jacob, T. Löffler, and H. G. Roskos, Phys. Rev. B **65**, 125205 (2002)
2. P. Gaal, K. Reimann, M. Woerner, T. Elsaesser, R. Hey, and K. H. Ploog, Phys. Rev. Lett. **96**, 187402 (2006).
3. A.K. Malik and H.K. Malik, 2nd Int. Conf. on Attosecond Physics – 2009**"** Kansas State Univ., USA.
4. H. Hamster, A. Sullivan, S. Gordon and R. W. Falcone, Phys. Rev. E **49**, 671 (1994); Z.-M. Sheng, K. Mima, J. Zhang, and H. Sanuki, Phys. Rev. Lett. **94**, 095003 (2005).
5. W. P. Leemans, J. vanTilborg, J. Faure, C. G. R. Geddes, Cs. Toth, C. B. Schroeder, E. Esarey, and G. Fubianif, Phys. Plasmas **11**, 2899 (2004).

Photonic Crystal Si-based Structures for Optics and Sensorics

A.I. Efimova, V.B. Zaitsev, L.A. Golovan, S.M. Afonina, A.D.Sladkov
Physics department, M.V. Lomonosov Moscow State University, Moscow, Russia
119991 Russia, Moscow, Leninskie Gory, MSU Physics Department
Phone/Fax (+7495) 939-15-66
e-mail: efimova@vega.phys.msu.ru

Photonic bandgap (PBG) structures can be used as a basis for new photonic devices fabrication to control light beams and for gas sensors. Stacks of porous silicon (PS) layers with alternating high and low porosity form one-dimensional PBG crystals with steep slopes of PBG. A structure defect can be formed by varying either porosity or width of the porous layer between two Bragg reflectors. The defect layer results in a narrow transparency window in the PBG, where reflectivity decreases almost to zero [1-3].

The sensor under construction is formed from a porous silicon PGB structure with a defect layer technologically tuned to a characteristic wavelength of the target gas. The structure may have several operation modes in either transmission or reflectance. Each gas having unique infrared absorption lines, infrared gas sensors provide conclusive identification and measurement of the target gas with little interference from other gases.

Nonlinear optical interactions in porous silicon, resulting in nonlinear refraction under high density laser irradiation, can shift PBG edge. A possibility of several nanometers PBG edge shift in PS-based photonic crystals was shown at the intensities below the breakdown threshold for PS. Thus, a genuine photonic band gap porous silicon multilayer structure for optical switching has been designed.

References

1. L.A. Golovan, V.Yu. Timoshenko, P.K. Kashkarov, "Optical properties of nanocomposites based on porous systems", *Uspehi Fisicheskif Nayk*, **177**, N6, 619-637 (2007).
2. J. J. Saarinen, S.M. Weiss, P.M. Fauchet and J.E. Sipe, "Reflectance analysis of a multilayer one-dimensional porous silicon structure: Theory and experiment", *J. of Appl.Physics*, **104**, 013103-1-013103-7 (2008).
3. T.V. Dolgova, A.I. Maidikovsky, M.G. Martemyanov, G. Marovsky, G. Mattei, D. Shumacher, "Giant second harmonic in microresonators based on porous silicon photonic crystals", *JETP Letters*, **73**, N1, 8-12 (2001).

Thermally Induced Depolarization Ratio in 23 and m3 Symmetry Classes of Cubic Crystals

A. G. Vyatkin, E. A. Khazanov
Institute of Applied Physics of the Russian Academy of Sciences 603950 Nizhniy Novgorod/Russia
Main author email address: anton.vyatkin@gmail.com

Nowadays several m3 symmetry group oxides (Y2O3, Sc2O3, Lu2O3) are becoming available for optical applications. The photoelastic tensor of these crystals as well as of 23 symmetry group crystals has a different structure than most known cubic crystals including garnets have: $\pi 12 \neq \pi 21$ [1]. We investigated thermally induced depolarization ratio in a m3 crystal.

We assumed long rod geometry and top-hat heating and scanning beam profiles. Strain field in an isotropic approximation is available in [2]. The local depolarization rate in both cases of small and strong birefringence has been derived. The global depolarization rate, the optimal and the worst crystal orientations have been calculated numerically.

The local depolarization rate depends on two parameters: □=2πxyxy/(πxxxx□½(πxxyy+πyyxx)) is the common photoelastic anisotropy parameter [3], □d=(πxxyy□πyyxx)/(πxxxx□½(πxxyy+πyyxx)) is a novel parameter.

The optimal orientations are mainly determined by the □d/(□□1) ratio and are not the same as found in [3] for a "common" cubic crystal. In case of small birefringence the minimal depolarization rate is always larger for a "novel" crystal than for the "common" one with the same □. In case of strong birefringence it can be either smaller or larger depending on both heating and scanning beam diameters.

References

1. J. F. Nye: Physical properties of crystals, (University Press, London, 1964).
2. A. V. Mezenov, L. N. Soms and A. I. Stepanov: Thermooptics of solid-state lasers, (Mashinostroenie, Leningrad, 1986).
3. B. Mukhin, O. V. Palashov, E. A. Khazanov and A. I. Ivanov: JETP Letters 81, 120 (2005).

Thermally Induced Light Scattering in Laser Ceramics with Arbitrary Grain Size

A. G. Vyatkin, E. A. Khazanov

Institute of Applied Physics of the Russian Academy of Sciences 603950 Nizhniy Novgorod/Russia
Main author email address: anton.vyatkin@gmail.com

Laser ceramics combines large aperture like glasses and high thermal conductivity like crystals but is affected by thermally induced light scattering. The special case of the grain size d to wavelength λ ratio $R>>1$ was studied in [1] in geometrical optics approximation. We considered a medium with an arbitrary R value and isotropic variations of dielectric permeability ε in case of small fluctuations magnitude and small mean scattered power to incident power ratio K.

The scattered electric field was calculated by small perturbations method [2]. Only once scattered light term was considered. We figured out that mean scattered light intensity depends on ε fluctuations intensity spatial spectrum (correlation function (CF) Fourier-transform).

The magnitude of ε CF can be estimated as $<\varepsilon_{xx}^2>$. The CF shape was evaluated in spherical grain shape approximation in both cases of single scale grains and grain size varying in the range of (d□□, d+□). The actual difference between these cases is sufficient for □/d>0.33.

The K ratio obtained was compared with mean fundamental mode power loss ratio 1□<χ> [1]. □he curves fit qualitatively in the range R>1 where 1□<χ> calculation is valid. However the amount of scattered power is overestimated by ~8 in the current study.

References

1 I. B. Mukhin, O. V. Palashov, I. L. Snetkov and E. A. Khazanov: Proc. SPIE. 6610. 66100N-1 (2007).
2 S. M. Rytov, Yu. A. Kravtsov and V. I. Tatarskiy: Introduction to statistical radiophysics, Vol. 2, (Nauka, Moskva, 1978).

Spectral-Luminescent Properties of Nd^{3+} Ions in Semiconductive Glasses of $La_2S_3 \cdot 2{,}3Ga_2O_3$

G.I.Abutalybov, A.A. Mamedov

Institute of Physics of the National Academy of Sciences of Azerbaijan
AZ-1143, H. Javid ave., 33, Baku
Fax: (+99412)4470456 e-mail: mamedov_arzu@mail.ru

Interest to $La_2S_3 \cdot 2{,}3Ga_2O_3$ glasses doped by Nd^{3+} as a perspective active elements of lasers has been aroused that there has been existed possibility off – center optical excitement for lasers of semiconductive matrix by light corresponding to basic absorption with subsequent energy transmission of active impurity[1]. Investigation shows that in oxosulphide glasses Nd^{3+} ions are luminescenced at excitement in intrinsic absorption band of base. At high concentration of Nd^{3+} this fact manifests clearly in excitement spectre.

At high delay time and T=300K neodymium ion luminescence in $La_2S_3 \cdot 2{,}3Ga_2O_3$ has been observed in transition $^4F_{3/2} \rightarrow {}^4I_J$. By temperature rise up to ~600K at high delay time there have been observed lines related with transitions not only with $^4F_{3/2}$ but with the levels of the nearest multiplets $^4F_{5/2} + {}^2H_{9/2}$, moreover relationship of band intensities does not change in time, i.e. decay of excited established that at high temperatures thermal occupancy of $^4F_{5/2} + {}^2H_{9/2}$ state has a considerable influence on population of upper laser level $^4F_{3/2}$ of neodymium in $La_2S_3 \cdot 2{,}3Ga_2O_3$.

To determine microscopic constants of nonradiative donor-donor(C_{DD}) and donor-acceptor(C_{DA}) interactions of $Nd^{3+} - Nd^{3+}$, knowledge of them allows such important properties of material as quantum efficiency of luminescence optimal concentrations of active impurity and etc. to be predicted, we analyze curves of excited states $^4F_{3/2}Nd^{3+}$. These value parameters are following:

$$C_{DD} = 4.5 \cdot 10^{-40} cm^6 \cdot \sec^{-1} \qquad C_{DA} = 1.2 \cdot 10^{-40} cm^6 \cdot \sec^{-1}$$

$$R_{\min.} = 4A^{0} \quad (R_{\min.}\text{-minimum distance between interacting particles})$$

To reveal prospect of $La_2S_3 \cdot 2{,}3Ga_2O_3 - Nd^{3+}$ as active mediums of lasers with diode pumping there has been carried out comparison of calculated (spectrographic data) threshold power at various configuration of pumping with corresponding values for glass $ED-2$ and $YAG - Nd^{3+}$, on which generation at pumping by semiconductive diodes have been taken. Carried calculations allows to suggest that $La_2S_3 \cdot 2{,}3Ga_2O_3 - Nd^{3+}$ can be effective active medium of miniature lasers with laser pumping.

Reference

1. Glushkov M.V., Mamedov A.A., Prokhorov A.M. and others. Resonance excitement in semiconductor single crystal. Letters to JETP,1980, v.31, ed.2, pp. 114-117

A Multi-Angle Laser Light Scattering Aerosol Spectrometer

A. Nagy [1], A. Czitrovszky, A. Kerekes, W.W. Szymanski

Research Institute for Solid State Physics and Optics
Hungarian Academy of Sciences
Budapest 1525, P. O. Box 49, Hungary

Light scattering from sub and super micron particles has been studied both theoretically and experimentally for many years and it became clear that correct particle sizing is not possible by using single scattering geometrics and simple data reduction methods. By extending the examined refractive index range from the refractive index of the calibration aerosol one have to face with significant over or under sizing.

A new method was introduced for the real time measurement of the size and the complex refractive index of aerosol particles [1]. The method is based on a dual wavelength illumination system where the scattered light is collected over four angular ranges, forward and backward scattering directions compared to the two illumination laser light beams. The measured and digitalized quartet is than compared to a pre-computed table calculated using the Mie scattering theory. The rows of the table contain a size, a complex refractive index and the corresponding four scattered signals from the four angular ranges.

The resolution and the accuracy of the method depend on many parameters, e.g. instabilities in the sample flow system, uncertainties in the illumination and detection electronics, on the applied analog-to-digital converter and also on the dimensions of the evaluation table. A comprehensive numerical and experimental study showed the feasibility of the method recently [2].

The calibration of the instrument was performed using laboratory particle standards (PSL). Initially, scale factors were determined for each detector to link the scattered intensities calculated using the Mie theory with the detector responses.

To evaluate the performance of the method particles were generated from a suspension using pneumatic atomization and electrostatic classification (DMA) were used to obtain monodisperse distributions. These particles were then introduced to the instrument's measuring volume after aerodynamic focusing. The four signals from the four detectors were catch by a four channel peak detection system which utilizes certain logic to minimize the effects of possible crosstalk between channels. The detected signals were digitized and using the scale factors a search was performed in the evaluation table to obtain the particle size and complex refractive index.

PSL particles with different sizes from aqueous suspension, DEHS particles generated from an Isopropyl Alcohol-DEHS solution, Paraffin oil and carbon-like absorbing particles generated from black ink diluted in pure distilled water were used for the test measurements.

References

1 W.W. Szymanski, A. Nagy, A. Czitrovszky, P. Jani, "A new method for the simultaneous measurement of aerosol particle size, complex refractive index and particle density", *Measurement Science and Technology*, **13**, 303-307 (2002).

2 A. Nagy, W.W. Szymanski, A. Golczewski, P. Gál, A. Czitrovszky, "Numerical and experimental study of the performance of the Dual Wavelength Optical Particle Spectrometer (DWOPS)", *Journal of Aerosol Science*, **3**8 467-478 (2007).

A New Approach for Developing Highly effective Solid-State HV Pulse Generators for Laser Pumping

S. I. Moshkunov

Russian Academy of Sciences, Institute for Electrophysics and Electric Power, Moscow, Russia

Main author email address: serg-moshkunov@yandex.ru

A new approach for developing highly effective solid-state HV pulse generators for laser pumping is described. The generators are based on a new high voltage solid state switches comprising a number of insulated gate bipolar transistors (IGBT) connected in series/parallel and magnetic pulse compressor circuits. These switches are capable to replace modulator vacuum tubes and gas-discharge switches (thyratrons) [1-2], which are currently used in most power pulse generators for supplying of lasers and many other electric discharge devices.

The effectiveness of the approach in developing a number of pulse laser pumping systems with working voltages up to 30 kV, current amplitude up to 2000 A, average power up to 2 kW, pulse repetition rate up to 20 kHz and pulse width of 50 - 1000 ns was demonstrated.

The main advantages of the new approach as compare to generators based on thyratrons are: high reliability, long life, high stability, low losses, small dimension and weight.

References

1 I.S.Kolokolov, V.I.Klimenko, N.A.Lyabin, G.M.Paramonova, A.D.Churkin, M.A.Kasaryan, N.M.Lepehin, Yu.S.Priseko, V.G.Filippov, "The industrial laser on base of desolder active elements of a series "KULON" on pairs copper (LT-10CU), gold(LT-1,5AU), mix pairs of gold and copper (LT-AU-CU)", *Applied physics,* No. 3, 80-89, (2003)

2 N. M. Lepekhin, Y. S. Priseko, V. G. Philippov, "Nanosecond pulse generator for excitation copper vapor lasers", *Applied physics,* No. 5, 40-45, (2001)

Laser scattering and diffraction assessment of the effect of diamond nanoparticles on blood microrheology

Alexander V. Priezzhev[1], Andrei E. Lugovtsov[1], V.G. Ionova[2], Chia-Liang Cheng[3], and E. Perevedentseva[3]

[1] *Physics Department and International Laser Center, M.V. Lomonosov Moscow State University, Moscow 119992, Russia*

[2] *Research Institute of Neurology of RAMN, Moscow 125367, Russia*

[3] *Physics Department, National Dong Hwa University, Hualien 97401, Taiwan*

Main author email address: avp2@mail.ru

Nanodiamond particles (NDs) are perspective fluorescent markers that can potentially be used for biomedical diagnostics. Although they seem to be not toxic and not to destroy vitally important organs, tissues and cells as was shown in a number of biological experiments both in vitro and in vivo, their implementation into clinical experiments is highly debated nowadays. There are fears about small ND particle penetration and accumulation into other cells than those tested. In general, the problems of biocompatibility of nanoparticles, nanotoxicity and nanosafety are gaining more and more attention nowadays.

The aim of our work was to study the effect of NDs on blood microrheology, in particular, on the ability of red blood cells (RBCs) to deform in shear flow and to spontaneously aggregate. This was motivated by the fact that the administration of NDs and other nanoparticles into a live organism is usually performed intravenously, i.e. via blood vessels. However the effect of nanoparticles on blood and on its ability to normally flow though the vessels of different radii is usually not accounted for. The only information available at this time concerning the interaction of nanoparticles with RBC is that the administration of carbon nanoparticles into blood leads to the lysis of RBCs, aggregation of platelets and that small NDs (around 5 μm- sized) penetrate though the membranes of RBCs and interact with the hemoglobin (Hb) molecules. The latter fact can potentially lead to the reduction of RBC deformability which may further lead to the impairments of the blood flow through smaller vessels.

In order to study the effect of NDs on RBCs we have conducted a series of in vitro measurements of the deformability index and several parameters of aggregation kinetics using the optical measurement techniques based on the detection of diffraction patterns from dilute suspensions of RBCs and diffuse reflection from a layer of whole blood. In our experiments, we used suspensions of NDs with sizes from 5 to 500 μm in bidistilled water of different concentrations, added to samples of freshly drawn human blood. The ND particles were either bare or corboxilated (cND) to improve their biocompatibility.

We have shown the there is a remarkable negative effect of NDs and cNDs on both deformability and aggregation kinetics of RBCs in the in vitro experiments. The effect is concentration dependent. In particular, smaller NDs and cNDs (around 5 μm characteristic size) in smaller concentrations (around 33 μg/ml) seem to decrease the time of formation of both linear and 3D RBC aggregates and enhance the amplitude of spontaneous RBC aggregation in whole blood, which are overall negative physiologic effects. Larger NDs and cNDs (around 500 μm characteristic size) as well as smaller ones in higher concentrations (around 330 μg/ml) lead to smaller negative effects which can be speculated as a result of small particles aggregation in concentrated suspensions and nonpenetration of relatively large ND particles and their aggregates into the RBCs through their membranes. Carboxilation of ND particle surface makes the negative effect of small cNDs less pronounced but does not totally abolish it.

The effect of ND particles on shear deformability of RBCs is negative as well: the RBC deformability index is reduced all through the range of shear stresses (from 3 to 60 Pa). However the reduction of the defomability index becomes evident at higher concentrations (around 100 μg/ml).

These initial results are indicative of the importance of thorough studies of the effect of nanoparticles on blood rheologic properties, given the particles are to be delivered to the targets via the blood flow. The effect of nanoparticles on the macromolecules constituting the blood plasma is still an open issue, which should be studied as well, because blood proteins also play a significant role in RBC microrheologic properties.

The authors thank Russian Foundation for Basic Research and National Science Council

Lasers in Confocal Raman Research of Prehistoric Stones and Painted Hellenistic Potteries in Anatolian Archaeology

A. Ulubey[1], B. Erdogu[2], A.Seçgin[3], S.Özbek[3]
[1]*University of Thrace, Faculty Art and Science, Department of Physics, 22030 Edirne, Turkey*
[2]*University of Thrace, Faculty Art and Science, Department of Archaeology, 22030 Edirne, Turkey*
[3]*TUBITAK, Marmara Research Center, Materials Institute, P.K.21,41470 Gebze/Kocaeli,Turkey*
E-mail: aydinulubey@trakya.edu.tr

The high information content of laser techniques has been coupled with analysis on the micro scale to provide imaging techniques for scientists from many varied research fields. The encouraging results achieved with this work propose the improvement of such a sort of considerations on wider archaeological samples for a statistical study of spectral properties.

Raman Spectroscopic methods were developed for chemical and physical characterization of different materials, and it is now commonly used in archaeology. The chemical nature of the black and red pigments of some samples of Hellenistic pottery from the Salt Lake (Tuz Golu) region of Central Anatolia has been identified by Confocal Raman Spectroscopy. The black and red pigments are found to be magnetite (Fe3O4) and hematite (□-Fe2O3). A piece of prehistoric polished stone axe from Turkish Thrace has also been investigated by home made Confocol Raman Spectroscopy setup developped and installed at the TUBITAK MRC, Materials Institute, Laser Spectroscopy Lab. The result show that the spectrum recorded from the rock matrix is actinolite.

Investigation on the Mode Hope Free Tunability of a 852 nm Laser Diode without Anti Reflection Coating

C. Birlikseven, E. Şahin, M. Çelik, R. Hamid
National Metrology Institute (UME),
Scientific and Technological Research Council of Turkey (TÜBİTAK),
Gebze-Kocaeli, Turkey

One of the key parameter of external cavity diode laser is the single mode tuning capability. Most applications require that the wavelength scan is free of mode-hops. Setting up and maintaining a large mode-hop free tuning range is difficult, since the external and the internal cavity formed by the end facets of the semiconductor itself need to be tuned synchronously. One of the method is simultaneous ramping of PZT and laser injection current. External cavity length is changed by applying a ramp voltage to the PZT. The varying current adjusts the internal cavity length and keeps the internal and external cavities synchronized. Mainly, two problems occur. First, the components do not generally respond in a linear fashion. Second, vibrations and thermal fluctuations lead to mode-hops. [1, 2].

To investigate the tunability of a 852 nm laser diode without an anti-reflection coating, we constructed a simple ECDL cavity. A weak optical coupling is achieved using a very thin glass piece placed directly opposite to laser facet allowing the coarse and fine alignment of external cavity [3]. We used Spectra diode Labs SDL-5410-C series 100 mW Fabry-Perot laser diode at 852 nm which is suitable for Cesium D_2 line spectroscopy. In our system, wavelength selection is accomplished by directly changing the cavity length. Cavity length is changed by a Piezo-mechanic HPST 500/10-5-5 type PZT. We adjusted the cavity length and laser current together to achieve large single mode tuning range. PZT voltage and laser injection current was controlled with a DAC card and sophisticated control software.

References

1. T. Führer, D. Stang and T.Walter, "Actively controlled tuning of an external cavity diode laser by polarization spectroscopy", *Optics Express*, **17**, 4991 (2009).
2. T. Führer and T. Walther, *Optics Letters*, "Extension of the mode-hop-free tuning range of an external cavity diode laser based on a model of the mode-hop dynamics", **33**, 372–374 (2008).
3. A.V. Carr, Y.H.Sechrest, S.R.Wauitukaitis, J.D. Perreault, P.A.V. Lonij, A.D.Cronin, "Cover slip external cavity diode laser", *Rev.Sci. Inst*., **78**, 106108-106108-3 (2007).

Turkish Accelerator Complex, FEL Resonator System

H. Duran Yildiz[1]
[1]*Physics Department, Dumlupınar University, Kütahya, Turkey*

Accelerator technology is a comprehensive tool of the development in almost all fields of science and technology. Considering the importance of accelerator technology, a feasibility report and conceptual design report (CDR) on Turkic Accelerator Complex in Turkey has been completed by a small research group in 2005. It is proposed that the complex will contain a collider, light sources (SR and FEL) and a proton accelerator. Beginning of 2006, third phase of the TAC project is started with the collaboration 10 Turkish Universities. There are three main goals of this phase: to built Institute of Accelerator Technologies, to write the Technical Design Report of TAC, and to construct linac based infrared free electron laser facility to use in basic, applied research, and to get experience on related technologies. TAC IR FEL will be covered range of 2-185 microns that based on 15 - 40 MeV e-linac.

In this presentation, the main system of TAC project will be briefly presented. Behind this, calculated resonator and mirror system parameters for TAC IR-FEL Resonator and in optic cavity system, maximum density, saturation density, power, pulse energy, RMS pulse length are obtained and will be presented in more detail. In this research, diffraction losses are calculated by using mirror parameters in GLAD Program. In order to maximize FEL efficiency, controlled optic cavity system, stability and beam quality of the out-coupled signal are needed [1, 2, 3].

References

1 F. Ciocci, G. Dattoli, A. Torre, A. Renieri, *Insertion Devices for Synchrotron Radiation and Free Electron Laser*, World Scientific, Singapore, 2000.
2 D. C. Tyte, *Advances in Quantum Electronics*, Vol.1, Academic Press, New York, 1970.
3 N. Hodson, *Laser Resonators and Beam Properties*, Optical Sciences, 2004.

Photovoltaics in X-İrradiated Inse–Gase–Inse Heterojunctions

MirSalim Asadov

mirasadov@gmail.com

The purpose of this work was to investigate photovoltaic and X-ray dosimetric characteristics of InSe–GaSe–InSe epitaxial heterojunctions, obtained by melting of low-temperature component. Indium was used as a contact material. The thicknesses of GaSe and InSe single crystals were equal to 200 and 50 μm, correspondingly; the distance between the In contacts was equal to 0.6 cm. As an X-ray source, we used a URS instrument with a BSV-2(Cu) tube. The X-ray intensity was controlled by varying the electric current in the tube at each specified value of the accelerating voltage (U). The absolute values of the X-ray dose were measured on a DRGZ-02 dosimeter. All measurements were carried out at the temperature T = 300 K. Voltage-dose characteristics of InSe–GaSe–InSe heterojunction have been investigated in the ventilated regime, i.e. without of supply voltage. The e.m.f. created in studied heterostructure increases with increasing dose rate E from 0.75 to 78.0 R/min. Maximal value of e.m.f. was equal to 170 mV at E = 78.0 R/min and U = 50 keV. From analyzing the current – dose characteristics of InSe–GaSe–InSe heterojunction, it follows that the dependence of the steady-state X-ray current on the dose rate can be adequately described by a power law. The dose sensitivity of studied heterojunctions made 1e-10 – 1e-9 A•min/R in the range of the measured power E = 0.75 – 78.0 R/min. The registered range of the X-rays energy made 25–50 keV. The results obtained have demonstrated that InSe–GaSe–InSe heterojunctions are characterized by a high X-ray sensitivity and can be used in the design of operable at room temperature roentgen detectors.

Photoalignment in a Dye-doped Liquid Crystal by Linearly Polarized Laser Light

R. Karapinar[1], D. Fedorenko[2], E. Ouskova[2] and Y. Reznikov[2]
[1]*Department of Physics, Faculty of Arts and Sciences, Yuzuncu Yil University, Van,Turkey*
[2]*Institute of Physics, National Academy of Sciences, Kyiv,Ukraine*

In recent years photoalignment of liquid crystals (LCs) has become particularly important because of its potential display applications [1]. Conventional photoalignment technique uses photo-chemical processes that induce optical anisotropy on a photoaligning polymer layer because of the absorption of polarized ultraviolet light. Another type of photoalignment (light-induced anchoring) can be achieved on non-photosensitive aligning layer due to light-induced adsorption of dye molecules on the alignment layer. It was found that irradiation of a planar LC cell doped with an azo dye under illumination with polarized light produced an easy orientation axis on the non-photosensitive aligning surface [2]. This study focuses on the light-induced anchoring in a LC 5CB doped with a dye Methyl Red (MR). It has been found that the photoalignment depends strongly on the intensity of the pumping beam in MR doped LC system and is governed by light-induced adsorption and desorption of a dye to/from the polymer surface at a presence of a light-induced bulk torque [3]. We report on dynamical studies of photo-induced adsorption of methyl red molecules onto polymer surface. Dependence of the twist angle on the exposure time of the pumping beam is also studied. A typical behavior of twist angle as a function of the exposure time is given in Fig.1. The factors that determine the light-induced anchoring energy of the LC on the polymer layer are analyzed. These dye-doped liquid crystals can be used for photonics applications.

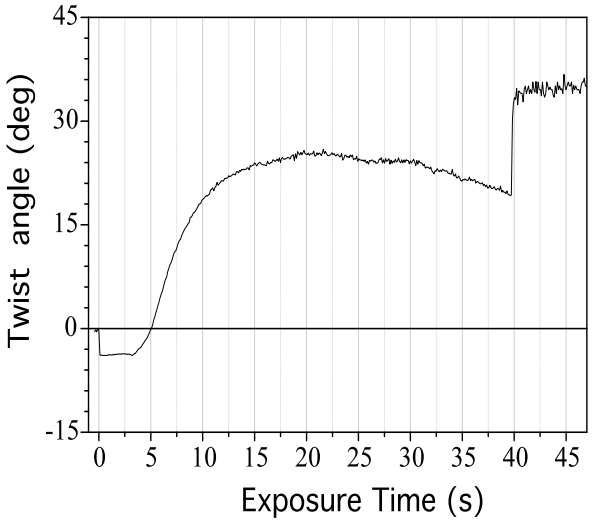

Fig.1. Dependence of the twist angle on the exposure time.

References

1 M. O'Neil and S.M. Kelly, J. Phys. D 33, 'Photoinduced surface alignment for liquid crystal displays' *J. Phys. D: Appl. Phys*., **33,** 67-84 (2000).
2 D. Voloshchenko, A. Khizhnyak, Yu. Reznikov and V. Reshetnyak, 'A control of an easy axis on a nematic-polymer interface by a light action to a nematic bulk', *Jpn .J. Appl.Phys*.,Part 1 **34,** 566-571 (1995).
3 D. Fedorenko, K. Slyusarenko, E. Ouskova, V. Reshetnyak, K-R. Ha, R. Karapinar, and Yu. Reznikov, 'Light-induced gliding of the easy orientation axis of a dye-doped nematic liquid crystal', *Phys. Rev. E,* **77**, (061705) 1-9 (2008).

Wakefield excited by Laser Pulses of Different Field Profiles: Contribution of Electron Thermal Energy

Hitendra K. Malik
Plasma Waves and Particle Acceleration Laboratory, Department of Physics, Indian Institute of Technology Delhi, New Delhi – 110 016, India

The acceleration of charged particles to high energies has diverse applications in the field of nuclear physics, harmonic generation, high energy physics, nonlinear phenomena observed during laser plasma interaction, etc. Therefore, the subject of charged particle acceleration has been an interesting field for both the experimentalists as well as the theoreticians. Appreciable attempts have also been made to achieve compact ultrahigh gradient accelerators using high intensity short pulse lasers in the plasmas [1 – 5]. Among various acceleration schemes, the wakefield excitation by short pulse lasers has been very effective mechanism for the particle acceleration. However, such schemes need to employ ultrashort and ultrahigh intensity lasers because of which it costs high to achieve large energy gain.

In the present article, we propose to focus on different field profiles of the laser pulses rather than their ultrahigh intensities. The present calculations show that the wakefield of large magnitude can be achieved with a moderate intensity laser pulse if the shape of the pulse is maintained such that its rising and fall time is short. A more realistic situation is examined by taking into account the finite temperature of the electrons, which was neglected in earlier investigations. A differential equation is derived in terms of electrostatic potential from which we obtain the expression for the wakefield excited by different laser pulses. We have done calculations for three types of the pulses namely triangular pulse, sawtooth decreasing front pulse and sawtooth increasing front pulse. For sawtooth increasing pulse, the phase for the electrostatic potential or the wakefield comes out to be opposite to the ones for the triangular and the sawtooth decreasing front pulses. A comparative study reveals that the sawtooth increasing front pulse is the most useful for particle acceleration as it generates largest wakefield among the three types of the pulses. The effect of electron thermal energy is to enhance the wakefield and it becomes more significant in the range of high temperatures. So for high temperature applications it is not advisable to neglect the electron temperature.

References

[1] H.K. Malik, J. Appl. Phys. **104**, 053308 (2008) , and references therein**.**
[2] D. Umstadter, Phys. Plasmas **8**, 1774 (2001), and references therein.
[3] H. Suk, J. Appl. Phys. **91**, 487 (2002).
[4] T. Katsouleas, Plasma Phys. Controlled Fusion **46**, B575 (2004).
[5] S. Kawata, Q. Kong, S. Miyazaki, K. Miyauchi, R. Sonobe, K. Sakai, K. Nakajima, S. Masuda, Y. K. Ho, N. Miyanaga, J. Limpouch, and A. A. Andreev, Laser Part. Beams **23**, 61 (2005).

Application of digital in-line holographic microscopy (DIHM) for 4D tracking of the colloid particles

D. A. Ekimov[1,2]

[1] *Measurement and Sensors Laboratory, University of Oulu, Kajaani, Finland*

[2] *Information and Measurement Systems Department of physics faculty, Petrozavodsk State University, Petrozavodsk, Russia*

Digital in-line holographic microscopy (DIHM) is a powerful method to study the moving micro objects in the volume1-2 whereas conventional microscopy provides the information only about the focus plane because the working distance limited by numerical aperture. As a single hologram contains all the information about 3D volume, any cross-section of the volume can be reconstructed at the various distances from CCD numerically by post processing. After that it is possible to measure positions of the particles in the volume. We have made the setup to record the holograms of the colloid and develop the program to reconstruct the tracks of the micro particles in order to see agglomeration process in the time.

References

1 M. Kanka, R. Riesenberg and H. J. Kreuzer, "Reconstruction of high-resolution holographic microscopic images", *Optics Letters* **34**, 1162-1164 (2009).

2 M. H. Jericho, and H. J. Kreuzer, "Digital in-line holographic microscopy", *G.I.T. Imaging and Microscopy* 63-65 (2007).

GaSe and InSe Crystals in Quantum Electronics

V.M.Salmanov[1], A.A.Salmanova[2], E.M.Kerimova[3], D.A.Huseinova[3]

1.Baku State University
2.Azerbaijan State Oil Academy
3.Institute of Physics, National Academy of Sciences

ekerimova@physics.ab.az

The nonlinear light absorption and its time evolution in the exciton resonance region at high optical excitation levels in GaSe and InSe layered crystals have been investigated experimentally. The observed time dependences of the absorption coefficient of GaSe and InSe crystals and its excitation intensity dependences are determined by exciton-exciton interaction and exciton screening by the plasma of no equilibrium carriers. Optical bistability in the GaSe at excitation by dye laser results from the interplay of absorptive excitonic non-linearity and feedback effect. The observed hysterics loop agrees well with the semi empirical non-linear Fabry-Pero cavity approximation. Fast uncoiled GaSe and InSe detectors that can record ultra short laser pulses in the visual and near-IR ranges are developed. The optical filters are capable to reduce intensity of radiation of various lasers more, than on two order and can be used as cut-off filters. The bleaching of band-edge absorption which manifests itself as an apparent blue shift of the absorption edge can be interpreted on the base of band filling nonlineartities.It is shown that the observed negative absorption change in GaSe crystal is the basis of optical amplification and the semiconductor laser.

πShaper - Beam Shaping Optics for Advanced Laser Technologies

Alexander Laskin

Molecular Technology (MolTech) GmbH, Berlin, Germany

Performance of plenty of scientific and industrial laser applications can be essentially improved when original intensity distribution of a laser beam is transformed from non-uniform profile to uniform or flattop one. The task of such a transformation is solved by series of refractive beam shaping optics ***πShaper*** ®. This solution is important in irradiating the cathode of Free Electron Lasers, confocal microscopy, biomedical fluorescence techniques, many industrial technologies like welding, cladding or hardening, homogenizing of pump radiation by building powerful femtosecond lasers, and many other applications. The ***πShaper*** ® can be used with TEM_{00} and multimode laser beams, achromatic design lets it possible to provide the same conditions of beam shaping for several lasers of a certain spectrum range simultaneously, particular models can be implemented either as a Telescope of Galilean type without internal focusing (collimated input / collimated output), or as a Collimator (divergent input / collimated output).

This paper will describe the principles of operation, design features of the ***πShaper*** ®, there are, also, presented examples of beam intensity transformation and effects on material processing achieved in several applications.

.Improving spatial resolution of infrared image converter based on the semiconductor-liquid crystal structure for real time optical application

N.J.Ismailov, T.D.Ibragimov

Institute of Physics of Azerbaijan National Academy of Sciences.
Baku, Azerbaijan.

The using of coherent radiation makes it possible to carry out transmission, processing and storage the high densities optical information. The great merit of information processing in coherent light is a possibility of fast image processing, because coherence allows the parallel processing of separate elements. The solid state image converter based on photoconductor layer and liquid crystal using for conversion incoherent image to coherent one is very effective in holography, correlation computing system and Fourier transforms analysis. A development of effective image converter for infrared application is very actually, mainly because of existence atmosphere windows and decreasing of losses in infrared fiber-optic channels. However, the decreasing of spatial resolution, sensitivity and the problem of balance between resistance of photosensitive layer and liquid crystal arise for realization of these devices.

In this report the working principle of the solid state image converter based on semiconductor –liquid crystal layered structure with high spatial resolution and cut-off wavelength extended more than 1.2 μm is described. The photosensitive layer in this structure is produced as plan array of Scottky microdiodes, which makes it possible to increase the infrared boundary and resolution of the device. The cut-off wavelength is determined by spectrum of electron photoemission process in metal-silicon MIS structures with barrier potential height that is less than optical band gap of silicon. The photons with wavelength more than 1.2 μm, passing through silicon wafer, are absorbed in metal, exiting electrons. Exited electrons, passing to space charge region of semiconductor, where their avalanche multiplication is occurred. In this case the spatial resolution is determined by sizes of one metallic pixel. In order to decrease liquid crystal resistance for balance with differential resistance of microdiodes, the 0.3-0.5 μm silver particles in 0.05% weight quantity were added to nematic liquid crystal mixture EBBA-MBBA with molar ratio 1:1 . In this case, the resistance and threshold voltage of electrohydrodynamic instability decrease, while contrast ratio, rise and decay times of switching are not changed. The possessed device may be useful in telecommunication, medicine, industrial and military applications.

The work has been supported by Scientific and Technology Center in Ukraine.

Optical Methods and Systems for Distance and Contact Dangerous Matters Detection

S.Yu.Strakhov

Laser Systems Ltd., Krasnoarmeyskaya str., 1, 190005, Saint-Petersburg, Russia

E-mail: Strakhov@lsystems.ru

Optical methods for dangerous matter detection have essential advantages in comparison with other methods - chemical, electrochemical, biosensor and etc. These advantages are possibility of distance detection, high performance, sensitivities.

In this report the range of perspective optical methods and devises are presented, in particularly:

- The attenuated total reflection method for detection of explosives traces on different objects (documents, clothes, fingers) is considered. The results of experiments with Fourier spectrometer and ATR attachment for explosive trace detection are presented. The new devise "*X-Tracer*" developed in *Laser systems Ltd* (St.-Petersburg, Russia) is presented. This devise can detects dangerous matters (explosives, drugs) traces in quantity about 1 g during detection time about 1 sec.
- Compact LIDAR system on the base of DFB lasers for remote fumes of dangerous matters detection. In particularly, the distance detector of alcohol fumes in the car is presented. This devise can detect alcohol fumes on distance 10…30 m in concentration about 100 mg/m^3.
- The using of Raman spectrometer for remote detection of dangerous liquid and solid samples is considered.

Spectroscopic Measurements and Modelling of the Spectrum Emitted from Laser-Induced Argon Plasma

B. Genc[1], S. Sipahioglu[2], E. Akman[1], P. Demir[1, 2], E. Kacar[1, 2], A. Demir[1, 2]

[1]Kocaeli University, Laser Technologies Research and Application Center, Yeniköy, Kocaeli 41275, TURKEY

[2]Kocaeli University, Faculty of Arts and Science, Department of Physics, Umuttepe, Kocaeli 41380, TURKEY

Main author email address: belgingenc@kocaeli.edu.tr

The emission spectra of the laser-induced argon plasma were investigated at different laser energies in low-pressures. The laser-induced breakdown was generated by focusing a 532-nm, 6 ns pulse from a Q-switched Nd:YAG laser with pulse energy varied from 50 to 200 mJ. Spectral lines were recorded between 390 nm and 470 nm at a pressure of 0.1-1 Torr. The electron temperature was determined by Boltzmann plot method using ArI and ArII lines. The electron density was calculated from Stark broadening of Ar I lines. Also, collisional radiative code was used to simulate the ArI and ArII spectral emission and to compare the results with the experimental data for electron density and temperature determination.

Phase-Lock and Frequency Stabilization of Nd:YAG Lasers

Ramiz. Hamid, Cihangir Erdogan

Electromagnetic Group Laboratory, Wavelength Standards Division,
TÜBİTAK-UME Po. Box. 54 Gebze-Kocaeli, (41470) Turkey

Tel: +90-262-679 50 00, Fax: +90-262-679 50 01,
E-mail: ramiz.hamid@ume.tubitak.gov.tr, cihangir.erdogan@ume.tubitak.gov.tr

In this work we will present results of phase lock of Nd:YAG laser to fs Ti:Sa Comb generator and frequency stabilization of Nd:YAG lasers on Doppler-free absorption spectrum of I_2 molecular gas.

Recently developed comb system gives a great contribution to measure the optical frequencies and it has an ability of precise measurement of absolute frequency of the stabilized Nd:YAG lasers. Offset and repetition frequency of femtosecond Comb generator with spectral bandwidth of 525–1100 nm and the repetition frequency which is 800 MHz was stabilized on 10 MHz reference signal of Cs atomic clock. Green laser beam of Nd:YAG laser was beat with the fs Ti:Sa Comb beam and the error signal was send to PZT of Nd:YAG laser for phase locking. By using this method Nd:YAG laser was locked to fs Ti:Sa Comb generator with an uncertainty of 3 Hz.

We measured the beat frequency between UME Nd:YAG-L1 and UME Nd:YAG-L2 which are iodine-stabilized Nd:YAG lasers. We have used the technique of saturated absorption spectroscopy (SAS), for realizing the stabilization of the laser we have chosen the method of frequency modulation and third harmonics spectroscopy technique.

Our laser systems are accessible with the absorption lines of P53 (32-0) - line 1111 and R(56)32-0 - line 1110 in molecular iodine. The frequency of two similar Nd:YAG lasers was stabilized on Doppler-free absorption spectrum of I_2 molecular gas. Second harmonic (Green-532 nm) laser beam passed trough 15 cm I_2 cell, reflected back from mirror and detected on the photodiode. PZT of the laser was modulated with a frequency of 24 kHz and third derivative of iodine 1110 R(56)32-0 line was used in frequency stabilization of lasers. One of laser stabilized on iodine 1110 R(56)32-0 a_{10} line ($\approx$ 563 260 223 513 kHz) and second laser on iodine 1110 R(56)32-0 a_6, a_7, a_8, a_9 lines and beat signal was measured with a PC controlled frequency counter and a spectrum analyzer. External iodine cell pressure, modulation frequency and power of the beam versus laser output frequency investigated at 532 nm. The hyperfine line differences were measured by the beat frequency technique. In addition to this, the finger print of line 1111 - P53 (32-0) has been detected.

Laser Refractography – the Technology for Diagnostic of Optically Inhomogeneous Media

B.S.Rinkevichyus, O.A.Evtikhieva, I.L. Raskovskaya, A.V.Tolkachev

V.A.Fabrikant Physics Department Moscow Power Engineering Institute (Technical University), Krasnokazarmennaya 14, Moscow, 111250, Russia

rinkevbs@mail.ru

The basic principles of laser refractography, a technology for diagnostics of optically inhomogeneous media and flows are described. This technology is based on the theory of the structured laser beam (SLB) refraction in transparent inhomogeneity also experimental digital registration and differential computer processing of the two refraction images (refractograms). The experimental setup allows quantitative visualization of the transparent media by using 2D (passed radiation) or 3D-refractograms (scattered radiation). The discrete character of SLB makes the refractograms adapted for digital registration and processing. The 3D- refractograms are used for visualization of the boundary layer near the hot or cold metallic bodies in water are present. The comparison of the parameters for experimental and corresponding calculated refractograms allows recognizing the temperature fields in the boundary layer, i.e. gives quantitative information. The technology is modified for studying edge effects and micro layers in liquids and gases.

Measurement of Refractive Index Variation of Water as Function of Temperature and Wavelength with a Fiber Optic Sensor

S. Yaltkaya, E. Kendir and S. Bayır

Physics Department, Akdeniz University, Faculty of Sciences & Arts, 07058 Antalya, TURKEY

The refractive index n(□) is basic optical properties of materials. While the refractive index and its temperature coefficient (dn/dT) are significant parameters of liquids for the optically controlling systems, such as the direct measurement of liquid solution concentrations and the optical paths. They also play a key role in index-matching measurement and anomalous effect like water. Water is the most abundant and life-critical substance in the world. The optical properties of water pose challenging scientific problems that require knowledge of the refractive index in order to be resolved [1]. The refractive index of water has been measured by many researchers for over a century. In this study variation of refractive index of water in liquid phase with temperature is measured and obtained dn/dT values at 980 nm, 1426 nm and 1550 nm (FWHM) wavelength respectively. For this aim the refractive index sensors is constructed with single mode optical fibers. The fiber optic sensor mainly consists of a diode laser, a fiber optic splitter, an optical isolator and a detector, connected to a computer via an ADC.

References

1 P. Schiebener, J Straub, J. M. H. Levelt Senger and J. S. Gallagher, " Refractive Index of Water and Steam as Function of Wavelength, Temperature and Density" J. Phys. Chem. Ref. Data, **19-3,** 677-717 (1990).

A Review of Laser Ablation Propulsion

C. Phipps[1], W. Bohn[2], T. Lippert[3], M. Michaelis[4], A. Sasoh[5], W. Schall[6] and J. Sinko[7]

[1] *Photonic Associates, LLC, 200A Ojo de la Vaca Road, Santa Fe NM 87508, U.S.A.*
[2] *Bohn Laser Consult, Weinberg Weg 43, Stuttgart, Germany*
[3] *Paul Scherrer Institut, CH 5232 Villigen PSI, Switzerland*
[4] *University of KwaZulu Natal, King George V Avenue, Durban, South Africa*
[5] *Department of Aerospace Endineering, Graduate School of Engineering, Nagoya University, Furo-cho, Chikusa-ku, Nagoya, Japan*
[6] *DLR Institute of Technical Physics, Stuttgart, Germany (Retired)*
[7] *Micro-Nano GCOE, Graduate School of Engineering, Nagoya University, Furo-cho, Chikusa-ku, Nagoya, Japan*

Main author email address: crphipps@aol.com

Laser Ablation Propulsion is a broad field with a wide range of applications. Laser-induced re-entry of space debris or launch to low planetary orbit involve a laser system which is remote from the propelled object (on another spacecraft or planet-based). Other applications use a laser which is a part of the propulsion engine onboard the spacecraft. Propulsion is due to the ablation jet created when an intense laser beam (pulsed or CW) strikes a condensed matter surface and produces a vapor or plasma jet. A universal advantage for this idea is that specific impulse (exhaust velocity) of a laser-ablation engine is adjustable and covers a broader range than is available from chemistry, because of the very high temperatures which can be attained. Adjustable exhaust velocity matches instantaneous requirements during a mission, giving much better energetic efficiency than possible with a fixed velocity. Practical realizations often lead to lower mass and greater simplicity for a payload delivery system, and ground-based launch concepts can dramatically reduce launch cost by using low-cost energy and facilitating high launch frequency.

We review the 30-year history of the subject from the transition from earlier pure photon propulsion concepts of Oberth and Sänger through Kantrowitz's original laser ablation propulsion idea to the development of air-breathing "Lightcraft" and advanced spacecraft propulsion engines. The polymers POM and GAP have played an important role in experimental realizations. Liquid ablation fuels show great promise, made possible by the realization of low vapor pressure, viscous polymers or, alternatively, by the use of thin liquid films.

We summarize the underlying theory, buttressed by extensive experimental data. Earlier workers, e.g., Pirri [1], treated laser-surface interaction primarily as an aerodynamic problem for the vapor regime in atmosphere. Phipps, et al. [2] addressed the vacuum plasma regime with a treatment that permitted ablation pressure predictions within a factor of two over a broad range of pulse duration and wavelength, but with intensity limits excluding ICF extremes and very short pulses. We discuss a new result [3] which provides a simple 1D model that spans the vapor and plasma regimes, with a smooth transition between the two.

References

1. Pirri A.N., *Phys. Fluids* **16** 1435-40 (1973)
2. C. R. Phipps, Jr., T. P. Turner, R. F. Harrison, G. W. York, W. Z. Osborne, G. K. Anderson, X. F. Corlis, L. C. Haynes, H. S. Steele, K. C. Spicochi and T. R. King, *J. Appl. Phys.*, **64**, 1083-1096 (1988).
3. C. R. Phipps, M. Birkan, H.-A. Eckel, H. Horisawa, T. Lippert, M. Michaelis, Y. Rezunkov, A. Sasoh, W. Schall, S. Scharring and J. Sinko, *J. Propulsion and Power*, to appear (2009)

Evaluation of Ammonia Absorption Coefficients by Photoacoustic Spectroscopy for Detection of Ammonia Levels in Human Breath

C. Achim, D. C. Dumitras, D. C. A. Dutu, R. Cernat

Department of Lasers, National Institute for Laser, Plasma and Radiation Physics,
P. O. Box MG-36, 409 Atomistilor St., 077125 Bucharest, Magurele, Romania
E-mail: cristina.achim@inflpr.ro

Photoacoustic spectroscopy has become a powerful technique for measuring extremely low absorptions independent of the path length and offers a degree of parameter control that cannot be attained by other methods. The absorption of laser radiation by a gas creates a pressure signal which is detected by a microphone. The resulting signal, processed by a phase sensitive detector, is directly proportional to the absorption coefficient and laser power [1].

We report precise measurements of ammonia the absorption coefficients at the CO_2 laser wavelengths by using a photoacoustic (PA) cell in an extracavity configuration and we compare with other values reported in the literature. Ammonia, presents a clear fingerprint spectrum and high absorption strengths in the CO_2 wavelengths region [2]. Because more than 250 molecular gases of environmental concern for atmospheric, industrial, medical, military, and scientific spheres exhibit strong absorption bands in the region 9,2 μm – 10,8 μm, we have chosen a frequency tunable CO_2 laser (73 different vibrational-rotational lines) with an output power up to 50 W.

In the present work, ammonia absorption was measured at both branches of the CO_2 laser lines by using a calibrated mixture of 10 ppm NH_3 in N_2 .

The measurement of absorption coefficients by the methods of photoacoustic spectroscopy has been applied to many gases that have a characteristic absorption spectrum in the CO_2 laser wavelength range [1, 2]. We obtained the ammonia absorption coefficients and we found the maximum absorption in the 9 μm region, at 9R30 line of the CO_2 laser. One of the applications based on the absorption of 9R30 line in ammonia, is used to measure the ammonia levels in expired human breath. This can be used to determine the exact time necessary at every session for an optimal degree of dialysis at patients with end-stage renal disease.

References

1. D. C. Dumitras, D. C. Dutu, C. Matei, A. M. Magureanu, M. Petrus, C. Popa, ''Laser photoacoustic spectroscopy: principles, instrumentation, and characterization", Journal of Optoelectronics and Advanced Materials **9**, No.12, pp. 3655-3701 (2007)

2. S. Cristescu, D. C. Dumitras, D. C. Dutu, "Ammonia and ethane absorption measurements with a tunable CO2 laser-based photoacoustic trace gas detector", International Conference on Advanced Laser Technologies ALT'99, Potenza-Lecce, Italy, September 20-24 (1999)

Photoacoustic Spectroscopy: Low vs. High Laser Power

D. C. Dumitras, D. C. A. Dutu, A. M. Bratu, M. Patachia, C. Achim,
M. Petrus, C. Matei, S. Banita

Department of Lasers, National Institute for Laser, Plasma and Radiation Physics,
409 Atomistilor St., P.O. Box MG-36, 077125 Bucharest, Romania
E-mail: dan.dumitras@inflpr.ro

In previous works[1,2] we presented an instrument based on the principles of laser photoacoustic spectroscopy designed for trace gas measurements at sub-ppb level. This laser photoacoustic spectrometer equiped with a low-power, continuous wave CO_2 laser was fully characterized in terms of laser tunability and frequency stability, cell parameters (cell constant, responsivity, electrical, acoustical and background noises) and overall characteristics of the spectrometer (pressure amplitude response, limiting sensitivities of the cell and of the system, limiting measurable concentration of ethylene, minimum measurable signal in nitrogen, minimum detectable pressure amplitude, minimum detectable concentration, minimum detectable absorption cross section, minimum measurable absorption coefficient, and cell sensitivity for 1 ppb of ethylene). A comparison of these parameters (coherent acoustic background noise 2.6 μV, coherent photoacoustic background signal 2.7 μV/W, cell responsivity 280 V cm/W) with the best results reported by other authors demonstrates that we succeeded to achieve the best value for the minimum detectable concentration (0.9 ppb) reported to date.

By analyzing the dependence of the minimum detectable concentration (c_{min}) on the minimum measurable voltage signal (V_{min}) obtained at SNR (signal-to-noise-ratio) = 1, on the gas absorption coefficient (α), on the laser power (P_L) and on the cell responsivity (R): $c_{min} = V_{min}/\alpha P_L R$, we see that it is possible to get a smaller detectable concentration by increasing the laser power. In our experimental set-up we replaced the low-power CO_2 laser (5 W) with a line-tunable, high power CO_2 laser (50 W) in an extracavity configuration. In this case we may expect also the increase of the coherent photoacoustic background signal (which is the main component of V_{min}) and the appearance of saturation effects, similar to those observed in intracavity configurations[3].

We have optimized all components of the experimental set-up and we have measured the relevant parameters to characterize this new high-power, extracavity laser configuration. We found that the cell responsivity can be increased by 10% (310 V cm/W) (value confirmed by the measurements of absorption coefficients in ammonia), while the coherent photoacoustic background signal can be reduced by a factor of near 4, to 0.7 μV/W. In ethylene (α = 30.4 $cm^{-1}atm^{-1}$) and at a laser power of 15 W (10P(14) line of the CO_2 laser) through the photoacoustic (PA) cell, we were able to reduce further the minimum detectable concentration to a value of 0.3 ppb (an improvement with a factor of 3 compared to the best previous reported value). When the laser power through the PA cell is increased from 2 W to 15 W, the saturation effect is evidently, manifesting by a decrease of the cell responsivity by a factor of 6 (from 310 V cm/W to 52 V cm/W). To measure the influence of the laser power to the saturation factor and to the coherent photoacoustic background signal, we introduced in the laser beam several water-cooled apertures with diameters of 1.4 - 5 mm (the measured $1/e^2$ laser beam diameter is 7.09 mm). The saturation is negligible only when the laser power is reduced under 2 W (1.9 W with an aperture of 1.9 mm). Unfortunately, the coherent photoacoustic background signal increases tremendously (50 times) for each aperture, owing to diffraction effects at the edges of the aperture. Our conclusion is that the increase of laser power is advantageous, but saturation effects must be taken into consideration.

This laser photoacoustic spectrometer is very useful for implementation in medical and environmental applications, because it is possible to identify and measure quantitatively hundreds of molecular trace gases with an accuracy of several parts per billion.

References

1. D. C. Dumitras, D. C. Dutu, C. Matei, A. M. Magureanu, M. Petrus, C. Popa, *"Laser photoacoustic spectroscopy: principles, instrumentation, and characterization"*, Journal of Optoelectronics and Advanced Materials **9**, No. 12, pp. 3655-3701 (2007)

Optoacoustic Phenomenon in Submicron Metal Coating Covered by a Transparent Liquid: Theory and Application for Evaluation of Coating Properties

Kopylova D.S., Pelivanov I.M., Podymova N.B., Karabutov A.A.
International Laser Center, Moscow State University, Moscow, Russia

Optoacoustic (OA) conversion in the system consisting of a metal film deposited on a transparent dielectric substrate and covered by a liquid is considered theoretically and experimentally. This consideration implies a method for non-destructive evaluation of submicron metal coatings. The main principle of the method is the following. Irradiation of the metal film by a nanosecond laser pulse leads to transient heating and expansion of the film that in turn results in the excitation of an acoustic signal. The waveform of the signal consists of two contributions: the "primary" signal from the thermal expansion of the metal film and the "secondary" signal, that originates from the thermal expansion of the adjacent liquid layer. Due to low thermal conductivity of liquid compared to metal, the liquid accumulates heat that is released in metal and produces that "secondary" contribution into the OA conversion. This contribution is very sensitive to the properties of the film. The influence of the film thickness and its thermophysical parameters on the frequency-dependent efficiency of OA conversion and on the temporal profile of excited OA signals is discussed in detail.

Two different detection modes are considered. In the forward mode laser pulse irradiates the film from the side of the substrate and in the backward mode – from the side of the liquid. Detection of induced ultrasonic pulses is performed in the liquid in both cases.

Three chrome coatings of different thickness deposed on a quartz substrate were investigated experimentally. It is shown that the film thickness can be determined by the spectrum of the detected pressure signal with the error of 50 nm. The measuring thickness range is determined by the heat diffusion length within the laser pulse duration and at nanosecond laser impact estimated as: from 50 nm to 5 m [1]. Thermal diffusivity of the metal coatings can be evaluated as well.

References

1 D.S. Kopylova, I.M. Pelivanov, N.B. Podymova, A.A. Karabutov, "Thickness Measurement for Submicron Metallic Coatings on a Transparent Substrate by Laser Optoacoustic Technique", *Acoustical Physics,* **54**, 783-791 (2008).

Vertical concentration distribution measurement of atmospheric aerosols by laser light scattering

Daniel Oszetzky[2], Attila Nagy, Attila Kerekes, Aladár Czitrovszky
Research Institute for Solid State Physics and Optics
Hungarian Academy of Sciences
Budapest 1525, P. O. Box 49, Hungary
odani@szfki.hu

Measurement of aerosol concentration in the atmosphere by laser light scattering methods has a long history. The Laser Application Department of our Institute has been developing airborne particle counters for years [1,2]. With these devices one can determinate the local concentration and size distribution of aerosols. However to measure the vertical concentration distribution of atmospheric aerosols over a certain region (city, motorway, etc.) can be difficult. In this paper we offer a new approach for this problem using a special laser light scanning and detection method for different heights.

Our experimental set up consists of two 532 nm wavelength DPSS lasers with beam expanders. The lasers are pointed upwards and the overlapping beams appoint us the measurement volume. The scattered light from particles inside the measurement volume is detected by a single photon counting module (SPCM) focused precisely on the overlapping beams.

To filter all the scattering from the background we use a narrow bandwidth interference filter centered to the laser wavelength and lock-in detection. The particle concentration can be calculated from the detected signal and the measurement volume. Changing the geometrical alignment of the set up we can easily change the height where the beams overlap and therefore the vertical distribution of concentration can be determined. The range of this method can be increased to a few hundred meters by using more powerful lasers.

The proposed method can substitute the existing more complicated and more expensive systems.

References

1 W.W. Szymanski, A. Nagy, A. Czitrovszky, P. Jani, "A new method for the simultaneous measurement of aerosol particle size, complex refractive index and particle density", *Measurement Science and Technology*, **13**, 303-307 (2002).

2 A. Nagy, W.W. Szymanski, A. Golczewski, P. Gál, A. Czitrovszky, "Numerical and experimental study of the performance of the Dual Wavelength Optical Particle Spectrometer (DWOPS)", *Journal of Aerosol Science*, **38** 467-478 (2007).

Diffraction of plasmon-polariton beams on metal/metamaterial-dielectric interfaces

Daria O. Saparina[1] and Anatoly P. Sukhorukov[1]
[1] *M.V. Lomonosov Moscow State University, Faculty of Physics, Moscow, Russia*

Surface waves exist on interfaces of media with different signs of permittivity or permeability. Metals are known to possess negative permittivity, and recently artificial metamaterials with negative permittivity and permeability were manufactured. Surface waves in metamaterials [1,2] have several peculiarities, among which the most important one is existence of both *TE* and *TM* modes, in contrast to metal-dielectric interface supporting only *TM* waves. Due to the strong localization of surface waves their intensity can be sufficiently larger than excitant beam intensity, so nonlinear effects in surface waves propagation can be easily observed.

We present theory of surface wave diffraction on metal/metamaterial-dielectric interface. Previous works (for example, [1,2]), refer to case of plane wave propagation. Nonlinear effects, such as dark soliton trapping, are also considered in this paper.

Let's consider electromagnetic field of surface plasmon-polariton wave in the form

$$E(x,y,z,\xi) = A(x,y,\xi) f(z) \exp(i\beta x - i\omega_0 t), \quad (1)$$

where β is the plasmon-polariton wave vector, $\xi = x - v_{gr} t$ is co-moving with the group velocity $v_{gr} = \partial\omega / \partial\beta$ coordinate, *A(x,y,ξ)* is the slowly varying amplitude, *f(z)* describes mode structure. In the linear case structure of the surface mode can be described as $f(z) = \exp(-\gamma_j z)$, where constant γ_i (*i=1,2*) defines field localization; in nonlinear case $f(z) = f_0 \operatorname{sech}[\eta_j (z - z_{j0})]$ [2].

We derived diffraction equation for surface wave beams, while equation for propagation of pulses of infinite width in nonlinear media was obtained in [2]. Taking into account diffraction, dispersion and nonlinearity the equation for surface plasmon-polariton waves of finite width and duration can be written in the form:

$$\frac{\partial A}{\partial x} + iD_{dis}\frac{\partial^2 A}{\partial \xi^2} + iD_{dif}\frac{\partial^2 A}{\partial y^2} - i\alpha |A|^2 A = 0, \quad (2)$$

where diffraction and dispersion coefficients are $D_{dif} = \frac{1}{2\beta}$, $D_{dis} = \frac{1}{2}\frac{dv_{gr}^{-1}}{d\omega}\Big|_{k=k_0}$ respectively, and α is the effective nonlinear coefficient, sign and value of which depends on the media permittivities, permeabilities and nonlinearities. Equation (2) is the nonlinear Schrodinger equation having soliton solutions.

The form of equation (2) implies that spatio-temporal plasmon-polariton vortices can be generated (see, for example, [3]). The simplest case corresponds to a wave carrying unity-charged screw dislocation. Phase singularity appears to be in the center of such beam with zero amplitude. Amplitude of a vortex nested in a Gaussian beam is complex and is written as the following:

$$A(x,y,\xi) = A_0 \cdot (y + i\xi) \exp\left(-\frac{y^2}{a_0^2} - \frac{\xi^2}{b_0^2}\right) \quad (3)$$

The dynamics of such plasmon vortex is considered analytically and numerically. Energy flow trajectories are calculated. Equation (2) also has an approximate solution [5]:

$$A = A_0 \cdot \exp\left[-(y^2 + D_{dif}/D_{dis}\xi^2)^3 / a_0^6\right] \tanh\left(\sqrt{y^2 + D_{dif}/D_{dis}\xi^2}/r_0\right) \exp\left[i \arctan\left(\sqrt{D_{dif}/D_{dis}}\,\xi / x\right)\right] \quad (5)$$

in the form of spatio-temporal vortex-soliton in the case of defocusing effective nonlinear coefficient α.

References

1 Ruppin R. "Surface polaritons of a left-handed medium", *Phys. Lett. A* **277** 61 (2000)
2 Shadrivov I. V., Sukhorukov A. A., Kivshar Yu. S. et al. "Nonlinear surface waves in left-handed materials" *Phys. Rev. E* **69** 016617 (2004)
3 Sukhorukov A.P., Yangirova V.V. "Spatio-temporal vortices: properties, generation and recording" *Proc. of SPIE*, **5949** 594906 (2005)

Alternative Materials for High Power Lasers

David E. Zelmon[1], K.L. Schepler[2], Shekhar Guha[2], S. M. Hegde[2], Julie J. Lee[1], and Leonel Gonzalez[2]

[1]*Air Force Research Laboratory, Materials and Manufacturing Directorate, Wright Patterson AFB, OH, USA*

[2]*Air Force Research Laboratory, Sensors Directorate, Wright Patterson AFB, OH, USA*

The dominant material for fiber lasers is doped silica. However, as requirements for higher laser power increase, this material begins to show signs of significant limitations due to imperfections in the material, thermal management, and nonlinear effects such as stimulated Brillouin scattering. Polycrystalline YAG has the potential to overcome many of these problems due to its greater efficiency, higher thermal conductivity and lower SBS threshold. We present a series of measurements showing the optical properties of polycrystalline YAG and show that these properties will lead to superior performance in high power lasers.

Nonlinear optics at the single optical cycle limit

Eleftherios Goulielmakis

The decisive role of intense, nearly-single-cycle pulses for the generation of sub-100 attosecond soft x-rays [1], the precise metrology of light fields with attosecond resolution [2] as well as for the development of ultrashort and intense light sources in the deep ultraviolet [3],[4] will be discussed along with recent developments and results.

References

1. E. Goulielmakis *et al.*, *Science* **320**, 1614 (2008).
2. E. Goulielmakis *et al.*, *Science* **305**, 1267 (2004).
3. U. Graf et al., Optics Express **16**, 18956 (2008).
4. E. E. Serebryannikov *et al.,* New J. Phys. 10, 093001 (2008).

LIBS-study of Components Migration in Steel Weld Joints

Elena L. Surmenko[1,2], Tatiana N. Sokolova[1,2], and Ivan A. Popov[1,2]
[1] *Educational-Research Lab. of Laser Technics & Technology, Saratov State Technical University, Saratov, Russia*
[2] *Chair of Electronic Engineering and Welding , Saratov State Technical University, Saratov, Russia*

A weld joint is characterized by special element composition of the melt zone in depth and width. The type of element distribution depends on welded materials and welding modes. The result of migration of different components of the joint causes some changes in functional properties of the preform.

Welding of steel alloys is considered. The distribution of chemical elements in weld joints is studied by LIBS. Special LIBS-technique - scanning sampling [1] - by Q-switched Nd:YAG-laser is used. It allows the layer-by-layer analysis of weld joints to be implemented. Also the features of surface modification of weld joints was studied. The special analytical software [2] was used for experiment.

References

1 E.L. Surmenko, V.V. Tuchin, T.N. Sokolova, "Laser microspectral analysis of thin evaporations of unknown composition", *Proc. SPIE. Bellingham, SPIE*, 4241, 300-302 (2000).
2 Sert. RU.C.37.006.A □18673. Registrars of spectra, multichannel, measuring MIRS / Reg. □27644-0499109237; Brought □□ the state register 08.10.2004.

Intermittency and Chaos in a Semiconductor Laser Subjected to Strong Coherent and Incoherent Feedback

Enrico Randone and Silvano Donati

Department of Electronics, University of Pavia, Pavia/Italy

The dynamics of a semiconductor[1,2] laser subjected to strong feedback from a remote reflector is studied experimentally.

We employ a scheme of free space propagation to a reflecting mirror, and use a monitor photodiode to look at the outgoing laser beam. Time series, electrical frequency spectrum as well as optical spectrum of the laser are used to characterize the regime of oscillation at several levels of bias current of the diode laser.

When the level of injection is increased, at $k<0.1$ (in power ratio) first we observe an excess amplitude noise, then (at $k=0.5$) burst of damped oscillations at the relaxation frequency of the unperturbed laser, with a periodicity given by the roundtrip time of flight of the external cavity[3]. Correspondingly, the optical spectra is widened and shifted to the red. This is the so-called intermittency regime.

At even larger coupling ($k=0.8$) the time waveform of the oscillation exhibits strong pseudorandom fluctuations, the line-width of the optical spectrum is much widened (over 3 times the unperturbed value) and the electrical spectrum exhibits peaks at the inverse roundtrip time and its sub-harmonics. We have also noticed, for the first time in literature, a hysteresis of the curve describing the dynamical regime evolution as a function of the injection parameter.

References

1 G. Giuliani S. Donati: "*Optical Feedback Effects*" in: "*Unlocking Dynamical Diversity - Optical Feedback Effects on Semiconductor Lasers*", ed. by A.Shore and D.Kane, J.Wiley and Sons, Chichester (2005).

2 R.Ju, P.Spencer, "Dynamic Regimes in Semiconductor Lasers Subject to Incoherent Optical Feedback" *Journal Lightwave Technology* **23**, 2513-2522 (2005)

3 J. Otsubo: "*Semiconductor Lasers: Stability, Instability and Chaos*" Springer Verlag vol.111, Berlin 2006.

4 S. Donati, C.Mirasso (Editors): '*Optical Chaotic Cryptography*', Feature Issue of: IEEE Journal of Quantum Electronics, **38**, 1138-1184 (2002).

Laser pulse shape effects on the hardness of steel

E. Akman[1], L.Candan[1], M. Zeren[2], E. Kacar[1,3], A. Demir[1,3]

[1] *Laser Technologies Research and Application Center Kocaeli University 41380 Kocaeli/Turkey*
[2]*Metallurgical and Materials Engineering Department, Kocaeli University 41380 Kocaeli/Turkey*
[3] *Faculty of Arts and Science, Department of physics, Kocaeli University 41380 Kocaeli/Turkey*

Main author email address: erhan.akman@kocaeli.edu.tr

Laser beam hardening is used to locally enhance the surface properties of materials. The high heating and cooling rates capability of the laser on the material causes the changes on the microstructure and so good mechanical properties can be obtained. The laser hardening results depend on the properties of the material and the laser radiation parameters such as wavelength, pulse duration, pulse energy and the laser pulse-shape. Through the changes in shape of pulse, rate of the thermal gradient can be changed; therefore laser heat treatment efficiency can be improved.

In this study, changing the pulse shape of the millisecond Nd:YAG laser it has been aimed to reach the most convenient shape for the laser heat treatment. Triangular pulse shape (ramp up, ramp down) have been used to obtain maximum thermal gradient in laser treatment process. Also the experiments have been repeated in nitrogen environment in order to reach the maximum wear resistance on 2 mm thickness steel plates.

Theoretical and Experimental Characterization of Nanosecond-Laser-Induced Plasmas for Ignition

E. Wintner
Photonics Institute, Vienna University of Technology, Vienna, Austria

With the improvement of modern solid-state lasers new applications become more and more widespread, the initiation and diagnostics of chemical processes [1] being one special class of them. The initiation of a plasma by nanosecond laser pulses or shorter ones allows e.g. to reliably start combustion processes which is of special importance in case of internal combustion engines. Therefore a worldwide race towards the first realization of laser-ignited engines has been going on within the last years. Advantages may comprise higher efficiency and substantial reduction of pollutant emissions as well extended service intervals. The development of laser ignition comprises a lot of basic research like the investigation of the dependence of plasma threshold on various ambient parameters like pressure, temperature, combustible gas mixture, concentration of seed charges etc. On the other hand, the specifications of the laser pulses applied are of crucial importance: wavelength, pulse energy, pulse duration, focal diameter, and potentially the repetition rate of several pulses.

We have investigated all these specific aspects experimentally as well as theoretically in a long-term research effort. Recently, we succeeded to simulate the plasma threshold when applying ns laser pulses of ~ 1 µm wavelength representing the most likely candidate for an ignition laser – Nd:YAG. In this context, a kinetic model of electron cascade growth in the electromagnetic field of a focused intense laser pulse as generally used for laser spark generation in gases has been numerically implemented in Visual C code. The effects considered comprise Drude absorption, diffusive kinetic and inelastic losses as well as (three-particle) electron recombination. The objectives were to illustrate the dynamic process of gas ionization and to clarify the pressure dependence of known breakdown thresholds within a range of about $2 \cdot 10^4$ to $2 \cdot 10^6$ Pa of initial pressure. Exemplary results with laser pulse energy of 26 mJ applied to N_2 gas, pulse duration of 14 ns and 18 µm focal spot size illustrate the dynamic process of ionization within a very short time period of less than 0.5 ns. Identical laser parameters as in experiments conducted previously were used and the results are in excellent agreement with respect to curve shapes, i.e. MPE $\sim 1/p^{0.4}$ and $\sim 1/p^{0.3}$ in different experiments.

Furthermore, experimental investigations covering optical breakdown thresholds, plasma absorption efficiency, plasma scattering, and ultra-sound wave emission for the fundamental wavelength of Nd:YAG as well as its SH are reported. It turned out, that the minimum pulse energy for optical breakdown applying green laser radiation is somewhat lower compared to the case of 1064 nm due to better focusability. Plasma absorption of the infrared light was found to be stronger above approximately 10 mJ. Plasma transmission losses are much more dominant than scattering losses at both wavelengths.

References

1 M. Lackner, "Lasers in Chemistry - Probing and Influencing Matter", ISBN-13:978-3-527-31997-8 - Wiley-VCH, Weinheim, 2008;
2 H. Kofler, J. Tauer, E. Wintner, "Laser-induced ignition for combustion engines".

Roughness Measurement with Laser Speckle Pattern of Milled Metals Using Speckle Statistics Analysis

E. Kayahan [1], F. Hacizade[2], O. Gundogdu[3,4], H. Nasibov[2]

[1] *Kocaeli University, Gebze Vocational School, 41410, Çayırova, Kocaeli,Turkey*
[2] *TÜBİTAK-UEKAE, 41470, Gebze, Turkey*
3 Department of Physics, Faculty of Engineering and Physical Sciences, University of Surrey, Guildford, Surrey, GU2 7XH, United Kingdom
[4] *Kocaeli University,Umuttepe Campus,41384, Kocaeli, Turkey*

The laser beam, reflected from a milled surface contains both specular and diffuse components. The origin of the diffuse component is the surface asperities, whose randomly distributed pattern leads to the random interference of scattered coherent laser beam, i.e. to the optical phenomena called Laser Speckle [1], as seen Fig. 1(a). Laser speckle techniques play dominant role in noncontact surface roughness measurements [2]. In this study, we present an experimental investigation of milled metallic surface roughness by means of multicolor laser speckle patterns, generated by various wavelengths of 543 nm, 594 nm and 633 nm, of He-Ne (CW) laser. The optical measurements were carried out on the several steel specimens with different roughness values of R_a ranging from 0,5 µm to 2µm, measured by stylus. Used experimental setup is shown in Fig. 1(b). To determination of surface roughness of milled metal surfaces, optical method was used using properties of the speckle pattern. The laser speckle patterns of all specimens were captured at every highlighted wavelength and analyzed by utilizing statistical image processing approach to the surface roughness. In this method, the speckle images are converted to binary images and various parameters such as bright and dark regions pixel counts, areas and their ratios were calculated. The obtained speckle patterns statistical results for different specimens at every wavelength were compared with the stylus results of R_a, and it was found that, there is a good correlation between them. Optical method using properties of speckle pattern, it has great potential to be used for in-process measurement and automation due to the simplicity of optical system used.

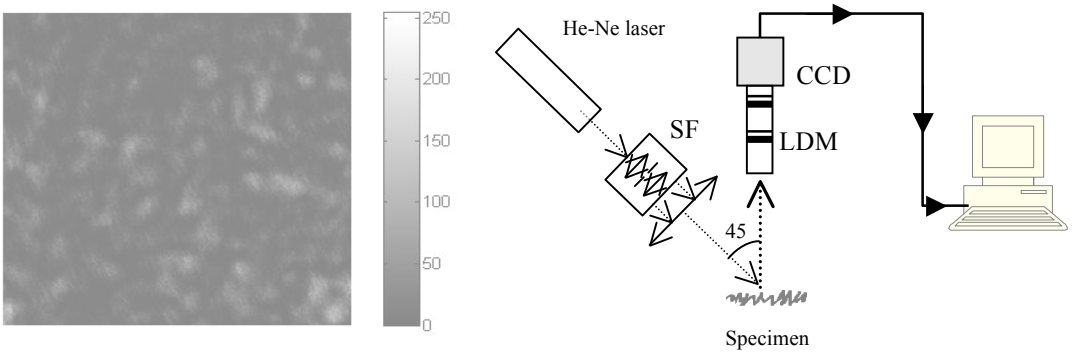

(a) (b)

Fig. 1. CCD image (1024x1360 pixels) of a speckle pattern (a) and schematic diagram for speckle pattern formation (b). Where, LDM and SF are long distance microscope and spatial filter, respectively.

References

1 U. Persson, ''Measurement of surface roughness on rough machined surface using speckle correlation and image analysis", Wear, **160**, 221-225, (1993).
2 E. Kayahan, H. Oktem, F. Hacizade, H. Nasibov, O. Gundogdu, '' Measurement of surface roughness of metals using binary speckle image analysis'', Tribology International, (article in press), (2009).

Thin disk laser: A versatile tool for micro machining

F. Dausinger

Dausinger + Giesen GmbH, Rotebuehlstr. 87, D-70178 Stuttgart,
dausinger@dausinger-giesen.de

On the fast growing market of precision micromachining of mechanical and electronic components as well as of photovoltaic elements lasers do not only compete with other methods of structuring. There is also strong competition among laser sources with different pulse duration. A comprehensive study of laser micro-machining with nanosecond, picosecond, and femtosecond laser pulses resulting in selection rules will be presented in the first part.

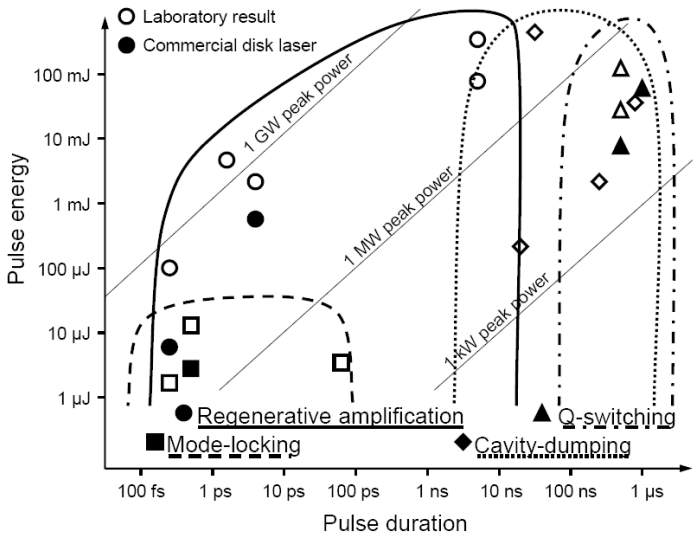

Figure 1 Pulse energy and duration values of thin disk lasers [1].

In the second part it will be shown, that the thin disk laser principle not only can be operated in all the mentioned pulse duration regimes but also offers pulse energy levels which neither fiber nor slab or rod lasers can reach, see figure 1. The contribution will summarize what has been reached so far in laboratory and commercial systems and give and outlook on what can be expected in the near future.

References

[1] C. Stolzenburg, A. Voss, T. Graf, M. Larionov and A. Giesen, Advanced pulsed thin disk laser sources, Proc. SPIE 6871, 68710H (Photonics West 2008)

New Multiwavelength Mie-Raman Lidar in Turkey for Aerosol Studies

K. Allakhverdiev [1,2], T. Baykara [1], M. Bekbolet [3], F. Huseyinoglu [1,3*], S. Ozbek [1], Z. Salaeva[1,2], A. Secgin[1], S. Vartapetov [4], I. Veselovskii [4]

[1]TUBITAK, Marmara Research Center, Materials Institute, P.K. 21, 41470 Gebze/Kocaeli,Turkey
[2]Institute of Physics ANAS, 370143, Baku, Azerbaijan
[3]Bogazici University, Institute of Environmental Sciences, P.K. 34342, Bebek/Istanbul, Turkey
[4]Physics Instrumentation Center of General Physics Institute, Troitsk, Moscow region, 142190 Russia

** E- mail: Fatih.Huseyinoglu@mam.gov.tr Fax: (+90 262) 641 23 09*

The multiwavelength Mie-Raman lidar based on a tripled Nd:YAG laser becomes an important tool for profiling aerosol physical parameters in the planetary boundary layer (PBL). Such lidar quantifies three aerosol backscattering and two extinction coefficients and from these optical data the particle parameters such as concentration, size and complex refractive index are retrieved through inversion with regularization [1]. In our presentation we give the description of new multiwavelength lidar installed in TUBITAK, MRC, Materials Institute, Laser Spectroscopy Lab., Turkey. The laser source in lidar system is the 5th Harmonic Generation Module Nd:YAG laser (QUANTEL - Brilliant B) emitting 855 / 400 / 240 / 95 / 17 / mJ in a pulse at 1064 / 532 / 355 / 266 / 213 / nm wavelengths, respectively. Laser repetition rate is 10 Hz. Laser beam is collimated by off axis parabolic mirrors with high reflecting dielectric coating at all three wavelengths. Laser beam diameter after collimation is 40 mm and divergence below 0.2 mrad.

Laser and collimator are mounted on the telescope side allowing operation at an angle to horizontal. Scattered radiation is detected by 400 mm aperture Newtonian telescope with the focal length of 1.2 m. The optical signals are separated and analyzed in 7-channels spectrum analyzer. In the process of measurements we monitor the elastic backscatters (355, 532, 1064 nm), depolarization at 355 nm, nitrogen Raman (387, 608 nm) and water vapor (408 nm) signals. Thus, the lidar will provide comprehensive information about aerosol parameters. The main directions of coming lidar research are:

- **Study of seasonal and diurnal variations of aerosol characteristics in Istanbul region;**
- **Separation of atmospheric aerosols of anthropogenic and natural origin;**
- **Investigation of African dust transport;**
- **Study of fuel burning aerosol distribution over Bosphorus;**
- **Comparison of aerosol parameters retrieved from lidar data with data from other instruments;**
- **Application of aerosol lidar data for estimation of climate forcing.**

Fluorescence channel is in development and will be installed. This channel will allow detection of the gas pollutions in the atmosphere and the water pollutions in the Bosphorus. The authors are indebted to the State Plan Committee (DPT) of Turkey for the support.

References

1 I. Veselovskii, A. Kolgotin, V. Griaznov, D .Muller, U. Wandinger, D. Whiteman, "Inversion with regularization for the retrieval of tropospheric aerosol parameters from multiwavelength lidar sounding", *Appl. Opt.* 41, 3685-3699 (2002).

Detailed theoretical analysis of thermal effects in Er-Yb phosphate glass microchip lasers

Feng Song, Teng Li ,Fang Wang, Shujing Liu, Hong Cai, and Jianguo Tian
Photonics Center, Nankai University, Tianjin 300071, China
Key Laboratory of Weak-Light Nonlinear Photonics, Ministry of Education, Tianjin 300457, China
fsong@nankai.edu.cn , Fax: 022-23501743

Laser diode(LD) pumped 1.54□m Er-Yb codoped solid state lasers have many advantages, such as compact structure, high efficiency, low cost. They can be applied in laser detection and medical diagnosis, because the wavelength belongs to the so called "eye safe" region. Therefore, laser diode pumped 1.54□m Er-Yb codoped solid state lasers attract more and more interest in the scholar and industrial field.

In Er-Yb-codoped phosphate glass laser, the temperature of the media increases due to such factors as low heat conductivity, the high absorbed pump power, and quantum defect. Excited sate absorption in this kind of material also contribute to the heat generation. Extra thermal load is deposited in the glass resulting in the thermal effects, which influence the laser performance and efficiency greatly. Many theoretical and experimental researches have concentrated on the study of thermal effects in various solid-state lasers recently, but most of them are focused on LD pumped Nd-doped and Yb-doped material lasers. However, the thermal effects in Er-Yb-codoped phosphate glass laser has received little attention. Thus analysis of thermal effects in Er-Yb phosphate glass microchip lasers is very necessary and important.

Thermal effects cause the dynamical change of the laser mode size. Subsequently, the threshold pump power and the laser slope efficiency also change dynamically. In this paper, an investigation of thermal effects in longitudinally LD end pumped Er-Yb-codoped phosphate glass microchip TEM_{00} lasers is made in detail numerically. The distributions of temperature and stress in the glass were calculated according to comparison of edge-cooling and end-cooling under identical conditions with finite element analysis. Based on the optical path difference distribution, thermal induced diffraction losses in end-cooling scheme were investigated. We find that the higher the pump power the higher the thermally induced diffraction loss is for a given mode-to-pump ratio. The diffraction loss at a fixed pump power is an increasing function of mode-to-pump ratio.

Investigation on Carriers Confinement in Photonic-Corral-Mode Quantum Ring Lasers

G. A. Stanciu[1], R. Hristu[1], S.G. Stanciu[1], O'Dae Kwon[2],

[1]Center for Microscopy- Microanalysis and Information Processing, University "POLITEHNICA" of Bucharest, Splaiul Independentei 313, 060032, Bucharest, Romania
[2]Department of Electrical Engineering, Pohang University of Science & Technology San31 Hyojadong, Pohang 790-784, Korea

Main author email address: stanciu@physics.pub.ro

Ultralow threshold microcavity lasers are ideal candidates for high-density optical interconnect light sources. PQR structure was fabricated on an n-type (100) GaAs substrate grown by the metal-organic vapor-phase epitaxy method. The structure consists of two distributed Bragg reflectors (DBRs) mirrors surrounding a one-l cavity, which has three 8 nm GaAs quantum wells (QWs), $Al_{0.3}Ga_{0.7}As$ barriers and spacers. The thickness of one-l cavity is 269.4 nm. There are 38.5 periods in the n-type bottom mirror and 8 periods in the p-type top mirror. The mirrors consist of alternating 41.98 nm $Al_{0.15}Ga_{0.85}As$ and 48.82 nm $Al_{0.95}Ga_{0.05}As$ layers. Between the layers, a 20 nm thick linearly graded AlGaAs layer was grown. The p- and n- DBR mirrors were doped to a dose $>10^{18}$ cm^{-3} with C and Si, respectively. The height of the PQR mesa structure is 4.5 □m. The investigation have been made using by laser scanning microscopy and laser beam induced current (LBIC) technique. The laser source was a He-Ne laser operating at 633 nm and 100 mW maximum output power. By using laser beam induced current technique technique we investigated the carriers confinement in the laser structure.

Sorption of the ions with different ionic radii on protein surface in the process of nanocluster formation

Khlapov V.P, G.P. Petrova, Yu.M. Petrusevich
Physics Department
of Lomonosov Moscow State University, Moscow, Russia
Fax:+7(495)932-882
petrova@phys.msu.ru

Laser light scattering method (Rayleigh – Debye) was used for sorption mechanism study of the ions with different value of ionic radius on the protein surface. In our research Bovine serum Albumin (BSA) water solutions containing K^+, Na^+ and Pb^{++} ions at different ionic strengths were investigated.

With the help of the automatized optical set-up scattering parameters of these solutions were studying, such as, Rayleigh scattering coefficients, the masses of scattering particles, intermoleculare interaction coefficients as the functions of pH, protein concentrations and ionic strengths. On the fig 1, 2 and 3 the ratios of scattering particles masses to molecular mass of Albumin are shown for protein water solutions contained NaCl (1), KCl (2) and $PbCl_2$ (3), as the function of ionic strength obtained in the region of protein isoelectric point.

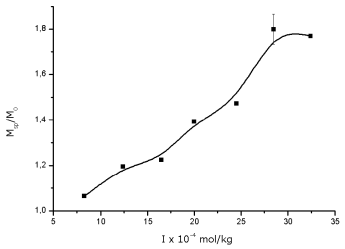

Fig.1 (pH5), NaCl

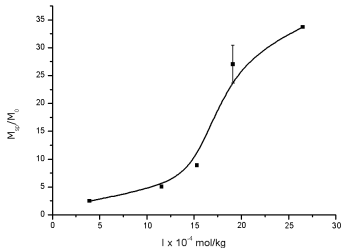

Fig.2 (pH5), KCl

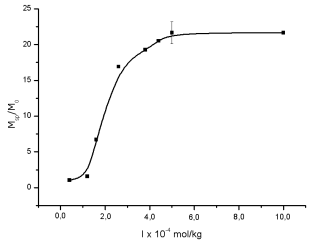

Fig.3.(pH5),$PbCl_2$

The main result is that the presence the ions with large ionic radii like K^+ (1,33 Å) and Pb^{++} (1,2 Å) stimulate the forming of nanoparticles with the mass more than one order to molecular mass of albumin M_o. In the presence of Na^+ (0,9 Å) in albumin solutions the nanocluster are absent, the maximum .of the scattering particle mass less than $1{,}8M_o$.

In the region of small ion concentration (I) the dependences of mass have a initial part practically linear (Langmuir monolayer). With the increase of ion concentration (I) the saturation in this dependences is observed , which can be connected with the difference in the sorption processes of the ions.

16.6 W, Near- and Mid-Infrared Optical Parametric Oscillator Pumped by an Yb Fiber Laser

S.Chaitanya Kumar[1], Ritwick Das[1], G. K. Samanta[1], and M. Ebrahim-Zadeh[1,2]

[1] *ICFO-Institut de Ciencies Fotoniques, Mediterranean Technology Park, 08860 Castelldefels, Barcelona, Spain*

[2] *Institucio Catalana de Recerca i Estudis Avancats (ICREA), Passeig Lluis Companys 23, Barcelona 08010, Spain*

Main author email address: goutam.samanta@icfo.es

High power, continuous-wave (cw), singly-resonant optical parametric oscillators (SROs), tunable in the near- and mid-IR, are of great importance for applications in spectroscopy, biomedicine, and atmospheric propagation. Such cw SROs based on the most widely used nonlinear material, periodically poled $LiNbO_3$ (PPLN), have been extensively demonstrated previously. However, attainment of high optical powers in the near- and mid-IR is an experimentally challenging proposition, essentially due to heavy thermal loading of the nonlinear crystal resulting from the high intracavity signal power at increased pump powers. This can lead to saturation and subsequently a substantial drop in efficiency, thus limiting the available output power. To date, a maximum of 10 W at 50 W of pump power at 20% efficiency has been reported in a cw SRO [1]. A substantial reduction in the thermal loading by out-coupling the resonating signal has enabled considerable increase in the overall extraction efficiency up to 59% resulting in a total power of 8.6 W (5.1 W signal, 3.5 W idler) for 15 W of pump power [2]. Recently, we also demonstrated that the use of output coupling can result in substantial enhancement in the overall performance of cw SROs without degrading output power and stability [3]. Using the out-coupling approach, we have now generated up to 16.6 W of output power (8.3 W of signal and 8.3 W of idler) from a cw SRO for 26.8 W of pump power at an extraction efficiency to 62%. Moreover, the device is based on a cw Yb fiber laser as the pump source, resulting in a highly compact, practical, and portable design.

The Yb fiber pump laser delivers up to 30 W of single-frequency radiation at 1064 nm in a linearly polarized beam with M^2 factor <1.01. The pump beam is focused to a waist radius of w_{op}~67 □m at the centre of the crystal, corresponding to a focusing parameter of □~1. The SRO is based on a 50-mm long multi-grating (Λ=29.5-31.5 μm) MgO:PPLN crystal and is configured in a compact ring cavity consisting of two plano-concave mirrors (r=150 mm) and two plane mirrors. All mirrors have R>99%@ 1.3-1.9 μm and T>90%@2.2-4 μm, thus ensuring SRO operation. For out-coupled SRO (OC-SRO) operation, we replaced one of the plane mirrors with an output coupler with T~5% across 1.3-1.9 μm.

We measured the output powers of SRO (idler-only extraction) and OC-SRO (both idler and signal extraction) as a function of input pump power at 100 °C crystal temperature corresponding to a signal wavelength of 1629 nm and idler wavelength of 3067 nm. Although the OC-SRO has higher threshold (11.6 W) compared to SRO (5.2 W), it can provide higher output power 16.6 W (8.3W of signal, 8.3W of idler) for 26.8 W of pump and higher efficiency of 62% compared to SRO, which provides 7.6 W of idler for 25 W of pump with a maximum efficiency of 30.4%. Under free-running condition and without any thermal isolation, the signal power shows higher peak-to-peak power stability (12%) than the idler (17.2%).

References

1. BD. Chen and T. S. Rose, Conference on Lasers and Electro-Optics (CLEO), paper CThQ2 (2007).
2. A. Henderson and R. Stafford, Opt. Lett. 32, 1281-1283 (2007).
3. G. K. Samanta and M. Ebrahim-Zadeh, Opt. Express 16, 6883 (2008).

Continuous-Wave, Single-Frequency Optical Parametric Oscillator Pumped by a Frequency-Doubled Fiber Laser

G. K. Samanta[1], S. Chaitanya Kumar[1], Ritwick Das[1], and M. Ebrahim-Zadeh[1,2]

[1]*ICFO-Institut de Ciencies Fotoniques, Mediterranean Technology Park, 08860 Castelldefels, Barcelona, Spain*

[2]*Institucio Catalana de Recerca i Estudis Avancats (ICREA), Passeig Lluis Companys 23, Barcelona 08010, Spain*

Main author email address: goutam.samanta@icfo.es

Continuous-wave (cw) singly-resonant optical parametric oscillators (SROs) represent versatile sources of widely tunable, high-power, single-frequency radiation in spectral regions inaccessible to lasers. Pumped at 1.064 μm, PPLN cw SROs can cover the 1-5 μm spectral range, but access to wavelengths <1 μm is precluded by photorefractive damage in PPLN. Due to its large photorefractive damage threshold at and relatively high nonlinearity (d_{eff}~10pm/V), MgO:sPPLT is an attractive alternative for frequency conversion below 1 μm. Recently, we demonstrated that by exploiting this material and pumping at 532 nm, we can achieve practical operation down to 850 nm [1], and as short as 425 nm in the blue [2]. Operation of these cw SROs was made possible only by deploying commercial, high-power, high-cost, frequency-doubled cw Nd:YVO_4 laser (Coherent, Verdi-10). Here, we demonstrate operation of such green-pumped cw SROs using a fiber-based laser pump source. To our knowledge, this is the first report of a cw SRO pumped by a fiber-laser-based pump source in the green.

The key to the successful realization of such a cw SRO has been efficient generation of high-power cw radiation in the green using simple single-pass second harmonic generation (SHG) of an infrared fiber laser in a suitable nonlinear crystal to provide the pump radiation [3]. A 30-W, cw single-frequency Yb fiber laser (IPG Photonics, YLR-30-1064-LP-SF) at 1.064 μm is frequency-doubled in a 30-mm MgO:sPPLT crystal (HC Photonics) with a single grating (Λ=7.97 μm) to provide up to 9.64 W of single-frequency green power at 532 nm [3]. The SRO is based on an identical MgO:sPPLT crystal and is configured in a compact ring cavity [1,2] comprising two concave mirrors of radius of curvature 100mm, and two plane reflectors. All mirrors have R>99%@840-1000 nm and T>85%@1100-1500 nm, except for one of the plane mirrors (output coupler, T=0.71%-1.1% @840-1000 nm), thus ensuring SRO operation. A 500-μm fused silica etalon (FSR=206GHz, finesse~0.6) is used for frequency control.

The SRO is tuned across 855-1408 nm by varying the crystal temperature from 59 °C to 236 °C [1]. With optimum output coupling (1.04%), we obtain a signal power of 800 mW in TEM_{oo} spatial profile (M^2<1.52) with simultaneous idler power of up to 2 W (M^2<1.26) across the tuning range for a pump power of 7.3 W. The out-coupled signal shows higher peak-to-peak power stability (<10.7%) than idler (<11.7%) over 40 minutes. The frequency stability of the signal at 971.14 nm was measured using a wavemeter (High finesse, WS/U-30). Under free-running conditions, the signal output exhibits a natural peak-to-peak frequency stability <75 MHz over 15 minutes with a short-term frequency stability <10 MHz over 10 seconds, confirming robust, high power, frequency-stable source and its potential for spectroscopic applications.

References

1 G. K. Samanta, G. R. Fayaz, Z. Sun, and M. Ebrahim-Zadeh, Opt. Lett. **32**, 400-402 (2007).
2 G. K. Samanta and M. Ebrahim-Zadeh, Opt. Lett. **33**, 1228-1230 (2008).
3 G. K. Samanta, S. C. Kumar and M. Ebrahim-Zadeh, Opt. Lett. **34**, No. 10 (2009).

Lasers in Spectroscopy to Study Materials Under Extreme Conditions

Hans Dieter Hochheimer
dieter@lamar.colostate.edu

The use of lasers in Raman- and Brillouin spectroscopy at high pressures will be discussed and several examples presented.In particular, the advantages to use different laser wavelengths to distinguish between Raman lines and luminescence will be demonstrated. In addition, the the advantages and disadvantages of useingof Raman spectroscopy to determine phase diagrams will be discussed.

Polycrystalline Yttrium Aluminum Garnet for Fiber Lasers

Randall S. Hay, Geoff Fair

Air Force Research Laboratory, Materials and Manufacturing Directorate, WPAFB, OH
FAX: 937-656-4296
Randall.Hay@wpafb.af.mil

Hee Dong Lee, Triplicane Parthasarathy, Kristin Keller, Pavel Mogilevsky
UES, Inc. Dayton, OH

Silica-glass fiber lasers can be small, powerful, and physically robust. However, the low thermal conductivity of silica creates thermal gradients which cause mechanical failure and thermal lensing that degrades beam quality. These problems can be reduced by using longer fibers, but this causes problems with nonlinear effects such as stimulated Raman scattering and stimulated Brillouin scattering (SBS). Fiber lasers with much higher power output can clearly be made with YAG as the laser host. Yttrium aluminum garnet ($Y_3Al_5O_{12}$, YAG) has much higher thermal conductivity than silica (~11 W/m°K vs 1.37 W/m°K for SiO_2). This enables higher power generation without wavefront distortion or failure from local hot spots. Published data suggest a higher laser damage threshold for YAG, and it is not known to photodarken like silica. YAG fiber may also have a higher SBS gain threshold than silica, but this needs verification. Analysis suggests there are three power limiting mechanisms for YAG fiber: SBS, thermal lensing, and pump-limited output.

One way to make YAG fiber is from growth of single crystal fiber from a melt. Minimum fiber diameters are limited to about 75 mm, which is insufficient for single mode operation. Optical clarity is often inadequate because of porosity, and dopant distribution can be non-uniform from segregation and zone refinement during growth. The low growth rates, limitations on fiber diameter, lower fracture toughness, and inhomogeneity of Nd-dopant distribution makes this method unattractive for fine diameter, low cost fiber.

Another way to make YAG fiber is by sintering and densification of polycrystalline YAG. The high sintering temperatures (>1700°C) used to make dense polycrystalline YAG for optical applications forms material with large grain sizes >3 µm. The low diffusion coefficients for YAG inhibit densification. Polycrystalline YAG fibers can be doped at higher levels than single-crystals, has higher fracture toughness, supports higher power densities, and can be made with fine diameters (< 10 mm). The processing methods are adaptable to larger and more complex shapes than single crystals. We discuss the mechanisms that may limit power in polycrystalline YAG fibers, and some processing methods for making polycrystalline fiber.

Multi-dimensional Laser Microscopy in Biomedical Sciences

Herbert Schneckenburger, Petra Weber, Thomas Bruns and Michael Wagner
Hochschule Aalen, Institut für Angewandte Forschung, 73430 Aalen, Germany

An overview on recent applications of laser-assisted fluorescence microscopy with high spatial, spectral and temporal resolution is given. Spectral imaging is used to characterize membrane stiffness as a function of temperature and cholesterol content [1]. Fluorescence lifetime seems to be an appropriate parameter of malignancy in tumour diagnostics, but also can be used to probe molecular interactions via Förster Resonance Energy Transfer (FRET), e.g. in studies of Alzheimer's disease [2] or in sensing of apoptosis [3]. Variable-angle total internal reflection fluorescence microscopy (VA-TIRFM) [4] as well as methods of structured illumination are used to obtain high axial resolution, whereas polarization microscopy is applied for measuring cell and membrane dynamics. All experiments are performed under controlled light dose in order to avoid damages to living cells. Finally microscopic techniques are modified for applications of fluorescence reader technology in various fields of diagnostics [5].

References

1 P. Weber, M. Wagner, H. Schneckenburger: "Microfluorometry of cell membrane dynamics", *Cytometry*, **69A,** 185-188 (2006).

2 C.A.F. von Arnim, B. von Einem, P. Weber, M. Wagner, D. Schwanzar, R. Spoelgen, W.S.L. Strauss, H. Schneckenburger: "Impact of cholesterol level upon APP and BACE proximity and APP cleavage", *Biochem. Biophys. Res. Commun.,* **370**, 207□212 (2008).

3 B. Angres, H. Steuer, P. Weber, M. Wagner, H.Schneckenburger: "A membrane-bound FRET-based caspase sensor for detection of apoptosis using fluorescence lifetime and total internal reflection microscopy", *Cytometry*, **75A,** 420–427 (2009).

4 M. Wagner, P. Weber, W.S.L. Strauss, H.-P. Lassalle, H. Schneckenburger: "Nanotomography of cell surfaces with evanescent fields", *Advances in Optical Technologies*, **Vol. 2008**, Article ID 254317 (2008).

5 T. Bruns, W.S.L. Strauss, R. Sailer, M. Wagner, H. Schneckenburger: "Total internal reflectance fluorescence reader for selective investigations of cell membranes", *J. Biomed. Opt*., **11**, 034011 (2006).

Spectroscopy of Multisites Chromium in Garnet Crystals

H. Orucu[1], J. Collins[2], B. Di Bartolo[3]
[1]*Department of physics, Ege University, Izmir, Turkey*
[2] *Department of physics, Wheaton College, Norton, MA, USA*
[3] *Department of physics, Boston College, Chestnut Hill, MA, USA*

Garnet crystals doped with Chromium ions are materials of great interest for their possible laser applications and for the possibility they allow to study the relation between their spectroscopic properties and the crystalline field symmetry and strength. The octahedral coordinated Cr^{3+} ion can function as a laser active center to achieve tunable laser output in the red and near infrared spectral region or it can act as an energy sensitizer in rare-earth ion-based laser materials [1, 2]. By changing the chemical composition of the garnet, one can systematically alter the crystal field strength experienced by the Cr^{3+} center and influence its luminescence properties. Four systems were the object of this work: $Y_3Al_5O_{12}:Cr^{3+}$ (YAG:Cr), $Gd_3Ga_5O_{12}:Cr^{3+}$ (GGG:Cr), $Gd_3Sc_2Ga_3O_{12}:Cr^{3+}$ (GSGG:Cr) and $CaMg_2Y_2Ge_3O_{12}:Cr^{3+}$ (CMYGG:Cr). In the kinetic and spectral luminescence measurements of each sample investigated, the R-line regions showed varying degrees of complexity. All systems exhibit evidence of multiple centers due to the different sites at which the chromium ion sits in each crystal. The simplest of these was the YAG:Cr system, though even that system exhibited as many as three distinct sites.

References

1 U. Hömmerich and K.L. Bray, "High-pressure Laser Spectroscopy of $Cr^{3+}:Gd_3Sc_2Ga_3O_{12}$ and $Cr^{3+}:Gd_3Ga_3O_{12}$", *Physical Review B*, **51**, 18, 12133-12141 (1995)

2 M. Yamaga, B. Henderson, K.P. O'Donnell, C. Trager Cowan, and A. Marshall, "Temperature Dependence of the Lifetime of Cr^{3+} Luminescence in Garnets Crystals I", *Appl. Phys. B,* **50**, 425-431 (1990).

Estimation of Thermal Influence of Infrared (λ=1064 nm) Laser Tweezer on Red Blood Cell

I. Krasnikov
Amur State University, 21, Ignat'evskoe shosse, Blagoveshensk, Russia, 675021,
Fax: +7 (4162) 394-525, drpooh@mail.ru;
A. Seteikin,
Amur State University, 21, Ignat'evskoe shosse, Blagoveshensk, Russia, 675021,
Fax: +7 (4162) 394-525, seteikin@mail.ru;
I. Bernhardt,
Universitat des Saarlandes, P.O. Box 151150, Saarbrucken, D-66041,
Fax: +49 (681) 3026690, i.bernhardt@mx.uni-saarland.de

Continuous-wave laser microbeams are generally used as diagnostic tools in laser scanning microscopes or, in the case of near-infrared microbeams, as optical traps for cell manipulation and force characterization. Because single-beam traps are created with objectives of high numerical aperture, typical trapping intensities and photon flux densities are, respectively, of order of MW/cm^2 and 10^{27} cm^{-2}s^{-1}. These extremely high fields may induce two-photon absorption processes and anomalous biological effects [1].

We studied such effects arising in red blood cell (RBC) radiated by near-infrared laser tweezer (□=1064 nm). We were interested in thermal reaction of RBC irradiated by laser microbeam. It is conditioned by the fact that many experiments on erythrocytes carried using laser near-infrared tweezers, and usually they are long lasting, but the thermal aspects of such experiments are not examined.

For simplicity of the simulation red blood cell is presented as a sphere of 7 □m diameter 100% consists of hemoglobin and situated in a water solution. Cell membrane was not considered in simulation because it is very thin (approximately 10 nm). Focused infrared laser tweezer (100 mW, 1 □m diameter) irradiates red blood cell. Light propagation in medium and inside the cell was simulated using Monte-Carlo method. Monte Carlo simulations of photon propagation offer a flexible yet rigorous approach toward photon transport in turbid tissues. This method simulates the "random walk" of photons in a medium that contains absorption and scattering [2]. Then, we solved standard heat-transfer equation to get the temperature dynamics inside the cell. Heat source for the equation was the density of absorbed energy received from Monte-Carlo simulation data. It is identified that laser influence on a cell with density of absorbed energy approximately 10 MJ/cm^3 causes temperature rise less than 10-15 ^{0}□.

References

1. König K., Liang H., Berns M.W., Tromberg B. "Cell damage by near-IR beams", Nature. 377, 20–21 (1995).
2. Wang L.-H., Jacques S.L., Zheng L.-Q. "MCML-Monte Carlo modelling of photon transport in multilayered tissues", Comp. Methods and Programs in Biomed. 47, 131-146 (1995).

Structure elucidation 4,4'''-Bis-(2-butyloctyloxy)-p-quaterphenyl in cyclohexane by the joint application of FTIR, Raman, UV and visible spectroscopy

Ş. İ. Karaaslan
Physics Department, Yeditepe University, Istanbul, Turkey

BBQ (4,4'''-Bis-(2-butyloctyloxy)-p-quaterphenyl) is one of the laser dyes, which appears as white, crystalline solid. A dye laser is a laser which uses an organic dye as the lasing medium, usually as a liquid solution. Some of the dyes are Rhodamine 6G, fluorescein, coumarin, stilbene, umbelliferone, tetracene and others. A dye can usually be used for a much wider range of wavelengths. The wide bandwidth makes them particularly suitable for tunable lasers and pulsed lasers. The tunable lasers are widely used in different areas. In order to enhance the efficiency of a blue-green laser through spectrum conversion of the pumping light, a converter dye BBQ was mixed in the laser dye solutions.

Cyclohexane is a cycloalkane. It is used as a nonpolar solvent for the chemical industry, and also as a raw material for the industrial production of adipic acid and caprolactam, both of which are intermediates used in the production of nylon. Over 90% of cyclohexane is used in the manufacture of nylon fibre and nylon molding resin. The remaining 10% of cyclohexane ends up as solvents for paint, resins, varnish and oils, or in plasticizers.

Fourier transform infrared, Raman, UV-vis absorption spectra of BBQ in cyclohexane were recorded at room temperature. BBQ from Exciton Co. used without purification.

Optoacoustic Measurement of Optical Properties in Biological Tissues

Pelivanov I.M., Barskaya M.I., Podymova N.B., Khokhlova T.D., Karabutov A.A.

International Laser Center of Moscow State University

GSP-1, Leninskie Gory, Moscow, Russia

E-mail: pelivanov@ilc.edu.ru

Optoacoustic (OA) method is a promising tool for visualization of absorption inhomogeneities in turbid media, such as biological tissues. In OA method the information on the optical properties of the medium under study is delivered by the acoustic waves, which are weakly distorted in soft tissues. OA measurements can be performed in two detection modes. In the forward mode the laser irradiation of a medium under study and wide-band piezoelectric detection of excited ultrasonic signals occurs at its opposite sides. In current study such scheme was used for direct in-vitro measurement of the spatial distribution of laser fluence in some biological tissues (porcine and bovine liver and bovine muscle) and for determination of their optical properties (light absorption and reduced light scattering coefficients). Application of the forward detection mode for in-vivo measurement is restricted only by a few special cases due to the requirement of the two-sided access to a tissue.

Detection of OA signals can occur also at the side of laser impact, i.e. in the backward mode. Such scheme allows to perform local in-vivo measurement of the light absorption coefficient in biological tissues, that makes it very important for practice. The measurement is based on the fact that the amplitude of the OA signal is proportional to the of absorbed laser power density (the product of light absorption coefficient and laser fluence) at the medium surface. Light absorption coefficients of the biological tissues being examined in the forward mode as well as that for human skin were determined in the backward mode. The comparison of the results obtained in both detection modes demonstrates a good agreement between them.

Temporal Optimization of 0.1-Hz 0.5-PW Laser Pulses

Jae Hee Sung, Tae Jun Yu, Seong Ku Lee, Tae Moon Jeong, Il Woo Choi, and Jongmin Lee
Center for Femto-Atto Science and Technology & Advanced Photonics Research Institute (APRI), GIST, Gwangju 500-712, Republic of Korea

We are developing a chirped pulse amplification femtosecond Ti:sapphire laser which generates 0.1-Hz 0.5-PW laser pulses with temporal optimization [1]. High-contrast laser pulses from a 1-kHz multi-pass amplifier system are used as seed pulses of amplifiers to enhance the temporal contrast of the 0.5-PW laser pulses. An acousto-optic programmable dispersive filter, which controls the spectral amplitude and phase of the laser pulse, is used to compensate for the gain narrowing and the high-order dispersions. The laser pulses are stretched to about 1 ns by a Öffner-triplet-type stretcher to prevent optical damages during amplification. The stretched pulses are amplified through a pre-amplifier and two power amplifiers. The amplified pulses are upcollimated with achromatic doublet lenses instead of two singlet lenses to minimize the chromatic aberration, which broadens the temporal profile of the focal spot [2]. The laser pulses are then injected into the high-energy booster amplifier. In the booster amplifier, the index-matched liquid is used as a cladding material of the Ti:sapphire crystal to suppress the parasitic lasing. When the booster amplifier is pumped by 80-J green laser pulses, the output pulse is expected to have energy over 35 J with 60-mm beam diameter after 3 passes. The booster amplifier will be developed soon. A grating compressor has been designed with a genetic algorithm to minimize the temporal duration of the recompressed pulse. The result calculated with the genetic algorithm shows that the recompressed pulse duration is close to the transform-limited pulse duration. The final laser pulses are expected to be optimized temporally with a peak power of 0.5 PW.

References

1 Jae Hee Sung, Tae Jun Yu, Seong Ku Lee, Tae Moon Jeong, Il Woo Choi, Do-Kyoeng Ko, and Jongmin Lee, "Design of a Femtosecond Ti:sapphire Laser for Generation and Temporal Optimization of 0.5-PW Laser Pulses at a 0.1-Hz Repetition Rate", *J. Opt. Soc. Kor.*, **13**, 53-59 (2009).

2 T. M. Jeong, D.-K. Ko and J. Lee, "Deformation of the Focal Spot of an Ultrashort High-Power Laser Pulse due to Chromatic Aberration by a Beam Expander", *J. Korean Phys. Soc.*, **52**, 1767-1773 (2008).

Stable laser-plasma picosecond kHz X-ray source using melted metal target

K.A.Ivanov, D.S.Uryupina, R.V.Volkov, A.B.Savel'ev, I.A.Ozheredov, A.P.Shkurinov
Physics faculty and International Laser Center of Lomonosov Moscow State University, Moscow, Russia

We have developed a new source of picoseconds hard x-ray pulses, which are generated under interaction of high intensity ultrashort laser radiation on a melted metal target. Using such target one could not renew the target surface after each laser shot, comparing to commonly used solid state targets. This permitted us to create a stable x-ray source with high repetition rate of pulses. Using a laser pulse with a prepulse and varying the energy of a prepulse it is possible to easily control the parameters of plasma. The size of the source is 4 μm, it has 1-10 ps duration of pulse at 1 kHz repetition rate, which allow to use this source in nanostructures investigation, x-ray spectroscopy with high temporal resolution, EXAFS spectroscopy, medical researches etc.

In our experiments plasma was created by laser pulse delivered by Ti:Sa laser system (pulse duration – 60 fs, wavelength – 800 nm, energy of pulse – 1 mJ, repetition rate – 10 Hz). As target we used melted gallium at temperature of 300 ^{o}C. In stability research experiment we have exploited the other similar Ti:Sa laser system (pulse duration – 100 fs, wavelength – 800 nm, energy of pulse – 2 mJ, repetition rate – 100-1000 Hz).

We have shown that usage of laser pulse with a prepulse, advancing the main pulse over few nanoseconds, can lead to appreciable increase in x-ray yield and hot electron energy. At prepulse energy ~50^{-1} of main pulse energy we achieved a 60 times increase in x-ray yield and almost fourfold growth of hot electron energy in plasma (from 20 keV to 75 keV), comparing to plasma, formed by a pulse without prepulse. Furthermore, excitation of linear radiation of plasma takes place, corresponding to $K_{\square}$ (9.3 keV) and $K_{\square}$ (10.3 keV) lines of gallium, which intensity also increases with prepulse energy growth. At the same time parameters of plasma do not depend on laser pulse polarization.

Optical shadowgraphy revealed that main pulse interacts with highly deformed target surface with 10 μm scale of convexity. That might lead to local electric field amplification and also independency of plasma parameters on polarization. Moreover, the main pulse propagates not in vacuum, but in a cloud of matter 130 μm in length, which can lead to additional self-focusing.

We also have demonstrated that liquid gallium can be used as a stable laser-plasma source of x-ray pulse with repetition rate up to 1 kHz. Without additional focusing such source remains stable about 30 seconds, whereas at additional focusing – up to few hours of continuous work with more than 10^{9} x-ray quantum per second power.

This work was supported by RFBR, grant # 07-02-00724-□.

Functional surface structures using femtosecond ablation

Päiväsaari Kimmo, Jääskeläinen Timo

University of Joensuu, Department of Physics
P.O.Box 111, FI-80101 Joensuu, Finland,
Fax +358 13 251 2721,

timo.jaaskelainen@joensuu.fi

Variety of surface micro- and nanostructures can be manufactured to wide range of materials using femtosecond ablation. Direct structure writing using ultrafast lasers to materials that are hard, or impossible, to process using traditional manufacturing processes can be advantageous in some applications. In addition to that, the femtosecond laser-matter interaction itself can produce the structures with new desired properties. The surface structures with feature sizes ranging from 100 nm to tens of microns can be manufactured using various self-organization processes related to the femtosecond ablation. Control over the shape and size of these generated surface features can be obtained by varying such laser parameters as polarization, incident angle, pulse number and energy. In addition to that structures can be generated using direct writing and the features can be controlled using various beam shaping techniques.

A wide range of material properties can be changed including wetting, frictional and absorption behavior by structuring the surface with micro- and nanosized features. We have studied the effect of femtosecond laser generated structures to the functionality of the surface mainly in order to control the hydrophobic and protein adsorption properties of the surface. The control over wetting properties of the material surface has a multitude of applications in the chemical, biological and medical sciences as well as in our everyday life. Simple example is self-cleaning surfaces, or so called Lotus-leaf effect, where superhydrophobic surfaces are obtained by combining specific micro- and nanostructures. Superhydrophobic surfaces are obtained using both, directly written and self-organized structures in stainless steel samples. The hydrophobic/philic properties of the surface can also have a major role in the biomaterial adsorption at interfaces. We have studied the controlling of the cell adherence and cell migration using micro- and nanostructured surfaces, both important aspects of the development of biocompatible materials.

Chemical Vapor Deposited (CVD) Diamond for Laser Applications

V.G. Ralchenko[1], V.I. Konov[1], A.P. Bolshakov[1], A.F. Popovich[1], V.V. Kononenko[1], M.N. Sinyavskiy[1], E.E. Ashkinazi[1], A.A. Kaminskii[2], A.Yu. Lukyanov[3], A.V. Khomich[4]

[1]A.M. Prokhorov General Physics Institute RAS, Moscow, Russia
[2]Institute of Crystallography RAS, Moscow, Russia
[3]Institute of Physics of Microstructures RAS, Nizhny Novgorod, Russia
[4]V.A. Kotelnikov Institute of Radio Engineering and Electronics RAS, Fryazino, Russia

Chemical vapor deposition (CVD) technology allows growth of optical quality polycrystalline diamond wafers of very large size (>100 mm in diameter) as well as extremely pure single crystals (of limited size). Exceptional properties of diamond – transparency in broad spectral range (from □=225 nm to radio frequencies), record high thermal conductivity (2000 W/mK @R.T.), high hardness (81-104 GPa) and Young modulus (1050 GPa), low thermal expansion ($1*10^{-6}$ K^{-1}) make this material very attractive for laser applications. The best quality CVD diamond films are produced in a microwave plasma using methane-hydrogen source gas. We will focus primarily on use of CVD diamond for Raman shifters [1] with Nd:YAG laser pumping and windows for CO_2 lasers [2]. In addition, solar-blind diamond-based UV detectors, fast bolometers, and heat spreaders for semiconductor lasers will be discussed, and examples of practical realizations will be given. Finally, a reverse topic, lasers for CVD diamond processing, will be considered to illustrate the effectiveness of lasers for treatment of this hardest material.

References

1. A.A. Kaminskii, V.G. Ralchenko, V.I. Konov, "CVD-diamond – a novel $\chi^{(3)}$-nonlinear active crystalline material for SRS generation in very wide spectral range", *Laser Phys. Lett.*, **3**, 171-177 (2006).
2. A.Yu. Luk'yanov, V.G. Ralchenko, et al. "Measurement of optical absorption in polycrystalline CVD diamond plates by the phase photothermal method at a wavelength of 10.6 μm", *Quantum Electronics*, *(Moscow)* **38**, 1171-1178 (2008)

LIBS-assisted laser cleaning of metals: physical processes and applications

Vadim P. Veiko, Timofej Yu. Mutin, Elena A. Shakhno, Valentin N.Smirnov, Sergey A.Volkov
Laser–based Technologies department, St.Petersburg State University of Information Technologies, Mechanics and Optics, St.Petersburg, Russia

There are some tasks, arising by metal surfaces, such as corrosion protection, cleaning of environmental contaminations (for sculptures and architecture), of heat exchanger elements from operating contaminations, contamination of resources worked-off components of nuclear reactors and so on. Traditional technologies turn out to be not effective to solve them. In this paper basics of laser technologies for metal surfaces cleaning as well as its applications for solving of such tasks are considered. The main regimes of laser cleaning such as shock waves and explosion evaporation are considered being applied to the surface contaminations. Main areas for laser cleaning of metal surfaces developed by authors are described –Laser technology for cultural heritage conservation –Cleaning of the internal surfaces of heat exchanger pipes. – Remote cleaning and deactivation of nuclear power station components. There are different ideas to combine laser cleaning of metal surfaces with other surfaces treatment will be represented, such as anticorrosive treatment of structural steels for example.

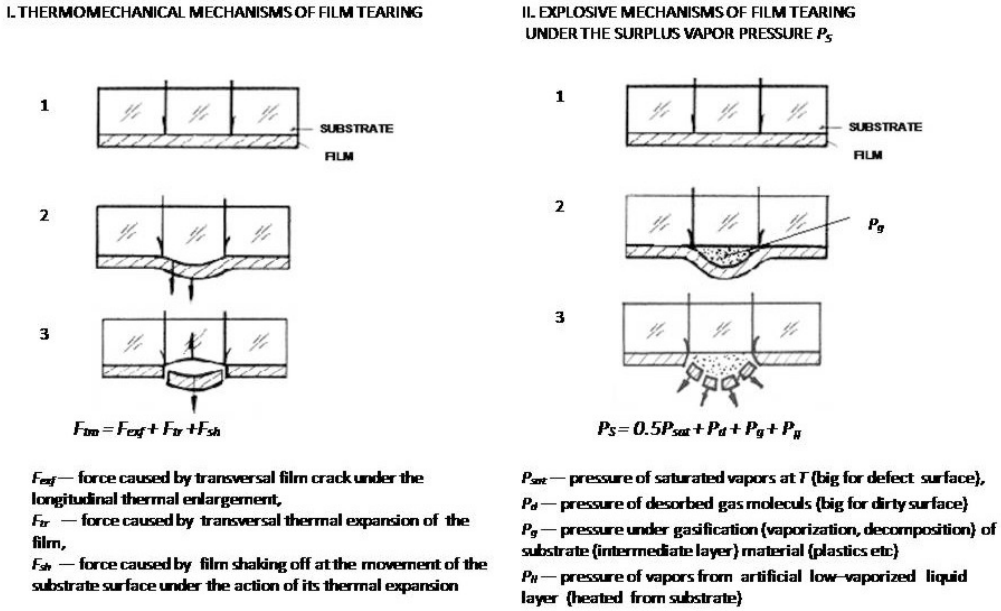

Fig. 1. Low energy mechanisms of laser ablation of surface films and layers

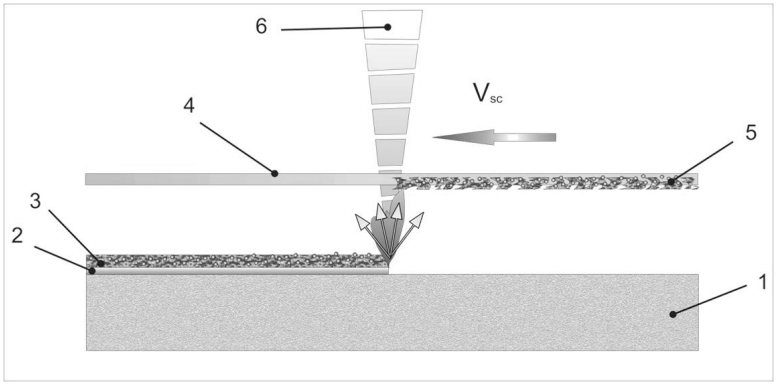

Fig. 2. Deactivation with transparent collector film:
1 – base material, 2 – densed thin oxide layer, 3 – corroded porous thick layer (150-200 mm), 4 – transparent film-collector, 5 – allated and collected products (nuclides contaminated), 6 – scanning laser beam.

The work supported by RFBR Grant 07–02–00887.

High-Power Coherent Beam Combination from two and four Fiber Lasers

Jun Zhou, Bin He,Wei Wang, Qihong Lou

Shanghai Institute of Optics and fine Mechanics, Shanghai Key Laboratory of All solid-state Laser and Applied Techniques Shanghai 201800, China

email address: junzhousd@mail.siom.ac.cn

As the output power of a single fiber lasers has been improved rapidly and has exceeded kilowatt magnitude. However, the ultimate output from a single fiber laser is limited by the nonlinear and thermal effects. Beam combination is an effective geometry which can improve output power with excellent beam quality. At present, many researchers have brought up various techniques of coherent beam combination. Fiber laser arrays with self-imaging resonator have been realized under low power condition.

We have demonstrated experimentally the phase locking of two fiber lasers by means of a self-imaging resonator and a special spatial filter. The pattern of the coherent beam profile exhibits the steady interference strips. The phase locking is due to a self-adjusting process of the fiber laser array with the long lengths, broad gain bandwidth, and low-Q value. The coherent output power of 256W is obtained and the coherent power combination is about 85%. There is no doubt that the coherent output power can be increased by the same method if we optimize the parameters of the resonator and the fiber laser array.

By using a self-imaging resonator and a spatial filter, coherent beam combination of a 4 fiber laser with two-dimensional is demonstrated. The phase locking fiber array with in-phase mode has produced 26 W coherent output. The experimental results show that the far-field beam profile from the fiber laser array can be controlled by adjusting the position of spatial filter. The in-phase mode, out-of-phase mode, and an antisymmetric eigenmode are observed.

References

[1]Qihong Lou, Jun Zhou, Bing He and Hongming Zhao; OPN ,2008,47
[2]Bing He, Qihong Lou, Wei Wang, Jun Zhou et al,; Appl.Phys. Lett., 92,(2008) 251115
[3]P. K. cheo, A. Liu, and G. G. King; IEEE Photonics Technol. Lett., 13(2001) 439
[4]E. J. Bochove, P. K. cheo, and G. G. King,; Opt. Lett. 28,(2003)1200

Stable laser-plasma picosecond kHz X-ray source using melted metal target

K.A.Ivanov, D.S.Uryupina, R.V.Volkov, A.B.Savel'ev, I.A.Ozheredov, A.P.Shkurinov
Physics faculty and International Laser Center of Lomonosov Moscow State University, Moscow, Russia

We have developed a new source of picoseconds hard x-ray pulses, which are generated under interaction of high intensity ultrashort laser radiation on a melted metal target. Using such target one could not renew the target surface after each laser shot, comparing to commonly used solid state targets. This permitted us to create a stable x-ray source with high repetition rate of pulses. Using a laser pulse with a prepulse and varying the energy of a prepulse it is possible to easily control the parameters of plasma. The size of the source is 4 μm, it has 1-10 ps duration of pulse at 1 kHz repetition rate, which allow to use this source in nanostructures investigation, x-ray spectroscopy with high temporal resolution, EXAFS spectroscopy, medical researches etc.

In our experiments plasma was created by laser pulse delivered by Ti:Sa laser system (pulse duration – 60 fs, wavelength – 800 nm, energy of pulse – 1 mJ, repetition rate – 10 Hz). As target we used melted gallium at temperature of 300 ^{o}C. In stability research experiment we have exploited the other similar Ti:Sa laser system (pulse duration – 100 fs, wavelength – 800 nm, energy of pulse – 2 mJ, repetition rate – 100-1000 Hz).

We have shown that usage of laser pulse with a prepulse, advancing the main pulse over few nanoseconds, can lead to appreciable increase in x-ray yield and hot electron energy. At prepulse energy ~50^{-1} of main pulse energy we achieved a 60 times increase in x-ray yield and almost fourfold growth of hot electron energy in plasma (from 20 keV to 75 keV), comparing to plasma, formed by a pulse without prepulse. Furthermore, excitation of linear radiation of plasma takes place, corresponding to K□ (9.3 keV) and K□ (10.3 keV) lines of gallium, which intensity also increases with prepulse energy growth. At the same time parameters of plasma do not depend on laser pulse polarization.

Optical shadowgraphy revealed that main pulse interacts with highly deformed target surface with 10 μm scale of convexity. That might lead to local electric field amplification and also independency of plasma parameters on polarization. Moreover, the main pulse propagates not in vacuum, but in a cloud of matter 130 μm in length, which can lead to additional self-focusing.

We also have demonstrated that liquid gallium can be used as a stable laser-plasma source of x-ray pulse with repetition rate up to 1 kHz. Without additional focusing such source remains stable about 30 seconds, whereas at additional focusing – up to few hours of continuous work with more than 10^{9} x-ray quantum per second power.

This work was supported by RFBR, grant # 07-02-00724-□.

High Power Quantum Cascade Lasers and Applications to High Sensitivity, High Selectivity Detection of Chemical Warfare Agents and Explosives

C. Kumar N. Patel[1,2]
[1] *Pranalytica, Inc., Santa Monica, CA, USA*
[2] *Department of Physics & Astronomy, University of California, Los Angeles, CA, USA*

In this paper I will describe the recent developments in the midwave infrared (MWIR) and longwave infrared (LWIR) quantum cascade lasers (QCLs) and their applications to ultra high resolution infrared spectroscopy and high sensitivity (low probability of false negatives), high selectivity (low probability of false alarms) detection of chemical warfare agents (CWAs), toxic industrial chemicals (TICs) and explosives.

In the area of QCLs, I will describe the significant improvements in the laser power output and its wall plug efficiency. Using a novel design for the epitaxial structure for the QCLs, we have shown continuous wave (CW) room temperature (RT) QCL (single emitter) operation in a Fabry-Perot geometry with single ended power output of 3 watts with wall plug efficiency (WPE) of >13 %. In external grating cavity configuration, we have been able to obtain single frequency tunable power output in excess of 300 mW tunable over >200 nm in the MWIR region. At present, we can generate any wavelength in the 4.5 mm to 12 mm region with ~ 3 W CW/RT power in the shorter wavelengths and ~ 0.5 W at the longer wavelengths. Both the relatively broad band Fabry-Perot configuration QCLs and the single frequency broadly tunable external grating cavity QCLs are now finding a broad range of applications in research, defense, homeland security and industrial arena.

The availability of high power CW/RT single frequency radiation tunable over the entire spectral region covering 4.5 mm to 12 mm has led to numerous applications. For ultra high resolution spectroscopy, we have used the saturation spectroscopy of NO_2 to demonstrate that the linewidth of a free running but moderately stable external grating cavity QCL operating at ~ 6.3 mm is less than 4 MHz. The high tunable powers available have made QCLs ideal sources for high sensitivity detection of gases through the use of photoacoustic spectroscopy which is a very rugged and proven technique. Photoacoustic spectroscopy, however, derives its capability of high sensitivity detection from the availability of high tunable optical powers, which heretofore were not available in the MWIR and LWIR region except for the molecular lasers that provide high powers but tunability is discrete. Using discretely tunable CO_2 lasers as sources, for example, laser photoacoustic spectroscopy (L-PAS) detection is possible only when there is an accidental coincidence between the discreet CO_2 laser line and the absorbing transition. The high power tunable QCLs have made it possible to use photoacoustic spectroscopy over the entire spectral region from 4.5 mm to 12 mm, where the strong optical absorption features of all of the CWAs, almost all of the TICs and explosives are to be found. Thus, our extension of L-PAS to the use of QCLs has made it possible for us to detect CWA surrogates at ppb levels with false alarm rates below $1{:}10^{-7}$. Detection of explosives has especially benefited from QCL-PAS because for non-nitrate based explosives, such a triacetone triperoxide (TATP), conventional explosives detection techniques do not work well and nitrate based fertilizers cause a significant interference problem for the detection of traditional explosives using conventional techniques. We have demonstrated very high sensitivity detection of TNT with excellent probability of false alarms (PFA) even in a nitrate saturated environment. Since the optical spectroscopy is based on probing the chemical structure of a target molecule, it is able to distinguish between TNT and nitroglycerine, the two which are different chemical compounds but accidentally have nearly identical molecular masses. We have also succeeded in high sensitivity, low PFA detection of TATP and its precursor acetone.

In the presentation, I will describe in detail the field of high power QCLs and their applications.

Electric properties of heterogeneous transitions between n - and p - type ZnO films and n - and p - type silicon substrates.

L.S. Parshina[1], O.A. Novodvorsky[1], V.Ya. Panchenko[1], O.D. Khramova[1], Ye.A. Cherebilo[1], A.A. Lotin[1], C.Wenzel[2], N. Trumpaicka[2], J.W. Bartha[2]

[1] *Institute on Laser and Information Technologies, Russian Academy of Sciences (ILIT RAS) Shatura, Moscow Region, Russia e-mail:* onov@mail.ru, fax: 8(49645)22532

[2]*Dresden University of Technology, Institute of Semiconductor and Microsystems Technology, D-01062 Dresden, Germany*

The growing demand for solid-state sources and receivers of light in the blue and UV regions has in recent years stimulated an intensive study of several kinds of wide-gap semiconductors. The main development efforts in this field focus on GaN (energy gap width E_g = 3.5 eV), ZnO (E_g = 3.4 eV), ZnSe (E_g = 2.9 eV), 6H-SiC (E_g = 3 eV). The impressive advances have been made in the GaN based materials. GaN and its alloys have been used in production of light-emitting and laser diodes operating in the visible (460 nm) [1]. Nevertheless, effective radiation is attained at high concentration of indium in the InGaN structure, which enhances the absorption in the UV region and casts some doubt on GaN based materials application in producing UV light-emitting and laser diodes [2].

Zinc oxide is of great interest as an alternative to GaN based devices. Possessing high radiation and chemical resistance and thermal stability, ZnO is widely used in various devices, in particular, in fabrication of low-resistance contacts for solar cells. Owing to its unique optical, acoustic and electric properties, ZnO has found application in producing transparent electrodes for solar cells, gas sensors, varistors, and SAW generation devices [3]. Being transparent over a broad spectral region, zinc oxide shows high resistance to irradiation; it is prone to chemical etching and rather cheap which makes him attractive for microelectronic applications [4].

Zinc oxide has the greater exciton binding energy (60 meV), that is record for the solid-state binary semiconductors (for comparison the exciton binding energy in GaN - 25 meV, in ZnSe - 20 meV). The greater exciton binding energy of ZnO and its alloys is especially attractive to creation of the radiating devices and photodetectors of the UV region on the ZnO basis. The decision of ZnO with Si integration problems causes also particular interest, that can open the real overlapping opportunities of the unique functional abilities of these materials at the creation of the photoconverters on the silicon substrates. Heterostructures created at the deposition on the semiconductor substrate of the material layer with the greater bandgap width, are usually characterized by the higher photosensivity because of so-called "window effect" [5]. If the heterolayer was created by the chemical- and radiation-resistant substance, that is characteristic for ZnO, the photosensitive structure will not demand of creation on the surface of the additional protective coating. Thus the cheap ZnO/Si heterostructures should have the comparable and even surpassing characteristics of the existent photodetectors.

The goal of the present work was the creation ZnO/Si heterostructures and the investigation of the electric properties anisotype and isotype heterojunctions received by the ZnO layers creation on silicon substrates. The epitaxial ZnO films doped by gallium, nitrogen, phosphorus were deposited by the pulse laser deposition method on monocrystal n- and □- type Si (001) substrates. The volt-ampere characteristics of n-ZnO/p-Si-, n-ZnO/n-Si-, □-ZnO/p-Si- and □-ZnO/n-Si- heterojunctions were obtained. It was established, that in case of the isotype heterojunction it was possible to receive both the ohmic contact and the rectifying contact by changing of the contacting materials conductivity. For the anisotype heterojunctions in all cases considered us the rectifying contacts were observed only.

References

1. T.Mukai, D.Morita, and S.Nakamura, **"**High-Power UV InGaN/AlGaN Double-Heterostructure Leds", J.Crist. Growth v.189, 778 (1998).
2. H.Tampo,A.Yamada, P.Fons, H.Shibata et al., "Degenerate layers in epitaxial ZnO films grown on sapphire substrates", Appl.Phys. Lett. v.84, n.22, 4412 (2004).
3. Y.Chen, D. Bagnall, T.Yao, "ZnO as a novel photonic material for the UV region", Mater.Sci.Eng.,B 75,190 (2000).
4. D.C.Look, D.C.Reynolds, C.W.Litton et al. "Characterization of homoepitaxial *p*-type ZnO grown by molecular beam epitaxy" Appl. Phys. Lett., Vol.81,No.10, 1830 (2002).
5. A.Milns, D.Foiht, Heterojunctions and metal- semiconductor junctions, Moscow (1975)

TEM_{00}, 30mJ, 2.94-μm Q-switched Er:YAG laser working at the repetition rate up to 25Hz

M. Skorczakowski[1], J. Swiderski[1], A. Zajac[1], W. Pichola[1],
S. Gross[2], A. Heinrich[2], T. Bragagna[2]

[1] *Institute of Optoelectronics MUT, 2 Kaliskiego Str., 00-908 Warsaw, Poland*

[2] **Pantec Biosolutions AG, Industriering 21, LI-9491 Ruggell, Liechtenstein**

Main author email address: mskorczakowski@wat.edu.pl

A high-repetition rate, mechanically Q-switched Er:YAG laser operating at 2.94-μm has been developed. For a single generator at 25Hz, pulses of about 300-ns duration and 30-mJ energy characterized by TEM_{00} distribution have been achieved. It corresponds to the peak power of over 100 kW.

The laser set-up is depicted in Fig. 1. A ϕ4x100 mm Er^{3+}-doped YAG crystal was used as an active medium. It was AR-coated on both end surfaces. The laser rod was pumped by a single xenon flashlamp, with typical pump energy of up to 60 J, housed in a single diffuse (ceramics) 80 cm-long cavity formed by two mirrors: rotating mirrors M1 and an output mirror M3 with reflectivity of 100% and 90%, respectively. A convex mirror M2 was characterized by 100% reflectivity at 3 μm and curvature of 50-cm. Mirror M1 placed in the resonator functioned as a high reflective Q-switch driven by a suitable controller which triggered the pump source according to the chosen repetition rate, pump pulse length and delay time.

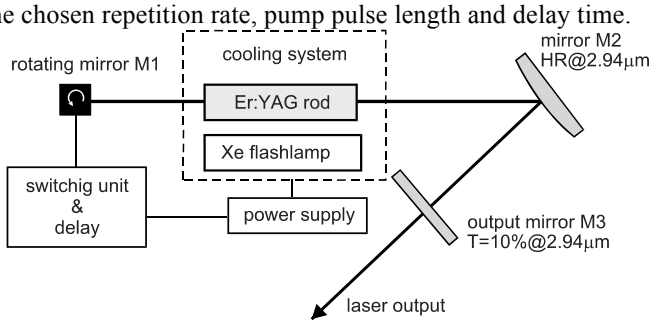

Fig. 1. Experimental set-up of a Q-switched Er:YAG laser.

The laser resonator was dynamically stable. The laser rod and the flashlamp were cooled with circulating distilled water. The flashlamp was supplied by means of the home-made power supply system PPM-6kW whose voltage and repetition rate could be quickly adjusted to keep thermal lensing in check.

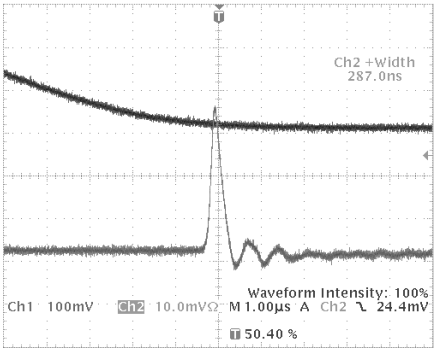

Fig. 2. Oscilloscope picture of the shortest Q-switch pulse generated by Er:YAG laser. Lower trace – laser pulse, upper trace – current applied to the pump lamp.

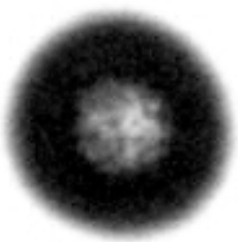

Fig. 3. TEM distribution of single pulse generation.

In Er:YAG laser set-up presented in Fig. 1 generation of nanosecond pulses has been achieved. The shortest pulse width was less than 290 ns at the output energy of 30 mJ and 25 Hz repetition rate (Fig. 2). The supply voltage in this case was 375 V; the pump pulse duration and time delay equalled 300μs and 3140μs, respectively. The TEM distribution for single pulse generation was depicted in Fig. 3.

The laser worked with a stability of several percent for many hours without any fractures. The level of pulse energy obtained, especially at 25 Hz repetition rate, is sufficient to ablate most of biological tissues. The laser developed can be successfully applied in microsurgery, laryngology or ophthalmology.

Histological studies of pathological ENT tissues irradiated by laser diode and CO_2 laser surgical system

M. Petrus, D.C. Dumitras, D.C. Dutu
Department of Lasers, National Institute for Laser, Plasma and Radiation Physics, 409 Atomistilor St., PO Box MG-36, 077125 Bucharest, Romania
e.mail: mioara.petrus@inflpr.ro

The CO_2 laser is one of the most widespread gas lasers. It successfully manage to combine many positive characteristics, inherent to gas lasers: a) easy to be build up; b) cheap gases, the active medium; c) pulse or continuous operation; d) a stable level of laser radiation power/intensity during the operating time. All these characteristic makes the CO_2 laser one of the most used in the medical field applications. In the ENT field, the CO_2 laser is used especially to correct the physico-morphological defects which give an optimal recovery time by using the innovative therapies of the affected structures. Also, the CO_2 laser is used in the treatment of certain diseases and disorders [1, 4].

In spite of this large number of applications, the process of laser- ENT tissue interaction was not thorough investigated. This fact is due to the complexity of experimental investigations, the specificity of investigated materials, the variety of lasers with different wavelengths and energies, the complexity of physico-chemical and physiological processes [2].

More recently, the development of high power near infrared laser diode (810 nm and 980 nm) offers a new surgical alternative in ENT laser surgery. The 810 nm diode laser delivers light with similar physical characteristics to the 1064 nm Nd:YAG laser. The 980 nm diode laser is highly absorbed by both water and hemoglobin, this combined with precise hemostasis making excision, incision or vaporization very effective. For example, the penetration depth of the 980 nm laser radiation is less compared to the longer Nd:YAG wavelength. This allows safe and precise procedures close to very delicate structures. The diode laser is a suitable surgical alternative to the Nd-YAG laser, with substantial advantages in terms of reliability and low cost ownership [3].

Histological studies of ENT tissues were performed by irradiation with CO_2 laser surgical system and laser diode.

We report a parallel study of laser diode and CO_2 laser beams on ENT tissues, nasal polyps and tensile cytolysis. We have used a 15W 810 nm laser diode surgical system with optical fiber delivery system and a CO_2 laser with an output power of 15W, equipped with an opto-mechanical articulated arm. Based on the examination of histological specimens under optical microscopy and the examination in vivo of the surgical site with a contact endoscope, the study relives the main advantages and limitations of this laser technique in ENT surgery.

References:

1. Ben Cox, "Optics in Medicine. Introduction to Laser-Tissue Interactions", Photoacoustic Imaging Group, Department of Medical Physics and Bioengeneering,University College London,2007 (*www.medphys.ucl.ac.uk/~**bencox/laser-tissue**.pdf*).
2. V. Oswal, M. Remacle, S. Jovanovic, J. Krespi, "Principle and Practice of Lasers in Otolaryngology and Head & Neck Surgery", Kulger Publications, 2002.
3. M.G. Dilkens, I. Cameron, S.J. Quinn and G.S. Kenyon, "Preliminary experience with an 810 nm wavelength diode laser in ENT surgery", Laser in Medical Science, Vol. 9, 261-264 (2007).
4. D.C. Dumitras, "Biophotonics", All Publishing, Bucharest, 1999.

High Power Fiber Lasers

Bulend Ortac
buelend.ortac@uni-jena.de

Rare-earth-doped fibers are one of the most promising solid-state laser concepts for efficient diode-pumped high power continuous wave and pulsed laser systems. Their main performance advantages are due to the outstanding thermo-optical properties of an actively doped fiber. The large ratio of surface to active volume of such a fiber ensures excellent heat dissipation; furthermore the beam quality is given by the refractive index profile of the active core and is therefore independent of the pump power. Due to the recent developments of reliable high brightness all solid state pump sources and the advances in fiber manufacturing technology these devices are no longer restricted to low-power operation. Mode-locked fiber lasers fibers offer a number of advantages as they have a large amplification bandwidth supporting ultra short pulse generation from picosecond to femtosecond range. In addition, they are suitable for high-energy applications and offer compact design with inexpensive components. In the first part, we will briefly introduce the generation of picosecond or femtosecond pulses from different kind of the fiber laser concepts. However, depending on the experimental set-up, these lasers can operate in very different regimes with different pulse profiles that can be detrimental for some applications. These fiber sources can generate pulses with output energies from some tens of picojoules to microjoule, duration from sub-100 fs to picosecond range at repetition rate from few tens of MHz. Within this seminar, different cavity designs (ring, linear and sigma) and different mode-locking regimes (stretched, wave-breaking free and all-normal) will be also discussed. Fiber concept has well established them as a very attractive gain medium for ultra short pulse amplification. Firstly, the influence of nonlinearity on different pulse shapes during amplification will be compared. We will demonstrate that the special parabolic pulse shape allows for the generation of high-quality femtosecond pulses in the direct pulse amplification systems beyond nonlinearity limits. For higher extraction of power and pulse energies, the nonlinear effects can lead to severe pulse distortions and even to damage to the fiber. A common way to overcome this limitation is the application of the well known chirp-pulse amplification (CPA) technique. Secondly, we will show the different fiber based CPA system employing the new generation of low-nonlinearity fibers and generating up to average power of 100 W with pulse energies well above millijoule.

Investigation of Radio-Optic Resonances on Far Field and Free Space Condition

M. Çetintaş, R. Hamid, S. Çakır and O. Şen
National Metrology Institute (UME),
Scientific and Technological Research Council of Turkey (TÜBİTAK),
Gebze-Kocaeli, Turkey

The investigations on radio-optic resonances and using of them for frequency locking of quantum oscillators on the three energy levels atoms with divided two hyperfine levels of ground state are realized generally in the microwave cavities. Frequency tuned laser beam to the atomic energy levels is passed through the atomic vapor and detected by photodiode. While, the atomic vapor in microwave cavity interacts to the microwave that its frequency detuned to two hyperfine levels of ground state, laser absorption will become decrease and so radio-optic resonance is observed [1-5].

In our work, the radio-optic resonances were investigated in far field and free space conditions. Cs atomic vapor cell included laser beam passed through in it was installed to the certain distance from horn antenna tip and exposure to the microwave. The laser beam tuned frequency to the Cs atoms 6S1/2(F=4) - 6P3/2(F¢=4) levels was passed through the Cs cell and detected by photodiode. The power density of the laser beam was changed between 1 mW/cm2 and 100 mW/cm2 and cell temperature was kept at T=23oC (N=3x1010atoms/cm3) during the experiment. The microwave was transmitted to the cell by horn antenna. The diagonal length of horn antenna is 12 cm and to create the far field condition, the distance from horn antenna to the cell was kept at 1 m. The radio-optic resonance was observed when the frequency of microwave (≈ 9.2 GHz) was tuned to the 6S1/2(F=3) - 6S1/2(F=4) hyperfine levels of Cs atoms. In order to create free space condition, the experiment was realized in semi-anechoic room with 40 GHz cut-off frequency. The amplitude dependency of radio-optic resonance to the both laser and microwave powers was investigated [6]. The splitting of radio-optic resonance at constant magnetic field was observed. The creation time of radio-optic resonance was investigated by pulsed modulation of microwave for different pulse parameters.

References

1. A.S. Zibrov, A.A. Zhukov, V.P. Yakovlev, V.L. Velichansky, "Shape of the signal of double radio-optical resonance in 85Rb atomic vapors in strong fields" JETP Letters, **83**, 136-140 (2006)
2. A. Litvinov, G. Kazakov, B. Matisov, I. Mazets, " Double radio-optical in 87Rb atomic vapor in a finite size buferless cell" J. Phys. B: At. Mol. Opt. Phys. **41**, 125401 (2008)
3. D. Budker, L. Holberg, D.F. Kimball, J. Kitching, S. Pustelny, V.V. Yashchuk, "Microwave transitions and nonlinear magneto-optical rotation in anti-relaxation –coated cells", Physical Review A, **71**, 012903 (2005)
4. D. Paulusse, N. Rowell, A. Michaud, "Realization of a atomic microwave power standard", Proc. Conf. on Precision Electromagnetic Measurements, Ottawa, Ontario, Canada, 16 - 21 June, 2002, pp. 194-195.
5. T. P. Crowley, E. A. Donley, T. P. Heavner, "Quantum-based microwave power measurements: Proof-of-concept experiment", Review of Scientific Instruments, **75**, 2575 – 2580 (2004)
6. M. Çetintaş, R. Hamid, O. Şen, S. Çakır, "Traceable measurement of field strength" Topical Session TP-2 20th International Zurich Symp. Electromagn. Compat. 2009.

High accuracy TN optical commutator of laser radiation for application in space navigation

V. Pokrovsky*, S. Studentsov**, L. Soms*, M. Tomilin***

* S.Vavilov State Optical Institute, St.-Petersburg
** Volga-Modulator Ltd., Saratov
*** Physical Department of State University of Information Technologies, Mechanics and Optics, Kronversky pr. 49, St.-Petersburg, 197101, Russia. Tel. 8-812-714-0565, e-*mail:* *mgtomilin@mail.ru*

We describe a new laser based high accuracy space navigation system for landing on a large area surface (200 km^2). The laser system during landing generates four subsecutive pulses (1 Hz, 5 ms, 1.06 □) in direction to four fixed angles by using liquid crystal twist nematic (TN) optical commutator. The signals reflected from landing surface are detected and analyzed with control system that generates signals for movement correction.

The subject of innovation is a new high accuracy TN optical commutator that gives exact addressing laser pulses to four fixed angle beams being propagated to the landing surface. For space navigation system the parameters of applied nematic liquid crystal mixture were optimized.

The efficiency of the commutator system is confirmed experimentally.

In conclusion the advantages and disadvantages of TN commutator system are discussed.

New Frontiers in Tunable Laser Technology: Optical Parametric Oscillators Spanning the Ultraviolet to Mid-Infrared

M. Ebrahim-Zadeh

ICFO-Institut de Ciencies Fotoniques, Mediterranean Technology Park, 08860 Castelldefels, Barcelona, Spain
Institucio Catalana de Recerca i Estudis Avancats (ICREA), Passeig Lluis Companys 23, Barcelona 08010, Spain
Tel: 0034-93 553 4047; Fax: 0034-93 553 4000
e-mail: majid.ebrahim@icfo.es

The development of practical solid-state laser sources in different regions of optical spectrum has been an important goal of research in laser science and technology, since Maiman demonstrated red laser action in ruby in 1960. Major efforts have been devoted to provide coherent radiation in difficult spectral regions using conventional laser techniques, yet, after nearly 50 years, extended wavelength bands across the ultraviolet (UV), visible and infrared (IR) still remain inaccessible to lasers. The potential of optical parametric oscillators (OPOs) for the generation of widely tunable laser light at new wavelengths was recognized soon after the invention of the laser, and the first experimental device was demonstrated in 1965. However, for nearly two decades thereafter, there was little progress in practical development of OPO devices due to the absence of viable nonlinear materials and laser pump sources. With the advent of a new generation of birefringent nonlinear crystals such as β-BaB_2O_4 and LiB_3O_5 in the mid-1980s, and quasi-phase-matched materials, particularly periodically-poled $LiNbO_3$ (PPLN), in the mid-1990s, there began a resurgence of interest in OPO technology for the generation of coherent radiation in new spectral regions. In the intervening period, OPO devices have been transformed from laboratory prototypes into practical light sources, capable of accessing difficult spectral regions and addressing real application areas beyond the reach of conventional lasers. With an exceptionally broad wavelength coverage from a single device, temporal flexibility from the continuous-wave (cw) to femtosecond time-scales, high output power and efficiency, and compact solid-state design, OPOs are now firmly established as truly viable alternatives to conventional lasers and other technologies for the generation of coherent light in difficult spectral and temporal domains.

In the femtosecond time-scales, the absence of viable ultrafast solid-state lasers has confined the choice of laser pump source for OPOs to the Kerr-lens mode-locked Ti:sapphire laser, providing ultrashort pulses in the 1-5 μm spectral range. In the cw regime, the deployment of cw semiconductor diode lasers, high-power Nd-based solid-state lasers and fiber lasers in combination with new QPM materials has similarly led to the realization of a new generation of coherent cw light sources with unprecedented performance capabilities for the 1-5 μm spectral range. On the other hand, extension of operation of ultrafast and cw OPOs to shorter wavelengths below 1 μm has been more challenging because of increased demands on nonlinear materials and the absence of short-wavelength laser pump sources to achieve wavelength generation in the visible and UV using direct parametric down-conversion. However, through application of novel schemes based on frequency up-conversion in combination with parametric down-conversion, it is now also possible to access short wavelengths into the UV and across the visible, making OPO technology a powerful tool for practical generation of coherent radiation across an expansive spectral range from the UV to mid-IR. Here, we describe such techniques for spectral extension of ultrafast femtosecond and cw OPOs into the visible and UV, review the important developments in OPO sources in the near- and mid-IR, and highlight new applications in science and technology.

Manfred Berger

II-VI Deutschland GmbH, Im Tiefen See 58, D-64293 Darmstadt / Germany
eckert@ii-vi.de / www.ii-vi.de

With the advent of reliable Yb:YAG disk lasers and Yb-doped fibre lasers the industry is now adopting these novel sources in their laser material processing systems. Not only superior beam quality and brightness in comparison to conventional technological high power lasers, but also the simplified handling via multi-kW-fibres open up new high performance industrial applications. Recent results underline the importance of 1µm wavelength disk- and fibre-lasers. The advantages and present limitations of 1 µm solid state lasers will be discussed.

High-intensity terahertz pulses: methods of generation and applications.

S.V. Garnov[1], V.V. Bukin[1], A.I. Ritus[1], A.A. Sirotkin[1], T.V. Shirokih[1] and A.G. Stepanov[2]

[1] *A.M. Prokhorov General Physics Institute RAS, Moscow, Russia, garnov@kapella.gpi.ru*
[2] *Institute for Spectroscopy RAS, Troitsk, Moscow region, Russia*

Among a variety of methods and techniques developed for generation of terahertz (THz) beams there are four of them which we discuss in the present talk. Aiming to reach a possibly higher THz electric field amplitude – to be able to study nonlinear processes in gas and condensed media; to test and *to teragraph* high-absorbing biological media; etc. – we studied and applied in the experiments: i) photoconductive antennas – high-voltage biased photoconductors (GaAs and diamonds), ii) laser-induced gas plasma discharges – gas breakdown by femtosecond laser pulses in the presence of the external dc electric field, iii) optical rectification of femtosecond laser pulses with tilted pulse front in lithium niobate crystals, and iv) difference frequency mixing of two laser lines in nonlinear optical crystals.

The developed experimental setups, the results obtained and the prospective applications of high-intensity THz radiation are described and discussed in details.

This work was partially performed under Russian Academy of Sciences Programs: "Extreme light fields and their applications", "Fundamental optical spectroscopy and its applications", and Russian Foundation for Basic Research project # 09-02-00861-□.

Selective Laser Sintering of Magnesium Powder for Fabrication of Porous Structures

Ng Chi Chung[1]

[1] *The Advanced Manufacturing Technology Research Centre, Department of Industrial and Systems Engineering, The Hong Kong Polytechnic University, Hung Hom, Hong Kong, China*

Main author email address: eddyncc1@yahoo.com.hk

In past decades, considerable research effort has been reported in the area of direct metal laser sintering (DMLS). However, rarely work has previously been found on the laser sintering of magnesium powder. Magnesium possesses of low density, good mechanical properties and high degree of biocompatibility, making it become a potential candidate for the fabrication of biological implants. The novelty of the present research lies in the fabrication of porous structures by laser sintering of magnesium powder using a continuous wave (CW) Nd:YAG laser. The laser sintering of single tracks and single layers of magnesium powder were carried out for demonstrating the process feasibility and for examining the influences of two main processing parameters in terms of laser power and scan speed on microstructural characteristics and mechanical properties of the final porous structures. The experimental results demonstrated that porous structures of magnesium compacts have been successfully fabricated by selective laser sintering technique. The results also give sufficient and reliable information about microstructural evolution of magnesium powder under a continuous wave (CW) Nd:YAG laser irradiation, which would facilitate the fabrication and controllability of porous structures by deliberating the associated effect of different processing parameters, whilst achieving superior quality for the laser sintered parts.

Nano-imaging and nano-patterning with compact EUV lasers: new opportunities in nanotechnology with a table top system

Mario Marconi, Przemyslaw Wachulak, Lukasz Urbanski,
Carmen S. Menoni, Jorge J. Rocca
NSF Engineering research Center for Extreme Ultraviolet Science and Technology
and
Electrical and Computer Engineering Department, Colorado State University. USA

The realization of compact table-top size extreme ultraviolet lasers that emits in the 10-50 nm spectral region had opened new scientific opportunities that so far were restricted to large synchrotron facilities. In this talk I will review the last achievements in the development of compact EUV coherent sources, emphasizing two particular applications we are pursuing with table-top EUV lasers: holographic nano-imaging and table top nanopatterning.

We demonstrated wavelength-limited, sub-50 nm holographic imaging with a table-top extreme ultraviolet (EUV) laser operating at 46.9 nm.[1] Table-top nano-holography is demonstrated using as the test object carbon nanotubes. This imaging technique does not require special optics or critical beam alignment. Additionally this technique allows to image macroscopic size objects, several millimeters square and simultaneously sustaining in all the image sub-50 nm spatial resolution. Furthermore, an adequate processing of the hologram using a numerical optical sectioning allows also retrieving depth information, to completely determine the object in the three spatial coordinates.[2]

Using the EUV lasers in a nanopatterning tool, we demonstrated printing of large arrays of nano-pillars and nano-holes with a typical size around 50 nm, and periods in the hundreds of nanometers over millimeter square areas.[3] Using holographic projection lithography and Talbot self imaging we expanded the versatility of this nanopatterning tool making this technique a viable alternative to e-beam lithography for small size prototyping.[4]

References

1. P.W. Wachulak, M.C. Marconi, R.A. Bartels, et al., "Soft x-ray laser holography with wavelength resolution". *Journal of the Optical Society of America B-Optical Physics.* **25**, 1811-1814, (2008)
2. P. Wachulak, Marconi M.C., Bartels R., Menoni, C.S., Rocca, J.J, "Volume extreme ultraviolet holographic imaging with numerical optical sectioning". *Optics Express.* **15**, 10622-10628, (2007)
3. P.W. Wachulak, M.G. Capeluto, M.C. Marconi, et al., "Patterning of nano-scale arrays by table-top extreme ultraviolet laser interferometric lithography". *Optics Express.* **15**, 3465-3469, (2007)
4. J.F. Isoyan A., Cheng Y.C., Wachulak P., Urbanski L., Rocca J.J., Menoni C.S., Marconi M.C., Cerrina F. , "Extreme ultraviolet holographic lithography with a table-top laser". *Proc. SPIE.* **7271**, (2009)

HCN detection in human breath using a cw Optical Parametric Oscillator

M. Spunei[1], D. Arslanov[1], S. Persijn[2], S. Cristescu[1], P. Merkus[3], F. J.M. Harren[1]

[1] *Radboud University Nijmegen, Life Science Trace Gas Facility, Nijmegen, the Netherlands*
[2] *VSL, Delft, the Netherlands*
[3] *Radboud University Medical Centre, Dept. of Pediatrics, Nijmegen, the Netherlands*

Hydrogen cyanide (HCN) is a very potent poison that can cause death through irreversible inhibition of mitochondrial oxidative phosphorylation. Although its toxicity due to smoke inhalation injuries in humans is well described, the role of HCN in human diseases is poorly characterized. Since recently it was proposed that HCN could be an important virulence factor related to bacterial-infected cystic fibrosis (CF) and contributes to long-term lung damage and impairment of the local host immune system.
From the spectroscopic perspective, the "fingerprint" spectrum of HCN in the mid-infrared region shows narrow and strong absorption lines, making this molecule well suited for detection with laser-based spectroscopic techniques. Over the years several techniques have been developed in our laboratory for trace gas detection with applications in Life Sciences. For HCN measurements we shall use the Optical Parametric Oscillator (OPO) recently renewed with a fiber power amplifier in combination with photoacoustic spectroscopy and cavity ring down spectroscopy. The HCN is on line monitored in gas phase around 3 μm at below ppbv detection limit.

The OPO consists of a singly-resonant bow-tie cavity with a 5% MgO-doped PPLN crystal and a low-finesse intracavity etalon. The OPO is pumped by a 14 W cw Nd:YAG laser with 1.3 cm^{-1} continuous tunability and a 5 kHz linewidth over 1 ms. The OPO covers the mid-infrared region between 2.8 and 4.8 μm and provides output powers up to 2.7 W. The passive wavelength and power stability of the OPO system have been improved by embedding the complete OPO setup into a temperature-stabilized monolithic aluminum block. All the passive measures only result in a very narrow linewidth of 7 KHz over 20 μs and 8 MHz over 200 s, with an absolute frequency accuracy that is limited by the wavelength meter (Bristol Instruments 621A). The same combined pump laser and intra-cavity etalon scanning method has been used as described previously [1]. This allows high-resolution scans covering approximately 7 cm^{-1} at a fixed crystal temperature.

We would like to investigate the ability of several bacteria strains involved in airways infections and CF pathogenesis to produce HCN *in vitro*. Furthermore, our goal is to expand this research to *in vivo* tests in order to establish whether HCN in exhaled breath (or in sputum) may be a reliable marker of bacterial activity that can be used to evaluate the treatment efficiency in cystic fibrosis.

Reference

1. A.K.Y. Ngai, S.T. Persijn, G. von Basum, and F.J.M. Harren, "Automatically tunable continuous wave optical parametric oscillator for high resolution spectroscopy and sensitive trace gas detection," Appl. Phys. B **85** 173-180 (2006)

Accurate Spectral Measurement of Absorption and Scattering

Markku A. Lehto, Ville T.J. Keränen, and Anssi J. Mäkynen

Measurement and Sensor Laboratory, University of Oulu, Kajaani, Finland
markku.a.lehto@oulu.fi

The goal of this study was to design and build an accurate instrument for measuring the absorption and scattering coefficients of a thin sample. Performance of instrument was evaluated using absorption and scattering references, made of two different materials. Ultimate goal of this study was to have an instrument for non-contacting measurements for industrial applications.

The instrument set-up consists of two integrating spheres, two channel fibre optic spectrometer, cuvette for liquid samples and references and collimated fibre optics illuminator, all represented in Figure 1. The diameters of the integrating spheres are 210 mm and sample port diameters are from 25 mm to 63 mm. Solid sample is placed directly between integrating spheres and liquid samples are placed in cuvette. Sample is illuminated with collimated fibre optics illuminator through the first sphere. Reflected and transmitted light intensities are measured with two channel fibre optic spectrometer. The measured spectral intensities are then converted to absorption coefficient and reduced scattering coefficient using inverse adding doubling method [1].

Instrument performance was evaluated with Intralipid-10% fat emulsion with concentrations from 3% to 10% and results were compared with documented Intralipid-10% absorption and scattering properties. Also polyurethane reference samples with various amounts of India ink and TiO_2 were measured and results were compared to absorption and scattering properties measured in Oregon Medical Laser Center from the same samples.

Preliminary measurements show promising results which justify the continuation of the study. More testing and improvements are needed for this setup to prove its soundness in optical parameter determination. A more detailed description of the measurements and results will be presented in the final paper.

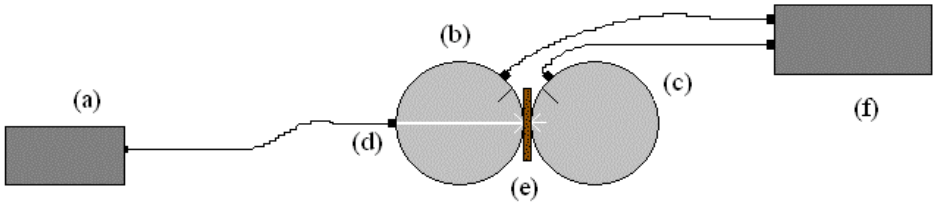

Fig. 1. Measurement setup. (a) Tungsten halogen light source (b) Reflectance sphere (c) Transmittance sphere (d) fiber collimator (e) Sample (f) Two channel fibre optic spectrometer.

Reference

1 http://omlc.ogi.edu/software/iad/

Biophotonic methods for the assessment of burn injury in human skin

Martin J. Leahy

Dept. of Physics University of Limerick, IRELAND
Email: martin.leahy@ul.ie

Of particular interest in laser safety for exposed skin is the effect of high energy photons since these constitute ionising radiation and as such raise complications such photo-chemical reactions and cancer. Therefore, a priori knowledge of the threshold light dose would be useful. However, prediction of the effect a particular light dose on human skin suffers from inter- and intra-individual variables. Even today the quantity of light required to cause burns is assessed by phototesting and visual inspection to determine the minimum energy deposition rate required to cause a burn for a particular subject. This paper will examine the use of biophotonic imaging techniques to remove observer variability in the assessment of burn injury in human skin.

Assessment of minimal erythemal UVB dose by diffuse reflectance imaging

Martin J. Leahy

Dept. of Physics University of Limerick, IRELAND
Email: martin.leahy@ul.ie

In routine clinical phototesting, naked eye dermatological assessment remains the "gold standard" for determining the patient's minimal erythemal dose (MED). Bioengineering methods such as colourimetry and laser Doppler perfusion imaging (LDPI) have been used as complementary methods to help reduce intra-observer variability in results. Divergent beam UV-B testing has used LDPI to give quantitative description of reactivity to doses above the MED as well as a "single-dose" objective determination of the MED itself. The recently developed Tissue Viability (TiVi) imaging is proposed as a reliable, easily acquired, high-resolution alternative to LDPI in the divergent beam testing concept.

TiVi offers advantages over LDPI in the acquisition and analysis of data collected during divergent beam testing. The data is easily obtained and increases applicability in the clinical environment.

Medical Applications of Laser Spectroscopic Gas Analyses

Department of Physics, ETH Zurich, Zurich, Switzerland

The detection and analysis of gases and vapors has attracted considerable interest in recent years owing to an enhanced concern of increasing concentrations of climate-relevant compounds in the earth atmosphere, of workplace safety in industry or of homeland security. Furthermore, gas sensing is important in numerous further applications, e.g., in agriculture or in medical diagnostics. Apart from conventional and well-established techniques such as gas chromatography, mass spectrometry, chemi-luminescence, electrochemical sensors or Fourier-Transform Infrared (FTIR) Spectroscopy, laser-based systems offer some unique advantages like minimal sample preparation and often good time resolution.

The performance of a laser-based device is crucially connected to the laser source itself. Since most gases have their fundamental absorptions in the mid-infrared range, easy and continuous tunability of the laser wavelength is mandatory to enable selective recordings in multi-component gas mixtures. At the same time the linewidth should be sufficiently narrow to permit differentiation between interfering absorption lines of different compounds or of isotopes or isomers. Although alternatives are sometimes available the choice of tunable mid-IR lasers is essentially limited to interband and quantum cascade lasers and nonlinear optical systems (optical parametric oscillators (OPOs) and difference frequency generation (DFG)). In addition to a suitable laser source a sensitive detection scheme (multipass trans-mission, photoacoustics, cavity ring-down or variations therefore) has to be implemented. An important issue concerns the analysis of spectra which requires databases of molecular spectra and an algorithm to fit a measured spectrum of a multi-component sample with spectra of individual compounds. In this paper we demonstrate the performance but also limitations of laser spectroscopy by discussing two applications in medical diagnostics: breath analysis and surgical smoke.

Breath analysis represents a promising tool for non-invasive medical diagnostics [1]. It is – however – a challenging task to identify ppb concentrations (or their enhancement in the presence of a disease) of specific compounds in a mixture of hundreds of other compounds, some of them like water vapor or CO_2 in the percent range. Here we present the example of a stable isotope used as tracer in clinical research and medical diagnosis. After ingestion of a small amount of D_2O (heavy water) by a person, we subsequently analyzed her breath at different time intervals by measuring the D/H isotope ratio [2]. This tracer is of interest to determine glucose and cholesterol synthesis rates, total body water or energy expenditure. We were able to determine an enhanced D/H isotope ratio in the exhaled breath for up to several weeks after the ingestion of only 5.1 mL of D_2O. The measurements were performed with a pulsed DFG system in the wavelength range around 3.6 μm where strong HDO lines and weak H_2O lines are present without interference by other relevant breath components like CH_4, NH_3, CO and CO_2. The breath samples were collected in a heated Tedlar bag and transferred to the heated multipass cell without any preliminary sample preparation.

A second example concerns analyses of so-called surgical smoke. In minimally invasive (laparoscopic) surgery with lasers or electroknives, surgical smoke is produced whose composition and potential danger to both the patient and the operation team are of great interest. We produced smoke samples in vitro by cauterization of animal meat in a CO_2 atmosphere (as is common in laparoscopic surgery). The DFG source with a pulsed Nd:YAG laser (1064.5 nm) as pump, a CW external cavity diode laser (1520-1600 nm) as signal laser and periodically poled $LiNbO_3$ (PPLN) as nonlinear mixing material enabled a (fully computer-controlled) broad tuning range between 2900 and 3144 cm^{-1} for a single PPLN poling period. We recorded spectra of smoke samples in the multipass cell and analyzed them with a newly developed algorithm using quantitative spectra of 360 compounds of a database [3]. The algorithm introduces a rating and an adaptive filter and produces a list of substances with their concentrations within a few minutes. First studies revealed the four compounds water, methane, ethane and ethene in all samples. Currently the accessible spectral range is extended to search for additional relevant species, also under *in vivo* conditions of smoke generation.

References

1 A. Amann, D. Smith, eds., *Breath Analysis for Clinical Diagnosis and Therapeutic Monitoring*, World Scientific, Singapore, 2005.

2 R. Bartlome, M.W. Sigrist, "Laser-based human breath analysis: D/H isotope ratio increase following heavy water intake", *Opt. Lett*., **34**, 866-868 (2009).

3 M. Gianella, M.W. Sigrist, "Improved algorithm for quantitative analyses of infrared spectra of multicomponent gas mixtures with unknown compositions", *Appl. Spectr.*, **63**, 338-343 (2009).

Broadly tunable Tm,Ho:KYW laser around 2 μm and its mode-locked operation

A.A. Lagatsky[1], S. Calvez[2], M. Dawson[2], N.V. Kuleshov[3], W. Sibbett[1]

[1]School of Physics and Astronomy, University of St. Andrews, St. Andrews, KY16 9SS, UK

[2]Institute of Photonics, University of Strathclyde, Wolfson Centre, 106 Rottenrow, Glasgow, G4 0NW, UK

[3]Institute for Optical Materials and Technologies, Belarus National Technical University, 65 Nezavisimosti Ave., Minsk 220013, Belarus

Tm^{3+} doped and Tm^{3+},Ho^{3+} co-doped crystalline gain media represent an attractive option for creating of diode-pumped, efficient and broadly tunable lasers around 2 μm [1, 2] which can be further employed for ultrashort pulse generation through the modelocking techniques [3]. Such laser sources are of great interest for applications in time resolved spectroscopy, nonlinear frequency up-conversion, optical communications and photomedicine.

Here we report on the basic spectroscopic properties of a novel Tm,Ho:$KY(WO_4)_2$ crystal, together with its room-temperature continuous wave and mode-locked laser performance around 2 μm when pumped by a Ti:sapphire laser.

Single crystals of $KY_{1-x-y}Tm_xHo_y(WO_4)_2$ (Tm,Ho:KYW) were grown by using the modified Czochralski technique under conditions of low thermal gradient. By using b-cut seeds the crystals of typical size of 25(*a*-axis)×25(*c*-axis) mm^2 and up to 50mm-long (*b*-axis) were pulled with compositions of x=0.05 (5 at. % of Tm^{3+}) and y=0.004 (0.4 at. % of Ho^{3+}). Using a Ti:sapphire laser as a pump source at 802 nm, a maximum slope efficiency of up to 44% has been achieved with a corresponding output power of 460 mW at 2056 nm during continuous wave operation of Tm,Ho:KYW laser at room temperature. A tunability covering the 1890-2080 nm spectral range has been demonstrated. It was observed that up-conversion losses play a significant role in reducing the slope efficiency and the output power of Tm,Ho:KYW laser when high transmission (T>1%) output couplers are employed.

The laser experiments on passive modelocking of Tm,Ho:KYW laser were performed using a semiconductor saturable absorber mirror (SESAM) which incorporated a GaSb/AlAsSb DBR structure having a high reflectivity at ~1930-2150 nm and 2×InGaAsSb quantum wells acting as the absorber. Stable mode locking was readily achieved at around 2057 nm with the generated pulse durations of 3.3 ps at an average output power of 230 mW. The corresponding spectral width of 1.3 nm implied a time-bandwidth product of 0.3. Using 2mm-thick Lyot filter, mode-locked pulses were tuned over the 2000-2070 nm range. In this case, the pulse durations ranged from 4.9 to 13 ps with a maximum average output power of 300 mW at around 2056 nm. Pulses as short as 570 fs were generated from Tm,Ho:KYW laser at 2055 nm using ion-implanted SESAMs.

In conclusion, it is believed that further optimization of Tm,Ho:KYW crystal and cavity parameters could lead to a superior modelocking laser performance thus making this type of novel gain medium highly suitable for the future development of practical and compact 2-μm ultrashort pulse lasers.

References

1 X. Mateos, V. Petrov, J. Liu, M.C. Pujol, U. Griebner, M. Aguiló, F. Diaz, M. Galan, G. Viera, "Efficient 2-μm Continuous-Wave Laser Oscillation of Tm^{3+}:$KLu(WO_4)_2$", IEEE J. Quantum Electron. **42**, 1008-1015 (2006).

2 X. Han, J.M. Cano-Torres, M. Rico, C. Cascales, C. Zaldo, X. Mateos, S. Rivier, U. Griebner, V. Petrov, "Spectroscopy and efficient laser operation near 1.95 μm of Tm^{3+} in disordered $NaLu(WO_4)_2$", J. Appl. Phys. **103**, 083110 (2008).

3 G. Galzerano, M. Marano, S. Longhi, E. Sani, A. Toncelli, M. Tonelli, P. Laporta, "Sub-100-ps amplitude-modulation mode-locked Tm-Ho:BaY_2F_8 laser at 2.06 μm", Opt. Lett. **28**, 2085-2087 (2003).

Laser resonator mode connection and change of this connection under influence of an external optical signal

V.P.Bykov

. *A.M.Prokhorov General Physics Institute, Vavilova 38 Moscow Russia*

The behaviour of the laser resonator filled by the active, not pumped laser medium (for example, $YAG:Nd^{3+}$), treated to action of the resonant laser radiation filling one of the resonator eigenmode, is investigated in the report. As the pumping radiation is absent and population on the working levels is not present, laser medium, despite of presence of resonant radiation, remains not excited . In the report it is shown, that at influence of an external resonant signal on such system, its state sharply varies. Connection of mode, excited by resonant laser radiation, with the second mode of the same resonant frequency, which is not excited before appearence of a resonant signal, appears. It is shown, that due to the appeared connection the amplitude of the second mode can reach significant values, and time of increase of this amplitude appears to be small $(10^{-8}\,\mathrm{sec})$. Thus the considered system allows to change optical radiation by means also by an optical signal. In the report possible practical schemes and their features are considered. Sensitivity of the system to an external signal is determined. The optimum sizes of the resonator and active medium are also given. Influence of initial parasitic communication between modes is estimated and shown, that this influence can be excluded. So, the considered system can be regarded as some sort of optical relay.

Influence of the resonator losses on the possible squeezing at the resonator parametrical excitation

V.P.Bykov

A.M.Prokhorov General Physics Institute, Vavilova 38 Moscow Russia

From the first observation of the squeezed light [1,2] has passed more than twenty years. Unfortunately, serious move, for example, in the squeezing factors has not occurred since then. Nevertheless, interest to the squeezed light there is, as from the basic point of view - the squeezed light is a macroscopical quantum object, and so from the point of view of practice since the squeezed light possesses some useful properties. First of all the opportunity to reduce quantum mechanical uncertainties and, accordingly, to raise accuracy, in particular, of interferometric measurements attracts the attention. We shall note also an opportunity of much more effective generation of high harmonics of light in nonlinear experiments. Now the phased high harmonics of radiation play the important role at generating attosecond pulses. Unfortunately, all these opportunities can be effectively realized only at great squeezing factors.

The contemporary interest to the squeezed light was manifested, in particular, in the appearing of two papers [3,4] in which the record, though still low squeezing factors ($\cong 10$), have been reached. At the same time, the reasons of the squeezing factor smallness have not been analysed in a due measure. However, at only deep understanding of these reasons it is possible to move to increased squeezing factors.

In this report it is found out, that a principal reason limiting squeezing factors is the resonator power losses, i.e. in other, spectral language - final width of its spectral line. Some possible ways of overcoming of this obstacle are planned also. The influence of losses on the possible squeezing factors is investigated at the resonator parametrical excitation. In frames of the iteration theory the following relation for the squeezed state dispersion is received

$$D^2(t)=\frac{1}{2}|F(t)|^2\left\{1+l\left[4t+\int_0^t dt'\cdot\left(|F(t')|^2+\left|\dot{F}(t')\right|^2\right)\right]\right\}-\frac{1}{4}l\left[F^2(t)\int_0^t dt'\cdot\left(F^{*2}(t')+\dot{F}^{*2}(t')\right)+\hat{e}.\tilde{n}.\right],$$

where $D(t)$ is the dispersion of the squeezed state, $F(t)$ is the solution of the equation

$$\ddot{F}+\kappa(t)F=0$$

and $\kappa(t)$ is the dependence on time of the squared resonator eigen frequency, l is the resonator loss factor. When last equation is the Mathieu equation

$$\kappa(t)=1+g\sin 2t,$$

the following limiting estimation for the squeezing factor is received

$$\mathrm{K}_{t\to\infty}^{\lim}\cong\sqrt{g/l}\ .$$

References
1.Slusher R.E., Hollberg L.W., Yurke B., Mertz J.C., Valley J.F. Phys.Rev.Lett. 55, p2409 (1985)
2.Wu Ling-An, Kimble H.J., Hall J.L., Wu Huifa Phys.Rev.Lett. 57, p2520 (1986)
3. Takeno Y., Yukawa M., Yonezawa H., Furusawa A.
Opt. Express **15**, 4321 (2007)
4. Vahlbruch H., Mehmet M., Chelkowski S., Hage B., Franzen A., Lastzka N., Goßler S., Danzmann K., Schnabel R. PRL **100,** 033602 (2008)

Direct-write of 3-dimensional materials structures from gaseous precursors and applications

Michael Stuke

Am Fassberg 11, D-37077 Göttingen

mstuke@gwdg.de

Free-standing 3-dimensional structures of different materials are generated by laser-direct-write from suitable gaseous precursor mixtures, with special emphasis on ceramic and metallic objects including Aluminum-oxide and Aluminum. In this way small stable and biocompatible electromagnetic cages for precise handling of objects in solution can be formed. Key processes and processing steps will be presented and examples shown including video clips of the main phenomena observed.

Reference

[1] "Direct-writing of three-dimensional structures using laser-based processes" Michael Stuke, Kurt Müller, Thorsten Müller, Kirk Williams, Rachel Oliver, Doug Ohlberg, Günter Fuhr, R.Stanley Williams

An Elliptically Polarized Laser Light for Characterization of Micro-Size Object(s) from Angular Scattering Profiles

Mustafa M. Aslan[1*], and Kerim Allakhvrdiev[1,2]
[1] *Materials Institute, TUBITAK Marmara Research Center, Gebze- Kocaeli, Turkey*
[2] *Institute of Physics ANAS. Baku, Azerbaijan*
**email: Mustafa.Aslan@mam.gov.tr*

By nature, laser light is the optimum tool for characterization of small object(s), as it is usually nonintrusive and allows real time measurements. If electromagnetic wave is incident on a cloud of objects, it is either absorbed or scattered. The extent of absorption and scattering depends on particle size, shape, optical properties, and the wavelength of the incident laser light. Object(s) can be in different structures and shapes such as particles, bubbles, fibers, structures [1]. Better characterization requires more experimental variables to be measured. Characterization of micro size objet(s) is possible with an elliptically polarized-elastic light scattering (EP-ELS) in terms of scattering matrix elements (S_{ij}'s). The scattering matrix elements as experimental variables provide information about intensity and polarization of scattered laser light. They can be measured and calculated as a function of scattering angle. The EP-ELS system that was built consists of three major parts: light source, optics and detector. Light source is a laser that can be employed to characterize micro-size objects in Mie/Ray Optics scattering regime. Optical components between the laser and the object are to control intensity and polarization of incident laser light. Optics between the object and the detector are to measure different polarization states of scattered laser light as a function of the scattering angle (θ).

In this poster we explain basic principle of the elastic light scattering system and summarize measurements taken by the system for three different problems: 1) Bubble size and concentration: In this section, potential use of the EP-ELS approach to monitor both bubble size and gas hold-up in a bubble laden medium is explored. It was observed that the change in the bubble size yields significant changes in S_{11}, S_{33}, S_{44}, and S_{34} profiles. An optimum single measurement angle of θ=120° was determined for a gas velocity range of 0.04 to 0.35 cm/s. The choice of the optimum angle depends on frit pore size, column diameter, gas pressure, and surfactant concentration. These results suggest that a simplified version of the present EPLS system can effectively be used as a two-phase flow sensor to monitor bubble size and liquid hold-up in industrial systems. 2) Size and shape prediction of colloidal metallic MgBaFeO particles: The size and structure of colloidal metallic (MgBaFeO) particles are determined using the system. The approach is based on a hybrid experimental/theoretical study where the experimental data are compared against predictions obtained using a T-Matrix model that accounts for particle shape irregularities. A power-law distribution function with two parameters is employed to account for the particle size distribution. The experiments are conducted using the second-generation EP-ELS system. If shape is the most desirable quantity to be determined, S_{22} profiles are the most important. However, if the size distribution is the most desired parameter, S_{11} and any other S_{ij} can be used. It is shown that the current EP-ELS measurements can effectively be used for identification of both the shape and the size of the colloids. 3) Measurement of milk fat ratio: In this part, we present an experimental approach to determine the milk fat content using scattered light intensity profiles. Three of the scattering matrix elements, specifically S_{11}, S_{12}, and S_{33}, were found to be sensitive to the number of fat particles in milk. These results indicate that it should be possible to develop a reliable sensor based on the measurement of these scattering elements, which will allow for the development of a robust, in-line sensor to be used in food processing. In addition an attempt was made to model the phenomena using a relatively simple approach based on single scattering with a size distribution. The disagreement between the model and experiments suggests that a more comprehensive model is needed which can account for multiple scattering.

Results from three different applications summarized above show such a flexible optical system would allow us to characterize micro-size features such as particle(s), bubbles, colloids as well as structures since it is capable to determine Mueller matrix elements as a function of scattering angle. Both the sample holder and optical components of the system can be modified very easily for other applications.

Reference

1. C.F. Bohren, and D.R. Huffman, *Absorption and scattering of light by small particles*, Wiley, New York, 1983.

CdTe Quantum Dots Embedded in Porous Silicon Oxide Matrix Photoluminensecence

N.A. Piskunov [1], E.D. Maslennikov [1], L.A. Golovan [1,2], V.Yu Timoshenko [1,2], P.K. Kashkarov [1,2]

[1] *Physics Department, Moscow State University, Leninskie gory 1/2, Moscow, 119991 Russia*

[2] *Russian Research Center "Kurchatov Institute", Kurchatov square 1, Moscow, 123182 Russia*
Phone: (+7 495) 9394657, fax: (+7 495) 9391944, e-mail: nickpsk@gmail.com

Semiconductor quantum dots (QDs) have attracted a lot of interest last years because of their intensive photoluminescence (PL), high quantum efficiency, and possibilities for optical and biomedical applications [1]. For some tasks of modern photonics such as light emitting devices, and IR-light visualizes, solid materials are preferable comparing to the suspensions. The simple way to form such materials is embedding of the QD in the solid matrix, and it's important to keep all necessary QD properties in the final medium. Fabrication and properties of the QD of A^2B^6 materials implemented in dielectric matrix haven't been studied earlier, despite of the practical interest to that topic [2].

In our present work CdTe QDs were successfully synthesized in double-step chemical reaction between $Cd(ClO_4)_2$, H_2Te, and thioglycolic acid [3]. That method allows to produce nanocrystals with diameters from 1,5 nm up to 5,5 nm, and to have emission peak in the range between 500 and 800 nm, depending on the QDs size. The free porous silicon films were used for the solid matrix preparation. The as-prepared films (thickness 25 □m) were oxidized in air under temperature 900° C during 2 hours, the stoichiometry coefficient x is between 1 and 2. Several drops of water-ethanol solution of QDs were sequentially put on the SiO_x film to produce nanocomposite material.

The implementation of the QDs in the depth of the film was tested by the cathodoluminescence method. For that purpose cathodoluminescence spectra were taken from different points on the film's profile. The presence of the QDs was detected on the both sides of the sample and from the middle part as well. That fact indicates the nanocrystal's deposition into the matrix pores.

The optical properties of the material with CdTe QDs, embedded in the porous silicon oxide matrix, were studied by the one- and two-photon photoluminescence methods. The QDs highly determine the optical characteristics of the nanocomposite, in the nanocomposite's PL spectrum QD's peak is two times more intense, than the matrix's one (fig.1).

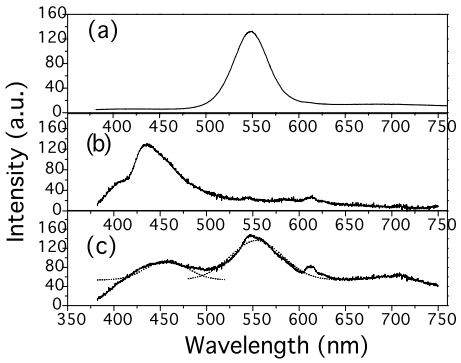

Fig.1.Photoluminescence spectra: CdTe QDs (a); SiO_x film(b); nanocomposite material CdTe/SiO_x (c).

The dependence of the PL intensity from the excitation power was linear in case of one-photon excitation by nitrogen laser (□ = 337 nm). For the two-photon excitation process by Nd:YAG ps-laser (□ = 1064 nm) the non-linear dependence was observed, which is in good correspondence with the theoretical model. The two-photon absorption coefficient of the CdTe QDs was estimated by approximation of the experimental curve with the theoretical formula, □ = 8 ±0.5 cm/GW. It's more than four times bigger then the value for the bulk CdTe. So, we fabricated easy-to- use nanocomposite material, which exhibits optical properties of QDs.

References

1. S. Ossicini, L. Pavesi, F. Priolo, Springer, Berlin, 2003.
2. L. Pan, A. Ishikawa, N. Tamai, "Detection of optical trapping of CdTe quantum dots by two-photon-induced luminescence", Physical Review B, **75**, 161305 (2007).
3. A.L. Rogach, T. Franzl, T.A. Klar, et al., "Aqueous synthesis of thiol-capped CdTe nanocrystals: State-of-the-art", J. Phys. Chem. C, **111**, 14628-14637 (2007).

Functionalized plasmon-resonant nanoparticles: Fabrication, optical properties, and biomedical applications

Nikolai G. Khlebtsov[1,2]
[1] *Laboratory of Nanobiotechnology, Institute of Biochemistry and Physiology*

[2] *Saratov State University, Saratov, Russia*

The metal (mainly gold) nanoparticles (NPs) [1] have attracted significant interest as a novel platform for nanobiotechnology and biomedicine [2] because of convenient surface bioconjugation with molecular probes and remarkable optical properties related with the localized plasmon resonance (PR) [3]. Recently published examples include applications of NPs to genomics, biosensorics, immunoassays, clinical chemistry, detection and control of microorganisms, cancer cell photothermolysis, targeted delivery of drugs or other substances, optical imaging and monitoring of biological cells and tissues by exploiting resonance scattering, optical coherence tomography, two-photon luminescence, or photoacoustic techniques. One of outstanding examples is rapid development of methamaterials with the optical negative refractive index [4].

Here, we give a short review of our recent work on fabrication, optical properties, functionalization, and biomedical applications of plasmon-resonant nanoparticles (more detailed information can be found in our recent review [5]). Three types of nanostructures are considered: gold nanospheres, gold or gold/silver nanorods, and gold nanoshells with silica cores. Several methods for spectral tuning of plasmon resonances through variations in size, shape, and structure of particles are described. We also discuss extinction, scattering, and depolarization of laser light scattered by gold and gold/silver nanorods. The multipole and coupled properties of interaction particles are discussed very shortly. Finally, we consider application of the functionalized nanoparticle bioconjugates to immunoanalysis, dark-filed light microscopy imaging of living cells, and laser photothermolysis of cancer cells *in vitro*.

References

1 E. Boisselier, D. Astruc, "Gold nanoparticles in nanomedicine: preparations, imaging, diagnostics, therapies and toxicity," *Chem. Rev*. **38**, 1759-1782 (2009).
2 N. R. Panyala1, E.M. Pena-Mendez, J. Havel, "Gold and nano-gold in medicine: overview, toxicology and perspectives," *J. Appl. Biomed*. **7**, 75-91 (2009).
3 N. G. Khlebtsov, "Optics and biophotonics of nanoparticles with a plasmon resonance," *Quant. Electron*. **38**, 504-529 (2008).
4 V. M. Shalaev, "Optical negative-index methamaterials," *Nat. Photon*. **1**, 41-48 (2007).
5 N. G. Khlebtsov, L. A. Dykman, "Optical properties and biomedical applications of plasmonic nanoparticles," *J. Quant. Spectr. Radiat. Transfer*. 2009. V.doi:10.1016/j.jqsrt.2009.07.012.

Controlled laser hyperthermia of subdermal neoplasms.

Nina A. Kalyagina*,**, Irina A. Shikunova*, Tatiana A. Savelieva*, Viktor B. Loschenov*

*General Physics Institute RAS, Moscow, Russia

**Institut National Polytechnique de Lorraine (INPL), Nancy, France

The capability of the Photodynamic Therapy (PhD) and Laser Hyperthermia (LH) methods is strongly restricted in the case of tumors located on the depth. The main problem, arising from the use of external irradiation, is caused by overheating tissue thin layers on the surface when required light power density in the soft tissues is reached.

The represented method includes tissue irradiation by laser light with synchronous cooling of the thin tissue layers with the special cooling system and real-time monitoring of the tissue surface temperature during that process. This system has a feedback with the use of which we can control the temperature inside the tissue, basing on the surface temperature.

We made several temperature distribution curves during the LH for different parametric variations: without cooling (the power of laser irradiation was 0.5W, 1W, 1.5W and 2W); with cooling and with cooling over the third minute of hyperthermia. Variation of the speed of cooling liquid and of laser power leads to variation of the depth of maximal heating area inside the tissue.

Optimal parameters of the light power and of the temperature in the cooling system were selected to control the temperature distribution of the tumor. We can receive profile of the temperature of thin (first) layers and inside the tumor to avoid overheating which leads to destruction of the normal tissues.

Determination of Heavy Metals in Waters by Thermal Lens Spectrometric Detection of Metal Colloids

Dorota Korte Kobylinska, Mladen Franko*

SI-5000 Nova Gorica, Slovenia,
Mladen.Franko@p-ng.si

Metal colloids dispersed in solutions play an important role in material science as well as in several technological and environmental processes and applications. They not only display novel catalytic properties in many chemical reactions but also change the optical parameters of materials which are a function of the metal nature, morphology of colloid particles and the state of their aggregation [1]. Due to the ability of influencing the physical and chemical properties of a wide range of materials, the metal colloids are commonly used in sensors for volatile organic chemicals, in DNA chips, data storage media, photonic devices, and also for fabricating magnetic and nanofluids [2-4].

Various methods are used for preparing metal colloids including laser ablation [5], photochemical [2] and chemical methods [6]. Transmission electron microscopy and atomic absorption spectrometry [2] are most frequently used for metal colloid detection and characterization but other techniques such as thermal lens spectrometry (TLS) was also used to monitor the process of metal colloid preparation [6].

In this work the possibility of exploiting the formation of metal colloids for detection of low concentrations of heavy metals was investigated. TLS [7] technique was applied for detecting metal colloids in solutions at 457.9 nm (100 mW excitation power). The colloids were prepared in a flow-injection (FIA) system by injecting a solution of metal ions into a flowing carrier stream and mixing it with a solution of a reductant (BH_4^-) in a mixing coil. Combination of FIA and TLS provides low limits of detection, which are at the levels of a few ng/mL as demonstrated for example for Ag. The measurment procedure is simple, fast and performed at a single wavelength. The described technique could therefore serve as a sensitive and universal detection scheme for metal ion detection in systems such as ion chromatography and capillary electrophoresis.

References

1. V. Vegera and A. D. Zimon Russian J. of Appl. Chem. 79 (2006), p. 1403.
2. T. A. Taton, C. A. Mirkin and R. L. Letsinger Science 289 (2000), p. 1757.
3. S. Sun, C. B. Murray, D. Weller, L. Folks and A. Moser Science 287 (2000), p. 1989.
4. B. Macalik, L. Krajczyk and T. Morawska-Kowal Phys. Status Solidi 4 (2007), p. 761.
5. J. Neddersen, G. Chumanov and T. M. Cotton Appl. Spectrosc. 17 (1993), p. 1059.
6. Z. Zhang and G. R. Long Appl. Spectrosc. 47 (1993), p. 2126.
7. M. Franko Appl. Spectrosc. Rev. 43 (2008), p. 358.

The possibility of wideband CO laser and Sr vapor laser using for atmosphere monitoring

Kharchenko O.V., Romanovskii O.A.

1, Akademicheski av., Tomsk, Russia, 634021, fax: 7 382 249 2086
mailto: olya@iao.ru

The development of laser remote IR-spectroscopy calls for the elaboration and promotion of new mid-IR laser radiation sources capable of lasing in the spectral range as wide as possible with small-step frequency tuning.

In the present paper the possibility of application of the wideband CO and Sr lasers for atmosphere monitoring is analized. A compact slit high-frequency-excited CO laser has generation range 4.7–8.2 □m for fundamental vibrational transitions and 2.5–4.2 □m for overtone transitions. Generation range for strontium vapor laser (SrI- SrII) is - 1-6.2 □m. These spectral ranges are most informative from the viewpoint of laser sensing of minor gaseous components (MGC) in the atmosphere.

The differential absorption lidar (DIAL) method based on the effect of resonant laser radiation absorption by gases is most widespread among the methods of laser sensing of gaseous atmospheric components. The effect of resonant laser radiation absorption has a maximum interaction cross section in comparison with other phenomena (Raman scattering and resonant fluorescence) used to determine gaseous composition of the atmosphere. To find CO-laser wavelengths suitable for sensing of the atmospheric MGC by the DIAL method, we used the justified criteria for line selection. The informative wavelengths of the substances N_2O, NO_2, H_2CO, CH_4, C_2H_2, HCl, HF, HBr, HCN for lidar technique have been found. Numerical modeling of lidar measurements of atmosphere MGC using wideband CO laser was carried out.

To retrieve wavelengths informative for MGC sensing by strontium laser we used the same technique. Results of these calculations demonstrates that it is rather difficult to use some of the strontium laser lines in base methods of gas analysis of the atmosphere because of the strong interfering component caused by the radiation absorption by water vapor. However, alongside with lines whose radiation is completely absorbed on the path 1 km long, there are lines in the Sr laser spectrum that fall within the atmospheric transparency micro-windows and can be used for remote sensing by DIAL. Strong water vapor absorption lines centered at 2.69 and 2.92 μm are promising for measurements of humidity profiles in the atmosphere on atmospheric paths of 10-100 m. As demonstrated the calculated results, the strontium laser line around 3 μm can be used to detect HCN emissions on a level of 0.1 ppm using paths 1 km long.

As a whole, our calculations have confirmed that the wideband CO and Sr vapor lasers are promising for remote laser sensing of the atmospheric MGC by the DIAL.

This work was supported in part by the Russian Foundation for Basic Research (grants Nos. 07-05-00765 a and 09-05-99035-r_ofi).

Application of the pulse laser deposition method for preparation film nanostructure of metals and semiconductors

O.A. Novodvorsky, E.V. Khaydukov, A.A. Lotin, L.S. Parshina, V.V. Rocheva, V.Ya. Panchenko

Modern tendencies in microelectronics demand creation of qualitative films of nanometer thickness, requirements to uniformity and smoothness of a surface of received structures constantly rise. For deposition of films of demanded quality the PLD method since in the processes of growth high-energy particles of plasma participate that allows to receive continuous films with high epitaxy and crystal perfection is perspective. The important advantage of a method is the exact control of speed of deposition of particles, roughness and uniformity [1].

We apply to deposition of ultra thin films two PLD modifications: the method of the crossed beams [2] and a method of high-speed mechanical separation [3]. The dimensional effect of static conductivity in thin films at PLD in vacuum was investigated at deposition of films ^{119}Sn, Fe, Cr, Si, ZnO. Isotopic pure ^{119}Sn films are received under various conditions of deposition. The AFM researching of ^{119}Sn films have shown dependence of structure of a film on power density of radiation on a target.

Using of quantum wells (MQW) as an active layer in optoelectronic devices essentially is more effective than usual p-i-n structures as charge carriers in quantum wells are spatially limited on one of three coordinates [4]. It promotes to increasing of probability radiating recombination of carriers and to reduction of a threshold of generation in lasers, and also to supervision various quantum dimensional effects connected with excitons. Therefore research of structures with quantum wells has both applied and scientific value. Research of dependence of width of the band gape and dependence of position of UV peak of a photoluminescence (PL) films MgxZn1-xO from Mg concentration in targets is researched.

For research of optical properties of $Mg_xZn_{1-x}O$ films the absorption spectra in short-wave area (250-400 nm) and the PL spectra were measured. The excitation PL of films was carried out by the He-Cd laser, the PL spectra in area 300 – 700 nm were registered by Ocean Optics HR4000 spectrometer in the temperatures range from 10□ to 400□. The increasing of magnesium concentration in the film leads to shift of edge of a fundamental strip of absorption and position of PL peak in dark blue area. MQW $Mg_xZn_{1-x}O$/ZnO received by us show good optical properties. Absorption MQW $Mg_xZn_{1-x}O$/ZnO observed in a spectrum separate lines corresponding to transitions between energy levels confirm presence of the connected electron-hole pairs and good repeatability of width QW and barriers.

The work has been supported by ISTC Project 3294, RFBR-09-07-00208-a and RFBR-09-08-00291-a.

References

1. V.Ya. Panchenko, O.A. Novodvorsky, V.S. Golubev, "The technology of pulse laser deposition of films of nanometer thickness", *The Science and Technologies*, **4**, 39 (2006).
2. A. Gorbunov, A. Tselev, W. Pompe, "Cross-beam laser deposition of ultrathin multilayer metal films", *Proceedings of SPIE*, **3688**, 351-358 (1999).
3. A.N. Zherihin, A.I. Khudobenko, R.T. Villjams, J. Wilkinson, K.B. User, G. Hionig, V.V. Voronov, *Quantum electronics*, **33**, 11 (2003).
4. G.-C. Yi, M.Y. Kim, S.J. Pennycook et al., "Quantum confinement observed in ZnO/ZnMgO nanorod heterostructures", *Adv. Mater*., **15**, 6 (2003).

Modulation for Compression Dynamics of Quadratically Phase-Modulated Few-Cycle Pulses in Dispersive Medium

Olga I. Paseka[1], Valery E. Lobanov[1] and Anatoly P. Sukhorukov[1]
[1] *Physics Department, Lomonosov Moscow State University, Moscow, Leninskie Gory d. 1, 119991, Russia*

We present novel effects for few-cycle pulses propagation and interaction in media with the dispersion management. The parametric processes, pulse compression and field differentiation are examined in the report.

Extremely short optical pulses, containing few electromagnetic field oscillations, find increasing application in nonlinear optics, medicine, spectroscopy and diagnostics of ultrafast processes and materials, laser physics (interaction of light with matter), telecommunication systems, and other fields [1]. Pulses containing only three to five field oscillations were experimentally obtained in the near-IR range using parametric generators [2]. Extremely short pulses are obtained using different methods of pulse compression with phase modulation in frequency-dispersive media (fibers, grids, etc.). In nonlinear media, the effect of self-compression is used for pulse compression [3]. Recently, compression of pulses with a spectral supercontinuum has been performed [4]. A significant compression was obtained at parametric amplification of chirp pulses [2, 5–7]. Hollow gas-filled photon fibers [8] have a very high dispersion, which is necessary for effective compression. The theory of picosecond pulse compression has been developed using the method of slowly varying amplitudes (SVA method) in the second-order approximation of the dispersion theory [2, 9]. However, this method is invalid for extremely short femtosecond pulses, because the spectral width of few-cycle pulses is comparable with the width of spectrum. Therefore, the propagation of extremely short pulses is described using either the SVA method with allowance for the higher order (third, fourth, etc.) dispersion [2] or the method of slowly varying profile (SVP method) of the pulse electric field. In this study, we used the SVP method to analyze the limiting compression of a few-cycle pulse with quadratic phase modulation. Complex numerical simulation of the equation for the optical wave electric field was performed with varying the phase-modulation index and the pulse width. More detailed equations are shown in [10].

A theory of compression of a few-cycle pulse with quadratic phase modulation has been developed within the SVP method. The equation for the electric field was numerically solved varying the phase modulation index, number of oscillations, and input pulse width. The optimal modulation index was found, at which a pulse can be compressed to one oscillation period. When the modulation index exceeds the optimal value, the width at the compression point increases. This study was supported by Grant NSh-671.2008.2 of the President of the Russian Federation for Support of Leading Scientific Schools and the Russian Foundation for Basic Research, project nos. 09-02-01028 and 08-02-00717.

References

1. J. Herrmann, B. Wilhelmi , *Laser für Ultrakurze Lichtimpulse*, Akademie, Berlin, 1984.
2. A. Baltuska, Z. Wei et al., "Optical pulse compression to 5 fs at a 1 MHz repetition rate", Opt. Lett, **22 (2)**, 102-104 (1997).
3. G. Agrawal, *Nonlinear Fiber Optics*, Academic, San Diego, 1995.
4. J. Dudley, S. Coen, *"Fundamental limits to few-cycle pulse generation from compression of supercontinuum spectra generated in photonic crystal fiber",* Opt. Express, **12(11),** 2423-2428 (2004).
5. P. Kinsler, G. H. C. New, *"Few-cycle pulse propagation",* Phys. Rev. A, **67**, 023813 (2003).
6. S. Witte, R. Zinkstok et al., *"Generation of few-cycle terawatt light pulses using optical parametric chirped pulse amplification"*, Opt. Express, **13(13)**, 4903-4908 (2005).
7. F Tavella, Y. Nomura et al, *"Dispersion management for a sub-10-fs, 10 TW optical parametric chirped-pulse amplifier",* Opt. Lett., **32(15)**, 2227-2229 (2007).
8. M. Nurhuda, A. Suda et al., *"Optimization of hollow fiber pulse compression using pressure gradients"*, Appl. Phys. B, **89**, 209-215 (2007).
9. A. Sukhorukov et al., *Theory of Waves*, Nauka, Moscow, 1990.
10. O. Paseka, V. Lobanov, A. Sukhorukov ,*"Compression Dynamics for Phase-Modulated Few-Cycle Pulses"*, Bulletin of the Russian Academy of Sciences, **72(12)**, 1628-1631 (2008).

High temperature effects at laser heating of ceramics in different ambient atmospheres.

Olga G. Tsarkova, Sergey V. Garnov
Oscillations Department, A.M. Prokhorov General Physics Institute of RAS, Moscow, Russia

Due to the unique resistance to high temperatures (thousands of degrees) and harsh environmental conditions, ceramics are widely used in modern technologies. The detailed studies of optical and thermal properties of ceramics are necessary for fundamental science as well as for optimization of technologies of laser processing of materials.

We describe here the complex optical method developed to study high temperature properties of solid states and some our results. The advantage of this method is the possibility to perform simultaneous measurements of true temperature, reflectivity, absorptivity, transmission, extinction, heat capacity, temperature conductivity, thermal conductivity of solids up to 2700 C [1, 2]. The obtained experimental results allow estimating values of heats of phase transitions of materials using a physical model of vacancies formations. The investigations of AlN, Si_3N_4, SiC, Al_2O_3 ceramics demonstrate noticeable influence of the ambient atmosphere (oxidizing – air, neutral – argon, vacuum – 10^{-3}atm) on the physical properties of these materials (the values of the optical and thermal characteristics, heat and temperature of the phase transitions, energy and concentration of the equilibrium vacancies and so on) at high temperature heating. In this connection a course of events occur as well as:

- a ceramic material degassing in vacuum;
- an evaporation of low temperature components of ceramics at laser heating;
- chemical reactions between components of the ceramics at the high temperatures in the neutral ambient atmosphere;
- an oxidation of studied ceramics in air at temperatures close to melting points transforming into combustion and stimulating structural and chemical modification of the material [2].

References

1. O.Tsarkova, S.Garnov, "Method of simultaneous measurements of optical and thermal properties of solids at high power laser heating up to 2700 C", *Processing of 6th International Seminar of Mathematical Models and Modeling in Laser-Plasma Processes (electronic version)*, Budva, Montenegro (May 30 – June 6, 2009).
2. O.Tsarkova, "Optical and thermal properties of metals, ceramics, and CVD diamond films upon high-temperature laser heating", *Physics of wave phenomena*, **15**, 1, 12-45 (2007).

Investigating Ultra-Intense Plasma-Based Soft X-ray Lasers

Philippe Zeitoun, Marta Fajardo, Pedro Velarde-Mayol, Frederic Burgy, Kevin Cassou, Julien Gauthier, Jean-Philippe Goddet, Guillaume Lambert, David Ros, Anna Barszczak Sardinha, Stéphane Sebban, Amar Tafzi

[2] *Instituto de Plasmas e Fusão Nuclear, Instituto Superior Técnico, Portugal*

[3] *Laboratoire d'Interaction du rayonnement X avec la Matière, CNRS/Université Paris Sud, France*

Main author email address: philippe.zeitoun@ensta.fr

For decades applications ranging from Biology, to Chemistry and Physics benefit from the availability of soft x-ray sources. So their short wavelength was interesting for nanometer imaging and fine material analysis thanks to the interaction of the photons with core electrons. With the completion of ultra-intense soft x-ray sources, based on both plasma or radiofrequency linac, a novel class of experiments emerged. These are taking full benefit of the outstanding intensities ($\geq 10^{16}$ Wcm^{-2}) achieved by focusing the beam down to 1 µm spot or smaller. Non-linear physics at short wavelength has been demonstrated. Such high intensity is achieved thanks to the unique combination of high number of photons per pulse (10^{10} to 10^{12}) and short pulse duration (picosecond to femtosecond), opening the path to single-shot imaging with femtosecond and nanometer resolution.

We will describe the theoretical, numerical and experimental developments we have undertaken with the aim to produce a *plasma-based* soft x-ray laser emitting pulses with duration around 100 femtosecond and containing 10^{12} photons. We demonstrated also the possibility to achieve fully coherent, diffraction limited beam.

Optimization of ultrashort pulsed laser radiation for precise and productive micromashining.

P. Pivovarov[1], S. Klimentov[1], V. Konov[1], D. Walter[2], M. Kraus[2], F. Dausinger[2]

[1] *Prokhorov General Physics Institute of the Russian Academy of Sciences*
Vavilov str.38, 119991 Moscow, Russia
tel. (499) 5038146, fax. (499) 234 9022, email: pablo@kapella.gpi.ru

Pfaffenwaldring 43, 70569 Stuttgart, Germany

Using of ultrashort laser pulses for micromashining is promising in terms of productivity enhancement and increased accuracy via minimization of melt and surface plasma effects. These advantage can only be noticeable in a definite range of radiation parameters, which calls for comprehensive optimization of incident beams and pulses by the pulse-width, wavelength, incident energy, focusing geometry etc. The optimization task is especially complex in the case of deep drilled channels, and the optimum found can typically be attributed only to a particular material. An explanation for that is a complex nature of ultrashort pulsed ablation implying variety of mechanisms sensitive to optical, electron and thermal properties of the medium gas, material of the target and the plasma created. In spite of diversity of materials to ablate, general trends can be derived for duration and wavelength of radiation. In many cases, using of short picosecond pulses and shorter wavelengths of radiation (harmonics) allows to avoid unwanted non-linear phenomena in ambient gases and plasma. Another significant advantage of optical harmonics is higher absorption in metals, higher plasma transparency, and elimination of long pedestal components in the incident pulse.

Significant attention in our work is paid to non-linear properties and ionization of the ambient gas at focusing of femtosecond and short picosecond pulses. The fundamental output and second harmonics of Ti:Sa and Yb:YAG laser (800 nm, 1030 nm, 400 nm and 515 nm) in combination with several gas environments were applied for direct comparison of scattered and absorbed energy, of the beam profiles and spectra with respect to the incident wavelengths and duration of laser pulses. In several cases, such combinations were shown to eliminate non-linear scattering in a broad range of incident energies (up to 300 J/cm2). Advantages of the visible pulses are illustrated in deep drilling experiments in metals. Theoretical estimations are made for explanation of the obtained optima.

Broadband optical illumination in a TD-OCT system for live imaging in developmental biology at 1300 nm wavelength

R.Cernat[12], G.Dobre[2], A.Bradu[2] and A.Gh.Podoleanu[2]

[1] *National Institute for Lasers, Plasma and Radiation Physics, Bucharest, Romania,*
ramona.cernat@inflpr.ro
[2] *School of Physical Sciences, University of Kent, Canterbury, UK*

The authors report the suitability of a comercially available broadband optical source (BBOS) to be used in a Time Domain Optical Coherence Tomography (TD-OCT) system at 1300 nm operating wavelength. OCT can perform high-resolution, cross-sectional tomographic imaging in materials and biological tissues by measuring the echo time delay and magnitude of back-reflected or backscattered light [1].

BBOS (Fianium SC 450, Fianium Ltd., Southampton, UK) covers a wide range of wavelength from 450 nm to 1700 nm and operates at a central wavelength of 1064 nm [2]. The entire spectrum of the BBOS was spectrally separated by using an optical filter unit containing a dichroic filter and a bandpass optical filter. Broadband input light with full at the half maximum (FWHM) of 268 nm value was obtained by selecting the appropriate waveband (1200–1500 nm) [3].

The TD-OCT arrangement was built around a two-coupler architecture in which object and reference beams were separated at a first fiber directional coupler, while the second directional coupler brought together object and reference light and allows balanced detection at its outputs. The photo-currents are further processed through rectification, envelope finding and grayscale encoding to provide the OCT signals.
The auto-correlation trace was measured in a zero-dispersion standalone Michelson interferometer in order to evaluate the axial resolution of the light source, which indicates a depth resolution value of ~ 3.4 □m (compared with the theoretical prediction of 3 □m). TD-OCT images from larval Drosophila Melanogaster were collected. Signal to noise ratio was experimentally measured for different values of the attenuation of the optical power in the reference arm and for the input optical power. Variation with wavelength of the cross-coupling coefficient of the second directional coupler was calculated in order to evaluate the noise cancelling effectiveness of balanced detection. BBOS has been used to obtain a depth resolution of 2 □m or better, high depth resolution which can make BBOS suitable for OCT imaging in cells culture and eye imaging.

References

1. Huang, D., E. A. Swanson, C. P. Lin, J. S. Schuman, W. G. Stinson, W. Chang, M. R. Hee, T. Flotte, K. Gregory, C. A. Puliafito, and J. G. Fujimoto," Optical coherence tomography", *Science*, **254**, 1178–1181 (1991a).
2. http://www.fianium.com
3. R. Cernat, G.M. Dobre, I. Trifanov, L. Neagu, A. Bradu, M. Hughes and A.Gh. Podoleanu, „Investigations of OCT imaging performance using a unique source providing several spectral wavebands", Coherence Domain Optical Methods and Optical Coherence Tomography in Biomedicine XII, edited by Joseph A. Izatt, James G. Fujimoto, Valery V. Tuchin, *Proc. of SPIE*, **6847**, 68470U (2008)

Nanostructured Thin Film Formation in Ultra-Short PLD of Vanadium Oxide

A. De Bonis[1], A. Galasso[1], A. Santagata[2], P. Villani[1], R. Teghil[1]

[1] *Dipartimento di Chimica, Università della Basilicata, Via N. Sauro, 85, 85100 Potenza/Italy*

E.mail: roberto.teghil@unibas.it

Vanadium oxide is an interesting material for its potential application in various areas such as sensors, catalysts and lithium ion batteries. New perspectives for these wide fields of uses can be however provided by further investigations on new deposition methods which can allow the formation of nanostructured thin film materials such as those induced by ultra-short Pulsed Laser Deposition. With this purpose, we have focused this work on the role played by nanoparticles forming the secondary plume produced during the ablation of V_2O_5 by a frequency doubled Nd:glass laser (250 fs pulse width) on the grown thin films. The nature of these nanoparticles, as well as their dynamics, compositional changes and their effects on films formation have been related to mass spectrometry, optical emission spectroscopy and fast imaging data. The results have been compared to those obtained for other molecular systems and metal alloys.

The films, deposited onto various substrate materials and over a wide temperature range, have been characterized using XRD, XPS, Micro-Raman, AFM, HR-TEM and SEM techniques. The experimental results obtained on the processes experienced by the nanoparticles evolution dynamics and the deposited thin film properties are compared and discussed.

Deposition of Iron and Chromium Oxide Films by Reactive Pulsed Laser Ablation for Photo Thermo Sensors

A.P.Caricato[1], A.Luches[1], M.Martino[1], S.A.Mulenko[2], N.T.Gorbachuk[3]
[1]*Department of Physics, University of Salento, 73100 Lecce, Italy*
[2]*Institute for metal Physics, NAS of Ukraine, 03142, Kiev-142, Ukraine,*
e-mail: mulenko@coriolan.kiev.ua
[3]*Kiev State University of Technology and Design, 03011, Kiev-11, Ukraine*

Films based on oxides of transitional metals have semiconducting properties that make them up-to- date materials for functional electronics. The reactive pulsed laser ablation (RPLA) allows the control of thickness and stoichiometry of deposits in order to obtain semiconductor structures with accurately tailored thickness and band gap. It is very important to study electrical, structural and optical properties of these semiconducting thin films, as sensing characteristics strongly depend on these properties.

We deposited iron oxide (Fe_2O_{3-X}; $0 \leq X \leq 1$)) and chromium oxide ($Cr_{3-X}O_3$; $0 \leq X \leq 2$) films on <100> Si substrate by RPLA using a KrF laser. The deposited nanometric thin films (thickness $\leq$ 80 nm) of iron and chromium oxides have large thermo electromotive force (e.m.f.) coefficient (S) and high photosensitivity. The S coefficient of iron oxide films varied in the range 0.8-1.65 mV/K in the temperature range 210-322 K. The maximum value of the S coefficient (1.65mV/K) was measured in the temperature range 270-290 K. The S coefficient value depends on the band gap (E_g) of semiconductor films: the largest value of this coefficient was measured for films with $E_g \cong$ 0.70 and 0.86 eV and the lowest one for films with $E_g \cong$ 0.43 and 0.93 eV. But the largest photosensitivity (F) of iron oxides films was about 44 V/W for white light at power density (I) of about $6x10^{-3}$ W/cm^2 for films with $E_g \cong$ 0.43 eV and the lowest value of F at the same I value was about 23 V/W for films with $E_g \cong$ 0.86 eV.

As regards chromium oxide films, S coefficient varied in the range 0.30-4.5 mV/K in the temperature range 210-333 K, with the maximum of 3.5-4.5 mV/K in the temperature range 270-290 K. Also in this case the S coefficient value depends on the band gap: the largest value of this coefficient was measured for films with $E_g \cong$ 0.40 and 0.71 eV and the lowest S coefficient was for films with $E_g \cong$ 0.32 and 0.38 eV. The largest photosensitivity of chromium oxide films was about 2.5 V/W at $I \cong 6x10^{-3}$ W/cm^2 for films with $E_g \cong$ 0.32 eV and $E_g \cong$ 0.71 eV and does not depend practically on E_g.

Our results show that RPLA can be used to synthesize iron and chromium oxide thin films with variable stoichiometry and, consequently, with different values of their band gap. The deposited films present large thermo e.m.f. coefficient and high photosensitivity.

Lasing properties of a new ytterbium-doped glass for miniature diode-pumped ultrashort pulse lasers

B.I.Denker[1], B.I.Galagan[1], I.N.Glushenko[1], V.E.Kisel[2], S.V.Kulchik[2], N.V.Kuleshov[2], S.E.Sverchkov[1]

1. A.M.Prokhorov General Physics Institute, Vavilova 38 Moscow Russia.

2. *Insitute forOptical Materials and Technologies, Belarussian National Technical University,*
65 Nezavisimosti Avenue, 220013 Minsk, Belarus ,Tel :+375 17 292 62 86,
e-mail : nkuleshov@bntu.by

It is known that the main drawbacks of phosphate-based laser glasses are their poor mechanical strength and thermal shock resistance that limits laser average power. Another one drawback is their poor resistance to air moisture.

The main structural component of phosphate glasses are PO_4 tetrahedrons having strong covalent bonds between the central ion and oxygen ions. But the glass properties are strongly determined by the bonds combining the tetrahedrons with each other. A well-known example of a thermal and mechanically stable glass is fused silica in which structure SiO_4 tetrahedron is connected with the 4 neighbor ones by bridge oxygen ions. These bonds form a strong 3D structure resulting in superb thermomechanical properties of fused silica. In case of phosphate glasses PO_4 tetrahedrons are bonded by bridge oxygen ions to no more than 2-3 other tetrahedrons and the physical properties of phosphate glasses are much poorer. Situation can be changed by addition of trivalent glass-forming ions (B^{3+}, Al^{3+}) that can also form strong tetrahedral complexes with oxygen. Alternating PO_4 and AlO_4 or BO_4 groups also form a strong 3D lattice with 4 bridge oxygen ions in each tetrahedron. Using these considerations we have found an alumino-boron-phosphate glass composition having air moisture stability, mechanical strength and thermal shock resistance close to silicate glasses. Nevertheless the absorption and emission cross-sections of Yb ions in it do not differ from the values typical for phosphate glasses.

It was found out that Yb ions luminescence in the glass exhibits unusually intensive quenching by OH groups. At technologically attainable dehydration level (at extinction level ~1.5 cm^{-1} @ 3.33 μm) Yb content should not exceed 10^{21} cm^{-3}. Laser quality glass having Yb content 5×10^{21} cm^{-3} was synthesized in ~250 ml platinum crucible using our original technology. Laser elements (5×5×2 mm plates) were fabricated from the glass. The elements were tested in free-run regime under longitudinal diode pumping. CW output of 783 mW has been obtained at 1054 nm (slope efficiency 28.9%). In preliminary ultrashort pulse laser experiments 150 fs pulses with peak power ~5kW were obtained. Further increase of output parameters requires modifications of the laser element geometry and its cooling conditions that are in progress now.

The work was supported by Russian and Byelorussian Foundations for Basic Research the joint project # F08R-180 – 08-02-90006-Bel.

Electric properties of heterogeneous transitions between n – and p - type ZnO films and n - and p - type silicon substrates

L.S. Parshina[1], O.A. Novodvorsky[1], V.Ya. Panchenko[1], O.D. Khramova[1], Ye.A. Cherebilo[1], A.A. Lotin[1], C.Wenzel[2], N. Trumpaicka[2], J.W. Bartha[2]
[1] *RAS, Institute on Laser and Information Technologies, Shatura, Russia*
[2] *TU Dresden, Institute of Semiconductor and Microsystems Technology, Dresden, Germany*

The growing demand for solid-state sources and receivers of light in the blue and UV regions has in recent years stimulated an intensive study of several kinds of wide-gap semiconductors. The main development efforts in this

The impressive advances have been made in the GaN based materials. GaN and its alloys have been used in production of light-emitting and laser diodes operating in the visible (460 nm) [1]. Nevertheless, effective radiation is attained at high concentration of indium in the InGaN structure, which enhances the absorption in the UV region and casts some doubt on GaN based materials application in producing UV light-emitting and laser diodes [2].

Zinc oxide is of great interest as an alternative to GaN based devices. Possessing high radiation and chemical resistance and thermal stability, ZnO is widely used in various devices, in particular, in fabrication of low-resistance contacts for solar cells. Owing to its unique optical, acoustic and electric properties, ZnO has found application in producing transparent electrodes for solar cells, gas sensors, varistors, and SAW generation devices [3]. Being transparent over a broad spectral region, zinc oxide shows high resistance to irradiation; it is prone to chemical etching and rather cheap which makes him attractive for microelectronic applications [4].

Zinc oxide has the greater exciton binding energy (60 meV), that is record for the solid-state binary semiconductors (for comparison the exciton binding energy in GaN - 25 meV, in ZnSe - 20 meV). The greater exciton binding energy of ZnO and its alloys is especially attractive to creation of the radiating devices and photodetectors of the UV region on the ZnO basis. The decision of ZnO with Si integration problems causes also particular interest, that can open the real overlapping opportunities of the unique functional abilities of these materials at the creation of the photoconverters on the silicon substrates. Heterostructures created at the deposition on the semiconductor substrate of the material layer with the greater bandgap width, are usually characterized by the higher photosensivity because of so-called "window effect" [5]. If the heterolayer was created by the chemical- and radiation-resistant substance, that is characteristic for ZnO, the photosensitive structure will not demand of creation on the surface of the additional protective coating. Thus the cheap ZnO/Si heterostructures should have the comparable and even surpassing characteristics of the existent photodetectors.

The goal of the present work was the creation ZnO/Si heterostructures and the investigation of the electric properties anisotype and isotype heterojunctions received by the ZnO layers creation on silicon substrates. The epitaxial ZnO films doped by gallium, nitrogen, phosphorus were deposited by the pulse laser deposition method on monocrystal n- and □- type Si (001) substrates. The volt-ampere characteristics of n-ZnO/p-Si-, n-ZnO/n-Si-, □-ZnO/p-Si- and □-ZnO/n-Si- heterojunctions were obtained. It was established, that in case of the isotype heterojunction it was possible to receive both the ohmic contact and the rectifying contact by changing of the contacting materials conductivity. For the anisotype heterojunctions in all cases considered us the rectifying contacts were observed only.

References

1. T.Mukai, D.Morita, S.Nakamura, **"**High-Power UV InGaN/AlGaN Double-Heterostructure Leds", *J.Crist. Growth,* **189**, 778 (1998).
2. H.Tampo, A.Yamada, P.Fons, H.Shibata et al., "Degenerate layers in epitaxial ZnO films grown on sapphire substrates", *Appl.Phys. Lett.*, **84**, 4412 (2004).
3. Y.Chen, D. Bagnall, T.Yao, "ZnO as a novel photonic material for the UV region", *Mater.Sci.Eng.,B* **75**,190 (2000).
4. D.C.Look, D.C.Reynolds, C.W.Litton et al. "Characterization of homoepitaxial *p*-type ZnO grown by molecular beam epitaxy" *Appl. Phys. Lett.*, **81**, 1830 (2002).
5. A.Milns, D.Foiht, *Heterojunctions and metal- semiconductor junctions*, World, Moscow, 1975.

Direct Laser Materials Nanostructuring in Absence of Melting

S.V. Nebogatkin[1], V.Yu. Khomich[1], V.A. Shmakov[2], V.N. Tokarev[2], V.A. Yamshchikov[1]

1- Institute for Electrophysics and Electric Power, Russian Academy of Sciences, 18, Dvortsovaya nab., Sankt-Peterburg, 191186, Russia
2- A.M. Prokhorov General Physics Institute, Russian Academy of Sciences, 38 Vavilov st., Moscow, 119991, Russia
snebogatkin@gmail.com

In the given paper a so-called "direct" laser nanostructuring is considered, when surface profile is modified by only one laser beam. As a result of performed theoretical studies [1] we found out that two types of nanostructures can be obtained in this case:

(1) A development of laser-induced surface instability in a form of wavy disturbances having characteristic periods $d < L_T$, where $L_T = 2(\chi\tau)^{1/2}$ is heat diffusion length for pulse duration τ. For action of nanosecond laser pulses ($\tau = 20$ ns) L_T becomes less than 1 μm and hence a formation of submicrometer reliefs is possible, if a material on a high-temperature stage of heating has a low thermal diffusivity: $\chi < 0.1$ cm^2/s. For example, for graphite, diamond films and ceramics, which have χ of the order of 10^{-2} cm^2/s, L_T is around 300 nm. For a number of polymers having χ of the order of 10^{-3} cm^2/s L_T is around 100 nm.

(2) Profile in the form of an array of cones having characteristic sizes along the material surface $d > L_T$. We have shown that for obtaining cones of minimal sizes both a short laser wavelength λ and a small heat diffusion length are important. Under nanosecond irradiation such situation is possible when ultraviolet lasers (λ = 157 and 193 nm) and materials having on high-temperature stage thermal diffusivity χ of the order of (1-3)×10^{-2} cm^2/s and less are used. Such materials are graphite and diamond films and also a number of ceramics and polymers. Obtained theoretical conclusions agree well with our experimental data on F_2 laser (λ = 157 nm) irradiation of diamond films, where cones with unusually small sizes d = 200-600 nm have been observed [2].

References

[1]. V.N. Tokarev, V.Yu. Khomich, V.A. Shmakov, V.A. Yamshchikov, Possibility of direct laser surface nanostructuring in absence of material melting, Physics and Chemistry of Materials Processing, No. 4, pp. 18-25 (2008) – in Russian.
[2]. K.E. Lapshin, A.Z. Obidin, V.N. Tokarev, V.Yu. Khomich, V.A. Shmakov, V.A. Yamshchikov, Direct laser surface nanostructuring of diamond film and silicon nitride by nanosecond pulses of F_2 laser radiation, Russian Nanotechnologies, vol. 2, No. 11, 12, pp. 50-57 (2007) – in Russian.

An Ultrafast Single-Photon Image Diagnostics Sensor with SPAD Arrays for Industrial and Bio-applications

Edoardo Charbon [1] and Silvano Donati[2],

[1] *Department of Electronics, University of Delft, Delft/The Netherlands*
[2] *Department of Electronics, University of Pavia, Pavia/Italy*

After a review of Single-Photon Detectors performances, (mainly PMTs versus APDs and SPADs), we present a new image sensor capable of performing photon counting and time-of-arrival single-photon analysis. The sensor comprises 32x32 pixels and each pixel consists of a single-photon avalanche photo-diode, a counter, and a chronometer. Each pixel operates independently and simultaneously, generating one time-interval measurement every 2 ms with a time resolution of 100 ps. The photosensitive area has a diameter of 6 mm, whereas the pixel size, allocating the electronics circuits for the time measurement, is 50 mm. To recover the loss due to the area fill-factor, we employ an array of plano-convex microlenses, one for each pixel, of 50-mm diameter. The microlens array boosts the power density by a factor ≈30, thus recovering almost completely the loss of efficiency due to the area-ratio $(50/8)^2$ =39. The sensor has been fully characterized and tested in a number of bio-setups.

References

1 S.Donati, *Photodetectors*, Prentice Hall, Upper Saddle River (NJ), 2000.

2 E. Charbon, "Will CMOS Imagers Ever Need Ultra-High Speed?" IEEE Intern. Conf. on Solid- State and Integrated-Circuit Techn., pp.1975-1980, Oct. 2004

3 S.Donati, G.Martini, M.Norgia: "Microconcentrators to recover fill-factor in image photo-detectors with pixel on-board processing circuits", *Optics Express*,**15**, 18066-18074 (2007)

Self-Mixing Interferometry

Silvano Donati

Department of Electronics, University of Pavia,Pavia/Italy

When a laser undergoes self-injection at weak level, amplitude and frequency modulation are generated, driven by external optical path length[1]. We will describe the developments of a displacement-measuring instrument, first by using the up/down counting of mode hops to resolve displacements[2] in steps of l/2=400 nm up to 1-2 m, then extending the principle of measurement to the case of a diffuse target, reflecting back a field affected by the

speckle-pattern statistics whose phase error and amplitude fading are corrected by a new technique of bright-speckle-tacking (BST) [3].

Then we will describe a two-channel (or, referenced) vibrometer, based on analogue processing of the self-mix signal, in which the speckle-related amplitude errors are removed thanks to a servo-loop concept, and the instrument is capable of true differential operation, on diffuse surface. A survey of applications to physical[4] and kinematic measurands[5] will conclude the talk.

References

1. S. Donati, *Electro-Optical Instrumentation* Prentice Hall, Upper Saddle River, NJ, 2004
2. M. Norgia, G.Giuliani, S.Donati: "Absolute Distance Measurement With Improved Accuracy Using Laser Diode Self-Mixing Interferometry in a Closed Loop", *IEEE Trans Instrum & Measur.*,**56**, 1894-1900 (2007).
3. E. Randone,, S.Donati: "Self-mixing Interferometer: Analysis of the Output Signals" *Optics Express*, **14**, 9788-9796 (2006).
4. Y.Yu, G. Giuliani, S.Donati: "Measurement of the Linewidth Enhancement Factor of Semiconductor Lasers based on the Optical Feedback Self-Mixing Effect" *IEEE Photonic Techn. Lett.*, **14**, 900-902, (2004).
5. S. Donati, G. Giuliani, S.Merlo: "Laser Diode Feedback Interferometer for Measurement of Displacement without Ambiguity", *IEEE Journal of Quantum Electronics*, **31**, 113-119 (1995).

Photovoltaic Spectra of Tlmse2 Single Crystals

Solmaz Mustafaeva

solmust@gmail.com

TlMSe2 single crystals (M=In, Ga) are semiconductors with chain and layer structure and characterized by high sensitivity to electromagnetic radiation in infrared and visible spectral range. These low-dimensional single

Electrically active intercalant ions impart radically new properties to the single crystals of the above compounds and favour the display of new and unusual physical phenomena in them. Here, we restrict ourselves to a report on the experimental results of the influence of lithium intercalation on photovoltaic spectra of chain TlInSe2 and layer TlGaSe2 single crystals. Lithium ions were chosen as the intercalant provided effective intercalation without destroying the crystals, owing to their rather small ionic radius. Intercalation was carried out by the method of a pulling electric field applied along the chain TlInSe2 and layer TlGaSe2 single crystals. The degree of intercalation jt (j is the current density, and t is the intercalation time) ranged from 6 to 20 C/cm2. The photovoltaic spectral characteristics of p-TlInSe2 single crystals undergo substantial variations as a result of their intercalation with lithium ions. In the short-wave region of the spectrum a maximum photosensitivity accompanied by the appearance of a series of new structures (1.27; 1.45; 1.60 and 1.85 eV) is observed in the spectral characteristics as a direct consequence of intercalation. After intercalation the photovoltaic signal in TlInSe2 single crystals increases by approximately one order of magnitude. In layer TlGaSe2 single crystals after intercalation the inner e.m.f. was created. The value of this e.m.f. was equal to 270 mV at darkness. Inner e.m.f. was sensitive to light and its maximum value was observed at energy of photons equal to 2.0 eV. The cause of the variations observed in photovoltaic processes in likely to lie in the partial removal of degeneracy in the course of intercalation, due to the elimination of the overlap of the wave functions of the carriers of neighboring chains (layers). The operation by the photovoltaic characteristics of the studied ternary single crystals due to intercalation gives perspective for the use of these objects as various transducers and detectors.

High Power CW and Pulsed Fiber Lasers with China-made Yb-doped LMA fiber at SIOM

Qihong Lou, Jun Zhou, Bin He and Songtao Du

Shanghai Institute of Optics and fine Mechanics, Shanghai Key Laboratory of All solid-state Laser and Applied Techniques Shanghai 201800, China

email address: qhlou@mail.shcnc.ac.cn

Fiber lasers hold great promise for a wide range of applications because fiber lasers have high efficiency and exceptional beam quality. Fiber lasers up to kW output power are now on high technological level, fiber laser systems for industrial applications are now on the market. The development of these lasers is not only in the cw and long pulsed mode operation but also in the short ps pulse mode operation.

In this paper, we report the development of fiber lasers and amplifiers in Shanghai Institute of Optics and fine Mechanics, It includes kW level CW fiber lasers, Q-switched pulsed fiber laser, and 156W average power, high repetition rate, nanosecond pulse from a LMA fiber amplifier.

A highly efficient Ytterbium-doped double-clad fiber laser, two-end pumped by 975 nm diode stack sources and generating up to 1758 W of continuous-wave (CW) output power at 1.1μm is reported. The slop efficiency is about 76% with respect to the launch pump power. A master-oscillator fiber power amplifier (MOPA) system with a 4.5-m-long Yb3+-doped China-made large mode area (LMA) double-clad fiber is reported. The system emits up to 156 W of amplified radiation with pulse duration of 24ns at a wavelength of 1064 nm and a repetition rate of 50 kHz.

References

1. J. Limpert, S. Hofer, A. Liem, et al., Appl Phys B, 75,(2002) 477
2. L. Kong, Q. Lou, J. Zhou, et al., Opt Eng., 45, (2006) 010502.
3. [4] S. Du, J. Zhou, Fangpei Zhang, et al., Microwave and Optical Technology Letters, 50,(2008)2546

Ultrafast Low-Noise High-Power Fiber Lasers: Applications from Material Processing to Next-Generation Accelerators

F. Ömer Ilday
Bilkent University, Ankara, TURKEY
ilday@bilkent.edu.tr

Fiber lasers are attracting intense worldwide attention in recent years due to their practical features, including high average power, low cost, ease of use, compact size and robustness. CW and nanosecond fiber lasers have already taken over a significant portion of the industrial laser-material processing market from Nd:YAG and CO2 lasers. Similarly, among mode-locked lasers delivering picoseconds and femtosecond pulses, fiber lasers are getting more established, particularly in applications such as ultrashort pulsed material processing, generation of THz pulses, optical frequency metrology, which demand uninterrupted operation over long periods of time. In recent years, niche applications of mode-locked fiber lasers to FEL-type accelerators, namely optical synchronization and electron beam diagnostics are being developed owing to the high stability and low noise of fiber lasers. This talk will begin with a brief review of the state of the art of fiber lasers and the physics underlying their operation, including a new mode-locking regime, soliton-similariton regime that we have

University: processing of biomedical materials, sub-cellular surgery, pulsed laser deposition as well as frequency metrology techniques applied to next-generation accelerators.

Laser-Assisted Fabrication of Silicon Nanocrystals in Liquids

Stanislav V. Zabotnov[1,2], Pavel A. Perminov[2], Alexander A. Ezhov[1], Irina O. Dzhun[1], Leonid A. Golovan[1], and Pavel K. Kashkarov[1,2]

[1] *Physics Department, M.V. Lomonosov Moscow State University, Moscow, Russia*

[2] *Russian Research Center "Kurchatov Institute", Moscow, Russia*

The laser-assisted nanoparticle formation by means of the ablation at a laser pulse action on solid state targets placed into different liquids stimulates the rising interest of researchers during last five years [1, 2]. This method has a set of advantages in comparison with the traditional laser nanofabrication at the laser ablation in gases: the nanoparticles are chemically pure, have the smaller size and spatial dispersion [3, 4].

In our work we studied the formation of the silicon nanocrystals at the laser ablation of monocrystaline silicon targets in such liquids as the water, glycerol and liquid nitrogen. We used a picosecond Nd:YAG and a femtosecond Cr:forsterite lasers as the pulse sources.

We studied the formed nanoparticles by the atomic-force microscopy. The nanoparticles have the spherical shape. The peak size (from 7 to 20 nm) and spatial dispersion depend on the buffer liquid (see Fig. 1). The Raman spectroscopy revealed the crystalline phase of the formed nanostructures.

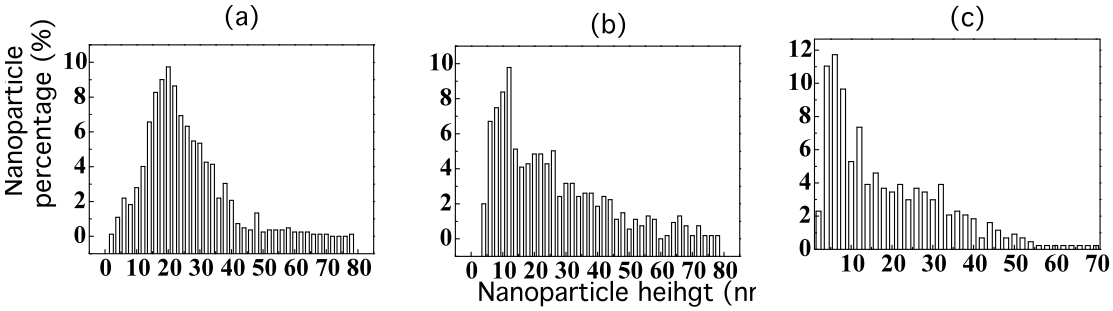

Fig. 1. The size distribution histograms of the silicon nanocrystals formed via laser ablation in the distilled water (a), the glycerol at 50 ºC (b) and the liquid nitrogen (c).

We suppose that the ablated silicon atoms decelerate because of collisions with molecules of the liquid and agglomerate into the nanocrystals.

Thus, we have shown a possibility to form the silicon nanocrystals of the desirable size and spatial dispersion via the laser ablation in the proper buffer liquid.

References

1. P.V. Kazakevich, A.V. Simakin, G.A. Shafeev, et al., "Laser-assisted shape selective fragmentation of nanoparticles", *Appl. Surf. Sci.*, **253**, 7831-7834 (2007).
2. R.A. Ganeev, M. Baba, A.I. Ryasnyansky, et al., "Laser ablation of GaAs in liquids: Structural, optical, and nonlinear optical characteristics of colloidal solutions", *Appl. Phys. B*, **80**, 595-601 (2005).
3. S. Besner, A.V. Kabashin, F.M. Winnik, and M. Meunier, "Ultrafast laser based "green" synthesis of non-toxic nanoparticles in aqueous solutions", *Appl. Phys. A*, **93**, 955-959 (2008).
4. A. V. Kabashin, and M. Meunier, "Femtosecond laser ablation in aqueous solutions: A novel method to synthesize non-toxic metal colloids with controllable size", *J. Phys.*, **59**, 354-359 (2007).

Development of Laser-Based Metrology Methods for Extreme Light Infrastructure Project

Czitrovszky, A.
Research Institute for Solid State Physics and Optics
Hungarian Academy of Sciences
Budapest 1525, P. O. Box 49, Hungary
czi@szfki.hu

One of the main aims of Extreme Light Infrastructure (ELI) international research project is the development and construction of a high intensity laser system, generating extremely high power (> 200 PW) short pulses. This will be the first facility dedicated to laser-matter interaction in the ultra-relativistic regime, providing

accelerators delivering > 100GeVparticles and photon sources. This facility will have a large benefit in medicine with new radiography and hadron therapy method, in material science with the possibility to unravel and slow down the ageing process in a nuclear reactor and in environment by offering new ways to treat nuclear waste. The scientific impact of such facility in relativistic quantum physics, high energy physics, nonlinear QED, attosecond laser science, etc., can be also considerable.
For design and construction of such laser system consisting of ~ 10 synchronized lasers, development and implementation of different optical measuring methods are needed.
In the presentation we will emphasise on two types of laser interferometry

- one - to measure the surface quality of the optical parts having big aperture (substrates and layers) with high resolution (<1nm),
- and second – Michelson-type - to study the mechanical stability and vibrations of the main optical parts of the system.

In the frame of this project we developed also a new measuring instrument for determination of the contamination sources in certain parts of the facility. This instrument can be applied for air quality testing in different other branches.
The utilization of the developed laser-based measuring methods and instruments and their fitting to the requirements of the ELI facility will be described.

Tunable Infrared Liquid Crystalline Filters

T.D.Ibragimov[1], N.J.Ismailov[1] , G.M.Bayramov[2], A.R.Imamaliyev[2]

[1] *Institute of Physics of Azerbaijan National Academy of Sciences, AZ1143 Baku, Azerbaijan*

[2] *Baku State University, AZ1148 Baku, Azerbaijan*

It is known that optical properties of small particles depend on the surrounding medium. In particular, at the sizes of particles comparable with a wavelength of incident light and certain conditions, the system passes radiation only in a narrow range of wavelengths (Christiansen effect). On the other hand, optical and dielectric properties of a liquid crystal (LC) along light propagation are easy for changing by means of the applied electric field (Frederickzs effect). In the present work the possibility of a combination of the indicated effects for operation of a position of transmission band maximum for infra-red radiation has been investigated.

The cell consists of two plane-parallel conductive germanium substrates of p-type which is transparent in the mid-infrared region. The aluminum oxide particles are precipitated on one of plates. The liquid crystal is located between substrates.

The two-frequency liquid crystal on the base of 4-n-pentyl-4□-cyanobiphenyl (5CB), 4-hexyloxyphenyl ester 4□-hexyloxy-3-nitrobenzoic acid (C2) and 4-n-pentanoyloxy-benzoic acid-4□-hexyloxyphenyl ester (H 22) which has nematic phase in the range of temperatures 11-65ºC with positive anisotropy of dielectric permeability at low frequencies and negative one at the high frequencies has been developed. The basic operated characteristics of the obtained mixture were defined.

Investigation of transmission spectra of pure liquid crystal 4-methoxybenzilidene - 4' – butylaniline (MBBA) and developed two-frequency liquid crystal has been shown that they are practically transparent up to 1650 cm^{-1} at small thicknesses except for a set of bands of 2850 -3050 □□$^{-1}$ corresponding to vibrations of CH, CH_2, and CH_3 groups. Extinction spectra of the small aluminum oxide particles-MBBA system reveal the transmission band with a maximum of 1896 cm^{-1} at room temperature, which starts to shift to short-wave part of spectra at application of direct electric field of 4 V to the system. Extinction spectra of the small aluminum oxide particles-the mixture 5CB-C2-H22 also show the transmission band with a maximum at one wavelength at application of alternative electric field of 1 kHz and another one at alternative electric field of 1000 kHz. The temperature dependences of transmission band position were studied in both systems.

The experimental results are explained by reorientation of LC molecules at application of electric field and passing of light through the system only at equality of effective refractive indices of particle and LC substances. Observed effects can be the base for creation of tunable infrared filters.

The work has been supported by Scientific and Technology Center in Ukraine (grant No 4172).

Effect of CO_2 Laser Focusing on Groove Cutting into Steel Surfaces

S. Bıyıklı[1], J. Yılmazkaya Süngü[2]

[1] *Mechanical Engineering Department, Okan University, Istanbul, Turkey*
[2] *Faculty of Arts and Science, Department of Physics, Kocaeli University, Kocaeli, Turkey*

Effect of lens focusing on evaporative laser groove cutting on thick steels with a moving continuous wave (CW) laser is described by solving a heat transfer model. A three dimensional heat transfer model which was developed by Bıyıklı and Modest [1] for non-dimensional parameters with a number of assumptions such as negligible convective losses, no multiple reflections within the groove, and negligible beam channeling is modified for this study. The thermal properties of carbon steel which are available in the literature [2, 3] are used in this model to study the focusing effects on the kerf geometry for a given scanning speed and laser power. Evaporative removal of steel is achieved by heating the steel surface with a high power CO_2 laser. The laser beam is highly-concentrated Gaussian Continuous-Wave at TEM_{00} mode and it is focused by a lens through which the laser beam passes and behind which it converges to a minimum beam waist and subsequently expands. The resulting non-linear partial differential equations were solved numerically by an explicit-implicit method. The results of this model are used to investigate the effect of lens focusing on the groove depth, thickness, and shape for some typical laser parameters such as the lens focal length (19cm) , laser power (9600 W), and scanning speed (8.5 cm/s). It is observed that when the lens is focused slightly inside the surface, as shown in Figure 1, groove depth reaches a maximum value and then starts decreasing.

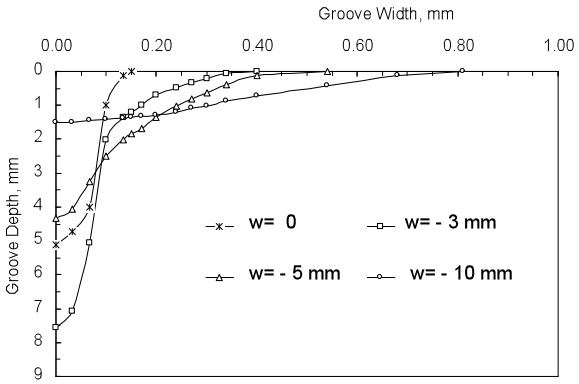

Figure 1 Effect of focal positions on the groove cross-section when focal point is in the steel, w shows the distances between the focal point of the lens and top surface of the steel.

References

1. S. Bıyıklı and M.F. Modest, "Beam Expansion and Focusing Effects on Evaporative Laser Cutting", Journal of Heat Transfer, 110, 529-532 (1988).
2. M. J. Hsu, P. A. Mollian," Thermochemical modelling in $C0_2$ laser cutting of carbon steel" Journal of Materials Science, 29, 5607-5611(1994).
3. B.S. Yilbas, S.B. Mansoor, R. Mansoor, "Laser pulse heating: Cavity formation into steel, nickel and tantalum surfaces" , Optics & Laser Technology, 40, 723–734 (2008).

Spectral Domain Optical Coherence Tomography Imaging of the Posterior Human Eye

Tapio Fabritius[1], Shuichi Makita[2], Risto Myllylä[1] and Yoshiaki Yasuno[2]
[1] *Optoelectronics and Measurement Techniques Laboratory, University of Oulu, Oulu, Finland*
[2] *Computational Optics Group, University of Tsukuba, Tsukuba, Japan*

Spectral domain Optical coherence tomography (SD-OCT) with 1.04 µm central wavelength for investigating a posterior human eye is presented. That approach enables the high-contrast and high resolution imaging (7.4 µm axial) of the posterior part of eye. The imaging depth (4.2 mm) was extended by using a full-range imaging

automatic and iterative retinal layer segmentation method, internal limiting membrane (ILM) and retinal pigment epithelium (RPE) can be identified [2]. Layer segmentation method is based on intensity variation of measured OCT signal. Healthy volunteer's eye and patients' eye with disease were measured and the obtained data were processed to evaluate presented method. The required measurement time for 5x5x4.2 mm^3 volume (1024x138x380 pixels) was 3.7 seconds and the total calculation time of ILM and RPE segmentation was 37 seconds. Results suggest that presented method is an effective tool for quantitative characterization of posterior human eye. In clinics, the obtained information can be used to diagnose many common eye diseases but it can be used also for treatment response evaluation.

References

1. S. Makita, T. Fabritius and Y. Yasuno, "Full-range, high-speed, high-resolution 1-μm spectral domain optical coherence tomography using BM-scan for volumetric imaging of the human posterior eye", *Optics Express*, **16**, 8406-8420 (2008).
2. T. Fabritius, S. Makita, R. Myllylä and Y. Yasuno, "Automated segmentation of the macula by optical coherence tomography", *Optics Express*, **17**, 15659-15669 (2009).

Point Spread Function of Array Transducers in 2D Optoacoustic Tomography

Tatiana D. Khokhlova[1], Ivan M. Pelivanov[2], Varvara A. Simonova[2]and Alexander A. Karabutov[2]

[1] *Applied Physics Laboratory, University of Washington, Seattle, WA, USA*
[2] *International Laser Center, Moscow State University, Moscow, Russia*

Optoacoustic (OA) tomography is a hybrid, laser-ultrasonic method for diagnostics of biological tissues. Ultrasound pulses, resluting from absorption of a laser pulse in tissue and its transient thermal expansion, contain the information on the distribution of laser-induced heat release and, therefore, the distribution of absorbing inhomogeneities. If these signals are detected by a transducer array, 2D or 3D distribution of heat release can be

reconstructed. 3D tomography is less widespread than 2D due to the complexity of transducer fabrication, therefore, in this work we only address the design of array transducers for 2D OA tomography.

One of the major characteristics of an array transducer is the spatial resolution it provides. This characteristic is primarily determined by the array design and can be inferred from the point spread function of the array, namely, the reconstructed 2D image of a point OA source. The relation between the resolution and the array dimensions (aperture, element width, element spacing) can not be determined analytically in 2D OA tomography, because, unlike 3D OA tomography, there is no rigorous solution to the inverse problem. Thus, the goal of this study was to find an empirical relation between image resolution and array dimensions using numerical simulations of direct and inverse problems of OA tomography.

First, the calculation of the output signals of the array elements detecting the OA pulse from an arbitrarily located point source, was performed using the approach described in [1]. Two array designs were considered: the elements were located either along a straight line (planar transducer) or along a curve (focused transducer). Each element was considered to have a limited frequency band Δf and to be shaped as a curved stripe (Fig.1). The number of elements N, their width b, the array aperture angle θ, were the variable parameters. For image reconstruction we employed the backprojection algorithm that is based on the time reversal concept: the detected signal, reversed in time, is reradiated back from each detector. The resulting acoustic field at zero time corresponds to the initial distribution of heat release. Longitudinal and lateral sizes of the obtained image, determined at ½ brightness level, corresponded to the in-depth Δx and transverse Δz spatial resolution, correspondingly.

According to the results of the simulations, Δz does not depend on the number of elements if $N > 4$. The relation between Δz and b is linear for the element widths that can be achieved technologically. The dependence $\Delta z(\theta)$ is close to the relation reported earlier [2] between the transverse size of the focal area of a single focused array element and its focusing angle.

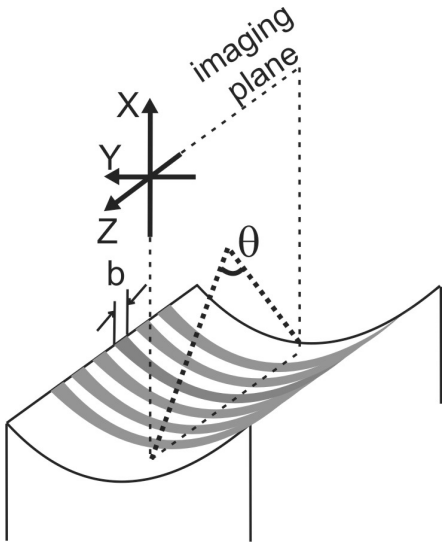

Fig. 1. The design of the array transducer used in the simulations.

High power femtosecond thin disk lasers

Thomas Südmeyer[1], C. R. E. Baer[1], C. Kränkel[1], Oliver H. Heckl[1], C.J. Saraceno[1], Matthias Golling[1], Rigo Peters[2], Klaus Petermann[2], Günter Huber[2], and Ursula Keller[1]
[1] *Department of Physics, Institute of Quantum Electronics, Zurich, Switzerland*
[2] *Institute of Laser-Physics, University of Hamburg, Hamburg, Germany*
südmeyer@phys.ethz.ch

The thin disk laser concept [1] avoids thermal problems occurring in conventional high power rod or slab lasers and enables high power TEM_{00} operation with broadband gain materials. Since its first demonstration in the year 2000, passively modelocked thin disk lasers [2] achieved higher pulse energies [3, 4] and average power levels

[5, 6] than any other modelocked oscillators. Stable and self-starting passive pulse formation is achieved with SESAMs. The key components of ultrafast thin disk lasers are used in reflection, which is an advantage for the generation of ultrashort pulses with excellent temporal, spectral and spatial properties, because the pulses are not affected by excessive nonlinearities inside the oscillator. Output powers close to 100 watts and pulse energies above 10 µJ are directly obtained without any additional amplification, which make these lasers interesting for a growing number of industrial and scientific applications such as material processing or driving experiments in high field science [7]. In this presentation, we review the development of ultrafast thin disk lasers with high average power levels. After a brief introduction to the modelocked thin disk laser technology, we discuss the power and pulse energy scaling limits of ultrafast thin disk lasers. Ultrafast thin disk lasers are based on a power-scalable concept, and average power levels of several hundred watts appear feasible by equally increasing pump power and the mode area on the disk and on the SESAM. The key challenges for further pulse energy increase are: 1. Generating sufficient average output power in fundamental transverse mode; 2. Achieving a balance between SPM and negative GDD for soliton modelocking with high pulse energies; 3. Optimizing the SESAM parameters for operation with high pulse energies. Already at the current state of technology, these challenges can be overcome and it appears feasible to increase the pulse energy into the 100-µJ regime. Furthermore, we discuss the minimum achievable pulse duration. So far, both the highest power levels and pulse energies are currently only achieved with Yb:YAG as gain material, whose restricted gain bandwidth limits the pulse duration to approximately 700 fs in efficient thin disk operation. The initial choice of Yb:YAG was not influenced by its suitability to support the generation of femtosecond pulses, but for its easy growth, high cross-sections, relaxed demands on the pump diodes, and thermo-mechanical strength to sustain high power levels. Other Yb-doped gain materials exhibit larger gain bandwidth, and it is important to evaluate their suitability for power scaling. We discuss the demands on the gain materials and compare different Yb-doped host materials. The recently developed sesquioxide materials are particularly promising [8], enabling the highest optical-to-optical efficiency (43%) [9] and shortest pulse duration (227 fs, [10]) of any modelocked thin disk laser.

References

[1] A. Giesen, et al., "Scalable Concept for Diode-Pumped High-Power Solid-State Lasers," Appl. Phys. B **58**, 365-372 (1994).
[2] J. Aus der Au, et al., "16.2 W average power from a diode-pumped femtosecond Yb:YAG thin disk laser," Opt. Lett. **25**, 859-861 (2000).
[3] S. V. Marchese, et al., "Femtosecond thin disk laser oscillator with pulse energy beyond the 10-microjoule level," Opt. Express **16**, 6397-6407 (2008).
[4] J. Neuhaus, et al., "Subpicosecond thin-disk laser oscillator with pulse energies of up to 25.9 microjoules by use of an active multipass geometry," Opt. Express **16**, 20530-20539 (2008).
[5] F. Brunner, et al., "Powerful red-green-blue laser source pumped with a mode-locked thin disk laser," Opt. Lett. **29**, 1921-1923 (2004).
[6] E. Innerhofer, et al., "60 W average power in 810-fs pulses from a thin-disk Yb:YAG laser," Opt. Lett. **28**, 367-369 (2003).
[7] T. Südmeyer, et al., "Femtosecond laser oscillators for high-field science," Nature Photonics **2**, 599-604 (2008).
[8] R. Peters, et al., "Broadly tunable high-power Yb:Lu_2O_3 thin disk laser with 80% slope efficiency," Opt. Express **15**, 7075-7082 (2007).
[9] S. V. Marchese, et al., "Efficient femtosecond high power Yb:Lu_2O_3 thin disk laser," Opt. Express **15**, 16966-16971 (2007).
[10] C. R. E. Baer, et al., "227-fs Pulses from a Mode-Locked Yb:$LuScO_3$ Thin Disk Laser," submitted to Opt. Express (2009).

$GaS_{0.4}Se_{0.6}$: relevant properties and potential for 1064 nm pumped mid-IR OPOs and OPGs operating above 5 µm

Valentin Petrov, Vladimir L. Panyutin, Aleksey Tyazhev, Georgi Marchev, Alexander I. Zagumennyi,* Fabian Rotermund, and Frank Noack
Max-Born-Institute for Nonlinear Optics and Ultrafast Spectroscopy, 2A Max-Born-Str., D-12489 Berlin, Germany,
**General Physics Institute of the Russian Academy of Sciences, 38 Vavilov Str., 117942 Moscow, Russia*
Phone: +49-30-63921272, Fax: +49-30-63921289, E-mail: petrov@mbi-berlin.de

The nonlinear optical properties of mixed GaS_xSe_{1-x} crystals with x=0.2 and 0.4 were studied as early as 1982 [1]. Relative SHG measurements gave d_{22}(x=0.2)=0.525 d_{22}(GaSe) and d_{22}(x=0.4)= 0.31 d_{22}(GaSe) for the nonlinear coefficients. Two essential advantages can be expected from adding S to the well known nonlinear crystal GaSe: increase of the band-gap value or the short wave cut-off limit (which is not the case using In as a dopant) and improved hardness which is one of the basic limitations of GaSe.

For our studies, GaS_xSe_{1-x} crystals were grown by the Bridgman-Stockbarger method in quartz ampoules with a diameter of 14 mm for compositions x = 0.0, 0.05, 0.10, 0.40 in the charge. The whole growth process took 20-25 days and uniform single crystals up to 60 mm in length were obtained. Interestingly, for the composition with x=0.4 the crystals grow without any "cap" at the top of the boule. This means that the charge and crystal compositions are identical, which is normally not the case even for pure GaSe. This observation could possibly mean congruent melting character which is equivalent to the existence of a separate compound in the system of solid solutions.

Characteristic unpolarized spectra corresponding to the o-wave were measured using thin (50-600 μm) cleaved plates and the direct band-gap was obtained from the linear fit to the $(\alpha hv)^2$ dependence on hv. The band-gap increases from 1.976 eV (628 nm) to 2.304 eV (538 nm) from x=0 to x=0.4. The nonlinear coefficient of the mixed compounds was re-measured by comparing the SHG conversion efficiency to that of pure GaSe. A $KNbO_3$ femtosecond optical parametric amplifier was used as a laser source, operating at 4.65 μm at a repetition rate of 1 kHz. The results obtained, $d_{22}(GaS_{0.05}Se_{0.95})$=0.9 d_{22}(GaSe), $d_{22}(GaS_{0.1}Se_{0.9})$=0.88 d_{22}(GaSe), and $d_{22}(GaS_{0.4}Se_{0.6})$= 0.83 d_{22}(GaSe) indicate much weaker dependence on the doping level. The measured dependence on the azimuthal angle suggests that either the symmetry of GaSe ($\bar{6}m2$) is preserved or the d–coefficient which is independent of the azimuthal angle (in 3m symmetry) has a negligible contribution. The index of refraction of $GaS_{0.4}Se_{0.6}$ was measured in the 0.633 – 10.0 □m spectral range using the auto-collimation technique on a prism with an aperture of 15x15 mm^2 and apex angle of 13.74°. Sellmeier equations with two-poles were then constructed and the SHG phase-matching curve was compared with experimental results at 2.79, 9.59 and 10.6 μm from the literature [2]. The damage threshold at 1064 nm was measured for the same composition both with 14 ns pulses at 100 Hz and CW radiation; it is roughly 50% higher than in pure GaSe. The two-photon absorption, TPA, (measured with ps pulses at 1064 nm) is lower than for GaSe.

The high nonlinearity of $GaS_{0.4}Se_{0.6}$, together with the improved thermo-mechanical properties, the increased band-gap and damage threshold, and the lower TPA make this crystal attractive for mid-IR optical parametric oscillators and generators operating above 5 μm for the idler and pumped by 1064 nm radiation (nanosecond and picosecond pulses, respectively).

References

[1] K. R. Allakhverdiev, R. I. Guliev, É. Yu. Salaev, and V. V. Smirnov, "Investigation of linear and nonlinear optical properties of GaS_xSe_{1-x} crystals," Sov. J. Quantum Electron. **12**, 947-948 (1982) [transl. from Kvantovaya Elektron. (Moscow) **9**, 1483-1485 (1982)].

[2] H.-Z. Zhang, Z.-H. Kang, Y. Jiang, J.-Y. Gao, F.-G. Wu, Z.-S. Feng, Y. M. Andreev, G. V. Lanskii, A. N. Morozov, E. I. Sachkova, and S. Yu. Sarkisov, "SHG phase-matching in GaSe and mixed $GaSe_{1-x}S_x$, x≤0.412, crystals at room temperature," Opt. Exp. **16**, 9951-9957 (2008).

Basic mechanisms of direct laser materials nanostructuring

V.Yu. Khomich[1], V.A. Shmakov[2], V.N. Tokarev[2], V.A. Yamshchikov[1,2]

[1] *Institute of Electrophysics and Energetics, Russian Academy of Sciences, 18 Dvortsovaya nab.,*
191186 Sankt-Peterburg/Russia
[2] *Centre for Development of Nanotechnologies and Nanomaterials, Group of Companies "Glenic",*
28-2, str. Zoologicheskaya 123056 Moscow/Russia

vtokarev56@mail.ru

Development of physical fundamentals of new simple nanostructuring methods, i.e. of creation of surface profiles with characteristic periods less than 1 μm on *high tech* materials, is of a great practical interest. In the given paper recent results of authors [1-6] on development of physical mechanisms and theoretical models of direct laser surface nanostructuring are reviewed. These models are based on concepts of laser-induced instability and self-organisation of surface profile under intense laser irradiation. The term "direct" means here that surface is modified in the simplest way – with a single laser beam instead of two beams crossed to form an interference pattern on a surface or in a volume of the material, without using any masks, without using a combination of laser beam with an atomic force microscope tip or optical fiber tip for writing profiles, as it was in a number of previous papers on laser nanostructuring. The attention is paid to nanosecond lasers, as they are cheaper and simpler in use compared to pico-, and femtosecond lasers, which is important for the development of further technological applications. The formation of so-called "non-resonant" structures, whose period is not directly related to laser radiation wavelength, is considered.

The discussed theoretical models are developed for different mass transfer processes (with or without melting, depending on radiation intensity and a material) – (i) laser-induced vaporisation, (ii) etching, (iii) deposition, (iv) a combined action of melting and vaporisation, (v) melting without intense vaporisation, and (vi) non-linear relaxation of laser-induced thermal stresses in absence of both melting and vaporisation. Corresponding experimental illustrations are given for various materials – metals, semiconductors, ceramics and diamond film.

Authors thank the Russian Fund for Basic Research for financial support of the work (Projects RFBR 07-02-12262 and 08-02-01192).

References

[1] F. Weisbuch, V. N. Tokarev, S. Lazare, C. Belin and J. L. Bruneel: Thin Solid Films, 453-454 (2004) 394.
[2] S. Lazare, V. N. Tokarev, A. Sionkowska, H. Kaczmarek, M. Wi□niewski and J. Skopi□ska, Appl. Phys. A, 81 (2005) 465.
[3] K. E. Lapshin, A. Z. Obidin, V. N. Tokarev, V. Yu. Khomich, V. A. Shmakov and V. A. Yamshchikov: Russ. Nanotech., 2 (2007) 50. – in Russian.
[4] V. N. Tokarev, V. Yu. Khomich, V. A. Shmakov and V. A. Yamshchikov: Doklady Physics, 53 (2008) 206.
[5] V. N. Tokarev, V. Yu. Khomich, V.A. Shmakov and V. A. Yamshchikov: Physics and Chemistry of Materials Processing, 4 (2008) 18. – in Russian.
[6] V. A. Shmakov: Doklady Physics, 52 (2007) 470.

Spectral response of molecular media under nanoporous confinement

V.G. Arakcheev, V.B.Morozov, A.N. Olenin, A.A.Valeev

International Laser Centre and Physics Department of M.V. Lomonosov Moscow State University
Moscow 119991, fax: +7(495)9393016
e-mail: morozov@phys.msu.ru

Coherent anti-Stokes Raman Scattering (CARS) spectroscopy proved to be an powerful tool for diagnostics of states and phase transitions of molecular media confined in nanopores [1, 2]. Contributions of gas phase, molecular layers adsorbed on the pores surface and liquid-like phase condensed inside pores can be recognized using the analysis of measured CARS spectra. Phase behavior of a molecular fluid under nanoporous

from phase behavior in bulk volume. In the present paper, we develop approach to spectral shape description as a function of pores diameter distribution.

Nanopopous glass sample was placed inside high-pressure cell filled with carbon dioxide. CARS spectra of high-frequency Fermi-dyad component Q-branch 1388 cm^{-1} were monitored. Typical spectral shape was defined by interference of two main spectral contributions: high-frequency peak caused by gaseous carbon dioxide in pores core area as well as from gaps between nanoporous glass sample and cell windows and low-frequency one attributed to carbon dioxide adsorbed on pore walls or condensed inside pores depending on pressure and temperature. Transition into condensed phase inside pores is recognized by substantial narrowing of low-frequency peak from ~4 cm^{-1} (corresponding to adsorbed molecules) to 1.6 cm^{-1} as in liquid in unconfined volume.

Spectra fittings were accomplished using the coherent sum of two Lorenzian profiles. Linewidth and centre frequency values measured in gaseous carbon dioxide in bulk were used as a substitute for high-frequency peak parameters. Low-frequency peak parameters were fitted as originating from molecules of the adsorbed and condensed fluid within a nanostructure. The diffusion process was presumed to be slow enough in order the molecule to stay within its phase the whole time of the scattering. Model porogram based on the measured one was used in our calculations. The porogram was modified with regard to the adsorbate layer thickness. Adsorption and condensation equations were used to simulate quantities and ratio of the both phases matter. The model spectra are in good agreement with the experimental results. The appearance of low-frequency peak at $T=21^{o}C$ was shown to be caused by gas adsorption and condensation to a dense liquid-like state inside nanopores at pressures lower than saturation pressure P_{SAT}.

The work is supported by Russian Foundation for Basic Research (07-02-01331).

References

1. V.G. Arakcheev, V.N.Bagratashvili, S.A.Dubyanskiy et al. *J.Ram.Spectr.*, **39**, 750-755 (2008);

2. V. G. Arakcheev, A. A. Valeev, V. B. Morozov, and A. N. Olenin. *Laser Physics*, **18**(12), 1451-1458 (2008).

Luminescent Porous Silicon for Biosensing Applications

Viktoriia Shevchenko
shevchenko@univ.kiev.ua

Porous silicon (PS) has found a new application in medicine and biology. This material is a promising one to make biochips, sensing devices. Because of the unique optical properties and morphology, porous silicon can be used as a matrix and signal transducer in a sensing application whose photoluminescence (PL) changes to detect various biochemical interactions. Here we study the effect of porous silicon surface treatment by water solutions of nucleic acids on the PS photoluminescent properties. Nanostructured porous silicon was prepared by anodic etching of 10 Ω*cm (100) p-Si wafers. The water solutions of polynucleotides were applied on the untreated surface of PS, and the photoluminescence spectra of samples are measured thereafter. The PL is excited by 337 nm laser beam, which is not absorbed by the nucleic acids. We have observed that the treatment of PS surface by the solutions of nucleic acids leads to PS PL intensity increase and short-wave shift of the peak. It is established

that the treatment of PS by the solutions of two-strand molecules of native DNA results in more essential changes of the PL parameters than that of single-strand molecules of poly(A) or molecules of denaturated DNA. We have supposed that the presence of nucleic acid molecules in water solution stimulates PS/water solution interacting. The water treatment of PS reduces the average size of silicon nanostructure, which can explain the PL intensity increase and blue shift of the spectrum within the quantum-size model of PS luminescence. The peculiarities of PS interaction with nucleic acid solutions are related, in our opinion, to the negative charge of polynucleotide molecules in water solutions. The accommodation of such a molecule near the PS surface can increase carrier change density of PS and affect the oxidation/hydrolyze progress. The oxidation/hydrolyze process in PS would be the most intensive for two-strand molecules of native DNA with highest density of negative charge and the PL parameters would be consequently modified to the greatest extent. The observed effects can be applied to determine the fact of hybridization of DNA oligonucleotides in solution to complementary sequences.

Determining resolution of a digital in-line holography microscope

Ville A. Kaikkonen and Anssi J. Mäkynen
Measurement and Sensor Laboratory, University of Oulu, Kajaani, Finland
Ville.Kaikkonen@oulu.fi

The resolution in DIHM is affected by several geometrical parameters and properties of the used equipment that can be affected. The pinhole size affects the quality of the point source and hence also to the achievable resolution in the reconstructions. Numerical aperture depends on the used camera chip size and the recording geometry. The pixel size of the camera is a factor that should be considered in relation to the setup geometry and the size of the particles one wishes capture into the hologram. Pixel size and the dynamic range of the camera affect both to the noise level in the hologram. And further more, a shorter wavelength of the point source allows a higher resolution but has to be considered in relation to the other properties listed above [1].

In this work various methods to determine the resolution of a digital in-line holography microscope that has been setup on to an inverted microscope have been studied. This type of setup allows the use of both conventional brightfield and digital in-line holography microscopy on the same platform. The DIHM instrument parts and reconstruction algorithm were delivered by Resolution optics from Canada. The work has been carried to determine the achievable lateral and depth resolutions for this integrated setup in setup geometries that are expected to be used in future applications. The DIHM system consists of a point source and a four mega pixel CMOS camera. The point source is implemented with a violet diode laser point source with wavelength of 405 nm and optical power of 25 mW. The digital camera has pixel size of 6 um. The DIHM system is integrated to a Zeiss Axiovert microscope so, that the point source is placed in the objective turret and the camera on top of the specimen stage.

References

1. H.J. Kreuzer, "Digital in-line holographic microscopy", *Applied Optics*, **45**, 838-839 (2006).

KDP crystal doped by anatase nanoparticles in Terahertz applications

V.A.Enikeeva[1], I.A.Ozheredov[1], A.P.Shkurinov[1]
V.Ya.Gayvoronsky[2], I.M.Prytula[3]

[1]Department of Physics and International Laser Center of M.V.Lomonosov Moscow State University, 119992 GSP-2, Leniskie Gory, Moscow, Russia
violetta.enikeeva@gmail.com
[2]Institute of Physics NASU, pr. Nauki 46, 03680 Kiev, Ukraine
[3]Institute for Single Crystals NASU, 61001, 60 Lenin Ave, Kharkov, Ukraine

The development of new THz sources is of great importance for scientific and technological applications. It was shown that potassium NLO crystals have promising capabilities for both THz generation by optical rectification and detection of THz pulses by electro-optic sampling [1]. In order

to optimize techniques for THz generation, it is of crucial importance to accurately know the optical characteristics of the material in far infrared range. An idea of synthesis of novel functional material – KDP crystals doped with TiO_2 (anatase polymorph) nanoparticles – was based on the approach of smart impact of the nanoparticles on defect subsystem of the crystal matrix via interaction of the hole polarons with extremely active surface of the incorporated nanocrystals. The defects have crucial influence on domain formation in ferroelectric phase. It is well known that KH_2PO_4 crystal undergoes the ferroelectric-ferroelastic phase transition from tetragonal to orthorhombic at T_c=122K, then changing from an optically uniaxial phase to another biaxial. KDP with the orthorhombic symmetry develops at low temperature a thin regular layered pattern of antiparallel ferroelectric domains which are also ferroelastic twins [2].

Experimental KDP samples doped by anatase nanoparticles were grown on the point seed from the solution by the temperature reduction method. Concentrations of TiO_2 particles in the initial solutions of KDP stoichiometric composition was 10^{-4} □%. Pure KDP crystals were grown at the same conditions from the same reagents. The samples had a form of plates with the main plane perpendicular to the growing axis with a size of 10×10×0,7 mm^3 with facets oriented along crystallographic axes.

We apply THz TDS technique for study of temperature dependencies and phase transition of pure KDP and KDP doped by anatase nanoparticles. For studying of dielectric properties of KDP crystals near phase transition point we used closed cycle helium cryostat DE - 210 S (Advanced Research Systems, Inc.) with temperature accuracy ±20 □□.

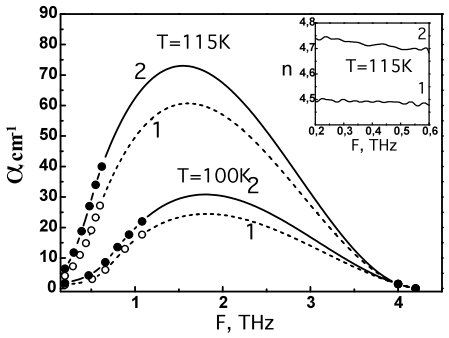

Fig. 1. Comparative absorption and refraction(inset) spectra of KDP crystals: 1) Pure KDP, 2) KDP:TiO_2

Experimental results of low frequency absorption of pure KDP sample for different temperatures below phase transition are shown at Fig.1. We noted a drastic decrease of absorption coefficient below phase transition. We approximated our absorption spectra using the model described in [3] for temperature dependence of imaginary part of the dielectric permittivity. Comparative refraction spectra of pure KDP and KDP:TiO_2 at 115K, which means below phase transition point, are shown in the inset of Fig.1. It is clearly seen for the same conditions absorption and refractive index of doped crystal are less correspondingly to pure KDP. The results of these measurements show the sensitivity of THz TDS technique to the crystal state and symmetry.

References

[1]. P. Mounaix, L. Sarger, J.P. Caumes, E. Freysz, *Opt.Com.*, **242**,631-639, (2004).
[2]. J.Bornarel. *Ferroelectics*, 71, 255, (1987).
[3]. F. Brehat and B. Wyncke, *Phys. Stat. Sol.*, **128**, 83, (1985).

Three-waves interactions of surface defect-deformational waves and their role in selforganization of nano and microstructures under laser action on solids

Vladimir.I.□mel'yanov, Dmitry.□.Seval'nev
Physics Faculty of Moscow State University, 119991, Moscow, Russia, emel@em.msk.ru

Selforganization of nano and microstrutures of the surface relief under the action of external energy (laser and ion) beams is considered as an instability of quasistatic surface defect-deformational (DD) waves formed by coupled quasistatic Lamb and Rayleigh acoustic waves and defect concentration waves [1,2]. It is shown that the dependence of the growth rate of DD waves on the wave number has two maxima that select the periods of two dominant surface relief modulations. The first period is equal to $2h$, where h is of the thickness of defect-enriched

surface layer created by irradiation and the second one is by an order of magnitude larger. Survey of experimental data on formation of surface relief under laser and ion beam irradiation of semiconductors and metals reveals the presence of two-scale surface relief modulation. A new approach to the obtaining of size distribution function of nanoparticles formed due to laser irradiation is developed that expresses it through the growth rates of the DD instability [2]. The calculated bimodal size distribution function is shown to reproduce well experimental bimodal size distribution functions regarding their shape and locations of maxima. It is shown that the DD surface instability is described by a closed nonlinear equation of Kuramoto-Sivashinsky (KS) type [3]. The KS equation with coefficients specific for ion sputtering of surface is widely used for the description of formation of ordered surface relief structures under ion beam irradiation of metals and semiconductors. The establishing of the universal DDKS equation supports the supposition [1] that the formation of similar surface relief structures under laser and ion beam irradiation has one and the same underlying DD mechanism. The computer solution of obtained two-dimensional DDKS equation is carried out that corroborates the formation of ordered surface relief structures. In the linear regime of DD instability computer analysis demonstrates the formation of characteristic lamellar surface relief structures that is frequently observed in experiments [4]. In the nonlinear regime formation of square and hexagonal structures occurs.

The three-DD waves interactions are considered for the first time including second and third harmonic generation, wave vector mixing [5] and generation of subharmonics. These DD wave interactions occur due to defect-deformational nonlinearity and are similar to optical and acoustical nonlinear wave interactions. The bimodal spectrum of DD waves excited by irradiation in the linear regime of the DD instability is shown to be enriched by nonlinear three DD waves interactions. Computer processing of experimental data on laser-induced generation of micro and nanostructures of surface relief in metals and semiconductors reveals the presence of the effects of second and third harmonic generation and wave mixing.

References

1. V.I. Emel'yanov, *Laser Physics* , **18**, N6, 682 (2008).
2. V.I.Emel`yanov, *Laser Physics* , **18**, N12, 1435 (2008).
3. V.I.Emel`yanov, *Laser Physics*, **19**, N3, 538 (2009).
4. V.I.□mel'yanov, D.□.Seval'nev, *J.Russian Laser Research*, **30**, N1, 21 (2009).
5. V.I.□mel'yanov, D.□.Seval'nev, *Quant.Electron.*, **39**, N7-8 (2009).

Characterization of Giant Photoacoustical Signals in Layered Crystals by a Novel Transient Free-Carrier Absorption Technique

V. Grivickas[1], V. Gavryushin[1], K. Gulbinas[1], V. Bikbajevas[1], K. R. Allakhverdiev[2,3], and D. A. Huseinova[3]

[1] *Institute of Applied Research, Vilnius University LT-10223, Vilnius, Lihuania*
[2] *TUBITAK Marmara Research Center, Materials Institute, 41470, Gebz, Turkey*
[3] *Institute of Physics ANAS, 370143, Baku, Azerbaijan*

The GaSe and $TlGaSe_2$ are layered indirect semiconductors. Recently, such crystals received a great deal of attention due to their optical and electrical properties in view of

possible optoelectronic devise application. Here, experimental evidence is presented that unusually strong longitudinal photoacoustic pulses (PAP) can be induced in these crystals [1,2].

Thick samples slabs were carefully polished on both sides of layers cross cut planes. The pump-probe technique with orthogonal geometry of pump and probe beams was used. The front sample face is homogeneously excited with 2 ns of a tunable wavelength pulses with photon energies tuned below and above the band gap energy. The free carrier absorption signal and the deflection changes caused by PAP propagation across probed area were detected. It is observed that giant longitudinal PAP arises and travel across the layer planes with the speed of the acoustic waves reflecting from the back and excited surfaces up to few hundred times. We show that the PAP is generated in close proximity of the sample surface and have very small dispersion and are orders of magnitude stronger than for isotropic indirect band gap semiconductors. Intensity dependences of PAP show that resonant two-photon absorption occurs above the indirect band gap. Tentative mechanism of the two-photon generation mechanism is discussed.

References

1. V. Grivickas, V. Bikbajevas, K. Gulbinas, V. Gavryushin, J. Linnros: Phys. Stat. Sol (b) **244** 4624-4628 (2007).
2. V. Grivickas. V. Bikbajevas, K. Allakhverdiev and J. Linnros: J. Phys.: Conf, Ser. **100,** 042008 (2008).

Nano-aquarium integrated with functional microcomponents in photostructurable glass by femtosecond laser microprocessing for microorganism analysis

Y. Hanada[1], K. Sugioka[1], H. Kawano[2], I. Ishikawa[2], A. Miyawaki[2], M. Iida[3], H. Takai[3], K. Modrikawa[1]

[1] *RIKEN-Advanced Science Institute 2-1 Hirosawa Wako Saitama 351-0198, Japan*
[2] *RIKEN-Brain Science Institute 2-1 Hirosawa Wako Saitama 351-0198, Japan*

Femtosecond (fs) laser direct writing followed by annealing and successive wet etching in dilute hydrofluoric (HF) acid solution results in formation of three dimensional (3D) hollow microstructures embedded in photostructurable glass. This technique enables us to fabricate micro fluidics, micro mechanics, and micro optics

inside the glass and thus to integrate these micro components in a single glass microchip. Fs laser refractive index modification further integrates buried optical waveguides in the microchip [1].

Meantime, observation of microorganisms is currently a challenging subject for cell biologists, since most of them are composed of a unit cell and thereby it is very important to explore their dynamic movement and physiologic energy generation mechanisms to understand the potential ability and function of the unit cells composing organisms including human beings. We proposed to use microchips fabricated by the fs laser microprocessing, referred to as nano-aquariums, for dynamic observation of microorganisms [2]. The nano-aquarium has several advantages over conventional observation methods using a glass slide with a coverslip or a Petri dish, such as great reduction of observation times, ability of 3D observations, easy stimulation of the cell using mechanical micro components integrated into the microchip, etc.

In this paper, we fabricate nan-oaquarium integrated with a micro pump to observe rheotaxis behavior of aquatic microorganisms and thus to explore mechanisms of sensing the water stream and of holding positions in the stream. Figure 1 shows the fabricated nano-aquaruim which consists of 4-mm long U-shaped microchannel connected to the embedded micro chamber containing a freestanding vaned wheel with a cross-shape. By rotating the wheel using a DC motor, one can control the flow rate of water in the microchannel. We also fabricate another integrated nano-aquarium for analyzing unique phenomenon of *Phormidium* moving toward a seedling root (*Phormidium* assemblage), which accelerates growth of the seedling.

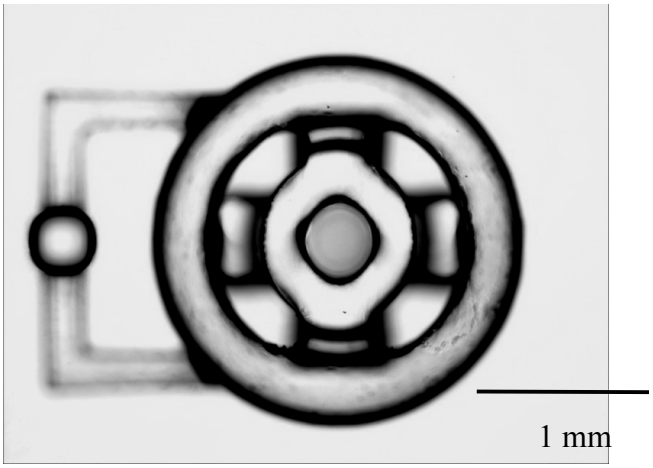

Fig. 1. Nano-aquarium integrated with micropump.

References

1. Z. Wang, K. Sugioka, Y. Hanada, K. Midorikawa: Appl. Phys. A88, (2007) 699.
2. Y. Hanada, K. Sugioka, H. Kawano, I. S. Ishikawa, A. Miyawaki, K. Midorikawa: Biomed. Microdevices, 10, (2008) 403.

Creation of ohmic contacts on n - and p - type ZnO films by PLD method.

Ye.A. Cherebilo[1], L.S. Parshina[1], O.A. Novodvorsky[1], V.Ya. Panchenko[1], E.V.Khaydukov[1], O.D. Khramova[1], C. Wenzel[2], N. Trumpaicka[2], J.W. Bartha[2]

[1] *Institute on Laser and Information Technologies, Russian Academy of Sciences (ILIT RAS) Shatura, Moscow Region, Russia* fax: 8(49645)22532

[2]*Dresden University of Technology, Institute of Semiconductor and Microsystems Technology, D-01062 Dresden, Germany*

e-mail: onov@mail.ru

Increasing necessity for solid-state sources and receivers of light in dark blue and UV areas stimulated last years intensive research of several broad-band semiconductors on the basis of which short-wave optical devices can be created. The zinc oxide, having band-gap zone 3.4 eV, it is characterized record energy of exciton conjuction (60 meV) at room temperature, possesses high stability an irradiation, it is pliable to chemical etching and it is rather cheap, that does its attractive to application in microelectronics. The method of pulse laser deposition (PLD) is applied to creation of thin-film structures on the basis of ZnO. This method favorably differs wide possibility of management process of the growth, in the lowered epitaxy temperature and the simplified technology of controllable entering of doping impurity that allows to grow up ZnO film with set crystal, electrical and optical properties. The PLD method provides congruence evaporation of targets of any composition and deep effective vacuum during of deposition owing to high density of particles in a plume [1]. Homoepitaxial ZnO films, doped by gallium, nitrogen, phosphorus were deposited on monocrystal sapphire substrates of by a method pulse laser deposition under various deposition conditions and methods of introduction of dopant in a film during deposition. Gallium was used for fabrication of n-type ZnO films. Nitrogen and phosphorus were used for fabrication of p-type ZnO films.

The ohmic contacts providing bilateral conductivity, are formed in places of connection of conclusions to semi-conductor layers. At creation of ohmic contacts it is necessary to receive the minimal resistance of contact [2]. The purpose of the given work is reception and research of metal contacts on epitaxial doped ZnO films for finding-out of an opportunity of creation of reliable ohmic contacts at manufacturing radiating devices and photodetectors of optical radiation on the basis of zinc oxide.

At contacts deposition on substrates very much preparation of a surface of substrates has great value. In our case of a substrate were degreased by acetone and got warm in vacuum before deposition process. The metal films of contacts Al, Au, Cu, Ta, Ti, Ni, Pt were deposited on substrates of silicon and ZnO films by PLD method. For creation of metal contacts on zinc oxide films of n-type on gallium doped ZnO film contacts were deposited of the titan and tantalum on various sites of a surface of a film also I-V characteristics were received. The received results show, that contacts have ohmic character. By a method of measurement U-I characteristics it was established, that contacts Au/Ni/p-ZnO, Au/Pt/p-ZnO, Au/n-Si and Au/p-Si are ohmic. The annealing influence on the films characteristics has been investigated.

Thus, for diodes on the basis of zinc oxide from a ZnO film of n-type it is possible to apply contacts from the titan or tantalum and for a ZnO film of p-type it is possible to apply contacts from the nickel and gold, platinum and gold.

References

1. A.N.Zherikhin et all. „Laser deposition ZnO films on silicon and sapphire substrates", Kvantovaja elektronika, 33(11) 975-980 (2003) (in Russian).
2. K.V. Shalimova, Physics of semiconductors, Energoatomisdat, Moscow, 1985.

Filamentation of femtosecond laser pulses: first experimental observation and real-time measurement of flying filament front

V.V. Bukin, S.V. Garnov, T.V. Shirokikh, V.A. Tserevitinov
A.M. Prokhorov General Physics Institute RAS
Main author email address: vbkn@kapella.gpi.ru

The spatiotemporal distribution of the refractive index and the electron density of the plasma filaments are studied with the precise interferometric pump-probe method. The laser-plasma

filament was produced in air by focusing ultrashort (~ 35 fs) pulses of Ti:Sa laser by lens with focal length F=500mm. The measuring technique and experimental setup for precise optical diagnostics of laser plasma is described. Our technique allows to measure phase objects with amplitude smaller than $2\pi/100$ with RMS noise ~ $2\pi/2000$. Measured electron density in filament was $1.5x10^{17}$ cm^{-3}. The process of moving of the plasma front in filament was observed for the first time.

This work was partially supported by: Russian Academy of Sciences Programs: "Extreme light fields and their applications"; "Fundamental spectroscopy and its application", and RFBR grant # 09-02-00861-□

Nonlinear Optical Properties of Biomineral Nanocomposite Structures

Yu.N. Kulchin[1], A.V. Bezverbny[1], O.A. Bukin[1], S.S. Voznesensky[1], S.S. Golik[1], A.Yu. Mayor[1], Yu.A. Schipunov[2]

[1] *Institute of Automation and Control Processes of Far Eastern Branch of RAS 690022 Vladivostok/Russia*

[2] *Institute of Chemistry of Far Eastern Branch of RAS 690022 Vladivostok/Russia*

Main author email address: kulchin@iacp.dvo.ru

The transmission of laser femtosecond pulses by spicules of marine glass sponges and monolithic nanocomposite silica biomaterials synthesized on the basis of natural polysaccharides has been experimentally investigated. The strong non-linear optical properties of these biominerals have been revealed in spectral characteristics of transmitted ultra-short pulses (USP). The multi-layer cladding of glass sponge spicules has an obvious analogy with some contemporary artificial microstructured optical fibers. Our researches have shown that the core diameter and cladding layers thickness of the spicules of *Hyalonema sieboldi*, *Pheronema sp.*, *Sericolopus* glass sponges are appropriate to cause photonic bandgaps in the infrared, visible, and ultraviolet wavelength regions. This enables singlemode waveguide and Bragg light propagation regimes in the spicules[1]. Also comparative analysis of the earlier transmission spectra of (USP) reveals that spicules exhibit much stronger non-linear optical properties than quartz optical fibers [2]. Recently new monolithic nanocomposite silica biomaterials were synthesized on the basis of various natural polysaccharides and completely water-soluble Si-precursor [3]. The shape of transmitted spectrums through both spicules and new nanocomposite biomaterials demonstrates major changes indicating the broadening and formation of dip due to self-phase modulation along with formation markedly strong anti-Stokes component in the output spectrum with generation of supercontinuum spectra. The carried out studies have showed that the nature combination of spongin protein with silicon dioxide extracted from seawater by silicatein protein in glass sponge spicules and monolithic nanocomposite silica biomaterials are biological and biomimetical nanocomposite materials with unique optical properties. These results provide exciting prospects of using the materials for the development of fundamentally new integrated optical elements based on their non-linear optical properties of such structures, e.g. for implementation of active optoelectronic devices such as optical fiber amplifiers and lasers.

References

1 Yu.N. Kulchin et al, Optics and Spectroscopy, (2009), in print.
2 Yu.N. Kulchin et al, Quantum Electronics, 38 (2008) 51
3 Yu.A. Shchipunov/ In Eds. Ruiz-Hitzky, E., Ariga, K., Lvov, Yu. M., Bio-inorganic hybrid nanomaterials, Weinheim: Wiley. 2007. P. 75-117

Development of Back-Mode Photoacoustic Transducer for Measuring Consistency of Paper Pulp Suspensions

Z. Zhao, M. Törmänen, R. Myllylä

Department of Electrical and Information Engineering and Infotech Oulu, University of Oulu, 90014 Oulu, Finland

zuomin@ee.oulu.fi

A back-mode photoacoustic transducer was developed, consisting of an optical fiber, a composite absorber, and a piezoelectric film. The transducer merit is simultaneously sensing optical reflectance and ultrasonic attenuation generated in suspensions. One probable application is in paper industry. The pulp consists of wood fibers, wood fines and filler particles, where fiber lengths range from sub-millimeters to millimeters and fines/particles have sizes of a few tens micrometers or smaller. Because of different size and shape, they have different properties of optical scattering and acoustic attenuation in suspensions [1]. Therefore, by measuring these two parameters, it is possible to determine the two-fractional consistencies. The experimental results showed that it can measure fibers consistency with good linearity at least in the range from 0.5% to 3 %, and distinguish the fines or filler (TiO_2) consistency from fiber one. Comparing with our former sideward mode measurement [2], this backward mode transducer greatly expands the measurement range of suspension consistency with better linearity. Moreover, it maximizes the efficiency of incident laser for PA generation, making it possible to use lower cost lasers, such as diode lasers, in this technique. Needless to say, the technique can expand to study suspensions in other industrial applications, and the transducer can also sense absorbing objects in scattering matrix.

References

1 M. Törmänen, J. Niemi, T. Löfqvist and R. Myllylä, Meas. Sci. Technol., 17, (2006) 695.
2 Z. Zhao, M. Törmänen and R. Myllylä, Meas. Sci. Technol. 17, 128-134 (2006).

Photodynamic Therapy on B16 Cells with Tetrasulphonated Porphyrin and Different Light Sources

S.F. Pop[1,2], R.M. Ion[1,2], M. Neagu[3] and C. Constantin[3]
[1] *Analytical Department, National Institute for Chemical and Petrochemical Research, ICECHIM , Bucharest, 202 Splaiul Independentei, Romania*
[2] *Valahia University, Targoviste, Unirii Blvd., 18-20, Romania*
[3] *Immunology Department, National Institute Victor Babes , Bucharest, 99-11 Splaiul*

Photodynamic therapy of cancer (PDT) has a major potential for medical practice.[1] PDT represents a local modality of treatment and, to be effective for eradicating tumors it is essential that an appropriate light dose reaches every relevant point of the tumor and also, to have an efficient photosensitizing drug administrated to a limited volume of tissue. Photodynamic therapy involves three key components: sensitizer, light and tissue oxygen. A sensitizer is a chemical compound that can be excited by light of a specific wavelength. 5,10,15,20-tetra-p-sulphonated-porphyrin (TSPP) was studied at different photodynamic dose from different laser types. [2] Also, this porphyrin belonging among the promising second generation of sensitizers was evaluated as an inducer of photodamage on B16 (mouse melanoma).

We report the influence of various concentrations of the sensitizer in combination with laser irradiation on the photodamage of cells. Viability of cells was determined by means of molecular probes (Calcein AM and ethidium homodimer) for fluorescence microscopy. The quantitative changes of cell viability in relation to sensitizer concentrations and laser irradiation were proved by fluorometric measurement. In addition, the viability studies showed that B16 mouse melanoma is sensitive to photodynamic damage induced by TSPP.

B16 melanoma cells were incubated with 1mM TSPP for either one, two, three or four hours. The control had TSPP added immediately prior to timelapse imaging (no incubation). They were then irradiated with red light He-Ne laser (= 6328 A, power 180 J/cm ^{2} for 20 minutes). Live cell timelapse imaging was done on a Nikon TE2000E inverted microscope (since the cells were in plastic culture dishes). An onscope incubator maintained temperature and CO_2 concentration. This setup has been able to maintain cells with no apparent ill effects for at least three days. A 375 W Hg medium pressure lamp provided a wavelength of 470nm +/- 20nm with bandpass filter. Also, it has been used a laser diode GaInAs 25 mW/cm^2, =650 nm;

The cells demonstrated clear morphological changes associated with apoptosis. Dendrites progressively shrank, while the nuclei first appeared to swell and then shrink relative to the total cell area. There were changes in texture, as expected. Changes appeared to occur more quickly at lamp irradiation than at HeNe and GaInAs diode laser. Addition of TSPP just prior to exposure and observation, with no incubation, did not result in changes in cell morphology or cell death.

References

1. RM Ion, Photodynamic therapy: a new concept and a clinical reality for medicine, *Acta Bio-optica et Informatica Medica,* **1**,37-49, (2006).
2. RM Ion, D.V.Brezoi, M.Neagu, G.Manda, C.Constantin, Laser effect in photodynamic therapy of tumors*, Proc.SPIE*, **6606**, 66061G-660671G (2007)

A novel pattern recognition approach for noisy frequency-resolved-optical-gating traces

Wei-Hong Su[1], Sung-Hui Lin[2], T. R. Tsai[3], A. K. Chu[4] and Chao-Kuei Lee [4*]
[1] *Department of Material science and technology, National Sun Yat-Sen University, Kaohsiung 804, Taiwan, ROC*
[2]*Department of Photonics and Institute of Electro-Optical Engineering, National Chiao Tung University, Hsinchu, 30010 Taiwan, ROC*
[3]*Institute of Optoelectronic Sciences, National Taiwan Ocean University, Keelong, Taiwan*

[4]*Department of Photonics, National Sun-Yat-Sen University, Kaohsiung 804, Taiwan*

Frequency-resolved optical gating (FROG) has been one of the most popular methods for measuring an ultrashort laser pulse [1-6]. It evaluates an autocorrelation signal by launching a tandem combination from two variably delayed replicas of the pulse into a nonlinear device. The spectrogram of this autocorrelation signal, or so-called FROG trace, is a two-dimensional function of frequency and time. With a suitable error comparison method, for example, by evaluating the deviation between the guessing and measured FROG traces [7], it is analyzable to retrieve the amplitude and phase of the pulse. One of the current trends in FROG is the accurate measurement of extremely weak pulses. Errors are inevitably introduced when the signal-to-noise ratio is too low. Several approaches have been proposed to enhance the tolerance of noise sensitivity, such as bandpass filtering [8] and OPA-FROG [6, 9]. Both approaches have limitations. In the method of bandpass filtering, most noises are eliminated by a frequency filter. However, it is a challenge to identify the filter's bandwidth, when the signal is unknown and extremely weak. In addition, noises which have the same frequency as the signals can not be thoroughly filtered out, resulting in enormous errors to retrieve the signal. An alternated solution is to enlarge the optical signal by OPA-FROG. Sensitivity in the atto-joule level can be achieved. Unfortunately, the systematic setup is relatively complicated. Challenges still remain to improve performance for practical applications. In this paper, we propose a method based on pattern recognition to characterize the error measurement of FROG traces for extremely weak laser pulses. This recognition algorithm is executed by cross-correlation rather than the conventional deviation method. There is no need to make any redundant experimental setup to enhance the signal-to-noise ratio. Data has shown that characteristics of the signal can be identified with very high repeatability, even though the signal-to-noise ratio is only 7. Advantages of this method also include (1) very sensitive to signal extraction, (2) very low computation cost, and (3) intensive application to various types of FROG traces [10].

References

1 D. J. Kane and R. Trebino, Opt. Lett. **18**, 823-825, (1993)
2 A. Assion, T. Baumert, J. Helbing, V. Seyfried, G. Gerber, Chem. Phys. Lett. **259**, 488-494, (1996).
3 J. W. Nicholson, F. G. Omenetto, D. J. Funk, and A. J. Taylor, Opt. Lett. **24**, 490-492, (1999)
4 R. Trebino, Kluwer Academic Publishers, (2001)
5 J. Kunde, B. Baumann, S. Arlt, and F. Morier-Genoud, J. Opt. Soc. Am. B **18**, 872-881, (2001)
6 J. Y. Zhang, C. K. Lee, J. Y. Huang and C. K. Pan, Opt. Exp. **12,** 574-581 **(**2004)
7 R, Trebino, and D. J. Kane, J. Opt. Soc. Am. A **10**, 1101-1111, (1993)
8 M. A. Krumbeuqel, D. N. Fittinghoff, K. W. DeLong, J. N. Sweetser, and R. P. Trebino, Proceedings of SPIE - The International Society for Optical Engineering **2762**, p 612-620 (1996)
9 J. Y. Zhang, A. P. Shreenath, M. Kimmel, E. Zeek, R. Trebino, and S. Link, Opt. Exp. **11**, 601-609 (2003)
10 .W. DeLong, and R. Trebino, J. Opt. Soc. Am. B **11**, 1595-1608, (1994)

Simulation of Optical Radiation Propogation in Plant Tissue

V. P. Zakharov, I. A. Bratchenko, E.V.Timchenko
Samara State Aerospace University, Samara, Russia

Three-dimensional mathematical model of simulating radiation-plant tissue interaction is developed. The model is implemented using Monte Carlo statistical technique for Henyey – Greenstein phase function and takes into account structural inhomogeneous and spectral properties of the medium and fluorescence effects. Dependencies of backscattering and fluorescence differential coefficients on the photosynthetic pigment (chlorophylls)

experiment is shown. The analytical approximate method based on expansion in perturbation series of diffuse and fluorescent fluxes is proposed. As shown the approximate solution allows to calculate backscattered radiation field with reasonable accuracy and gives only qualitatively description of fluorescence coefficient for large concentrations of chlorophyll.

Investigation of Thermal Diffusivity Temperature Dependence of Selected Laser Single Crystals

Jerzy Bodzenta, Anna Ka□mierczak-Ba□ata, Dominika Trefon-Radziejewska

Institute of Physics, Silesian University of Technology, 44-100 Gliwice/Poland

Growing powers dissipated in solid state lasers cause that thermal properties of laser crystals become very important. Crystals of high thermal capacity and high thermal conductivity are desired. In this work three groups of samples were investigated: yttrium aluminum garnet (YAG) crystals, yttrium orthovanadate (YVO_4) crystals and gadolinium calcium oxoborate (GdCOB) crystals. The thermal diffusivity was determined by the thermal wave method. The mirage effect was used for signal detection. The measurements were carried out for pure and doped samples in the temperature range (300÷500) K. Investigated crystals belong to different crystallographic systems. YAG is cubic crystal and its thermal diffusivity is fully characterized by single value. YVO_4 belongs to tetragonal crystallographic system. In this case the thermal diffusivity must be determined for two directions: parallel and perpendicular to crystallographic *c* axis. Description of the thermal diffusivity of monoclinic GdCOB crystal requires determination of three independent elements of thermal diffusivity matrix. Results of experiments confirmed the anisotropy of the thermal diffusivity of YVO_4 and GdCOB and revealed that the thermal diffusivity of all samples decreases with increasing temperature. Similarly to earlier experiments performed in room temperature [1], the results showed also strong influence of dopants on the thermal diffusivity.

References

1 J. Bodzenta, A. Ka□mierczak-Ba□ata, K. Wokulska, J. Kucytowski, T. □ukasiewicz, W. Hofman, Appl. Opt., 48 (2009) C46.

Laser Surface Treatment of Ceramic Material

M. Mutlu[1], E. Kacar[1,2], E. Suvaci[3], A. Demir[1,2] E. Akman[1]

[1] Laser Technologies Research and Application Center Kocaeli University 41380 Kocaeli/Turkey
[2] Faculty of Arts and Science, Department of physics, Kocaeli University 41380 Kocaeli/Turkey
[3] Materials Science and Engineering, Anadolu University, 26480 Eskisehir-Turkey

Main author email address: mesuremutlu@gmail.com

Laser surface treatment gives an opportunity to improve material properties (physical and chemical resistant) by applying high energy to the part of the substrate. During the laser treatment application laser beam as a heat source can be controlled and focused on substrate as desired position. Due to the hard and brittle nature of the ceramic materials it's difficult to process and some important properties of structural ceramics include: wear resistance, strength, hardness, fracture toughness, corrosion resistance, biocompatibility, and thermal shock resistance. Structural ceramics find applications in automotive, aerospace, printing, textile, metal cutting, and many other industries. Laser surface treatment is non-contact and low heat input application to maintain ceramic's desired properties and improve the erosion and corrosion resistance of materials.

In this study ceramic surfaces will be processed using ns and ms pulsed Nd-YAG laser with using ambient gases O_2, N_2 and Ar. Green alumina will be laser machined and the surface topographic, densification and porosity will be analysed in regard to laser wavelength, fluency and operation rate.

Laser Raman Microscopy, Pigments and the Arts/Science Interfaces

Robin J. H. Clark

Raman spectroscopy is a light scattering technique used historically in the characterisation of vibrational modes of molecules and thereby molecular structure. It provides a very effective means of identifying minute grains of any material such as a pigment. The technique has high specificity, sensitivity, reproducibility, spatial and spectral resolution, and is both non-destructive and applicable in situ. It is thus highly appropriate for the study

these attributes, leading to the identification of pigments on manuscripts, paintings, postage stamps, papyri, icons, ceramics, stuccoes, and archaeological artefacts, and to the establishment of artists' palettes at different periods and in different localities. At the arts/science interface, information has thereby been obtained which bears upon restoration, conservation and dating of artefacts, and upon the detection of forgeries. Complementary techniques are also used a needed, viz. XRF, XRD, IR and LIBS.

Important recent case studies include: the Lindisfarne Gospels (thought for centuries to involve illumination with the blue pigment lazurite, now identified as indigo; eight Gutenberg Bibles for comparative palette studies; the 36th Vermeer painting, the study involving the identification of key date-indicator pigments; the first scientific study of the archaeological finds (9th C stuccoes) of 1911 AD at Samarra; the pigments used on 16th-18th C Islamic manuscripts shown to differ only slightly from those used on secular ones; anatase (TiO_2) as a date marker material in Chinese kaolinitic clays; French miniatures by Bourdichon c.1500 AD involving the use of metallic bismuth as a mid-gray pigment; miniatures considered to be medieval French/Belgian, shown to be forgeries by the identification thereon of the modern pigments chrome yellow, Scheele's green, emerald green and ultramarine blue.

In conclusion, it is rare that an optical technique has made such an impact on seemingly unrelated areas.

Gas Pumping Through Membranes by Resonance Radiation

V.V. Levdansky[1], J. Smolik[2], P. Moravec[2]

[1] *Heat and Mass Transfer Institute NASB, 15 P. Brovka Str., 220072 Minsk, Belarus*

[2] *Institute of Chemical Process Fundamentals AS CR, v.v.i., Rozvojova 135, 165 02 Prague 6, Czech Republic*

Main author email address: vlev5@yahoo.com

Vacuum pumps are used in many branches of the modern technology (e.g. vacuum deposition of thin films, sublimation drying, manufacture of nanodevices, etc.). It is of interest to investigate the possibility of new principles of gas pumping. The paper deals with the theoretical study of gas pumping related to the influence of resonance radiation on the gas-membrane system that allows one, in particular, to carry out selective pumping a definite component of a gas mixture. This method does not demand mechanically moving elements as well as adsorbent regeneration (the latter is necessary in the adsorption pumps). As a source of resonance radiation the solid state tunable lasers can be used. Gas pumping through membranes under the influence of radiation is related to radiation-induced mass transfer in membranes. Resonance radiation can essentially change the character of the interaction between gas molecules and a surface due to the excitation of gas molecules and difference in the interaction of excited and non-excited molecules with the surface. Moreover, resonance radiation can affect the adsorption time of molecules adsorbed on the surface. It can evoke the radiation-induced drift of gas molecules in porous and non-porous membranes in the initially equilibrium gas-membrane system that leads to the pumping effect. The work was supported by GA AV CR project IAA400720804 and GA CR projects 104/07/1093 and 101/09/1633.

The project of High Power Cryogenic Laser Based on Yb:YAG Disks

E. A. Perevezentsev, I. B. Mukhin, O. V. Palashov, E. A. Khazanov

The Institute of Applied Physics of the Russian Academy of Sciences,
603950 Nizhny Novgorod/Russia

E. A. Perevezentsev: eperevezentsev@gmail.com

The aim of our project is a cryogenic Yb:YAG laser that combines the unique parameters: pulse energy 500mJ, pulse length 100ps (peak power 5GW), repetition rate 1kHz (average power 500W), high beam quality (M2~1).

Cooling Yb:YAG crystal with 10%at doping from 300K to 80K gives a ~0.8nm central laser wavelength shift. Three tunable generators are implemented experimentally: crystal cooling by liquid nitrogen; linear resonator with a birefringent filter (tuning to 1028.5…1033nm); crystal cooling using Peltier elements. At 80K, absorbed pumping power of ~200W and pumping beam diameter ~3mm, a depolarization ratio is less than 0.1%, and thermal lens focal length is implemented over 20m. The small signal gain after 8-passes the preamplifier is measured. The values coincide well with experimental results.

The stored energy with taking into account ASE, and thermal distortions of laser beam in the crystal are calculated. It is equals 0.6J in 2.7mm thick Yb:YAG crystal with 2.2%at doping, at 1.2kW pump power and 10mm diameter. It is possible to reduce thickness of a disk and increase doping concentration. Then it is necessary to use optically contacted Yb:YAG and YAG to reduce reflection of ASE from optical surfaces.

References

1. Krupke W.: IEEE Journal of Selected Topics in Quantum Electronics, 6, (2000) 1287.
2. Fan T.Y.: IEEE Journal of Quantum Electronics, 29, (1993) 1457.

Physical Properties, Phase Matching and Frequency Conversion in $GaSe_{1-x}S_x$, $Ga_{1-x}In_xSe$ and $GaSe_{1-x}Te_x$

Yu. M. Andreev[1], G. V. Lanskii[1], S. N. Orlov[2], Yu. N. Polivanov[2]

[1] *Institute of Monitoring of Climatic and Ecological Systems SB RAS 634055 Tomsk/Russia*

[2] *Prokhorov General Physics Institute RAS 119991 Moscow/Russia*

Main author e-mail address: [illegible]

Physical properties of modified GaSe (S, In, Te doped and mixed $GaSe_{1-x}S_x$, $Ga_{1-x}In_xSe$, $GaSe_{1-x}Te_x$) crystals are studied. Crystal structures are determined by both x-ray and proposed non-linear method. Main attention is paid to study of optical (linear, non-linear, damage threshold) and mechanical properties. $GaSe_{1-x}S_x$ crystals are found to be best choice for practical application due to a shift of transparency range toward short-wavelength range versus mixing ratio x and a set of it physical properties that are responsible for frequency conversion efficiency. Best dispersion equations for mid-IR are identified through SHG and DFG experiments, and modeling. Temperature dispersion of Er^{3+}:YSGG and CO_2 laser SHG within 100-560 K is analyzed in detail. First results on design of THz range dispersion equations will be discussed, so as different ways for THz emission generation in modified crystals.

A New Approach for Developing Highly effective Solid-State HV Pulse Generators for Laser Pumping

S. I. Moshkhunov

Russian Academy of Sciences, Institute for Electrophysics and Electric Power, Russia

Main author email address: serg-moshkunov@yandex.ru

A New approach for developing highly effective solid-state HV pulse generators for laser pumping is described.

bipolar transistors (IGBT) connected in series/parallel and magnetic pulse compressor circuits. These switches are capable to replace modulator vacuum tubes and gas-discharge switches (thyratrons), which are used in most power pulse generators for supplying of lasers and many other electric discharge devices.

The effectiveness of the approach in developing a number of pulse laser pumping systems with working voltages up to 30 kV, current amplitude up to 2000 A, average power up to 2 kW, pulse repetition rate up to 20 kHz and pulse width of 50 - 1000 ns was demonstrated.

Main advantages of the new approach as compare to generators based on thyratrons are: high reliability, long life, high stability, low losses, small dimension and weight.

Laser-Assisted Fabrication of Silicon Nanocrystals in Liquids

S.V. Zabotnov[1,2], P.A. Perminov[2], A.A. Ezhov[1], I.O. Dzhun[1], L.A. Golovan[1], P.K. Kashkarov[1,2]

[1] Physics Department, M.V. Lomonosov Moscow State University, 1/2 Leninskie Gory, 119991 Moscow/Russia
[2] Russian Research Center "Kurchatov Institute", 1 Kurchatov square, 123182 Moscow/Russia
e-mail: zabotnov@vega.phys.msu.ru

The laser-assisted nanoparticle formation by means of the ablation at a laser pulse action on solid state targets placed into different liquids stimulates the rising interest of researchers during last five years [1, 2]. This method has a set of advantages in comparison with the traditional laser nanofabrication at the laser ablation in gases: the nanoparticles are chemically pure, have the smaller size and spatial dispersion [3, 4].

In our work we studied the formation of the silicon nanocrystals at the laser ablation of monocrystaline silicon targets in such liquids as the water, glycerol and liquid nitrogen. We used a picosecond Nd:YAG and a femtosecond Cr:forsterite lasers as the pulse sources.

We studied the formed nanoparticles by the atomic-force microscopy. The nanoparticles have the spherical shape. The peak size (from 7 to 20 nm) and spatial dispersion depend on the buffer liquid. The Raman spectroscopy revealed the crystalline phase of the formed nanostructures.

We suppose that the ablated silicon atoms decelerate because of collisions with molecules of the liquid and agglomerate into the nanocrystals.

Thus, we have shown a possibility to form the silicon nanocrystals of the desirable size and spatial dispersion via the laser ablation in the proper buffer liquid.

References

1. P.V. Kazakevich, V.V. Voronov, A.V. Simakin and G.A. Shafeev: Quantum Electronics, 34, (2004) 951.
2. R.A. Ganeev, M. Baba, A.I. Ryasnyansky, et al., Appl. Phys. B, 80, (2005) 595.
3. S. Besner, A.V. Kabashin, F.M. Winnik, and M. Meunier, Appl. Phys. A, 93, (2008) 955.
4. A. V. Kabashin, and M. Meunier, J. Phys., 59, (2007) 354.

Neutral and Charged Species Produced Through Lasers in Solid and Gas Phase: Emission and Absorption Spectroscopy and Mass Spectrometry

A.Giardini[1], S. Orlando[1], A. Paladini[1], S. Piccirillo[2], F.Rondino[3], A. Santagata[1], P. Villani[1]
[1] *CNR – IMIP, Sede di Potenza, zona industriale, 85050 Tito Scalo (PZ), Italy*
[2] *Dip. di Scienze e Tecnologie Chimiche, Università di Roma 2 "Tor Vergata", Rome, Italy*
[3] *Dip. di Chimica e Tecnologie del Farmaco, Università di Roma "La Sapienza", Rome, Italy*
Main author email address: anna.giardini@uniroma1.it

This paper aims to review the characteristics of the process of laser desorption on non-

laser (532 nm emission wavelength, 6 ns pulse duration, 10 Hz repetition rate) and a Light Conversion doubled Nd:glass laser (529 nm emission wavelength, 250 fs pulse duration, 10 Hz repetition rate) are used for the ablation experiments. The highest laser fluences employed are 2.5 and 2.0 Jcm^{-2} in the fs regime and 18 Jcm^{-2} in the ns one.

The composition and temporal evolution of the transient products formed by short and ultrashort laser pulses are characterized to obtain structural and dynamical information. Different organic systems, as neurotransmitters, Schiff bases, and fluorinated drugs have been examined. To shed more light on the structure of these systems, complementary experiments of resonant enhanced multiphoton laser ionisation (REMPI) and mass spectrometric analysis, have been performed using a nanosecond dye laser pumped by a doubled Nd:Yag laser (0.1 Jcm^{-2}). For example, in the REMPI mass spectrum of (1S,2S)-N-methyl pseudoephedrine neurotransmitter, a fragmentation is observed, with breaking of the C_a-C_b bond [1]. At large fluences, an almost complete atomisation is observed in both femto and nanosecond regimes [2].

References

1 A. Giardini Guidoni, A. Paladini, S. Piccirillo, F. Rondino, M. Satta, M. Speranza, Org. Biomol. Chem., 4 (2006) 2012–18

2 P. Villani, S. Orlando, A. Santagata, A. De Bonis, S. Veronesi, A. Giardini, Appl. Surf. Sci., 253(19) (2007) 7783-86.

Power Scaling Approaches to Eye-Safe Bulk Solid-State Lasers

Mark Dubinskii
US Army Research Laboratory
2800 Powder Mill Rd, Adelphi, MD, 20783, USA

Author's e-mail address: mdubinskiy@arl.army.mil

The design of high power eye-safe lasers with nearly diffraction beam quality involves choosing the optimum host, dopant and its concentration, pump source, gain medium geometry, etc. In the quest for lowest possible thermal load, direct resonant diode-pumping offers many important practical advantages and much higher overall efficiency. Solid-state laser power scaling with high beam quality is only achievable in laser designs with maximum

possible reduction of heat generated by the absorbed pump along with efficient heat removal from the gain medium. The former can be achieved by minimization of the fundamental quantum defect (QD), $\square_{QD} = 1\square\square_P/\square_L$ (where $\square_P$ and $\square_L$ are the pump and laser wavelengths, respectively), while the latter is defined by the choice of the most thermally advanced host materials with thermal and thermo-optic properties superior to conventional YAG. It has already been demonstrated that QD less than 1.5% can be achieved while operating an eye-safe laser in a cryogenically-cooled regime [1]. Cryogenic cooling of gain medium is in all respects beneficial for power scaling due to: (i), favorable increase in laser transition cross-sections, (ii), significant population reduction of ground-state Stark sublevels closest to the "0"-level, and, (iii), great improvement of all major thermal and thermo-optic parameters of laser host [2]. This communication presents the most important and latest advances in resonantly-pumped eye-safe laser development at ARL, such as Er:YAG laser in cryogenically-cooled operation regime and intermediate temperature regimes [3], new thermally advanced Er^{3+}-doped laser materials – their spectroscopy and laser operation [1, 4], as well as totally new exploration of Pr^{3+} doped laser materials for efficient, low QD, resonantly-pumped 1.5-1.7 mm laser operation. Great emphasis is placed on Er-doped cubic sesquioxides such as Y_2O_3, Sc_2O_3 [1, 4], due to: (i) their superior thermal properties, and, (ii) the fact that they can be produced in a form of highly engineerable laser quality ceramics. Reported are Er-laser slope efficiencies as high as 70-80%, ultra-low quantum defect (QD) laser operation (QD ≈ 5%) and super-ultra-low QD (<1.5%) laser operation of Er-doped gain media, as it pertains to ultimate power scaling.

References

1. N. Ter-Gabrielyan, L. D. Merkle, A. Ikesue, and M. Dubinskii, Ultra-Low Quantum Defect Eye-safe Er:Sc_2O_3 laser. – Optics Letters **33**, 1524-1526 (2008).
2. T.Y. Fan, D. J. Ripin, R. L. Aggarwal, J. R. Ochoa, B. Chann, M. Tilleman, and J. Spitzberg, "Cryogenic Yb^{3+}-Doped Solid-State Lasers," IEEE J. Sel. Top. Quant. Electron. **13**, 448-459 (2007).
3. N. Ter-Gabrielyan, M. Dubinskii, G. A. Newburgh, A. Michael and L. D. Merkle, Temperature Dependence of a Diode-Pumped Cryogenic Er:YAG Laser, - OPTICS EXPRESS **17**, No. 9, 7159-7169 (2009).
4. N. Ter-Gabrielyan, L. D. Merkle, G. A. Newburgh, and M. Dubinskii. Resonantly-Pumped Er^{3+}:Y_2O_3 Ceramic Laser for Remote CO_2 Monitoring. - Laser Physics **19**, No. 4, pp. 867–869 (2009).

Supercontinuum Generation in Transparent Biomimetical Nanocomposites

Yu.N. Kulchin[1], A.V. Bezverbny[1], Yu.A. Shchipunov[2], S.S. Voznesensky[1], S.S. Golik[1], A.Yu. Mayor[1], I.V. Postnova[2]

[1] *Institute of Automation and Control Processes of Far Eastern Branch of RAS 690022 Vladivostok/Russia*

[2] *Institute of Chemistry of Far Eastern Branch of RAS, 690022 Vladivostok/Russia*

Main author email address: alexb62@mail.ru

The sol-gel technique is widely spread process of biomineralization, at which new nanocomposite silica biomaterials can be synthesized on the basis of various natural polysaccharides [1]. Small concentrations of polysaccharides radically change the structure and optical properties of synthesized biomaterials. The transparent materials with polysaccharides are expected to have large non-linear refractive index and ultrafast response time. The investigations of the dynamics of propagation of intensive ultra-short pulses (USP) through such biomimetical nanocomposites is of substantial interest in terms of creating a new, low-temperature technology for optical fiber production [2], as well as developing novel functional elements for photonics applications [3]. Laser complex Spitfire Pro 40F (Spectra Physics, USA) was used in experiments on propagation through samples of cylindrical and parallelepipedic patterns of nanocomposite silica biomaterials with various natural polysaccharides: Na-alginate, Na-hyaluronate, xanthan, carboxymethylcellulose. Input pulse duration was $T_0 < 40$ fs, maximum pulse energy 1 mJ, light beam diameter d ~ 10 mm, repetition rate 10-1000 Hz, pulse spectrum was centered at 800 nm. The transmitted spectrums of USP through the patterns of different lengths from 0.7 mm to 5 cm demonstrate significant non-linear optical properties. Most efficient generation of supercontinuum (SC) correspond with the pattern synthesized on the basis of Na-hyaluronate, which has non-linear refractive index $n_2 \sim 1.2\ 10^{-15}$ cm^2/W. These SC spectrums depend on concentrations of polysaccharides and extend to the region up to wavelengths of 300 nm for long patterns.

References

1. Yu.A. Shchipunov/ In Eds. Ruiz-Hitzky, E., Ariga, K., Lvov, Yu. M., Bio-inorganic hybrid nanomaterials, Weinheim: Wiley. 2007. P. 75-117
2. H.C. Schroder et al: Nat. Prod. Rep., 25, (2008) 455
3. Yu.N. Kulchin et al: Quantum Electronics, 38, (2008) 51

Residual Strain Study in Laser Cutting

Vladimir S. Mayorov[1], Sergey V. Mayorov[1], Maxim D. Khomenko[1], Roman V. Grishaev[1]

[1]*Institute on Laser and Information Technologies, Russian Academy of Sciences*

1 Svyatoozerskaya Str., Shatura, 140700, Moscow Region, Russia

Main author email address: top20072007@rambler.ru

The statement on the absence of deformations in laser processing often referred in the literature is generally not fair. Thermal laser effect results in local change of the material composition (in our case – metal) and appearance of inner stresses, which in a number of cases can lead to significant strain of the completed product. The results of investigation of residual strain in the samples after their cutting under different operating conditions are discussed. These samples are the disks of $0{,}5\text{-}1{,}0\cdot10^{-3}$ m thick polished AISI-304 stainless steel with the diameters from 30 to $100\cdot10^{-3}$ m. The laser system TRUMATIC-SL2530 was utilized, that allows both continuous and pulse-periodic regimes of laser cutting with laser power and impulse frequency varied. The behavior and value of residual strain of the samples were measured by the ZYGO GPI XP/D interferometer. Simultaneously, the sizes of heat-affected zone and rag were estimated. All the quality parameters improved with the cutting rate in continuous mode and significantly improved with the usage of pulse-periodic regime. The rag and heat-affected zone are considerable, and the strain (the deviation from flatness) makes fractions of a millimeter at small rates. When the operating regimes are optimal and the duration of the thermal cycle is short, the heat-affected zone is small and the strain makes several micrometers. If the operating mode is close to the critical cutting threshold, the quality and strain somewhat worsen again. The results of calculation of strain of the round disk, utilizing the differential equation of equilibrium with different boundary conditions proved adequate to those gained experimentally.

Imaging of Ultrasound Transmission Parameters in Photoacoustic Tomography

Srirang Manohar[1], Rene G.H. Willemink[2], Jithin Jose[1], Steffen Resink[1], Cornelis H. Slump[2], Ferdi van der Heijden[2] and Ton G. van Leeuwen[1,3]

[1]*Biophysical Engineering Group, University of Twente, Enschede, The Netherlands*

[2]*Signals and Systems Group, University of Twente, Enschede, The Netherlands*

Amsterdam, Amsterdam, The Netherlands

Main author email address: S.Manohar@utwente.nl

In photoacoustic imaging it is possible to image optical absorption contrasts deep in tissue with ultrasound-like contrasts. It is based on inducing ultrasound from absorbing structures in tissue using nanosecond laser pulses by the thermoelastic mechanism. Imaging can be performed in a computed tomographic geometry where modified acoustic backprojection is used for reconstruction. Recently, we have developed a modified photoacoustic imager that enables simultaneous measurements and imaging of the ultrasound transmission parameters of the object under investigation.

It is based on exciting ultrasound in a small absorber placed in the path of the light by the photoacoustic effect. This ultrasound is coupled to the object under investigation using water. The ultrasound propagates through the object and is detected using an ultrasound transducer at the far-end of the sample. Examination of the received signals and comparison with a reference measurement only in water allows integrated attenuation and inverse if the speed-of-sound to be ascertained as line integrals from the source to the individual detector elements. This traces a fan-beam as is well known from x-ray computed tomography. Taking projections around the object allows reconstruction of these parameters using algorithms that are based on standard fan-beam x-ray tomography. At each projection the light also illuminates the object producing ultrasound allowing conventional photoacoustic measurements as well. This method allows a hybrid of photoacoustic and ultrasound transmission parameter tomography.

The concept is introduced after a background to photoacoustic imaging. A miniature photoacoustic imaging setup is shown with a description of the phantoms that are used. Methods of estimation of integrated speed-of-sound and acoustic attenuation estimation at each projection are discussed showing simulations and phantom measurements. Finally imaging results on digital and real phantoms are shown.

References

S. Manohar, G. H. Willemink, F. van der Heijden, C. H. Slump and T. G. van Leeuwen: Appl. Phys. Lett., 91, (2007) 131911

Laser Designator and Range Finder Design

Birol Erentürk

ASELSAN MGEO Grubu, Çankırı Yolu 7.km Akyurt 06750 Ankara/Türkiye

erenturk@mgeo.aselsan.com.tr

Laser target designator and range finder design activities at ASELSAN will be summarized. Modern armed forces widely use laser technology in the battlefield. One of the main application areas of lasers in the battlefield

airborne platforms are explained. Another wide application area is range finding for fire control systems. Range finders designed for handheld use, armored vehicles, land and naval air defense systems are explained. Laser target designators use flashlamp or diode pumped Nd:YAG laser sources, new designs also include a switchable OPO for eye safe training modes. For new range finder designs eye safe Er:glass or Nd:YAG+OPO sources are preferred.

Evaluation of Microstructure of Severely Plastically Deformed Metals by Laser Ultrasound

Victor V. Kozhushko, Günther Paltauf, and Heinz Krenn
Institut für Physik, Karl-Franzens-Universität, Universitätsplatz 5, Graz, Austria

High pressure torsion (HPT) is a relatively new technique employed for severe plastic deformation of materials. Disk shaped specimens of iron and nickel have been prepared. Samples have a diameter of about 35 mm and a thickness of a few millimeters. The equivalent elastic strain of specimens linearly increases from zero at the centre of the disk up to hundred percent near the edge. The size and the orientation of grains in such materials are significantly changing with the radius and the strain status, respectively. Increasing strain yields refinement of the grains down to tens of nanometers, from which on saturation is reached. Nanocrystalline materials have special mechanical and magnetic properties making them attractive for various applications. Laser induced acoustic waves are employed for measuring the variation of the attenuation and the phase velocity of ultrasound

depends on the local grain size distribution and increases with frequency. The purpose of work is to correlate the results achieved by time-resolved optoacoustics with other methods of microstructural investigations.

The 5 ns pumping pulse of a Nd:YAG laser is used in two alternative experimental setups for excitation of longitudinal and surface pulses covering the frequency range below 100 MHz. The single longitudinal pulse is excited due to the absorption of the part of the laser pulse radiation on the surface of the specimen. The diameter of the laser spot is about 6 mm and the power density on the surface is below 20 MW/cm^2. The surfaces of specimens are polished to achieve high parallelism that is a crucial point in the experiments with longitudinal waves. The ultrasound pulse passes through the bulk to the opposite surface where the transient signal of particle displacement is detected by means of a Michelson interferometer. The time interval between echoes of the pulse allows the calculation of the phase velocity while Fourier spectra of separated echoes are used for the estimation of the attenuation of the longitudinal waves in frequency domain. The measurements show the broadening of the signal spectra from 30 MHz at the centre up to 90 MHz at the edge. The decreasing of the attenuation at high frequencies is explained in the frame of the established scattering theory.[1] Surface acoustic waves are induced by focusing the laser radiation to a line at the sample surface. The probe beam deflection method is used for calculation of the changes of the phase velocity. In this experiment the probe spot is fixed and the source is shifted. The increasing of the velocity at the edge is about 2%.

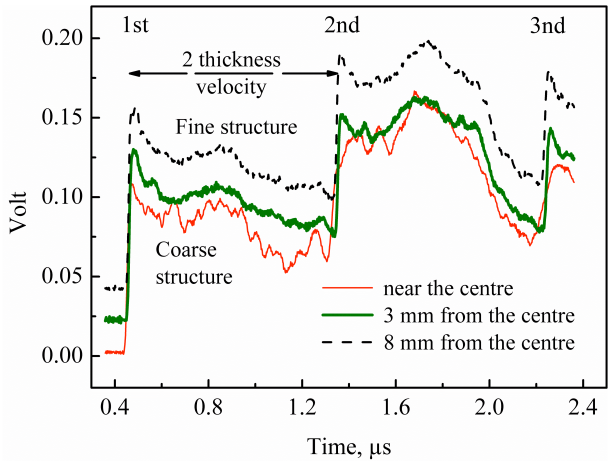

Fig. 1. The transient signals are induced by longitudinal pulses and measured by Michelson interferometer in nickel

The attenuation and the phase velocity of samples are changing during the translation of the excitation and detection spots along the radius of the sample and reflect the varying grain sizes. The grain size distribution is directly probed by electron microscopy. The measured attenuation fits well to calculated data in the Rayleigh scattering regime where the wavelength is at least 10 times larger than the mean value of the grain size.

References

1. E. P. Papadakis, "Revised grain-scattering formulas and tables", J. Acoust. Soc. Am., **37**, 703-710 (1965).

Hot-Air Atmospheric Turbulence Generator For The Improvement Of Laser Based Free-Space Communication Systems With Adaptive Optics Systems

O. Keskin[1], H. Nasibov[1], F. Hacızade[1]
[1] *The Scientific and Technical Research Council of Turkey - National Research Institute of Electronics and Cryptology (TÜBİTAK UEKAE), Gebze , Turkey*

The paper describes a simple, low-cost, characterized, statistically repeatable optical turbulence generator for the laboratory testing. Other techniques used to simulate the optical effect of the atmospheric turbulence, such as rotating phase etched screens are the usual devices used for adaptive optics (AO) tests. The possibility to test the robustness of the AO control system, used for the improvement of laser based free-space (FS) communication

systems, to turbulence variability becomes almost impossible to follow. For the given reasons, it is chosen to build a hot air optical turbulence generator, based on a previous version developed and characterized by Keskin et. All [1], referred as the prototype turbulator. In order to generate real optical turbulence (i.e. turbulent fluctuation of the index refraction), one needs to create dynamical turbulence, and temperature fluctuation of the turbulent air flow. This is achieved by mixing two air flows with different temperatures in a confined space- the turbulence chamber. It will be seen that the results obtained are in a good continuity with the prototype ones. Using equations from Le Louarn [2], it is calculated that we will be able, within the turbulence generator, to emulate a turbulence layer acceptable to see the effect of the deformable mirror conjugation. As the hot air turbulator is calibrated as a function of ΔT versus the Fried parameter, for the experimental bench, the optical beam can be sent through the turbulator in a single or multi-pass scheme, without overlapping to avoid spatio-temporal correlation between the two emulated layers. Indeed, the versatility of the turbulator makes it an ideal tool for emulating variable C_N^2 and wind velocity profiles, just by changing the temperature difference between the cold and hot air intakes, the air fans power, as it happens in the free atmosphere. The power spectrum analysis (Fig.1) shows a good agreement with Kolmogorov's homogeneous and isotropic atmospheric turbulence theory. Therefore, the device can be used with confidence to emulate a realistic turbulence in a controllable manner. Principles and characterization methodologies consist of full width at half maximum (FWHM), and angle of arrival (AoA) approaches.

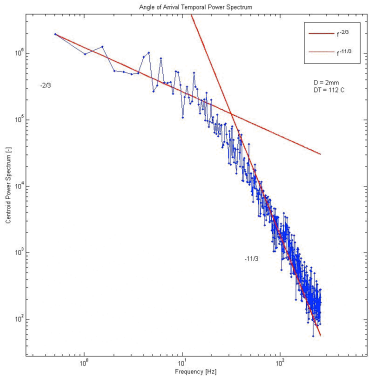

Fig. 2: Power spectrum of the centroid displacement (arbitrary units)

It is concluded that the hot-air turbulence generator can be used in particular in FSAO communication test bench developed at TUBİTAK UEKAE Optoelectronics Laboratory. Though the results are unique to the FSAO bench, the turbulator can also be used in testing other laser communication and atmosphere monitoring devices, which use AO schemes for compensation of optical disturbance effect due to laser light propagation through a turbide media.

References

1. O. Keskin, L. Jolissaint, and C. Bradley, " Hot-air optical turbulence generator for the testing of adaptive optics systems: principles and characterization," Applied Optics, 45, Issue 20, 4888-4897, (2006).
2. M. Le Louarn, N. Hubin, M. Sarazin, and A. Tokovinin, "New challenges for adaptive optics: extremely large telescopes," Mon. Not. R. Astron. Soc. , 317, 535–544 (2000).

Waveguides in Laser Crystals Inscribed by a Femtosecond Laser Beam.

A. G. Okhrimchuk[1], A.V. Shestakov[2], V. Mezentsev[1], and I. Bennion[1]
[1] *Photonics Research Group, Aston University, Birmingham, UK*
[2] *Elements of Laser Systems Co., Moscow, Russia.*

Waveguide design of laser components is a very attractive option for miniaturization of bright light sources, integration with fiber lasers components. Permanent micro modification of refractive index in dielectrics by means of femtosecond laser pulses is a novel enabling technology in photonics. It permits to inscribe low-losses active waveguides in laser crystals [1].

Few main distinct nonlinear absorption processes are relevant in femtosecond energy deposition and

electron-hole plasma and its resistive heating. Understanding of the relative contribution of these mechanisms is ultimately required for optimization of the inscription procedures [2, 3]. In this paper we present detailed experimental investigations of femtosecond energy deposition dealing with a Permanent Refractive Index Change in series of crystals and glasses. We also present theoretical and numerical modeling of the corresponding absorption processes.

We present series of waveguiding structures in laser crysatals: YAG:Nd, YAG:Cr^{4+}, $RbPb_2Cl_5$:Dy. Cross-section view of a typical structure is shown in Fig.1. Modified regions of the investigated crystals have the refractive index (1-5)*10^{-3} lower compared to unperturbed value. They are shaped as rods with oval cross section and all together comprise a waveguide cladding. A core is formed by a non-perturbed region of the crystal. Lasing properties of waveguide lasers fabricated in YAG:Nd, YAG:Nd/Cr^{4+} crystals were investigated from the point of view of efficiency and mode structure. Waveguide saturable absorber in YAG:Cr^{4+} crystal was characterized.

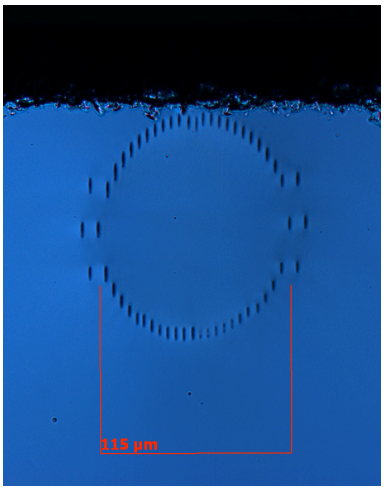

Fig.1. Microscope picture of depressed cladding waveguide in YAG:Nd crystal (end view).

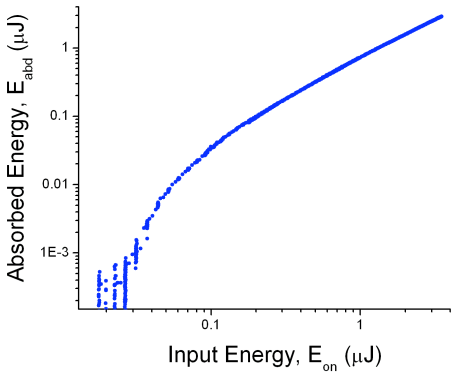

Fig.2. Dependence of a femtosecond pulse absorbed energy upon an input pulse energy.

References

1. A.G.Okhrimchuk, A.V.Shestakov, I. Khrushchev, J. Mitchell, "Depressed cladding, buried waveguide laser formed in a YAG:Nd3+ crystal by femtosecond laser writing", *Optics Letters*, **30**, 2248-2250 (2005).
2. V. Mezentsev et. al, Femtosecond laser microfabrication of subwavelength structures in photonics, *SPIE*, 6459 (2007).
3. L. Berge, S. Skupin, R. Nuter, J. Kasparian, J.-P. Wolf, Ultrashort filaments of light in weakly ionized, optically transparent media, *Reports on Progress in Physics,* V. 70, P. 1633-1713 (2007).

Phase-Lock and Frequency Stabilization of Nd:YAG Lasers

R.Hamid and C. Erdogan

National Metrology Institute (UME),
Scientific and Technological Research Council of Turkey (TÜBİTAK),
Gebze-Kocaeli, Turkey

In this work we will present results of phase lock of Nd:YAG laser to fs Ti:Sa Comb generator and frequency stabilization of Nd:YAG lasers on Doppler-free absorption spectrum of I_2 molecular gas.

Recently developed comb system gives a great contribution to measure the optical frequencies and it has an ability of precise measurement of absolute frequency of the stabilized Nd:YAG lasers [1]. In this work offset and repetition frequency of femtosecond Comb generator with spectral bandwidth

signal of Cs atomic clock [2]. Green laser beam of Nd:YAG laser was beat with the fs Ti:Sa Comb beam and the error signal was send to PZT of Nd:YAG laser for phase locking. By using this method Nd:YAG laser was locked to fs Ti:Sa Comb generator with an uncertainty of 3 Hz (Fig.1).

We measured the beat frequency between UME Nd:YAG-L1 and UME Nd:YAG-L2 which are iodine-stabilized Nd:YAG lasers. We have used the technique of saturated absorption spectroscopy (SAS), for realizing the stabilization of the laser we have chosen the method of frequency modulation and third harmonics spectroscopy technique. Our laser systems are accessible with the absorption lines of P53 (32-0) - line 1111 and R(56)32-0 - line 1110 in molecular iodine. The frequency of two similar Nd:YAG lasers was stabilized on Doppler-free absorption spectrum of I_2 molecular gas. Second harmonic laser beam (532 nm) passed trough 15 cm I_2 cell, reflected back from mirror and detected on the photodiode. PZT of the laser was modulated with a frequency of 14 kHz and third derivative of iodine 1110 R(56)32-0 line was used in frequency stabilization of lasers. One of laser stabilized on iodine 1110 R(56)32-0 a10 line ($\nu \approx 563\,260\,223\,513$ kHz) and second laser on iodine 1110 R(56)32-0 a6, a7, a8, a9 lines and beat signal was measured with a PC controlled frequency counter and a spectrum analyzer. External iodine cell pressure, modulation frequency and power of the beam versus laser output frequency investigated at 532 nm. The hyperfine line differences were measured by the beat frequency technique. In addition to this, the finger print of line 1111 - P53 (32-0) has been detected.

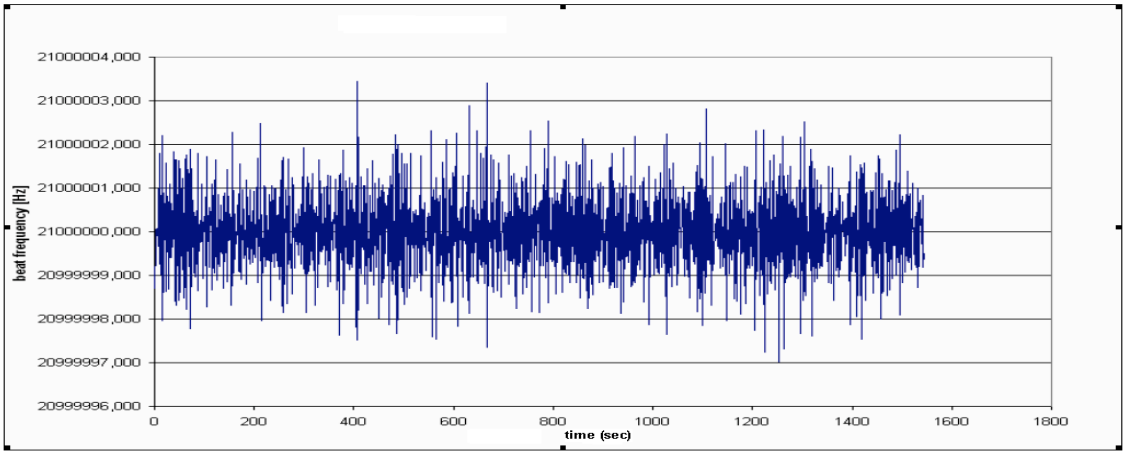

Fig 1. Time versus beat frequency of Nd:YAG laser which is phase locked to the Ti:Sa fs Comb system

References:

1. Jun Ye, Harald Schnatz, and Leo W. Hollberg, "Optical Frequency Combs: From Frequency Metrology to Optical Phase Control", IEEE Journal of Selected Topics in Quantum Electronics, **9**, 1041 (2003)
2. S. A. Diddams, D. J. Jones, J. Ye, S. T. Cundiff, and J. Hall, J. K. Ranka, and R. S. Windeler, R. Holzwarth, T. Udem, and T. W. Hansch, "Direct Link between Microwave and Optical frequencies with a 300 THz Femtosecond Laser Comb", Phys. Rev. Lett., **84**, 5102-5105 (2000)

Terahertz reflection response measurement using a phonon polariton wave

K. Katayama[1], H. Inoue[1], Q. Shen[2], T. Toyoda[2], K. A. Nelson[3]

[1] Department of Applied Chemistry, Chuo University, 112-8551 Tokyo/Japan

[2] Department of Applied Physics and Chemistry, The University of Electro-Communications, 182-8585 Tokyo/Japan

[3] Department of Chemistry, Massachusetts Institute of Technology, o2139 Massachusetts/USA

We have developed a technique for the measurements of terahertz reflection responses of various samples utilizing a propagating phonon polariton wave. Frequency tunable phonon polariton (PP) waves were generated by the recently developed continuously variable spatial frequency transient grating method.[1] The PP wave response was

In recent years, researches utilizing electromagnetic waves in a frequency range of 0.3–10 terahertz (THz) have progressed considerably. We have developed a compact optical setup for the generation and detection of phonon polariton (PP) waves with a frequency range on the order of terahertz, aiming at the development of a compact device wherein terahertz waves may be operated in a single platform. A PP wave is a coupled mode of an electromagnetic wave and polar lattice vibration, and generated in nonlinear crystals such as $LiNbO_3$ (LN) and $LiTaO_3$. Fig.1 shows the optical configuration for the generation and detection of PP waves. The tunable optical fringe pattern is used for the excitation of a PP wave. The frequency of the PP wave was controlled between the lens and grating distance, which provides a fringe pattern on a sample whose spacing can be continuously controlled. In this technique, PP waves in the frequency range of 0.4–1.5 THz can be generated. The PP wave propagates along x axis and reflected at crystal edge where a sample is to be positioned. After reflection, it comes back along the x axis, and the reflected response is measured again at the probing position. The reflected amplitude for a sample was compared with the reflected amplitude at the LN/air interface, i.e., in the absence of a sample. In this study, we measured reflection responses of PP waves when they were applied to various samples to demonstrate the terahertz spectroscopic measurements using PP waves. The refractive index and absorption was successufully obtaiend for water and luctose.[2] Since the terahertz light source, namely, a PP wave, does not need to be emitted outside a ferroelectric crystal, it is possible that the terahertz response of a sample can be obtained in an integrated form such as a microchemical cell.

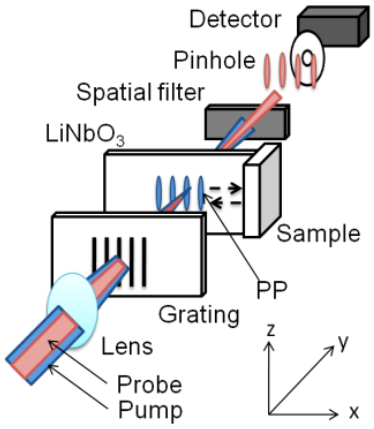

Fig.1 A schematic representation of the optical setup for the reflection measurement of a phonon polariton wave.

References

1 K. Katayama, H. Inoue, H. Sugiya, Q. Shen, T. Toyoda, K. A. Nelson, Appl. Phys. Lett. 92, 031906 (2008).
2 H. Inoue, K. Katayama, Q. Shen, T. Toyoda, K. A. Nelson, J. Appl. Phys. 105, 054902 (2009).

Lifetime and diffusion coefficient of active oxygen species generated in TiO_2 sol solutions

K. Katayama[1], M. Okuda[1], T. Tsuruta[1]
[1] *Department of Applied Chemistry, Chuo University, 112-8551 Tokyo/Japan*

TiO_2 is one of the most widely studied photocatalytic materials. It can decompose and mineralize pollutants and undesirable compounds in air and water. In general, such photocatalytic reactions start with the photoexcitation of electrons and holes(h^+) by irradiation of ultraviolet light, and generated superoxide anion and hydroxyl radical are the major reactive species produced during photocatalytic reactions. Since the efficiency of photocatalytic reactions depends on the quantity and properties of the active oxygen species, several techniques for detecting them have been developed, but there have been no methods for detecting active oxygen species in an in-situ manner.

The transient grating (TG) technique is a useful technique for detecting photoinduced reaction

species can be detected, and not only the lifetime of intermediate species but also the diffusion coefficient can be obtained. We have recently developed an improved TG method, the near-field heterodyne transient grating (NF-HD-TG) method[1], which features a simple optical setup and highly sensitive detection using a heterodyne technique. In this paper, we report a direct observation of active oxygen species without any reagents using the NF-HD-TG method.[2,3]

The principle of the NF-HD-TG method is explained in the paper [1]. The pump light was the third harmonic of a Nd:YAG laserwith a wavelength of 355 nm, pulse width of 4 ns, and pulse energy less than 0.5 mJ/pulse; the probe light was the second harmonic of an CW Nd:YAG laser with a wavelength of 532 nm. The optical cell has an internal thickness of 1 mm. The grating spacing was 40–90 μm. After a single-shot irradiation, the detected response was stored in a digital oscilloscope. The sample was a TiO_2 sol solution with a pH of 4.3 and viscosity of 4.3 mPa·s (Taki Chemical, AM-15). The average diameter of the TiO_2 particles was 30 nm.

A typical transient response of the TiO_2 sol solution is shown in Fig. 1 in the semi-logarithmic time scale for the grating spacing, 60 μm. the responses initially showed a negative signal, which increased beyond the baseline and gradually returned to it again. These responses were fitted with a sum of three exponential decay functions. To assign the three components, the change in responses due to addition of several scavengers was examined. The three components were assigned as OH•, H_2O_2, and $O_2^{\bullet}$, respectively.

The diffusion coefficients for the species OH•, H_2O_2, and $O_2^{\bullet}$ are now discussed. The diffusion coefficients of N_2 and O_2, which are similar in size to the observed active oxygen species, in aqueous solutions they are 2.3×10^{-9} and 2.5×10^{-9} m^2/s, respectively. Compared with these values, the obtained diffusion coefficients for active oxygen species were 1–3 orders of magnitude smaller. In actual, the diffusion coefficient for $O_2^{\bullet}$ was close to the value for the TiO_2 nanoparticles (4.4×10^{-12} m^2/s). Then, tt was suggested that active oxygen species are in the adsorbed state or under the adsorption isotherm on TiO_2.

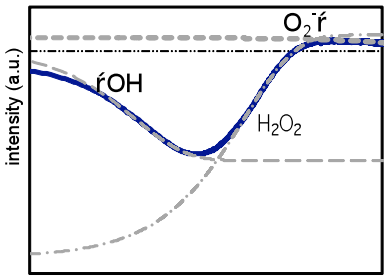

Fig.1 A NF-HD-TG response of a TiO2 sol solution after a 355 nm pulse laser irradiation. The response is consisted of three exponential decays.

References

1 Okuda, M.; Katayama, K. *Chem. Phys. Lett*. **2007,** *443,* 158.
2 Tsurata, T., Okuda, M., Katayama, K. *Chem. Phys. Lett.* **2008,** *456*, 47.

Specific character of the Sn thin films growth on amorphous Si by CBPLD method

V.V. Rocheva, E.V. Khaydukov, O.A. Novodvorsky, O.D. Khramova
RAS, Institute on Laser and Information Technologies, Shatura, Russia

The research of the Sn thin films growth on amorphous Si that is important for multilayered structures creation for spintronics have been investigated in the this paper.

The Sn thin films on silicon substrates (001) had been received by crossed-beam pulsed laser deposition method (CBPLD). Preliminary 40 nm thickness amorphous silicon films with 0,2 nm roughness were deposited on this silicon substrates. Further various thickness Sn films were deposited on amorphous Si without of unvacuumization procedure. Deposition was performed in the vacuum chamber at 10^{-6} Torr residual pressure, the Sn target was ablated by □=1,06 μm laser radiation at $5 \cdot 10^8$ W/cm^2 power density on the target. Pulse repetition frequency was equal 10 Hz. The substrate temperature was equal 30 ^{0}□. Similarly Si/Sn/Si multilayered periodical structures have been received.

The received films were investigated by atomic-force microscopy, electronic microscopy and X-ray reflectometry methods. It has been established that at Sn film thickness up to 3 nm it is possible to received atomic-smooth surfaces with 0,2 nm roughness (fig. 1a). At Sn film deposition greater thickness (more than 5 nm) was observed qualitative morphology changes of the film surface. On the surface started to appear local bulging (peeling) which height reached 50 nm (fig. 1b). At the further deposited films heightening to 40 nm all surface have been covered with it (fig. 1c). At the 100 nm film thickness surface character looked like densely located granules in the size about 100 nm (fig. 2).

The Si/Sn/Si multilayered periodical structures (Si - 3 nm, Sn - 3 nm, Si - 3 nm, 6 layers) on the silicon substrate (100) according to AFM data had a 0,2 nm surface roughness. According to X-ray reflectometry data the interface layers roughness also made 0,2 nm.

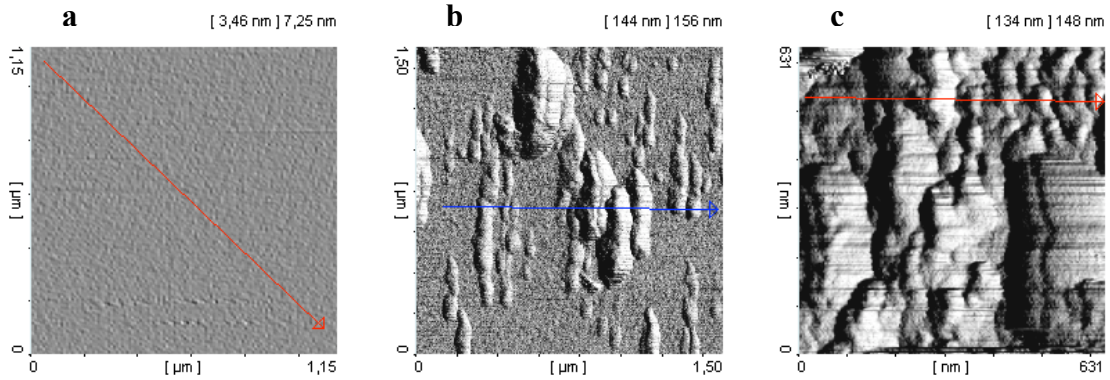

Fig. 1. AFM images of the various thickness Sn films.

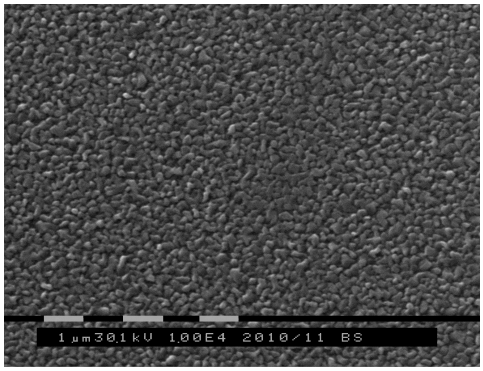

Fig. 2. Electronic microscope image of the 100 nm thickness Sn film.

Laser-based nanoengineering for biomedical applications

Boris N. Chichkov
Laser Zentrum Hannover e.V
Hollerithallee 8, 30419 Hannover, Germany

In this presentation, our research activities in laser-based micro- and nanostructuring of different materials, fabrication of nanoparticles, and biological laser printing will be reviewed. Special attention will be given to 3D microstructuring of photosensitive materials by two-photon polymerization (2PP), which is a rapidly-developing technology with a broad range of applications. The ability to produce complex 3D structures with high precision and reproducibility is very attractive for applications in regenerative medicine and, particularly, in tissue engineering for the fabrication of scaffolds. Scaffolds are highly porous 3D structures designed to support and guide cell growth, in order to artificially produce living tissue with a desired complexity and architecture. In comparison to other currently applied technologies, advantages of the 2PP technique for the fabrication of scaffolds are in the combination of unprecedented resolution, high reproducibility, and the ability to fabricate

arbitrary 3D structures directly from CAD models. Figure 1 shows an example of a highly porous 3D scaffold design (a) and SEM image of the fabricated structure (b).

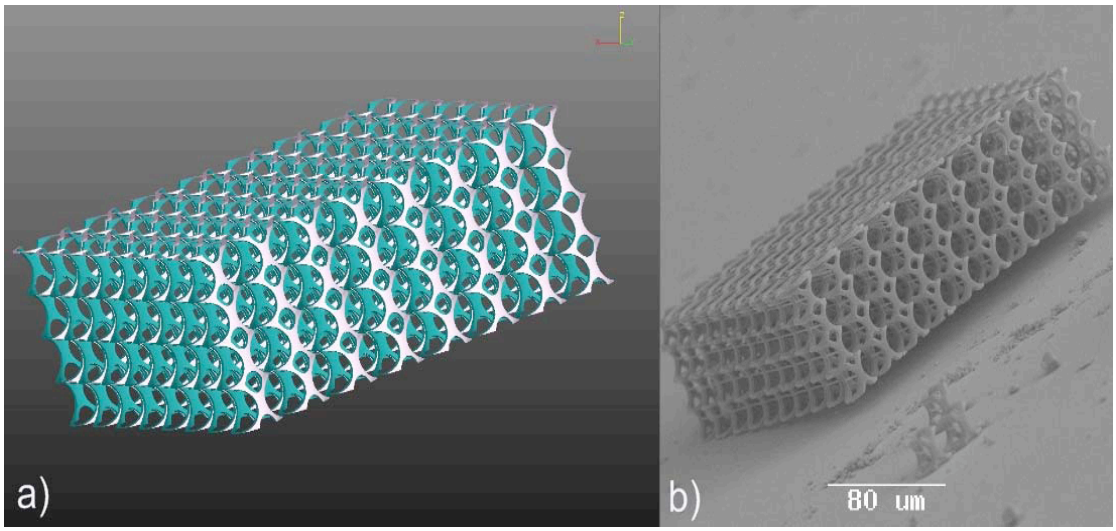

Fig. 1. Highly porous 3D scaffold with two distinct pore dimensions: a) CAD concept; b) SEM microscope image of according structure fabricated by the 2PP technique.

Further research topics and recent results obtained in cooperation with the Hannover Medical School (MHH) and related to the Rebirth Excellence Cluster will be presented

Laser stereolithography in cosmetic surgery

S.A. herebylo[1], A.V. Evseev[1], P.N. Mitroshenkov[2]
[1] *Institute on Laser and Information Technologies, Russian Academy of Sciences (ILIT RAS)*
[2] *Samara regional clinical hospital*
[1] *140700 Shatura, Moskow Region, Russia*
Fax. 8(49645)22533, e-mail: slana21@rambler.ru
[2] *443095 Samara, Russia, fax:(846) 9561260*

Computer modeling and laser stereolithography has found wide application for prepare and planning of complicated operations in reconstructive maxillofacial surgery. The base of laser stereolithography is special selectivity of laser induced polymerization of photosensitive materials. That is allow fabricate 3D plastic objects with practically any complication using, for example, layer-by-layer approach. In combination with modern CT (X-ray, NMR) inspection and computer modeling it allow rapidly fabricate practically any fragment of human body. The application of computer tomography, computer modeling and stereolithography enables the surgeons

children), increase the operation quality and, as a consequence, to reduce the rehabilitation period. In this report the results of using laser stereolithography for ear and nose reconstruction will be presented.

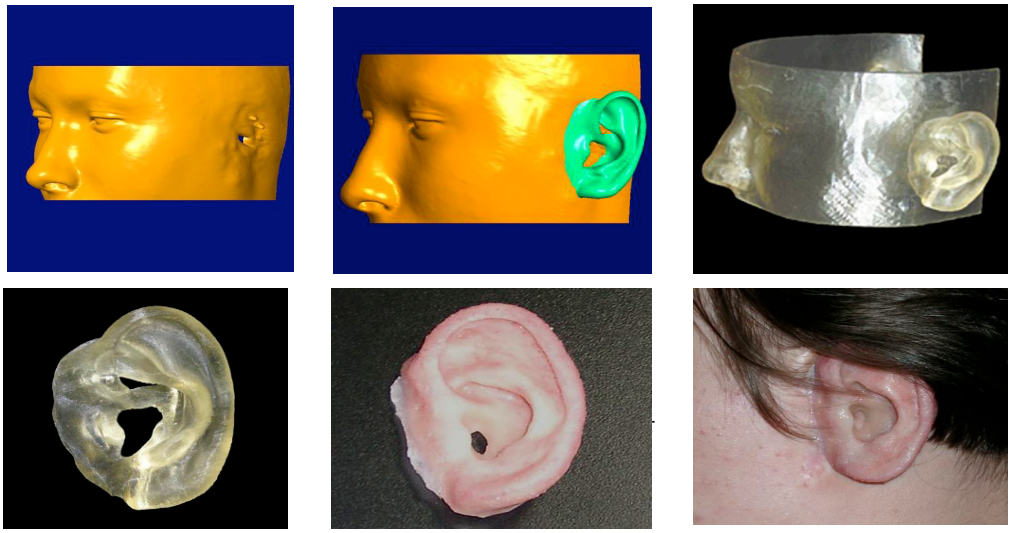

The Q-switched hybrid Er:YAG Laser

W. Zendzian[1], J. K. Jabczynski[1], L. Gorajek[1], J. Kwiatkowski[1], K. Kopczy□ski[1], H. Jelinkova[2], M. N□mec[2], J Šulc[2]
[1] *Institute of Optoelectronics, Military University of Technology, ul. gen. S. Kaliskiego 2, Warsaw, Poland*
wzendzian@wat.edu.pl, fax (4822) 666 8950
[2] *Czech Technical University,Prague, Czech Republic*

The eye-safe emission of Er^{3+}:YAG lasers at 1645 nm allows for various interesting applications such as remote sensing, free-space communications, range detection and designation [1,2]. The study describes the efficient, acousto-optic Q-switching of the Er:YAG laser at the 1645 nm eye-safe wavelength. For longitudinal pumping at the wavelength of 1532 nm, a linear-polarized 10 W erbium fiber laser radiation was used. The investigated Er:YAG crystals were 25 mm and 40 mm long and their erbium concentration was 0.25 % and 0.2 %, respectively. The active crystals were mounted in a copper heat-sink maintaining a 288 K temperature of coolant

oscillator near the output mirror of the resonator. Laser output characteristics were performed on the dependence on the parameters of output coupler reflectance (R= 95%, 90%, 85%) and the repetition rate (from 0.1 to 5 kHz), see fig. 1 and fig. 2.

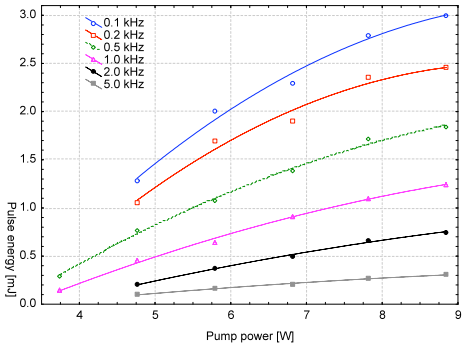

Fig. 1. Pulse energy of Er:YAG laser versus pump power for different repetition rate

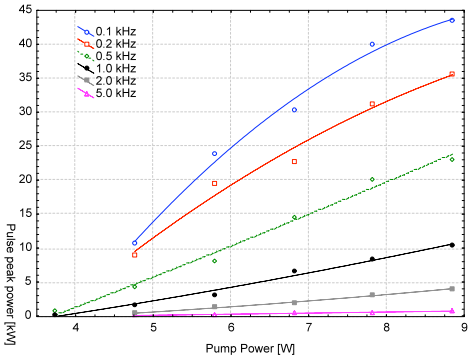

Fig. 2. Pulse peak power of Er:YAG laser versus pump power for different repetition rate

For maximum incident pump power of 8.9 W, pulse energy up to 3 mJ was generated with a pulse duration less than 70 ns at a 100-Hz repetition rate corresponding to a peak power of 43.5 kW.

This work was financed by Polish Ministry of Science and Higher Education under project NN515414834 and a Grant from the Czech Ministry of Education No. MSM6840770022.

References

1 Kalin Spariosu, Victor Leyva, Robin A. Reeder, and Matthew J. Klotz, "Efficient Er:YAG Laser Operating at 1645 and 1617 nm", *IEEE Journal of Quantum Electronics*, **42,** 182-186 (2006)

2 M. Eichhorn, Quasi-three-level solid-state lasers in the near and mid infrared based on trivalent rare earth ions", *Applied Physics B*, **93**, 269-316 (2008)

Pedestal Suppression in a Short-pulse Fiber-laser Output by Soliton Self-frequency Shift in a Photonic-crystal Fiber

D.A. Sidorov-Biryukov,[1] E.E. Serebryannikov[1], A. Voronin[1], A. Fernandez,[2] L. Zhu,[2] A. Pugzlys[2] , F.Ö. Ilday,[3] J.C. Knight,[4] A. Baltuška[2], and A.M. Zheltikov[1]

[1]*Physics Department, International Laser Center, M.V. Lomonosov Moscow State University, Russia*
[2]*Institute of Photonics, Vienna University of Technology, Vienna, Austria*
[3]*Physics Department, Bilkent University, Cankaya, Ankara, Turkey*
[4]*Centre for Photonics and Photonic Materials, Department of Physics, University of Bath, United Kingdom*

Discrimination of an ultrashort light pulse against an extended low-power pedestal is one of the key operations on a short-pulse laser output often needed for a clean, physically unambiguous high-intensity-laser--matter interaction experiment and for high-quality optical signal transmission. Fiber-format pedestal suppression is of special value for rapidly growing fiber-laser technologies. Nonlinear Kerr-effect-induced polarization phenomena offer an elegant solution to the problem of pedestal suppression in the fiber format [1]. However, for femtosecond fiber sources, pedestal suppression without a substantial temporal broadening of the main peak is often necessary for high-field physics and optical information technologies. Here, we show that soliton self-frequency shift [2, 3] of ultrashort light pulses in a highly nonlinear photonic-crystal fiber (PCF) [4, 5] allows a high-peak-power femtosecond pulse to be discriminated from a picosecond pedestal in the output of a positive-dispersion Yb fiber laser [6]. The central, most intense part of the laser pulse tends to evolve toward a soliton, experiencing a continuous red shift due to the Raman effect, which both spectrally and temporally isolates the soliton from the nonsolitonic, rapidly dispersing part of the field. As a result of this solitonic dynamics, high-contrast, pedestal-free 80-fs pulses with a milliwatt-range average power and kilowatt-level peak power have been generated at the output of an Yb-fiber-laser--PCF-discriminator system.

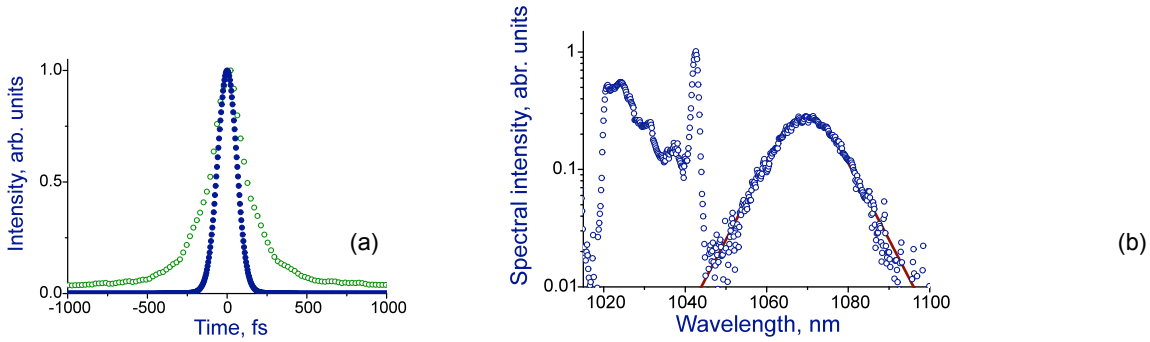

Fig. 1. (a) The autocorrelation of the compressed Yb-fiber-laser output (open circles) and PCF output (filled circle); (b) the spectrum of precompressed Yb-fiber-laser pulses transmitted through a 160-cm-long piece of PCF (open circles) and a hyperbolic-secant fit of the red-shifted solitonic feature (solid line).

This study was supported in part by the Russian Foundation for Basic Research (projects 09-02-01076, 09-02-12373, 09-02-91004)

References

1. R.H. Stolen, J. Botineau, and A. Ashkin, Opt. Lett. 7, 512 (1982)
2. F.M. Mitschke and L.F. Mollenauer, Opt. Lett., 11, 659-661 (1986).
3. E.M. Dianov, A.Y. Karasik, P.V. Mamyshev, A.M. Prokhorov, V.N. Serkin, M.F. Stel'makh, and A.A. Fomichev, JETP Lett. 41, 294-297 (1985).
4. P.St.J. Russell, Science 299, 358 (2003).
5. J.C. Knight, Nature 424, 847 (2003).
6. J. R. Buckley, F. W. Wise, F. Ö. Ilday, and T. Sosnowski, Opt. Lett. 30, 1888 (2005).

Formation dynamics of gold nanoparticles detected by single-shot near-field heterodyne transient grating method

K. Katayama[1], Y. Nakazato[1], K. Taniguchi[1],T. Eitoku[1]
[1] *Department of Applied Chemistry, Chuo University, 112-8551 Tokyo/Japan*

Gold nanoparticles have been used in catalysis, photoelectronics, and in various other applications. To use the particles effectively for these applications, monodispersed gold nanoparticles are necessary, and various synthetic methods for preparing them have been proposed. In general, the formation processes of nanoparticles start with nucleation, which involves aggregation of tens or hundreds of metal atoms, followed by the growth of the nuclei into particles. However the reaction mechanism is still not cleared because (1) the formation dynamics consists of multi-step complicated reaction processes and (2) the involved chemical species are typically difficult to detect, because intermediate chemical species have short lifetimes, and usually cannot be detected with a conventional spectrometer.

The transient grating (TG) technique is a useful technique for detecting photoinduced reaction dynamics. Because this technique is capable of monitoring refractive index changes, optically silent chemical species can be detected, and not only the lifetime of intermediate species but also the diffusion coefficient can be obtained. We have recently developed an improved TG method, the near-field heterodyne transient grating (NF-HD-TG) method,[1,2] which features a simple optical setup and highly sensitive detection using a heterodyne technique. In this paper, we report a direct observation of formation dynamics of gold nanoparticles triggered by UV pulse irradiation using the NF-HD-TG method.[3]

The principle of the NF-HD-TG method is explained in the paper [1]. The pump light was the third harmonic of a Nd:YAG laserwith a wavelength of 355 nm, pulse width of 4 ns, and pulse energy less than 0.5 mJ/pulse; the probe light was the second harmonic of an CW Nd:YAG laser with a wavelength of 532 nm. The optical cell has an internal thickness of 1 mm.. $HAuCl_4 \cdot 4H_2O$ was purchased and diluted without further purification; the concentration was 10 mM. Poly(vinylpyrrolidone) (K-30, average molecular weight: 40000) at a concentration of 0–1.0 mM was used as a protective agent for the gold nanoparticles.

Transient responses of $HAuCl_4$ for various PVP concentrations are shown in Fig.1 in the semi-logarithmic time scale. Successfully we could observe the response for the photoreduction reaction by a single-shot UV pulse irradiation. In general, the NF-HD-TG response consists of the sum of exponential decay curves with positive or negative signs. The negative and positive sign indicates that the observed reaction dynamics corresponds to the reactant species and product species, respectively. Then, we can distinguish whether the response is originated from the reactant or product species. In the absence of PVP, the response consisted of two exponential decay curves with a positive and negative signs. Then, they correspond to $HAuCl_4$ and $HAuCl_2^{2-}$ as reactant and product species, respectively. As the PVP concentration increased, not only the two species but also gold species making a complex with PVP were observed as another reactant and product species. Furthermore, another response was observed on the temporal order of a few seconds as a product species. Since the corresponding PVP concentration agreed with the threshold PVP concentration for nanoparticle formation, the component was assigned to the gold nanoparticle as a product species. From the diffusion coefficient of the response for the gold nanoparticle, the diameter was calculated, and it was 2-4 nm in diameter. Thus, it was confirmed that the component corresponds to the nanoparticle nuclei.

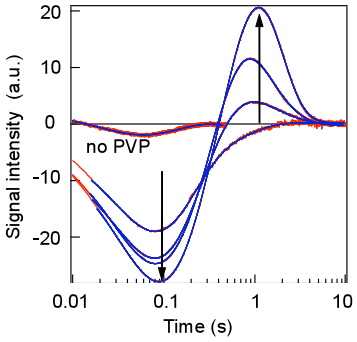

Fig.1 A NF-HD-TG response of a $HAuCl_4$ solution (10 mM) for various PVP concentrations. The arrow indicates the PVP concentration increase.

The erosive laser plume researches at the silicon ablation in vacuum

E.V. Khaydukov, V.V. Rocheva, A.A.Lotin, O.A. Novodvorsky, L.S. Parshina
RAS, Institute on Laser and Information Technologies, Shatura, Russia

The characteristics of erosion plume from the silicon target b□ the Langmuir probe method have been investigated. The YAG: Nd^{3+} laser (□=1,06 μm) for ablation was used. The ions energy spectra in the plume from one silicon target have been investigated. In the plasma plume formed by crossed plumes from two targets (crossed-beam pulsed laser deposition method (CBPLD)) has been investigated too. The ions time-of-flight curves at different probe-target distances in the 35-160 mm range have been received. It was established that ions time-of-flight curves of the one target erosion plume are represented the sum of one-dimensional velocity Maxwellian distributions for several ions groups.

It was established that at plumes crossing (CBPLD scheme, fig. 1) not all ions groups have been deviated.

The ions deviation and their energy spectrum were theoretically considered for crossed plumes. The satisfactory agreement at comparison with experimental researches results has been received.

The different sizes microparticles velocity distribution has been measured experimentally in the plasma plume formed from one Si target (fig. 2).

It was established that the plume is nonequilibrium even in connection of microparticles.

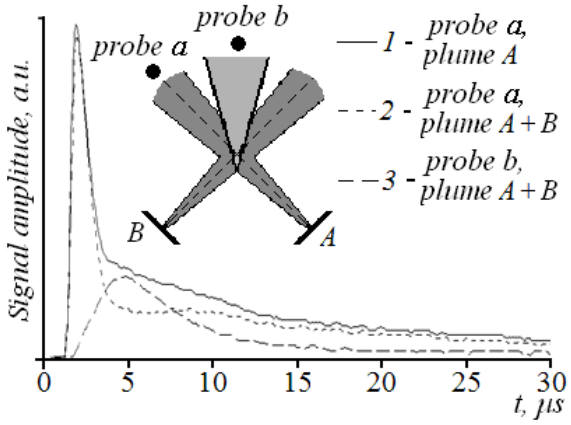

Fig. 1. The plume time-of-flight curves at the probe to a target 102 mm distance: 1 - a probe on the A plume axis at only A target ablation; 2 - a probe on the A plume axis at both A and B targets ablation, 3 - b probe on the bisector of angle between axes of plumes expansion at both A and B targets ablation.

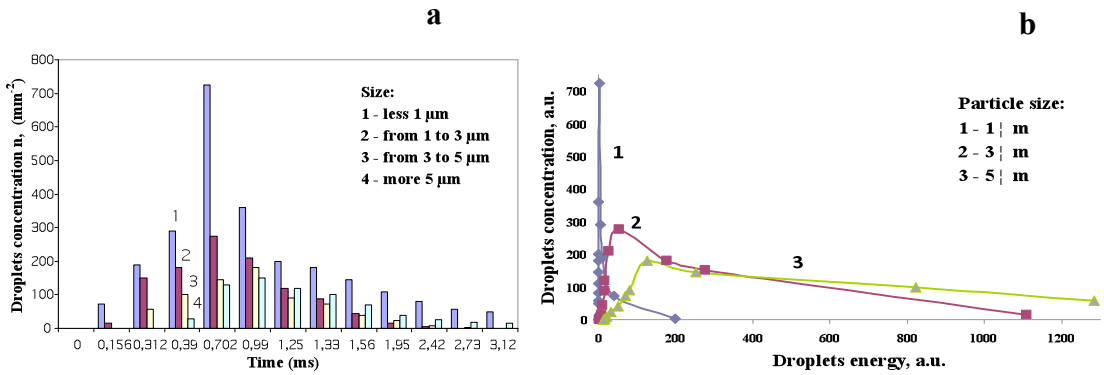

Fig. 2. The experimentally received different sizes droplets distribution during the various time moments from the Si targets ablation beginning: a) number n of the various size drops that got on 1 mm^2 of substrates during the various time moments from the ablation beginning; b) various sizes drops kinetic energy distribution.

Polymeric Surfaces during MEMS Fabrications

E. Mocanu[1] , P. Sterian
[1] *University Center for Optical Engineering and Photonics*
Bucharest Polytechnic University, 77206 Bucharest, Romania

This article tries to provide a comprehensive image of the recent state of the art of polymer based MEMS—including materials, fabrication processes, and representative application devices including medical sensors. In this paper we present results obtained with a ComPEX 205 KrF laser and an optical system that assures a working precision of 1 μm. Our main research area is the improving the parameters of microfabrication of the polymers used in the new generation of microelectronics. We try to obtain better results by understanding the chemical mechanism of laser polymer interaction. Polymer materials provide many advantages in terms of cost, mechanical properties, and ease of processing.

The type of material bond mainly determines the dominant UV excimer-material interaction mechanism, which drives the material removal process. The photolytic interaction is prevalent for covalent bonds, which are very

ceramics, glasses, and metals, tend to undergo pyrolytic dominated mechanism during irradiation by UV excimer beams [1]. Of major importance in patterning polymers is to have a clean operation without minimum thermal damage of the remaining material and a predictable ablation rate as a function of the laser energy flux. We want to establish the best laser parameters so that we may obtain holes without debris even if we use a longer wavelength, eg 308 nm. Considering that the ablation threshold for polymers is quite low longer wavelengths are sometimes more suitable.

We try to fully understand the mechanisms of photochemical ablation by measuring some very short time processes with an iStar ICCD camera [2]. The morphological behaviour and the dynamics are quite different from the classical photothermal processes. In this way we hope to improve the techniques of decomposition and ablation and to offer better alternatives to the existing polymeric materials and also to establish the best laser parameters according to the material and the purpose. Nevertheless we want to play an active role in the development of new biomaterials and biosensors.

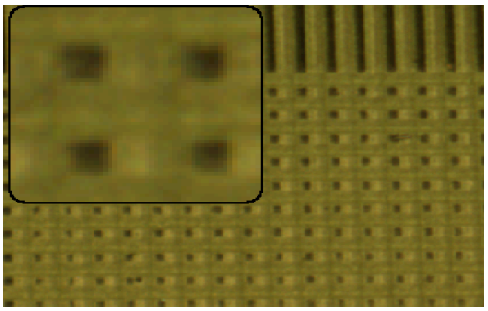

Fig 3 (a) A pattern of 100um x 100 um at 200mJ and 1Hz

References

1. R. Srinivasan, B. Baren, Chem. Rev. **89** (1989) 1303.
2. Tomokazu Masubuchi, Hiroshi Fukumura, Hiroshi Masuhara, Kenkichi Suzuki, Nobuaki Hayashi, „*Laser-induced decomposition and ablation dynamics studied by nanosecond interferometry . A polyurethane film"*, Journal of Photochemistry and Photobiology A: Chemistry **145** (2001) 215–222A. Paperauthor, B. Paperauthor, "The name of the journal paper", *Journal name*, **32**, 849-867 (2006).

Imaging of Live Mammalian Embryos with Confocal Microscopy and Optical Coherence Tomography

Kirill V. Larin[1*], Irina V. Larina[2], Saba Syed[1], Steven Ivers[2], and Mary E. Dickinson[2]
[1]*Department of Biomedical Engineering, University of Houston, Houston, Texas, USA*
[2]*Department of Medicine, Baylor College of Medicine, Houston, Texas, USA*
University of Houston, 4800 Calhoun Rd., N207 Engineering Bldg 1
Houston, TX 77204-4006
Phone: 713-743-4623
klarin@uh.edu

Defects in the cardiovascular (CV) system are the most common reasons of birth deaths. The mouse is a superior model for identifying and understanding mammalian CV birth defects. Currently, there is a lack of imaging

capabilities and limitations of confocal microscopy and Swept Source Optical Coherence Tomography (SSOCT) for live mouse embryo 2-D and 3-D imaging and hemodynamic measurements in 7.5-10.5 day embryos. For confocal imaging, we generated novel transgenic mouse model, Tg(Flk1-Myr:Cherry) that allows for visualization of cardiovascular development on the sub-cellular level (Fig 1). Our SSOCT data show that individual circulating blood cells can be visualized with structural SSOCT and the velocity of single moving blood cells could be measured during different phases of heartbeat cycle with Doppler SSOCT without use of any fluorescent markers (Fig 2). These results suggest that these complimentary imaging modalities could be extremely useful tools for structural and hemodynamic analysis at the earliest stages of mammalian blood circulation in different scales ranging from whole embryo (SSOCT) to sub cellular level (confocal microscopy).

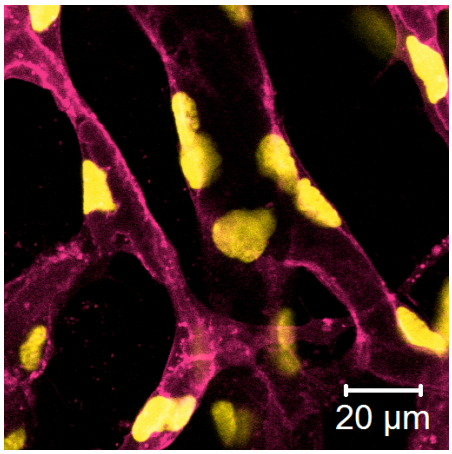

Fig. 1. mCherry Expression in the Embryonic Trunk on Embryonic Day 12.5

Fig. 2. Doppler OCT velocity signals from blood cells on the embryonic day 8.5. (A) Structural and corresponding color coded Doppler velocity images acquired at different phases of the heartbeat cycle. Green corresponds to zero velocity. Individual blood cells are distinguishable in the dorsal aorta. (B) Magnified view of the same area showing Doppler signal from single cells as well as a small group of cells.

Diamond *pn*-Junction for UV Streamer Laser

Sergei G. Buga, Vladimir D. Blank, Vitalii S. Bormashov, Victor N. Denisov, Sergei A. Terentiev, Alexei N. Kirichenko, Nikolai V. Kornilov, Michail S. Kuznetsov, Victor N. Mordkovich, Edyard G. Pel', and Sergei A.Tarelkin
Technological Institute for Superhard & Novel Carbon Materials, Troitsk, Russia

Diamond is a wide-band-gap (5.45 eV) semiconductor with outstanding electrical and optical properties. Diamond *p-n* junctions emit light in a wide spectral range from narrow UV band at 235 nm to a far red [1-3]. A narrow UV band is associated with the free-exciton recombination. UV-light emission realizes in a wide temperature range well above 300K, because the exciton binding energy in diamond is relatively high: 80 meV. A set of experimental light-emitting diamond diodes have been made by B, Li implantation of Ia, Ib, IIa diamonds [1] and homoepitaxial growth of B, S, P doped diamond films using microwave plasma chemical vapor deposition (MPCVD) technique [2-4].

We used an alternative method of formation of *p-n* junction on synthetic single crystal IIb type diamond grown by high-pressure-high-temperature method and investigated its light emission and electrical properties.

concentration ~ 10^{16} cm^{-3}. One side of the plate was implanted with P ions at the energy of 100 keV and the concentration of ~ $2 \cdot 10^{20}$ cm^{-3}. The opposite side was implanted with boron at 180 keV energy and the concentration of $1.3 \cdot 10^{21}$ cm^{-3}. In the other case *p-i-n*-structure have been fabricated by MPCVD growth of 5-8 μm thick pure diamond IIa layer on IIb type substrate with the following implantation of P donor ions. The electroluminescence spectra were investigated at different values of bias voltage and constant current in regular and *S*-part of the current-voltage characteristics. Strong exciton recombination emission was observed in UV range 235-250 nm at the current density up to 100 $A*cm^{-2}$. The spectrum in excitonic range transforms at transition from regular conductivity to forward electrical avalanche breakdown regime. Simultaneously a set of sharp EL lines appeared in the range of 250-652 nm on the broad A-band background (Fig.1, a).

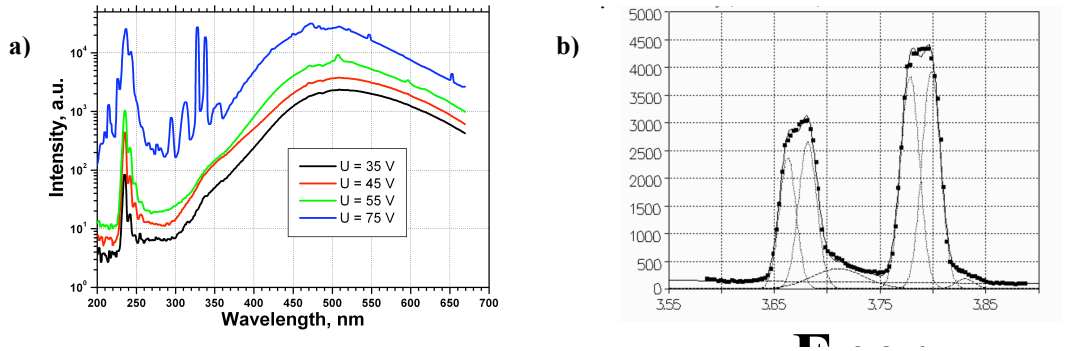

Fig 1. Semilogarithmic plots of EL spectra at different values of voltage and current in *p+-p-n* structure (a) and peak fit analysis of UV emission lines (b).

The BHWHM (band halfwidth at a half of magnitude) of Gauss peaks was in the range of 7-20 meV, that is significantly less than the temperature spread k_BT = 25 - 50 meV at temperatures 300 – 600 K (Fig.1, b).

We attribute appearance of narrow EL bands to superluminescence effect at electron transitions from P energetic level (0.6 eV below the conduction band) directly to boron acceptor level (0.37 eV above the valence band) or via intermediate nitrogen donor level (1.6 eV below the conduction band). The sublevels associated with defects have place, thus a set of lines appear in the 3.5-4.5 eV range. The superluminescence in diamond *p-n* junction opens a way to make streamer UV laser.

References

1. A.A. Melnikov, A.V. Denisenko, A.M. Zaitsev et al.,"Electrical and optical properties of light-emitting p-i-n diods on diamond", *J. Appl. Phys*., **84**, 6127-6134 (1998).
2. K. Horiuchi, A. Kawamura, T. Ide, et al., "Efficient free-exciton recombination emission from diamond diode at room temperature", *Jpn. J. Appl. Phys*. **40**, L275-278. (2001).
3. S. Koizumi K Watanabe, M. Hasegawa, H. Kanda, "Ultraviolet emission from a diamond pn junction", *Science*, **292**, 1899-1901 (2001).
4. H. Kato, S. Yamasaki, H. Okushi, "*n*-type doping of (001)-oriented single-crystalline diamond by phosphorus" *Appl. Phys. Lett*. **86**, 222111-222111-3 (2005).

Actively Q-switched diode pumped Tm:YLF Laser

J. K. Jabczynski[1], L. Gorajek[1], W. Zendzian[1], J. Kwiatkowski[1],
K. Kopczynski[1], H. Jelinkova[2], M. N□mec[2], J Šulc[2]
[1] *Institute of Optoelectronics, Military University of Technology,*
00908 Warsaw ul. gen. S. Kaliskiego 2, Poland,
[2] *Czech Technical University, Prague, Czech Republic*

jjabczynski@wat.edu.pl, fax (4822 6668950

We have demonstrated efficient Q-switched generation of diode pumped Tm:YLF laser end-pumped by 30-W fiber coupled laser diode bar [1,2]. The incident pump density exceeded above 5 times the saturation pump density, thus the drawbacks of quasi-three-level scheme have been mitigated. We have obtained the best output characteristics (slope and maximum power) for out-coupling losses of 20% evidencing the high roundtrip gain for maximum pump power. Above 7 W of output power for incident 26 W pump

power in free running regime was achieved in the best case of low duty cycle pumping for short 70-mm long cavity. Above 2 W of output power was demonstrated for CW pumping for elongated 220-mm cavity. The divergence angle was about 4.3 mrad and estimated parameter $M^2 < 1.3$. To improve the output characteristics in free running regime the optimization of pump size in the gain medium, application of longer rod and optimized cavity design should be examined.

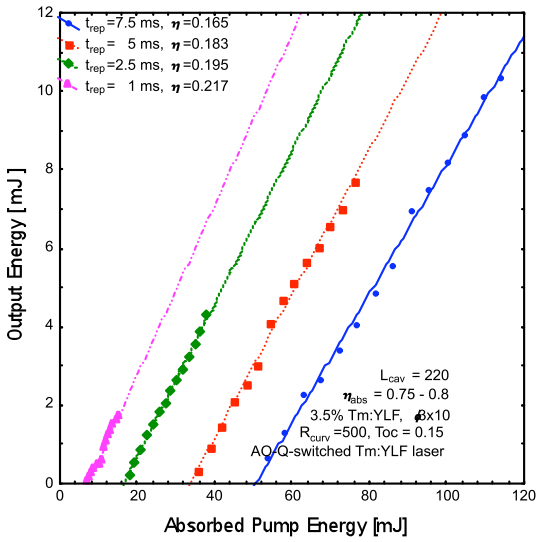

Fig. 1. Output energy vs. absorbed pump energy for different repetition periods

In the experiments on active Q-switching by means of acousto-optic modulator, up to 10-mJ output energy was demonstrated limited by damage of laser elements (see Fig. 1,2). Near 0.5 MW peak power with the pulse durations of 22 ns was achieved for 10-Hz repetition rate with 10% duty cycle of pumping regime. The 1.7-W of average power with 12 kW peak power and 1000 Hz repetition rate was demonstrated for cw pumping regime. The developed laser could constitute the basis for development of the tunable, Q-switched laser source operating at the 2-μm wavelength. Moreover, it could be used as a pump source for Ho:YAG and Cr:ZnSe lasers operating in gain switching regime for the longer (> 2 μm) wavelengths.

This work was financed by Polish Ministry of Science and Higher Education under projects: NN515345036, 0T00A00330, N515423033 and the Grant of the of Czech Ministry of Education No. MSM6840770022.

References

1 J.K. Jabczy□ski, W. Zendzian, J. Kwiatkowski, H. Jelinkova, J. Sulc , M. Nemec, „Actively Q-switched diode pumped thulium laser", *Las. Phys. Lett*, **4**(12), 863-867 (2007)

2 J.K. Jabczynski, □. Gorajek, W. Zendzian, J. Kwiatkowski, H. Jelinkova, J. Sulc and M. Nemec, „High repetition rate, high peak power, diode pumped Tm:YLF laser", *Las. Phys. Lett*, **5**, lapl.200810107 (2008).

Ho:YAG tunable hybrid laser pumped by a Tm-doped fiber laser

J. Kwiatkowski[1], J.K. Jabczynski [1], W. Zendzian[1], L. Gorajek[1], H. Jelinkova[2], J. Sulc[2], M. Nemec[2], P. Koranda[2]

[1] Institute of Optoelectronics, 2 Kaliskiego Str., 00-908 Warsaw, Poland
jkwiatkowski@wat.edu.pl, fax: +48 22 666 89 50
[2] Czech Technical University, Faculty of Nuclear Sciences and Physical Engineering, Břehová 7, 115 19 Prague 1, Czech Republic

Compact, tunable, laser sources operating in a 2-μm wavelength range are required in various applications. The hybrid configuration with the Tm:fiber laser as a pump source and the oscillator based on bulk holmium doped crystal offers wide possibilities due to the high energies and peak powers, scalability, compactness, modularity

spectroscopic, thermo-optic and mechanical properties. The aim of this work was to examine the feasibility of tunable oscillation of a compact hybrid laser based on the Ho:YAG crystal pumped by a continuously running Tm:fiber laser with the emphasis placed on potential tunability.

A Tm:fiber laser at 1908-nm was used for the pumping of the tunable Ho:YAG laser. The pump beam was focused on the 0.3 mm diameter waist located inside the 1% 20 mm long Ho:YAG rod. The 115 mm long cavity consisted of a rear flat dichroic mirror and curvature output coupler of 150 mm radius and 5% transmission for a 2000-2200 nm wavelength. For tuning, a Lyot filter consisting of a quartz plate of a 2.1 mm thickness was applied. The output power of 1.13 W with a 53% slope efficiency for 3 W of absorbed pump power was reached at the wavelength of 2132.8 nm.

The tunability between a 2075 – 2135 nm wavelength range was demonstrated (fig. 1). The linewidth of tunable oscillation was not wider than 1 nm (FWHM) for all the tuning range.

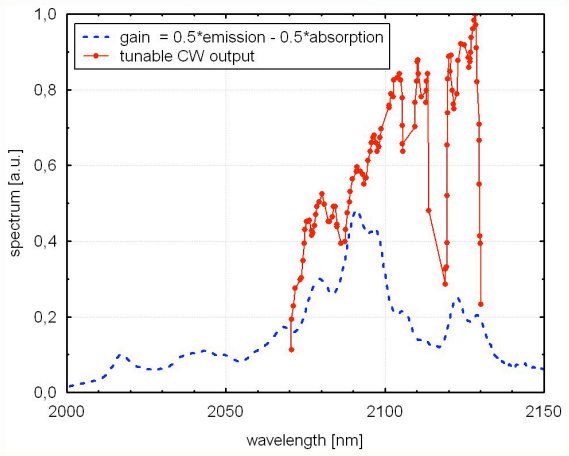

Fig. 1. Tunable output of the Ho:YAG hybrid laser vs wavelength (continuous curve), gain spectrum (dashed curve)

In the next step of experiments we intend to deploy the acousto-optic Q-switch to enable pulsed, tunable operation, similarly as was demonstrated in the case of the Tm:YLF laser [1, 2].

This research has been supported by The Polish Ministry of Science and Higher Education under project No. N N515 4230 33 and by a Grant from the Czech Ministry of Education No. MSM6840770022.

References

1 J.K. Jabczynski, L. Gorajek, W. Zendzian, J. Kwiatkowski, H. Jelinkova, J. Sulc, M. Nemec, "High repetition rate, high peak power, diode pumped Tm:YLF laser", *Laser Phys. Lett.* **6**, 109-112 (2009).

2 J.K. Jabczynski, W. Zendzian, J. Kwiatkowski, H. Jelinkova, J. Sulc, M. Nemec, "Actively Q-switched, diode pumped thulium laser", *Las. Phys. Lett.* **4**, 863-867 (2007).

Z-Scan Study of Concentration Dependency of Nonlinear Optical Responses In Triphenylmethane Dye Solutions

H. Nasibov, İ. Mamedbeili.

The Scientific and Technical Research Council of Turkey-National Research Institute of Electronics and Cryptology (TÜBİTAK-UEKAE), Gebze, Turkey

The results of the investigations of the continuous wave laser induced third-order nonlinear properties of Brilliant Green (BG) solutions, which belong to triphenylmethane organic dye group, is presented. The measurements were carried out by utilizing the single beam Z-scan technique (Fig.1 (a)) [1]. In our previous work [2], we have investigated third-order nonlinear properties of 1% BG medical solutions, which consists of 1gr of BG in 100 ml of 63% ethanol and 27% purified water solution. In present work we have investigated concentration dependency of third-order nonlinear properties of BG in different organic solvents: toluene, carbon tetrachloride (CCl_4) and acetone. Experiments were carried out at 470 nm, 535 nm and 633 nm laser wavelengths. The samples of BG were prepared in following concentrations (same for all solvents): 0.42 $x10^{-3}$

mol/L, 0.28x10^{-3} mol/L, 0.21x10^{-3} mol/L, 0.14x10^{-3} mol/L, 0.12x10^{-3} mol/L, 0.10 x 10^{-3} mol/L, and 0.07 x10^{-3} mol/L.

Fig. 1 (b) exhibits the open aperture (OA), close aperture (CA) and the division of the CA by OA normalized transmittance curves of BG solutions with concentration of 0.4x10^{-3} mol/L at 589 W/cm^2. The similar Z-scan traces were observed for all of the samples. The peak-to-valley signature (pre-focal peak followed by a post-focal valley) of the CA normalized transmittances indicate that the sign of the nonlinear refractive index n_2 of BG is negative ($n_2 < 0$), which is due to a self-defocusing effect.

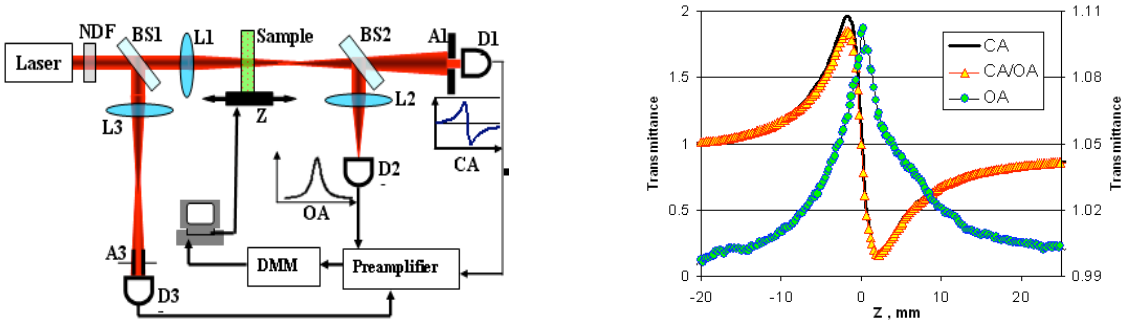

(a) (b)

Fig.1. (a) Schematic diagram of the experimental setup , (b) Normalized open aperture (right axis), close aperture and CA/OA (left axis) Z-scan transmittance of the BG.

The concentration dependency of the nonlinear phase-shift $\propto B_0$, of the nonlinear refractive index n_2, of the nonlinear absorption coefficient $\cup$(cm/W), of the real $\mathrm{Re}\left|\chi^{(3)}\right|$ and imaginary parts $\mathrm{Im}\left|\chi^{(3)}\right|$ of the third-order nonlinear optical susceptibility $\left|\chi^{(3)}\right|$ measurements were studied at following incident laser intensities: 207 W/cm^2, 283 W/cm^2, 353 W/cm^2, 412 W/cm^2, 471 W/cm^2, 589 W/cm^2. It was found that the increasing of both, the solution concentration and incident laser intensity increases nonlinear properties. The dependence of the nonlinear phase-shift and nonlinear refractive index from concentration is found to be linear in all investigated ranges and samples. However, due to the simultaneously presence of both the thermal and saturation absorption effects while propagation of continuous wave laser beam in the samples, the dependence of nonlinear absorption coefficient on the concentration exhibits nonlinear behaviour. More detailed study of nonlinear absorbing in BG solutions by employing high rate pulse lasers are subject of our future investigations. Overall results show a great potential of the BG for low-power cw laser nonlinear optical devices.

References

1 M. Sheik-Bahae, A. A. Said, E. W. Van Stryland, "High-sensitivity, single-beam n2 measurements," *Opt. Lett.*, **14**, 955-957, (1989)

2. I. Mamedbeili and H. Nasibov, "Large third-order optical nonlinearities in brilliant green solutions induced by cw He-He laser*", Laser Physics*, DOI 10.1134/S1054660X09190141, (2009).

Investigation of Formation Nanostructured Thin Films in Process of Femtosecond Laser Deposition

Gerke M.N, Kutrovskay S.V., Kucherik A.O., Prokoshev V.G., Arakelian S.M.
Department of Physics and Applied Mathematics, Vladimir State University,
Gorky st. 87, Vladimir, Russia
Phone: (4922) 533350
Fax: (4922) 533358
E-mail: laser@vlsu.ru

The purpose of this work was ablation investigation at interaction of radiation of femtosecond laser system Ti: Sp with a solid-state target in vacuum.

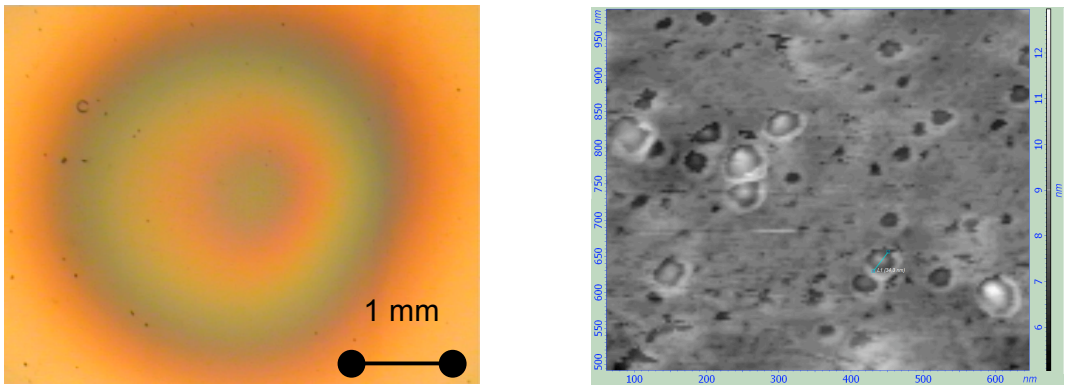

a) b)

Fig. 1. Formation thin film on the substrate: a) optic image of the deposition area; b) AFM image of the deposition structure.

After laser action samples were investigated on atomic-force microscope Ntegra AURA. Features of deposition area (see fig. 1) are found out.

Laser ablation, the subsequent carrying over and condensation of a target material on a substrate are applied in technology of laser carrying over to formation of film elements.

Phase Retrieval Method for Reconstructing Wavefront Aberration of Ultrashort High-power Laser Pulse

Jeong T. M., Kim C. M., and Lee J.
Advanced Photonics Research Institute, GIST, Gwangju, Republic of Korea

Wavefront aberration of a laser pulse determines the focal spot, together with an intensity profile of the laser pulse. In many cases, wavefront can be measured with a wavefront sensor or an interferometer [1, 2]. However, sometimes, it is not possible to measure wavefront of a laser pulse with a wavefront sensor or an interferometer. The wavefront reconstruction using the phase retrieval method can be an alternate approach to obtain information on a wavefront of a laser pulse. The phase retrieval method using iterative transform algorithm (ITA) is successfully demonstrated for the wavefront reconstruction of an ultrashort high power laser pulse from the intensity distributions [3]. In the presentation, a new wavefront reconstruction method using sets of

usually met in the reconstruction process. In this presentation, we will show the wavefront reconstruction of the 10-Hz, 100-TW Ti:sapphire laser pulse at Advanced Photonics Research Institute (APRI). The reconstruction performance of the method and the effect of intensity resolution and intensity noise on the performance will be shown in the presentation. The study on the wavefront reconstruction using phase retrieval algorithm can help building a wavefront-sensorless adaptive optics (WASLAO) system for a high-power laser system.

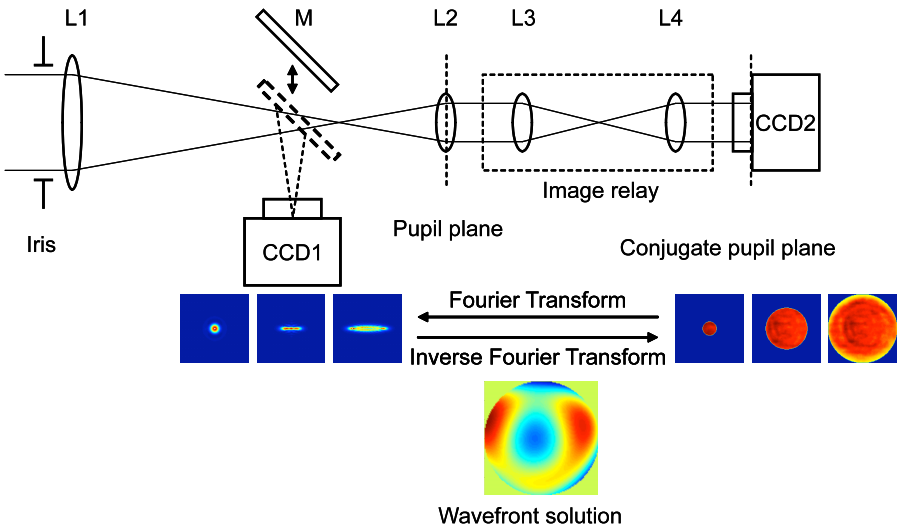

Fig. 1. Wavefront Reconstruction with the phase retrieval method using a set of intensity distributions.

References

1 T. M. Jeong, M. Menon, and G. Yoon, "Measurement of wave-front aberration in soft contact lenses by use of a Shack-Hartmann wavefront sensor", *Appl. Opt.*, 44, 4523-4527 (2005).

2 T. M. Jeong, T. M. Ko, D.-K. Ko, and J. Lee, "Method of reconstructing wavefront aberrations by use of Zernike polynomials in radial shearing interferometers", *Opt. Lett.*, **32**, 232-234 (2007).

3 T. M. Jeong, C. M. Kim, D.-K. Ko, and J. Lee, "Reconstruction of Wavefront Aberration of 100-TW Ti:sapphire Laser Pulse Using Phase Retrieval Method", *J. Opt. Soc. Kor.*, **12**, 186-191 (2008).

Development of photo-curable composition and technique for thin-layer (till 10 µm) objects manufacturing.

Evseev A (1) Kamayev S (1) Kotzuba E. (1) Markov M (1) Michrin V (2) Novikov M (1) Surovtsev M (2)

1 Institute on Laser and Information Technologies, Russian Academy of Sciences (ILIT RAS)
1140700 1 Svyatoozerskaya str, Shatura, Moskow Region, Russia
Fax. 8(49645)22533, e-mail:markov@shatura.laser.ru

2 OAO R&D Inst. "Yarsintez" 150040 88 Pr. Oktyabrya, Yaroslavl, Russia
Phone 8 (4852) 275570

The cycle of R&D was carried out for determination of components for the new photo-curable composition. New acrylic composition was prepared. Its has a low shrinkage, good low viscosity and ability to solidify in thin (till 10 □m) layer. Technological parameters foe manufacturing process were determined by experimentally. The first test models by 10 □m layer-by-layer technology were created.

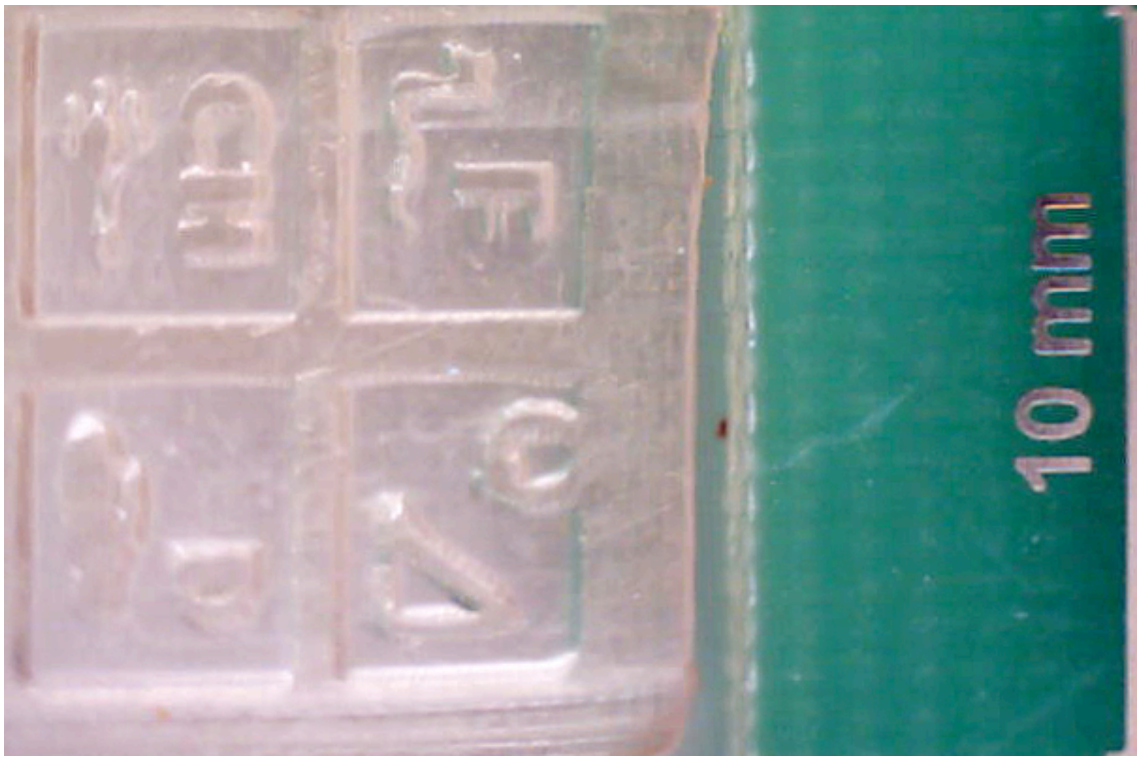

Structural Diagnostics of Polymer Materials by Raman Spectroscopy

K. A. Prokhorov[1], E. A. Sagitova[1,2], G.Yu. Nikolaeva[1], P. P. Pashinin[1], P. Donfack[2], and □. Materny[2]

[1] *A.M. Prokhorov General Physics Institute of RAS, 38 Vavilov St., 119991 Moscow, Russia*

[2] *Jacobs University, School of Engineering & Science, Bremen, Germany*

K. Prokhorov email address: cyrpro@gpi.ru

The manufacture of polymers as wide used materials and as the components for materials of a new generation is based on huge industry and long research experience. The physical properties of polymers and polymer-based composites directly depend upon the features of its molecular structure. But the methods of structural diagnostics of these materials remain conservative. Raman spectroscopy known as an effective tool for molecular diagnostics is hardly applied for the study of polymer-based materials.

It this research laser Raman spectroscopy was applied for the study of polymers, copolymers, and polymer-based composites, providing information on a molecular structure within nano scale.

Polyethylene and polypropylene as the most common polymers together with their mixtures and copolymers recently synthesized with the new catalysts were analyzed. Developing of Raman spectroscopy methods as applied to these specific materials helped us to determine their principal characteristics, such as molecular ordering, phase composition, and conformational structure.

Nanocomposites produced on the basis of polyethylene/polypropylene and cheap natural clay belong to another type of smart materials. Raman spectroscopy data allowed us to successfully study both the macromolecule structure of polymer matrix and the chain conformation of organic molecules of modifier, located in the clay interlayer space.

The conclusion is that Raman spectroscopy allows obtaining unique quantitative data on the structural characteristics of polymer materials, including information that is not revealed by traditional methods of polymer analysis.

This work was supported by the Russian Foundation for Basic Research (09-02-00587). This work is partially supported by the Grant of the President of the Russian Federation for Leading Scientific Schools (476.2008.2).

Efficient Pulse Sequence Generation with Positive and Negative Chirp

Chao-Kuei Lee*, A. K. Chu, H. C. Liu, W. C. Su and C. R. Wu

[1] *Department of Photonics, National Sun-Yat-Sen University, Kaohsiung 804, Taiwan*

**Main author email address: chuckcklee@yahoo.com*

In the past decade, development of pulse train generation have been attracted lots of attentions due to its wide applications, such as coherent control of chemical reactions, pulse train generation for tele-communications[1],

physics applications [3.4], multiple-pulse excitation of atoms, molecules, and solids [5], and generation of tunable narrow-band terahertz radiation [6.7]. In general, the reported pulse train generation methods are based on techniques, such as multi-Michaleson interferometer[8], amplitude-mask in 4f-pulse shaper[9], chirp-pulse mixing[10], a number of birefringent crystals[11], dark-soliton process in fiber[12] and so on. As high as energy transfer from single pulse to pulse sequence for linear polarization was demonstrated using multi-Michelson interferometer or a number of birefringent crystals. However, if the optics is unstable or the optical table mechanically vibrates, the time separation of the pulse pair produced by the interference optics will change temporally. As a result, this will decrease the beating frequency stability and further limit its application range. Meanwhile, all of the methods can only provide positive or negative chirp pulse train. For example, negative chirp sign can be obtained from chirp-pulse-mixing and birefringent crystals approach will generate positive chirp sign pulse train. This also restricts the possibility for coherent control experiment which is chirp sign sensitive. Therefore, an alternative approach with high energy transferring efficiency, high beating frequency stability and tunable sign and amount of chirp of pulse train are required. In their work, beam-splitter and relative temporal delayed can be obtained within pulse shaper. In this work, generation of not only negative but also positive chirp pulse sequences is reported for the first time using pulse shaping technique. Nearly 80% energy conversion efficiency, which is at least two fold to conventional approaches, is demonstrated. Compared to the previous methods, more flexibility for coherent control applications through this changeable sign of chirp is also discussed.

References

1 T. Feurer, J. C. Vaughan, T. Hornung, and K. A. Nelson, Opt. Letts. **29**, 1802-1804 (2004)
2 D. Umstadter, E. Esarey, and J. Kim, Phys. Rev. Lett. **72,** 1224–1227 (1994)
3 H. Tomizawa, T. Asaka, H. Dewa, H. Hanaki, T. Kobayashi, A.Mizuno, S. Suzuki, T. Taniuchi, and K. Yanagida, in *Proceedings of LINAC 2004*, 207–209 (2004)
4 I. V. Bazarov and C. K. Sinclair, Phys. Rev. ST Accel. Beams **8,** 034202 (2005)
5 R. J. Temkin, J. Opt. Soc. Am. B **10,** 830–839 (1993)
6 Y. Liu, S. G. Park, and A. M. Weiner, Opt. Lett. **21,** 1762–1764 (1996)
7 J. Ahn, A. Efimov, R. Averitt, and A. Taylor, Opt. Express **11,** 2486–2496 (2003)
8 C. W. Siders, J. L. W. Siders, A. J. Taylor, S. G. Park, and A. M. Weiner, Appl. Opt. **37**,5302-5305 (1998)
9 A. M. Weiner, J. P. Heritage, and E. M. Kirschner, J. Opt. Soc. Am. B **5**,1563-1572 (1988)
10 .S. Weling and D. H. Auston, J. Opt. Soc. Am. B **13**, 2783-2791(1996)
11 . Zhou, D. Ouzounov, H. Li, I. Bazarov, B. Dunham, C. Sinclair, and F. W. Wise, Appl. Opt. **46**, 8488-8492(2007)
12 . E. Rothenberg, H. K. Heinrich, Opt. Lett.**17,** 261-263(1992)

Laser-induced surface modification of organic polymers

Lokman Torun

TUBITAK MAM Chemistry Institute, Gebze, Kocaeli 41380 Kocaeli/Turkey

Main author email address: lokman.torun@mam.gov.tr

Laser-induced surface modification is a useful technique to change surface characteristic of materials without effecting bulk properties of the substrate. It is a powerful technological tool

hydrophilicity, dyeability, air and water purification, etc. The method has been successfully used in new applications such as coating, welding plastics, etc. Recent advancements on surface

Femtosecond laser applied to photovoltaic cell processing.

M. Sentis, Th. Sarnet and J. Hermann

Laser Plasma and Photonic Processing Laboratory
LP3 –UMR 6182 CNRS –Université de la Méditerranée
13288 Marseille Cedex 9, France
E-mail : Sentis@LP3.univ-mrs.fr

Two fields of femtosecond laser processing of photovoltaic cells will be presented: i) silicon surface micro/nano structuring and ii) CIS based photovoltaic cell scribing.

The formation of micro spikes and cones on crystalline silicon has been the subject of significant research during the past few years. The objective is to improve the unique optical properties that microstructured

photodetector and solar cells. These improved optical properties are due to the change in the topography as well as the chemical modification of the surface induced by laser irradiation in the presence of SF_6. We have chosen in this study to avoid the use of chemicals (NaOH, TMAH, NaOCl …) and corrosive gases (SF_6) by working under vacuum. In order to create an efficient junction for solar cells, we have doped our laser textured surface with a Plasma Immersion Ion Implanter. Significant optical absorption enhancement (more than 50 % in the UV and 35% in the IR) have been obtained, compared to a non-texturized silicon surface. The Internal Quantum Efficiency has also been increased, especially in the UV. Therefore the electrical performance is also drastically improved: we observed a 50% increase in the photocurrent.

Micromachining of CuInSe2 (CIS)-based photovoltaic devices with short and ultrashort laser pulses was also considered. Ablation thresholds and rates of ZnO, Mo and $CuInSe_2$ thin films have been compared for irradiation with nanosecond laser pulses of ultraviolet and visible radiation and sub-picosecond laser pulses of a Ti:sapphire laser. The experimental results were compared to the theoretical evaluation of the samples heat regime. In addition, the cells photo-electrical properties were measured before and after laser machining. Scanning electron microscopy (SEM) and energy dispersive X-ray (EDX) analyses were used to characterize the laser-induced ablation channels. Using nanosecond laser pulses, two phenomena were found to limit the laser-machining process. Residues of Mo that were projected onto the walls of the ablation channel and the metallization of the $CuInSe_2$ semiconductor close to the channel lead to an electrical shunt. The latter causes the decrease of the photovoltaic efficiency. As a consequence of these limiting effects, only ultrashort laser pulses allowed the selective or complete ablation of the thin layers without a relevant change of the photo-electrical properties.

Nonlinear photoluminescence of Gallium Selenide and related compounds: Caused by resonance-enhanced two-photon absorption rather than second-harmonic generation

K. Allakhverdiev [1,2*], D. Huseinova [2], T. Baykara [1], E. Salaev [2],
C. Angermann [3], P. Karich [3], and L. Kador [3**]

[1] *TÜBİTAK, Marmara Research Center, Materials Institute, 41470 Gebze/Kocaeli, Turkey*
[2] *Institute of Physics ANAS, 370143, Baku, Azerbaijan*
[3] *University of Bayreuth, Institute of Physics and Bayreuther Institut für Makromolekülforschung (BIMF), D-95440 Bayreuth, Germany*
[*] *E-mail: kerim.allahverdi@mam.gov.tr Fax: (+90 262) 641 23 09*
[**] *E-mail: lothar.kador@uni-bayreuth.de Fax: (+49-921) 55-3250*

Confocal Raman measurements on the layered chalcogenide semiconductor gallium selenide (GaSe) with a cw HeNe laser (632.8 nm) had shown that the material emits a strong photoluminescence signal which is mainly blue-shifted from the laser line and has a quadratic dependence on laser intensity [1,2]. A similar effect was found on mixed crystals of the form $GaSe_{1-x}S_x$ with sulfur content x below 0.05 [3]. The blue shift and the quadratic intensity dependence indicate that it involves a nonlinear-optical process. Since GaSe has a very high $\chi^{(2)}$ coefficient of 86 pm/V (1.9×10^{-7} esu, measured at 10.6 μm [4]), the effect was ascribed to second-harmonic generation in the laser focus which leads to the excitation of electrons into the conduction band and gives rise to the formation and radiative decay of Wannier excitons. Two-photon excitation as the origin was ruled out, since mixed crystals with higher sulfur content, which are known to have mainly centrosymmetric crystal structures [5], did not show the effect [3].

Recent experiments have proven that the direct observation of second-harmonic signals with the Maker fringe technique is indeed possible using weak cw diode lasers in the near infrared (at 1300 nm and 1550 nm). On the other hand, the nonlinear photoluminescence signal was found to be independent of the azimuthal orientation φ of the crystal with respect to laser polarization, which disagrees with the sin (3φ) dependence of the effective $\chi^{(2)}$ coefficient [4]. Moreover, temperature tuning of the absorption edge of GaSe and the mixed crystal $GaSe_{1-x}S_x$ with sulfur content $x = 0.1$ revealed that, under the condition of weak cw illumination, both compounds emit the nonlinear photoluminescence only if the laser wavelength is close to the absorption edge of the semiconductor. Hence, we are led to conclude that the mechanism behind the nonlinear photoluminescence is two-photon absorption rather than second-harmonic generation. At wavelengths close to the band edge, the $\chi^{(3)}$ effect two-photon absorption appears to become so strong due to resonance enhancement that it is more efficient than the $\chi^{(2)}$ effect second-harmonic generation (plus subsequent linear absorption of the generated second-harmonic wave). The authors are indebted to the State Plan Committee (DPT) of Turkey and the Deutsche Forschungsgemeinschaft (DFG) for support.

References

1. Y. Fan, M. Bauer, L. Kador, K. R. Allakhverdiev, and E. Yu. Salaev, ″Photoluminescence Frequency Up-Conversion in GaSe Crystals as Studied by Confocal Microscopy″, *J. Appl. Phys*. **91**, 1081 (2002).
2. Y. Fan, T. Schittkowski, M. Bauer, L. Kador, K. R. Allakhverdiev, and E. Yu. Salaev, ″Confocal Photoluminescence studied on GaSe Single Crystals″, *J. Lumin*. **98**, 7 (2002).
3. C. Pérez León, L. Kador, K. R. Allakhverdiev, T. Baykara, and A. A. Kaya, ″Comparison of the Layered Semiconductors GaSe, GaS, and $GaSe_{1-x}S_x$ by Raman and Photoluminescence Spectroscopy ″, *J. Appl. Phys*. **98**, 103103 (2005).
4. G. B. Abdullaev, K. R. Allakhverdiev, M. E. Karasev, V. I. Konov, L. A. Kulevskii, N. B. Mustafaev, P. P. Pashinin, A. M. Prokhorov, Y. M. Starodumov, and N. I. Chapliev, ″Efficient Geneartion of the Second Harmonic of CO_2 Laser Radiation in a Gase Ceystal ″ S*ov. J. Quantum Electron*. **19**, 494 (1989).
5. K. R. Allakhverdiev, M. Ö. Yetis, S. Özbek, T. K. Baykara, E. Yu. Salaev, ″Effective Nonlinear GaSe Crystal. Properties and Applications″, *Laser Physics*, **19**, 1092 (2006).

Nonlinear GaSe and $GaSe_xS_{1-x}$ Layered Compounds for Near IR Laser Light Visualization

Kerim R. Allakhverdiev [1,2*], Tarik K. Baykara[1], Sunullah Ozbek[1], Eldar Yu. Salaev[2]

[1] *TUBITAK, Marmara Research Center, Materials Institute, 41470, Gebze/Kocaeli, Turkey*
[2] *Institute of Physics ANAS, 370143, Baku, Azerbaijan*
[*] *E-mail: kerim.allahverdi@mam.gov.tr*

Near IR laser light converters are essential components in optical communication systems. These devices should have low power density limit (high energy sensitivity), high threshold damage, linear response and longer

of KDP, KTP or seramic ABO_3 (eg. PZT) and a special phosphor materials burried in a plastic foil. Each type of these converters reveal weak points, concerning with the sensitivity as well as with the possibility to observe the real spot size of the beam due to fluorescence of the regions of material which are close to the excited spot region. Besides this, both types do not give a possibility for visualization of distribution of the intensity of radiation over the cross section of beam and for investigation of content of laser radiation. Furthermore, the second type of converters must be charged by a short exposure to a daylight or fluorescent light prior to use. The sensitivity decreases after each exposure as a function of time.

Highly anisotropic GaSe (chemical family-metal selenide) and $GaSe_xS_{1-x}$ ($0.2 \le x \le 0.8$) semiconductors possess several outstanding physical properties, the best known of which is a very high non-linear susceptibility □(2), a wide optical transmission range and high birefringence that is used for phase-matched second harmonic generation in a middle-IR range [1,2]. The method of prerparation of laser radiation converters by the use of nonlinear optical materials was described [3]. Two important improvements come out by adding S to GaSe: the band gap and hardness of crystal increases. Conversion of pulsed and continuous IR (800-1360 nm) laser radiation into the visible range of spectra (400-680 nm) is achieved by using a transparent substrate covered with the particles (including nanoparticles) of effective nonlinear materials of $GaSe_xS_{1-x}$ ($0.2 \le x \le 0.8$). Converted light can be detected in transmission or reflection geometry as a visible spot corresponding to the real size of the incident laser beam. Developed device structures can be used for checking if the laser is working or not, for optical adjustment, for visualization of distribution of laser radiation over the cross of the beam and for investigation of the content of the laser radiation. Low energy (power density) limit for visualization of the IR laser pulses with 2 -3 *ps* duration for these device structures are: between 4.6 – 2.1 μJ ($3\cdot10^{-4}$ – $1\cdot10^{-4}$ W/cm^2) at 1200 *nm*; between 8.4 – 2.6 μJ ($4.7\cdot10^{-4}$ – $1.5\cdot10^{-4}$ W/cm^2) at 1300 *nm*; between 14.4 – 8.1 μJ ($8.2\cdot10^{-4}$ – $4.6\cdot10^{-4}$ W/cm^2) at 1360 *nm*. Threshold damage density is more than 10 MW/cm^2 at $\lambda = 1060$ *nm*, pulse duration $\tau = 35$ *ps*. The results are compared with commercially existing laser light visualizators.

The main conclusion from the present research is that pure GaSe and mixed $GaSe_xS_{1-x}$ are very effective for visualization of near IR laser light emissions. The authors are indebted to the State Plan Committee (DPT) of Turkey for the partial support.

References

[1] G. B. Abdullaev, L. A. Kulevskii, A. M. Prokhorov, A. D. Savel′ev, E, Y. Salaev, V, V, Smirnov, Sov. Phys.-JETP Lett. **16**, 90 (1972).
[2] K. R. Allakhverdiev, R. I. Guliev, E. Yu. Salaev, V. V. Smirnov, Sov. J. Quantum Electron. **12**, 947 (1982).
[3] K. Allakhverdiev, E. Salaev, D. Haarer, A. Seilmeier, Method of Preparation of Laser Radiation Converters by the Use of Nonlinear Optical Materials, Patent No97/00784, Registered 11.08.97 by Patent Institute, Ankara, Turkey.